

**Mechanism and dynamics of acyl-CoA mediated protein  
lysine acylation in mitochondria**

Dissertation

zur Erlangung des

Doktorgrades der Naturwissenschaften (Dr. rer. nat.)

der

Naturwissenschaftlichen Fakultät I – Biowissenschaften –

der Martin-Luther-Universität

Halle Wittenberg,

vorgelegt

von Herrn Zeljko Simic

geb. am 04.02.1982 in Bajina Basta

Gutachter: Prof. Dr. Mike Schutkowski  
Prof. Dr. Wolfgang Sippl  
Prof. Dr. Dirk Schwarzer

Tag der öffentlichen Verteidigung: 13.10.2016

# Table of contents

Abbreviations list .....	iv
List of figures.....	viii
List of tables .....	xi
Introduction.....	1
Lysine acetylation.....	1
Protein lysine acetylation in mitochondria .....	3
Induction of mitochondrial protein hyperacetylation.....	5
Mitochondrial lysine deacetylases .....	5
Mitochondrial lysine acetyltransferase .....	8
Proposed mechanisms of mitochondrial protein acetylation .....	8
Physiological conditions of mitochondrial matrix.....	11
Coenzyme A and its acyl-thioester derivatives.....	14
Acetyl-CoA .....	16
Acyl-CoA thioesters and PTMs of proteins in mitochondria .....	19
Aim of the thesis .....	22
Materials and Methods .....	23
Chemical synthesis .....	23
Synthesis of CPS1 peptide and CPS1 peptide derivatives .....	23
Synthesis of TNF $\alpha$ peptide derivatives .....	23
Synthesis and purification of acyl-CoA derivatives .....	24
Synthesis and purification of acetyl-adenylate (Ac-AMP) .....	24
Preparative HPLC .....	25
Analytical HPLC.....	25
Expression and purification of the enzymes .....	25
Expression and purification of human SIRT2 .....	25
Expression and purification of human SIRT3 and SIRT5 .....	26
Expression and purification of human SIRT4 .....	26
Expression and purification of human CypA.....	27

SDS-polyacrylamide gel electrophoresis (SDS-PAGE) .....	27
Native-PAGE .....	28
Dot-blot assay .....	28
4CN Colorimetric detection for Dot- and Western blot assays.....	29
Western-blot.....	29
Determination of protein concentration.....	30
Mass spectrometry (MS) .....	30
Sample preparation and MALDI-TOF/TOF MS .....	30
In-gel trypsin digestion.....	31
Nano-UPLC.....	31
ESI-QTOF-MS/MS-Analysis .....	31
Capillary electrophoresis (CE) .....	32
Continuous fluorescence assay for measuring sirtuin activity.....	32
Fluorescence spectroscopy .....	33
Circular dichroism spectroscopy (CD) .....	33
Peptide microarray .....	33
Results .....	35
Non-enzymatic lysine acetylation of model peptide using Ac-CoA .....	35
Kinetic and thermodynamic parameters of non-enzymatic lysine acetylation .....	37
Non-enzymatic acylation of CPS1 peptide by different acyl-CoA thioesters .....	41
Modulation of non-enzymatic lysine acetylation .....	42
Small molecules .....	42
Water content and ionic strength .....	43
The methylation of N- $\epsilon$ -amino group of lysine residue.....	45
Non-enzymatic acetylation of CypA .....	47
Non-enzymatic succinylation of CypA.....	53
Activity of acylated CypA.....	56
Structural alterations of acylated CypA.....	57
Desuccinylation of succinylated CypA by mitochondrial sirtuins .....	58
Acylation of CypA as a function of the lysine pK <sub>a</sub> values .....	61
Shift of acylation type by simultaneous action of SIRT3 and Succ-CoA .....	63
Expanding acyl specificity of SIRT4 .....	65

Enzymatic lysine acetylation.....	68
Citrate synthase.....	68
Acetyl-CoA acetyltransferase, mitochondrial .....	69
Hydroxymethylglutaryl-CoA synthase, mitochondrial .....	69
Carnitine O-acetyltransferase.....	69
Acetyl-CoA synthetase .....	70
Diamine acetyltransferase 1 .....	73
Protein modifications using modifying agents other than CoA thioesters. Introducing thioacetyl groups into the protein.....	77
Discussion .....	81
Summary .....	96
Zusammenfassung.....	97
Appendix.....	98
Bibliography .....	131
Acknowledgments .....	149
Curriculum Vitae.....	150
List of publications.....	151
Eigenständigkeitserklärung.....	152

# Abbreviations list

4CN	4-chloro-1-naphthol
Å	Ångström (unit of length equal to $10^{-10}$ m)
Abz	aminobenzoic acid
Ac	acetyl
AcAc	acetoacetyl
ACAT1	acetyl-CoA acetyltransferase 1
ACN	acetonitrile
ACS	acetyl-CoA synthetase
ADH	alcohol dehydrogenase
ADP	adenosine diphosphate
ALDH2	acetaldehyde dehydrogenase
APS	ammonium persulfate
Arg	arginine
Asp	aspartic acid
ATP	adenosine triphosphate
Benz	benzoyl
Boc	tert-butyloxycarbonyl protecting group
BSA	bovine serum albumin
But	butyryl
Bz	benzoyl
CD	circular dichroism
CE	capillary electrophoresis
CoA	coenzyme A
CPS1	carbamoylphosphate synthetase 1
CR	calorie restriction

CypA	cyclophilin A
CypD	cyclophilin D
Cys	cysteine
Da	dalton
DBU	1,8-diazabicyclo[5.4.0]undec-7-en
DCM	dichloromethane
dd H <sub>2</sub> O	double distilled water
DIPEA	N,N-diisopropylethylamine
DLAT	PDH E2 component dihydrolipoyllysine acetyltransferase
Dma	4-N,N-dimethylamino-1,8-naphthalimid-acetic acid
DMAP	4-(dimethylamino)-pyridine
DMF	dimethylformamid
DMSO	dimethyl sulfoxide
DNA	deoxyribonucleic acid
DTT	dithiothreitol
eq	equivalent
ES complex	enzyme substrate complex
ESI	electrospray ionization
ETC	electron transport chain
Fmoc	9-fluorenylmethoxy-carbonyl
GCN5L1	general control of amino acid synthesis 5 - like 1
GDH	glutamate dehydrogenase
Glu	glutamic acid
Glut	glutaryl
h	hour
HAT	histone acetyltransferase
HBTU	(2-(1H-benzotriazol-1-yl)-1,1,3,3-tetramethyluronium hexafluorophosphate)
HDAC	histone deacetyltransferase
HIF1 $\alpha$	hypoxia inducible factor-1 $\alpha$

His	histidine
HMG	3-hydroxy-3-methylglutaryl
HMGCS2	3-hydroxy-3-methylglutaryl-CoA synthase 2
HPLC	high-performance liquid chromatography
IMS	intermembrane space
I $\kappa$ B $\alpha$	nuclear factor of kappa light polypeptide gene enhancer in B-cells inhibitor, alpha
K	lysine
KAT	lysine acetyltransferase
KDAC	lysine deacetylase
LC	liquid chromatography
Lys	lysine
mA	milliampere
MALDI	matrix-assisted laser desorption/ionization
MBHA	4-methylbenzhydramine
MDH2	malate dehydrogenase 2
MDM2	E3 ubiquitin-protein ligase Mdm2
Me	methyl
MeCPS1	N-methyl-CPS1
MeSuccCPS1	N-methyl-N-succinyl-CPS1
min	minute
MS	mass spectrometry
NAD <sup>+</sup>	nicotinamide adenine dinucleotide
NADP <sup>+</sup>	Nicotinamide adenine dinucleotide phosphate
NAM	nicotineamide
NF- $\kappa$ B	nuclear factor kappa-light-chain-enhancer of activated B cells
OXPPOS	oxidative phosphorylation
PCR	polymerase chain reaction
PDC	pyruvate dehydrogenase complex



PDHA1	A1 subunit of the pyruvate dehydrogenase complex
PDP1	pyruvate dehydrogenase phosphatase 1
PPIase	peptidylprolyl cis/trans isomerase
Prop	propionyl
psi	pound-force per square inch (1 psi ~ 6894.6 Pa)
PTM	posttranslational modification
PyBOP	benzotriazole-1-yl-oxy-tris-pyrrolidino-phosphonium hexafluorophosphate
R	arginine
ROS	reactive oxygen species
RP-HPLC	reversed-phase high-performance liquid chromatography
RT	room temperature
SDS	sodium dodecyl sulfate
PAGE	polyacrylamide gel electrophoresis
Ser	serine
STAT3	signal transducer and activator of transcription 3
Succ	succinyl
TBS	tris buffer saline
TCA	tricarboxylic acid
TCEP	tris-(2-carboxyethyl)-phosphine
TEMED	N,N,N',N'-tetramethylethane-1,2-diamine
TFA	trifluoroacetic acid
THF	tetrahydrofuran
Thr	threonine
TNF $\alpha$	tumor necrosis factor alpha
TOF	time of flight
Tyr	tyrosine
UV	ultraviolet
Vis	visible

## List of figures

<b>Figure 1.</b> Chemical structure of free L-lysine and its N-( $\epsilon$ )-acetylated form. ....	1
<b>Figure 2.</b> Proposed mechanisms of mitochondrial protein acetylation. ....	10
<b>Figure 3.</b> Schematic illustration of animal mitochondrion. ....	12
<b>Figure 4.</b> Chemical lysine acetylation mechanism - schematic illustration. ....	12
<b>Figure 5.</b> Schematic illustration of the energy production metabolism in mitochondria. ....	14
<b>Figure 6.</b> The structure of CoA. ....	15
<b>Figure 7.</b> The biosynthesis of CoA. ....	16
<b>Figure 8.</b> Illustration of possible sources of Ac-CoA in the living organisms. ....	17
<b>Figure 9.</b> Reactivity of Ac-CoA. ....	18
<b>Figure 10.</b> Ac-CoA mitochondrial – cytosolic shuttle. ....	19
<b>Figure 11.</b> Known acyl-lysine posttranslational modifications found in mitochondrial proteome. ....	20
<b>Figure 12.</b> Non-enzymatic lysine acetylation of Bz-GVLKEYGV-NH <sub>2</sub> (CPS1 peptide). ....	36
<b>Figure 13.</b> Determination of kinetic and thermodynamic parameters of non-enzymatic lysine acetylation by Ac-CoA. ....	39
<b>Figure 14.</b> Comparison of non-enzymatic CPS1 peptide acylation by different thioesters. ....	42
<b>Figure 15.</b> DMAP accelerates Ac-CoA-mediated non-enzymatic acetylation of the CPS1 peptide in a concentration dependent manner. ....	43
<b>Figure 16.</b> Non-enzymatic acetylation of CPS1 peptide by Ac-CoA in the reaction system with reduced water content. ....	44
<b>Figure 17.</b> Non-enzymatic acetylation of CPS1 peptide by Ac-CoA in the presence of different salt concentrations. ....	45
<b>Figure 18.</b> Methylation of the $\epsilon$ -amino group of lysines residues prevents non-enzymatic acetylation by Ac-CoA. ....	46
<b>Figure 19.</b> Methylation of the $\epsilon$ -amino group of lysines residues is not able to prevent non-enzymatic succinylation by Succ-CoA. ....	47
<b>Figure 20.</b> Non-enzymatic lysine acetylation of the protein substrate CypA. ....	49
<b>Figure 21.</b> Schematic illustration of protein digestion with trypsin and LC-MS/MS analysis of tryptic peptides. ....	50
<b>Figure 22.</b> Analysis of the lysine acetylation pattern of CypA. ....	51

<b>Figure 23.</b> Deacetylation of acetylated CypA by mitochondrial sirtuins.....	52
<b>Figure 24.</b> Analysis of the lysine succinylation pattern of CypA by LC-MS/MS. ....	54
<b>Figure 25.</b> Analysis of CypA acylation by CE. ....	55
<b>Figure 26.</b> Effect of acylation on PPIase activity of CypA.....	56
<b>Figure 27.</b> Location of lysine residues in the X-ray structure of CypA.....	57
<b>Figure 28.</b> Analysis of acylated CypA by CD spectroscopy. ....	58
<b>Figure 29.</b> Organization of the secondary structure of the CypA. ....	58
<b>Figure 30.</b> Desuccinylation of CypA by SIRT3 and SIRT5. ....	59
<b>Figure 31.</b> Desuccinylation of CypA by SIRT5 followed by CE.....	60
<b>Figure 32.</b> Lysine acylation as a function of lysine $pK_a$ .....	62
<b>Figure 33.</b> Shift in “Acylation landscape” caused by the simultaneous action of specific sirtuin deacetylase and acyl-thioester. ....	64
<b>Figure 34.</b> Structure of synthesized TNF $\alpha$ peptide substrates.....	65
<b>Figure 35.</b> HPLC based assay of TNF $\alpha$ peptide substrates for SIRT4.....	66
<b>Figure 36.</b> Michaelis-Menten plots of TNF $\alpha$ substrate 1 and 2 for SIRT4.....	67
<b>Figure 37.</b> Acetylation of CPS1 peptide by ACS.....	71
<b>Figure 38.</b> Acetylation of CPS1 peptide by Ac-AMP. ....	72
<b>Figure 39.</b> Structure of small polyamines molecules.....	73
<b>Figure 40.</b> SAT1 lysine acetyltransferase activity detected by peptide microarrays. ....	74
<b>Figure 41.</b> Substrate specificity of SAT1. ....	75
<b>Figure 42.</b> Chemical structure of free lysine, N- $\epsilon$ -acetyl-lysine and N- $\epsilon$ -thioacetyl-lysine.....	77
<b>Figure 43.</b> Modification of CypA by ethyl dithioacetate. ....	78
<b>Figure 44.</b> CypA is successfully modified by ethyl dithioacetate at multiple lysine sites. ...	79
<b>Figure 45.</b> Schematic diagram of intramolecular catalysis in Succ-CoA and succinic anhydride formation.....	85
<b>Figure 46.</b> Potential role of ACS in the mitochondrial protein acetylation. ....	90
<b>Figure 47.</b> Sources and fate of mitochondrial Ac-CoA.....	92
<b>Figure 48.</b> Schematic representation of the possible role of non-enzymatic protein acetylation in energy storage.....	94

<b>Figure A1.</b> Analytical HPLC chromatogram of CPS1 peptide.....	99
<b>Figure A2.</b> Analytical HPLC chromatogram of N-methyl-CPS1 peptide. ....	100
<b>Figure A3.</b> Analytical HPLC and MS-spectrum of TNF $\alpha$ peptide 1.....	101
<b>Figure A4.</b> Analytical HPLC and MS-spectrum of TNF $\alpha$ peptide 2.....	102
<b>Figure A5.</b> Analytical HPLC and MS-spectrum of TNF $\alpha$ peptide 3.....	103
<b>Figure A6.</b> Analytical HPLC and MS-spectrum of TNF $\alpha$ peptide 4.....	104
<b>Figure A7.</b> Analytical HPLC and MS-spectrum of TNF $\alpha$ peptide 5.....	105
<b>Figure A8.</b> Analytical HPLC chromatogram of Benz-CoA. ....	106
<b>Figure A9.</b> Analytical HPLC chromatogram of But-CoA .....	107
<b>Figure A10.</b> Analytical HPLC chromatogram of Glut-CoA.....	108
<b>Figure A11.</b> Analytical HPLC chromatogram of Prop-CoA. ....	109
<b>Figure A12.</b> Validation of the HPLC method. ....	110
<b>Figure A13.</b> Calibration curves for TNF $\alpha$ peptides 1 and 2.....	111
<b>Figure A14.</b> Comparison of non-enzymatic lysine acetylation in the presence of a variety of different buffers.....	111
<b>Figure A15.</b> Hydrolytic stability of Ac- and Succ-CoA.....	112
<b>Figure A16.</b> Modification of CPS1 peptide by Succ-CoA. ....	113
<b>Figure A17.</b> Modification of CPS1 peptide by Glut-CoA.....	114
<b>Figure A18.</b> Modification of CPS1 peptide by Prop-CoA.....	115
<b>Figure A19.</b> Modification of CPS1 peptide by But-CoA. ....	116
<b>Figure A20.</b> Modification of CPS1 peptide by HMG-CoA.....	117
<b>Figure A21.</b> CypA and CypD sequence alignment.....	118
<b>Figure A22.</b> SDS-PAGE of CypA. ....	120
<b>Figure A23.</b> RP-HPLC separation of acetylated CypA. ....	124
<b>Figure A24.</b> Fluorescence spectra of CypA. ....	125
<b>Figure A25.</b> Analytical HPLC and MS of SAT1 substrate peptide 1 .....	126
<b>Figure A26.</b> Analytical HPLC and MS of SAT1 substrate peptide 2.....	127
<b>Figure A27.</b> Analytical HPLC and MS of SAT1 substrate peptide 3.....	128
<b>Figure A28.</b> Excitation and emission spectra of TNF $\alpha$ peptide 1 and 2.....	129
<b>Figure A29.</b> Simultaneous measurements of sirtuin activity using two substrates.....	130

## List of tables

<b>Table 1.</b> Classification of KDACs enzymes.....	3
<b>Table 2.</b> List of SIRT3 protein substrates. ....	6
<b>Table 3.</b> pK <sub>a</sub> values of the CypA lysine residues.....	62
<b>Table 4.</b> Kinetic constants for TNF $\alpha$ peptide 1 and 2 and SIRT4. ....	67
<b>Table 5.</b> Selected mitochondrial enzymes which use Ac-CoA as a cosubstrate.....	68
<b>Table 6.</b> Top 10 peptide substrates for SAT1. ....	76
<b>Table 7.</b> Kinetic parameters for SIRT5 mediated deacylation of acylated CPS1 peptide derivatives. ....	84
<b>Table A1.</b> Posttranslational lysine modifications of CypA.....	119
<b>Table A2.</b> List of CypA not-modified tryptic peptides.....	121
<b>Table A3.</b> List of tryptic CypA peptides containing acetylated lysine residue.....	122
<b>Table A4.</b> List of tryptic CypA peptides containing succinylated lysine residue.....	123

# Introduction

Protein posttranslational modifications (PTMs) represent covalent modifications of amino acid residue subsequent to protein biosynthesis. PTMs are components of the mature protein and mainly positioned on the side chains of the amino acids or on the C- or N-terminus of the protein. Introduction of additional groups into the proteins increases the diversity and functionality and overcomes proteome complexity specified by the genome. PTMs are very important factors in regulation of protein function in living cells including change of enzymatic activity, subcellular localization, protein stability, interactions with other proteins and DNA binding efficiency. A variety of different PTMs are discovered and the number is still going up with development of analytical techniques. Some of them include phosphorylation of Ser and Thr, acylation of Lys, glycosylation of Arg and lipidation of Cys. Hydrolysis of peptide bonds, establishing of disulfide bonds or peptidyl-prolyl-cis/trans isomerisation are also phenomena covered with the term of PTMs.

## Lysine acetylation

Lysine acetylation is one of the most common PTMs found on cellular proteins. The acetyl group is positioned at  $\epsilon$ -amino group of the lysine residue (Figure 1).

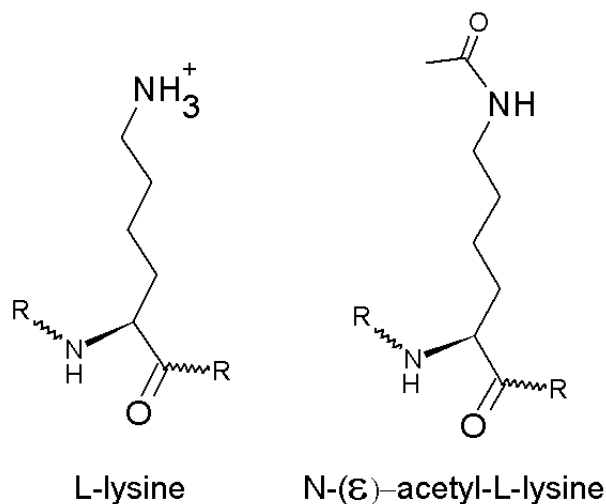


**Figure 1.** Chemical structure of free L-lysine and its N-( $\epsilon$ )-acetylated form.

Lysine acetylation was discovered and described for the first time fifty years ago on histones (Allfrey et al., 1964; Phillips, 1963). Shortly after that, protein lysine acetylation

was discovered also on nonhistone proteins (L'Hernault and Rosenbaum, 1983). Until now, protein lysine acetylation represents one of the most abundant PTM from bacteria to humans (Kim and Yang, 2011). Lysine acetylation is a reversible PTM. Three types of enzymes are responsible for the fluctuation in the acetylation state of the cellular proteins.

Lysine acetyltransferases (KATs) are enzymes catalyzing the transfer of an acetyl-group from the cosubstrate Ac-CoA to the  $\epsilon$ -amino group of the target lysine residue. Based on the sequence and structural differences these enzymes are divided into five subfamilies: HAT1, Gcn5/PCAF, MYST, P300/CBP and Rtt109 (Yuan and Marmorstein, 2013). Until now, about 30 human enzymes showing histone acetyltransferase activity have been identified (Glozak et al., 2005). Many of the histone acetyltransferases show significant ability to acetylate a wide range of non-histone proteins (Gu and Roeder, 1997).

Acetyl group is removed from the lysine residues by lysine deacetylases (KDACs). There are 18 different KDACs in humans (Shirakawa et al., 2013) subdivided into four classes (Table 1).

KDACs classes I, II and IV utilize  $Zn^{2+}$  as a cofactor. Although many of those enzymes are described to have a variety of substrates beyond histones, these enzymes still retained the traditional name histone deacetylase (HDACs). Class III lysine deacetylases are named sirtuins, because of the first identified Yeast Sir2 homolog (**S**ilent mating-type information regulation **2**) (Shore et al., 1984). Sirtuins use  $NAD^+$  as a cosubstrate.

One of the first roles of protein acetylation was described shortly after histone acetylation was discovered. Early studies suggested that abundant histone acetylation could affect gene expression (Allfrey, 1966; Vidali et al., 1968). The introduction of the acetyl group into the proteins neutralizes positive charge on the  $\epsilon$ -amino group of the lysine residue, resulting in a significant impact on a protein activity, protein-protein interaction, protein-DNA interaction, protein subcellular localization and protein stability (Glozak et al., 2005).

Gu and Roeder clearly demonstrated that acetylation at the C-terminal domain of p53 dramatically stimulates its DNA binding activity (Gu and Roeder, 1997). Additionally, Ito et al. showed that MDM2 can promote HDAC1 mediated deacetylation of p53, which leads

to its degradation, suggesting that acetylation promotes p53 stability and plays a crucial role in its function (Ito et al., 2002). It has been reported that HDAC3 mediated deacetylation of NF- $\kappa$ B promotes its binding to I $\kappa$ B $\alpha$ , demonstrating how acetylation can prevent protein-protein interaction (Chen et al., 2001). Wang and colleagues showed that CBP/p300 acetylated STAT3 at K685, resulting in its translocation from cytoplasm to nucleus and increasing its sequence specific DNA binding (Wang et al., 2005).

**Table 1.** Classification of KDACs enzymes.

Class	Isoform	Yeast homolog	Cofactor	Subcellular localization
I	HDAC1		Zn <sup>2+</sup>	nucleus
	HDAC2		Zn <sup>2+</sup>	nucleus
	HDAC3	Rpd3	Zn <sup>2+</sup>	nucleus/cytosol
	HDAC8		Zn <sup>2+</sup>	nucleus/cytosol
	HDAC4		Zn <sup>2+</sup>	nucleus/cytosol
IIa	HDAC5		Zn <sup>2+</sup>	nucleus/cytosol
	HDAC7	HDA1	Zn <sup>2+</sup>	nucleus/cytosol
	HDAC9		Zn <sup>2+</sup>	nucleus/cytosol
IIb	HDAC6	HDA2	Zn <sup>2+</sup>	nucleus/cytosol
	HDAC10		Zn <sup>2+</sup>	nucleus/cytosol
III	SIRT1		NAD <sup>+</sup>	nucleus/cytosol
	SIRT2		NAD <sup>+</sup>	cytosol
	SIRT3		NAD <sup>+</sup>	mitochondria
	SIRT4	Sir2	NAD <sup>+</sup>	mitochondria
	SIRT5		NAD <sup>+</sup>	mitochondria
	SIRT6		NAD <sup>+</sup>	nucleus
	SIRT7		NAD <sup>+</sup>	nucleus
IV	HDAC11	Rpd3/HDA1	Zn <sup>2+</sup>	nucleus

## Protein lysine acetylation in mitochondria

Large scales proteomics surveys have demonstrated that lysine acetylation is enriched in mitochondria (Choudhary et al., 2009; Kim et al., 2006; Zhao et al., 2010). Notably, mitochondrial protein acetylation exhibits a high degree of conservation between flies, worms, zebrafish, mice and humans (Weinert et al., 2011). These studies suggest a critical role of protein lysine acetylation in a wide range of key mitochondrial functions including fuel oxidation, energy generation, waste disposal, and detoxification of reactive oxygen species. Hebert et al. identified 3285 acetylation sites from 2193 mitochondrial proteins (Hebert et al., 2013). The authors claim that 65 % of all mitochondrial proteins



have at least one acetylation site. Almost every enzyme in the glycolysis, gluconeogenesis, tricarboxylic acid cycle, urea cycle, fatty acid metabolism has been found to be acetylated in human liver (Zhao et al., 2010). Interestingly, carbamoyl phosphate synthase 1 (CPS1) was found to be acetylated at 52 lysines in mouse liver (Weinert et al., 2013). These data are not surprising, because CPS1 is an abundant protein in the liver and has a relatively large molecular weight. Interestingly, the vast majority of metabolic enzymes are inactivated in the acetylated form. Acetylation at K642 inhibits mitochondrial acetyl-CoA synthetase 2 (Schwer et al., 2006). Hyperacetylation also negatively regulates activity of ornithine transcarbamoylase, an enzyme involved in the urea cycle (Hallows et al., 2011). Recently, MS study revealed that long-chain acyl-coenzyme A dehydrogenase is negatively regulated by acetylation at K42 (Hirschey et al., 2010). Hyperacetylation inhibits Complex I of the electron transport chain, showing its implication in the energy metabolism (Ahn et al., 2008). Despite these, a wide range of other enzymes involved in key mitochondrial functions are found to be inhibited by acetylation like isocitrate dehydrogenase, enzyme involved in the redox metabolism (Yu et al., 2012); superoxide dismutase 2, a major mitochondrial antioxidant enzyme (Qiu et al., 2010); 3-hydroxy-3-methylglutaryl CoA synthase 2 (HMGCS2) a mitochondrial enzyme involved in ketone body synthesis (Shimazu et al., 2010) and malate dehydrogenase, an enzyme of the TCA cycle (Schlicker et al., 2008). Interestingly, for all these enzymes hyperacetylation has been observed after knock out of SIRT3, a prominent mitochondrial lysine deacetylase (Lombard et al., 2007). Re-expression of SIRT3 could recover the function of a wide range of mitochondrial metabolic enzymes (Hirschey et al., 2010).

It is important to note that, although less prevalent, acetylation can also activate enzyme activity. Acetylation at K301, K307 and K314 significantly increases enzymatic activity of malate dehydrogenase 2 during adipocyte differentiation (Kim et al., 2013). Recently, Fernandes et al. have demonstrated that acetylation at multiple lysine residues increases aconitase activity in heart mitochondria. Additional investigation has shown that K144 is mainly responsible for aconitase activation and that SIRT3 successfully reverses acetylation at multiple lysines including K144 (Fernandes et al., 2015).

Mitochondrial protein hyperacetylation has been linked to the pathophysiology of different disorders, such as diabetes through acetylation of enzymes implicated in the regulation of oxidation, reactive oxygen species production and insulin resistance in skeletal muscle (Jing et al., 2011). SIRT3 expression is induced in human breast cancer,

which correlates well with up-regulation of HIF1 $\alpha$  target genes indicating that lysine acetylation plays a crucial role in cancer (Finley et al., 2011a). Additionally, mitochondrial protein acetylation is implicated in metabolic syndrome (Hirschey et al., 2011), cardiac hypertrophy (Hafner et al., 2010) and other mitochondrial disorders such as Friedreich's Ataxia (Wagner et al., 2012).

## Induction of mitochondrial protein hyperacetylation

It is well known that acetylation of metabolic enzymes depends strongly on extracellular nutrient availability (Zhao et al., 2010).

Hyperacetylation of mitochondrial proteins in mouse liver has been reported during calorie restriction (CR) (Hebert et al., 2013). CR is a dietary regimen characterized by lowering in nutrient input up to 50 %, without lowering in essential nutrients. CR extends life span of different organisms including yeast, mice or monkeys (Colman et al., 2009; Mattison et al., 2012; Weindruch et al., 1986). Molecular mechanism of CRs effected life span remains elusive. It is believed that in yeast sirtuins play a crucial role in CR mediated extension of life span (Lin et al., 2000). Mitochondrial hyperacetylation observed during obesity and high fat diet was mainly caused by downregulation of SIRT3 (Alrob et al., 2014). Recently, Fritz et al. have reported that chronic alcohol consumption induces increase in acetylation of 91 mitochondrial proteins targeting mainly fatty acid metabolism (Fritz et al., 2012).

## Mitochondrial lysine deacetylases

Mitochondria represent harbor for three of seven sirtuin isoforms (SIRT3, SIRT4 and SIRT5) which represent the main mitochondrial lysine deacetylases (Gertz and Steegborn, 2016). There are a limited number of evidences that nuclear encoded lysine deacetylase HDAC7 is located in the mitochondrial inter-membrane space of prostate epithelial cells (Bakin and Jung, 2004). However, presence of HDAC7 in the lumen of mitochondrial matrix has been poorly described and additional investigations are required.

SIRT3 is the only mitochondrial lysine deacetylase and appears to be a primary regulator of mitochondrial protein acetylation (Lombard et al., 2007). SIRT3 is a widely expressed sirtuin isoform with increased presence in mitochondria-rich tissues such as liver, heart and skeletal muscle (Onyango et al., 2002). Expression level is highly regulated by changing nutrient availability, especially by fasting, high-fat diet and CR

(Hirschey et al., 2010; Jing et al., 2011; Schwer et al., 2009). SIRT3 is implicated in a variety of diseases primarily in obesity and metabolic syndrome (Hirschey et al., 2011). SIRT3 mediates insulin signaling in skeletal muscle (Jing et al., 2011) and regulates mouse pancreatic  $\beta$ -cell function (Caton et al., 2013) demonstrating its crucial role in diabetes mellitus type 2. Strong evidence has been provided which describes involvement of SIRT3 in cardiovascular, heart diseases (Grillon et al., 2012; Sack, 2011) and cancer (Liu et al., 2014). Until now, a variety of SIRT3 protein targets are described. Some of them are listed in Table 2. SIRT3 is responsible for regulation of wide range of mitochondrial proteins especially enzymes related to energy metabolism.

**Table 2.** List of SIRT3 protein substrates.

SIRT3 Protein Substrate	Cellular Function	Reference
Acetyl-CoA Synthetase 2 (ACS2)	Acetate Metabolism	(Hallows et al., 2006; Schwer et al., 2006)
Glutamate Dehydrogenase (GDH)	Amino Acids Catabolism, TCA Cycle	(Schlicker et al., 2008)
NADH Dehydrogenase 1 $\alpha$ Subcomplex 9 (NDUFA9)	OXPHOS	(Ahn et al., 2008)
3-Hydroxy-3-Methylglutaryl CoA Synthase 2 (HMGCS2)	Ketone Body Formation	(Shimazu et al., 2010)
Long-Chain Acyl CoA Dehydrogenase (LCAD)	Fatty Acid Oxydation	(Hirschey et al., 2010)
Isocitrate Dehydrogenase 2 (IDH2)	TCA Cycle	(Someya et al., 2010)
Superoxide Dismutase 2 (MnSOD)	ROS	(Qiu et al., 2010; Tao et al., 2010)
Ornithine Transcarbamoylase (OTC)	Urea Cycle	(Hallows et al., 2011)
Cyclophilin D	Mitochondrial Permeability Transition Pore	(Hafner et al., 2010; Shulga et al., 2010)
Succinate Dehydrogenase Complex, Subunit A (SdhA)	OXPHOS, TCA Cycle	(Finley et al., 2011b)
Aldehyde Dehydrogenase 2 (ADH2)	Ethanol Metabolism	(Xue et al., 2012)

SIRT4 displays a very weak lysine deacetylase activity. Recently, the first deacetylation substrate was described. SIRT4 deacetylates malonyl CoA decarboxylase at lysine K471 and represses its activity, which in turn leads to promote lipogenesis (Laurent et al., 2013). Most prominent action of SIRT4 is ADP-ribosylation. SIRT4 uses NAD<sup>+</sup> to ADP-ribosylate and downregulate GDH activity resulting in decreased insulin secretion in pancreatic  $\beta$ -cells in response to increased level of amino acids (Haigis et al., 2006). Insulin-producing  $\beta$ -cells show increased insulin production in response to the

glucose level when SIRT4 is depleted (Ahuja et al., 2007). Mathias et al. recently discovered a SIRT4 delipoylase and debiotinylase activity (Mathias et al., 2014). The authors clearly demonstrated that SIRT4 physically interacts with pyruvate dehydrogenase complex and removes lipoamide cofactor from the E2 component dihydrolipoyllysine acetyltransferase (DLAT), decreasing its activity *in vivo* in mouse liver. SIRT4 represent a tumor-suppressor protein which connects mitochondrial glutamine metabolism with carcinogenesis (Zhu et al., 2014). These findings strongly confirm SIRT4 implication in key mitochondrial metabolic pathways. Taking together, almost negligible SIRT4 deacetylase activity lead to conclusion that the enzyme is highly specific for the acyl residues other than acetyl which are still remain to be discovered or it may require additional ligands and/or cofactors for its successful action as lysine deacetylase.

SIRT5 is a known sirtuin enzyme primarily localized in mitochondria (Pirinen et al., 2012; Zhong and Mostoslavsky, 2011). SIRT5 is found in the mitochondrial intermembrane space (IMS) (Schlicker et al., 2008) and also in the cytoplasm (Matsushita et al., 2011; Park et al., 2013). It shows weak but not insignificant deacetylase activity. SIRT5 has a role in the regulation of ammonia metabolism by deacetylating and activating CPS1, the first enzyme in the urea cycle (Nakagawa et al., 2009). SIRT5 transgenic mice show significant decrease in CPS1 acetylation, with upregulation of urea production in the liver hepatocytes (Ogura et al., 2010). SIRT5 knockout mice show no significant abnormalities in the metabolism under the basal conditions (Yu et al., 2013), but during high protein diet hyperammonemia was observed (Nakagawa et al., 2009). The newest published data described SIRT5 as lysine desuccinylase, demalonylase and deglutarylase (Du et al., 2011; Roessler et al., 2014; Tan et al., 2014; Weinert et al., 2013).

The three mitochondrial sirtuin isoforms seem to be highly specific for different acyl moieties attached to the side chains of lysines of mitochondrial proteins. Together, mitochondrial sirtuins are able to deal with the most demanding challenges which come with diversity of acyl modifications within the mitochondrial proteome. Very recently, it was shown that SIRT3, SIRT4 and SIRT5 successfully remove even long acyl-chain moieties from the lysine residues including myristoyl-, dodecanoyl-, decanoyl-, and octanoyl-moieties, widening the spectrum of its activity (Feldman et al., 2013).

## Mitochondrial lysine acetyltransferase

Conventional lysine acetyltransferase localized in the mitochondrial matrix remain unknown until now, making the phenomenon of mitochondrial protein acetylation even more complicated. Only few attempts were made to identify a mitochondrial protein which is able to transfer the acetyl group from Ac-CoA to lysine residues. GCN5L1 (General Control of Amino Acid synthesis 5 - like 1) is the first acetyltransferase proposed to have significant effects on protein lysine acetylation in mitochondria (Scott et al., 2012). It is clearly demonstrated that the enzyme is localized in the mitochondrial matrix and in the mitochondrial inter-membrane space. Authors further showed that knockdown of GCN5L1 results in disruption of mitochondrial protein acetylation homeostasis, but they did not provide evidences whether such change in acetylation state results from direct action of GCN5L1 enzyme. Additionally, it was shown that histone H3 is successfully acetylated by GCN5L1-enriched mitochondrial fraction. Here it is not clear why mitochondrial enriched fraction is used instead of recombinant GCN5L1 protein. Evidences in the form of peptide substrates *in vitro* are absent and kinetic parameters were not determined. All together, it is clear that there is reasonable suspicion about the role of GCN5L1 protein in the global mitochondrial protein acetylation. However, additional investigation will be required.

Recently, it has been shown that the known mitochondrial metabolic enzyme ACAT1 (acetyl-CoA acetyltransferase 1) successfully operates as lysine acetyltransferase (Fan et al., 2014). ACAT1 is a well described enzyme involved in ketone bodies production during low glucose diet (Haapalainen et al., 2007; Kano et al., 1991). Here, Fan et al. demonstrated that ACAT1 successfully acetylates and inhibits PDHA1 at lysine K321 and PDP1 at lysine K202. PDHA1 is a subunit of the pyruvate dehydrogenase complex (PDC) highly regulated (inhibited) by phosphorylation at S232, S293 and S300, whereas PDP1 represents a specific phosphatase which dephosphorylates PDHA1 and restores its activity (Roche et al., 2001). The acetylation reaction was confirmed *in vitro* using recombinant ACAT1, PDHA1 and PDP1 protein. Nevertheless, information about peptide substrates and kinetic parameters were not provided.

## Proposed mechanisms of mitochondrial protein acetylation

Mitochondrial protein acetylation combines two extreme opposites. On the one hand mitochondria are cellular compartments with highest abundance of acetylated proteins and on the other hand lacking enzymes responsible for such modifications. A relative

large diversity between acetyltransferase sequences makes identification of novel mitochondrial acetyltransferases even more challenging (Yuan and Marmorstein, 2013). Considering already known facts, there are few proposed ways to explain how mitochondrial proteins undergo acetylation, summarized in Figure 2 (Ghanta et al., 2013). Based on the current knowledge, each of the proposed mechanisms appears failed in attempt to fully explain mitochondrial protein acetylation. The first proposed mechanism is not able to explain the obvious dynamics in mitochondrial protein acetylation in response to nutrient availability (Zhao et al., 2010). We cannot completely exclude the second and the third mechanism. The second mechanism is currently unlikely. In the human genome there are 71 acetyltransferase encoded genes and many of them are well characterized (Fan et al., 2014). There is some evidence about the existence of mitochondrially localized proteins which even does not contain mitochondrial targeting sequence at all (Joiner et al., 2012; Sastri et al., 2013). The third mechanism could be promising in particular because of the fact that new enzymes as potential candidates for the mitochondrial acetyltransferases have been discovered recently. GCN5L1 has been the first enzyme proposed to be responsible for the mitochondrial protein acetylation (Scott et al., 2012).

Knockdown of GCN5L1 results in hypoacetylation of mitochondrial proteins indeed, but is such phenotype result of direct action of GCN5L1 enzyme still remains questionable. Moreover, the fact that this enzyme is not found in yeast reduced its evolutionary importance as a global and widespread protein acetyltransferase. It is more prominent that an already known metabolic enzyme could possess the ability to transfer an acetyl group from the Ac-CoA to the lysine residue of the targeted protein. ACAT1 was recently discovered to be an efficient lysine acetyltransferase harbored in the mitochondrial matrix (Fan et al., 2014). In addition to its already known and well described role in the ketone bodies synthesis ACAT1 acetylates the PDHA1 subunit of the large PDH complex and PDP1 phosphatase; both are mitochondrial enzymes.

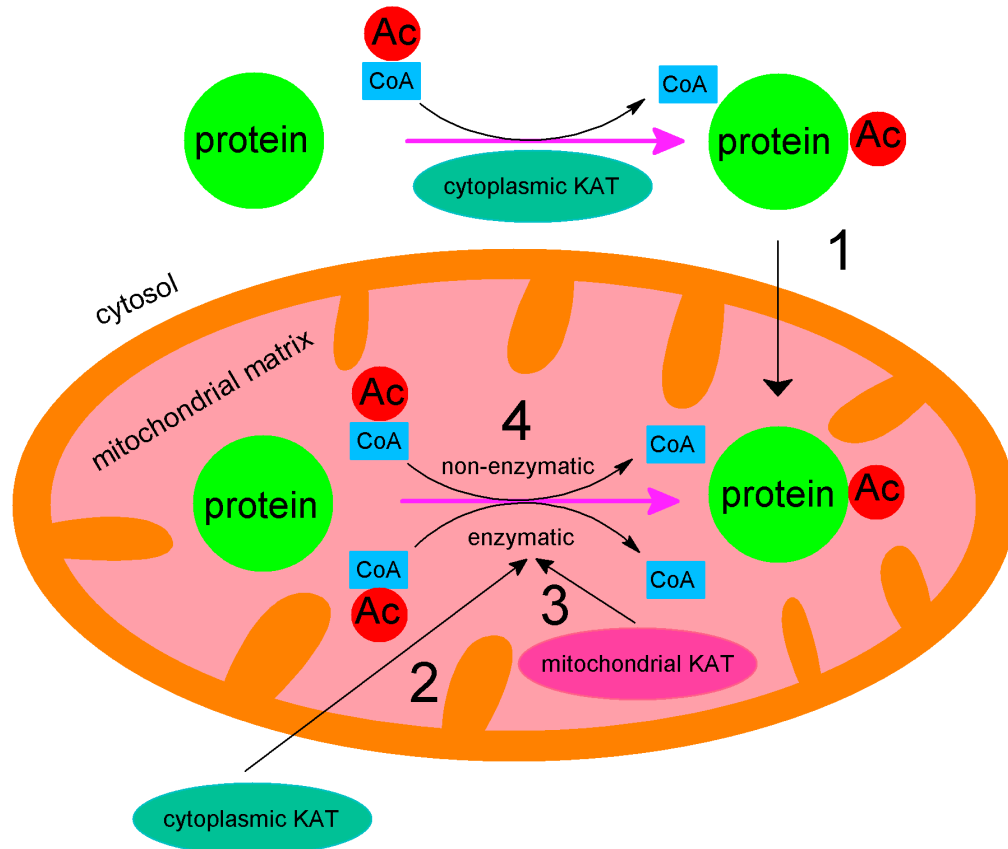


**Figure 2.** Proposed mechanisms of mitochondrial protein acetylation. Mitochondrial proteins are acetylated in the cytoplasm by known nucleocytoplasmic acetyltransferases prior to its translocation to mitochondria or mitochondrial proteins might shuttle between mitochondrial matrix and cytoplasm where they can be acetylated (1); mitochondrial proteins are acetylated by known nucleocytoplasmic acetyltransferase which are able to enter in the mitochondrial matrix (2); mitochondrial proteins are acetylated by mitochondrial residential protein which have lysine acetyltransferase function (3); mitochondrial proteins are acetylated non-enzymatically (4).

The fourth and the most prominent mechanism is that mitochondrial proteins are acetylated chemically without the need of any enzyme. The idea of chemical acetylation of proteins is 60 years old now. Ac-CoA represents a highly reactive compound with the capability to acetylate proteins *in vitro* without presence of enzymes or other catalytic compounds (Baddiley et al., 1952). Almost twenty years after such findings Paik et al. have demonstrated that Ac-CoA acetylates histones non-enzymatically (Paik et al., 1970) and that the introduced acetyl-group is most likely located at the N-ε-amino groups of lysine residues. Furthermore, non-enzymatic mechanisms for other intracellular lysine modifications by endogenous metabolites, such as glycation and carbamylation are already recognized (Verbrugge et al., 2015; Wautier and Schmidt, 2004). Proteine lysine residues can also react with glycolytic intermediate 1,3-bisphosphoglycerate to form 3-

phosphoglyceryl lysine derivatives (Moellering and Cravatt, 2013). Conditions of the mitochondrial matrix (pH value, availability of Ac-CoA) represent a favoring contribution to the non-enzymatic mechanism of mitochondrial protein acetylation.

At the beginning of this study, very little was known about the nature of the non-enzymatic protein acetylation. Several other groups in parallel investigated such phenomena and their published results also strongly support the idea which explains protein acetylation in mitochondria as product of non-enzymatic reaction driven by basic pH value and relatively high Ac-CoA concentration (Baeza et al., 2015; Kuo and Andrews, 2013; Wagner and Payne, 2013).

## Physiological conditions of mitochondrial matrix

Mitochondria are cellular organelles and represent a place where nutrients are degraded for the purpose of energy production. The mitochondrion consists of two membranes with an intermembrane space inbetween (Figure 3). Area of the inner membrane is about five times larger than outer, organized in a cristae, a specific structure which enlarges innermembrane area enhancing its ability to produce ATP. The inner membrane successfully maintains the small molecule transport. In particular, water molecules are controlled through special transporters so-called aquaporines, ensuring osmotic balance between mitochondrion and cytosol. The inner mitochondrial membrane enclosed space is filled with mitochondrial matrix.

Mitochondrial matrix is a dense, viscous, gel-like fluid containing enzymes and small molecules involved in different metabolic processes. About 65 % of all mitochondrial proteins are located in the matrix, as well as mitochondrial DNA and mitochondrial ribosomes. Majority of the proteins are nuclearly encoded and posttranslatory translocated to the mitochondrion.

Several physiological differences between mitochondria and cytoplasm are very important and might point out that mitochondrial protein acetylation could occur non-enzymatically. One of the most important differences is the mitochondrial matrix pH value and Ac-CoA concentration.



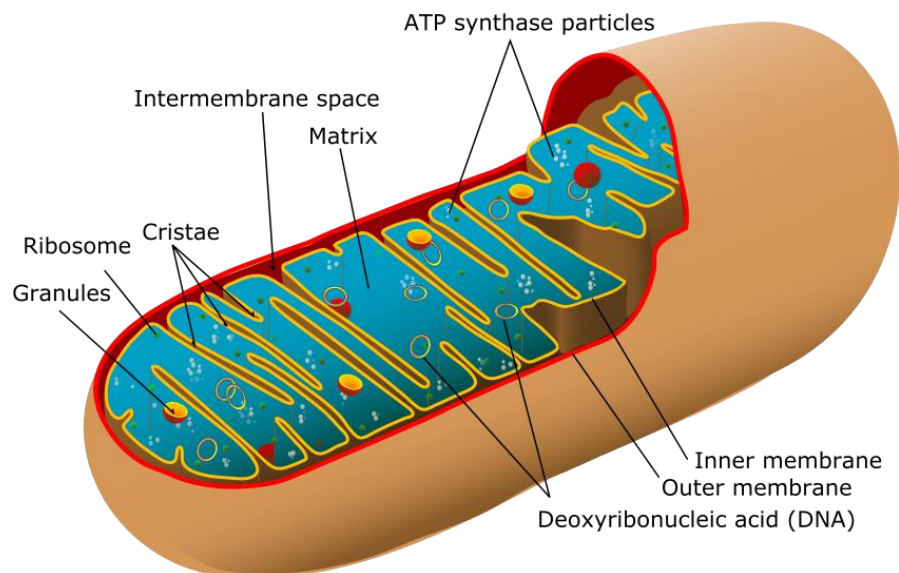


**Figure 3.** Schematic illustration of animal mitochondrion. Figure is free available at [https://commons.wikimedia.org/wiki/File:Animal\\_mitochondrion\\_diagram\\_en.svg](https://commons.wikimedia.org/wiki/File:Animal_mitochondrion_diagram_en.svg)

It was noted earlier that the  $\epsilon$ -amino group of lysine residues is highly ionizable with a  $pK_a$  value of 10.5. At physiological pH, usually referred to 7.4 (Zager et al., 1993), the amino group is in its protonated form and thus not available for acetylation by Ac-CoA. With basic pH values concentration of deprotonated amino groups increase leading to chemical acetylation (Figure 4).

The mitochondrial matrix pH value was found to be slightly basic in comparison to the pH value of the cytoplasm and can rise up to 8.2 (Llopis et al., 1998; Santo-Domingo and Demarex, 2012; Shen et al., 2013). In eukaryotic mitochondria energy-rich ATP can be produced using the metabolites generated in the TCA cycle, fatty acid oxidation or amino acid oxidation.

When nutrients are available in a large quantity, their degradation raises the mitochondrial pool of Ac-CoA up to a concentration in the millimolar range (Garland et al., 1965; Hansford and Johnson, 1975). Ac-CoA is mainly utilized for energy production through its oxidation in the TCA cycle. During the running of the TCA cycle, ETC pumps protons in the mitochondrial intermembrane space to ensure proton gradient (protonmotive force) which is necessary for operation of ATP synthase and production of ATP.

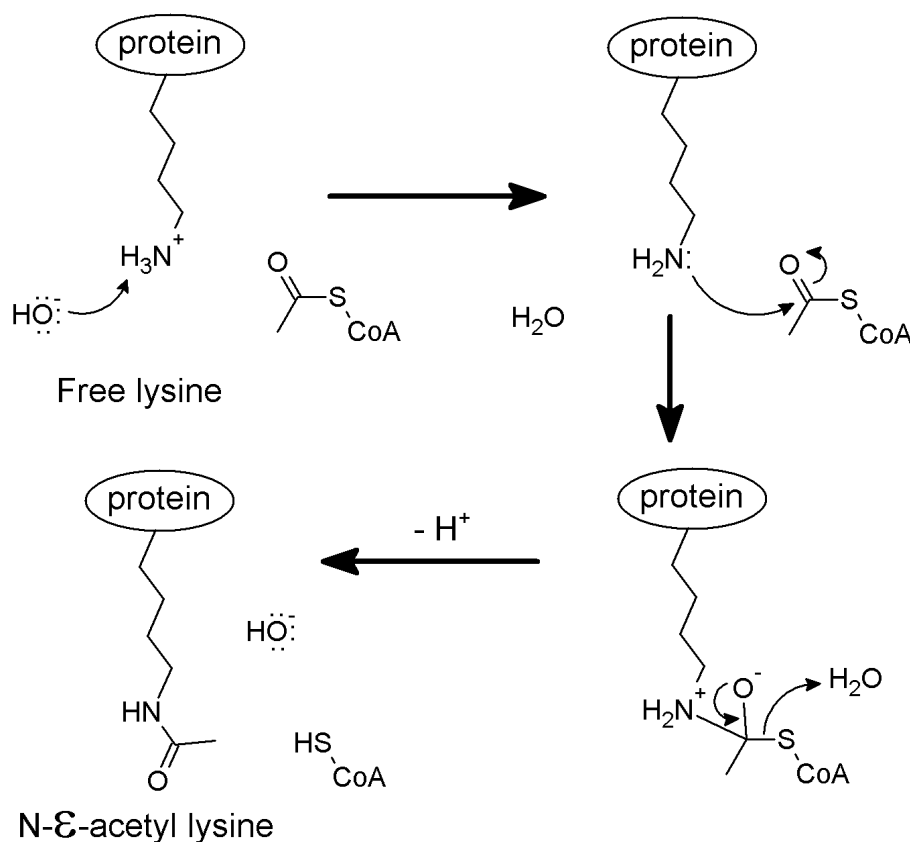


**Figure 4.** Chemical lysine acetylation mechanism - schematic illustration. Proposed mechanism is based on the GCN5 acetyltransferase mechanism (Roth et al., 2001; Yuan and Marmorstein, 2013), which used general base catalysis to deprotonate  $\epsilon$ -amino group of the lysine in the initial phase of the reaction. In the enzyme-free reaction, at the basic pH value,  $\text{OH}^-$  group acts as a base and deprotonates lysine amino group which is now able to attack the thioester carbonyl moiety of the Ac-CoA. After rearrangement free CoA is released thereby forming the acetylated lysine.

During such process mitochondrial intermembrane space is maximally acidified remaining mitochondrial matrix consequentially alkalized (Figure 5). Such conditions which are found especially in the mitochondrial matrix (high concentration of Ac-CoA and high pH values) represent an ideal environment for the non-enzymatic protein acetylation.

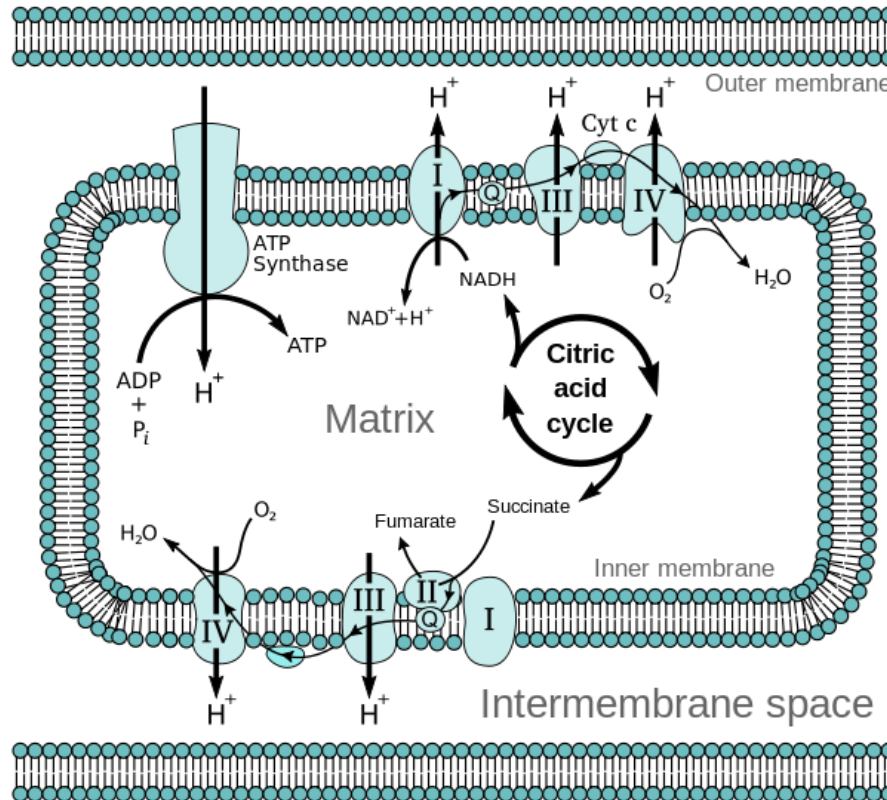


**Figure 5.** Schematic illustration of the energy production metabolism in mitochondria. Figure is free available at [https://en.wikipedia.org/wiki/File:Mitochondrial\\_electron\\_transport\\_chain%E2%80%944.svg](https://en.wikipedia.org/wiki/File:Mitochondrial_electron_transport_chain%E2%80%944.svg)

## Coenzyme A and its acyl-thioester derivatives

Coenzyme A (CoA) is a cosubstrate used by many enzymes involved in acyl-group transfer reactions. Around 4 % of proteins in the human genome are using CoA as a cosubstrate in different metabolic reactions (Daugherty et al., 2002). It was discovered seventy years ago by Fritz Lipmann (Lipmann, 1945) for which he received the Nobel prize in medicine 1953. In the beginning of the fifties of the last century, shortly after its discovery the structure of CoA was successfully determined (Baddiley, 1955; Baddiley et al., 1953). CoA shows a relatively complex structure, but its functionality is limited mostly to a reactive thiol group (Figure 6).

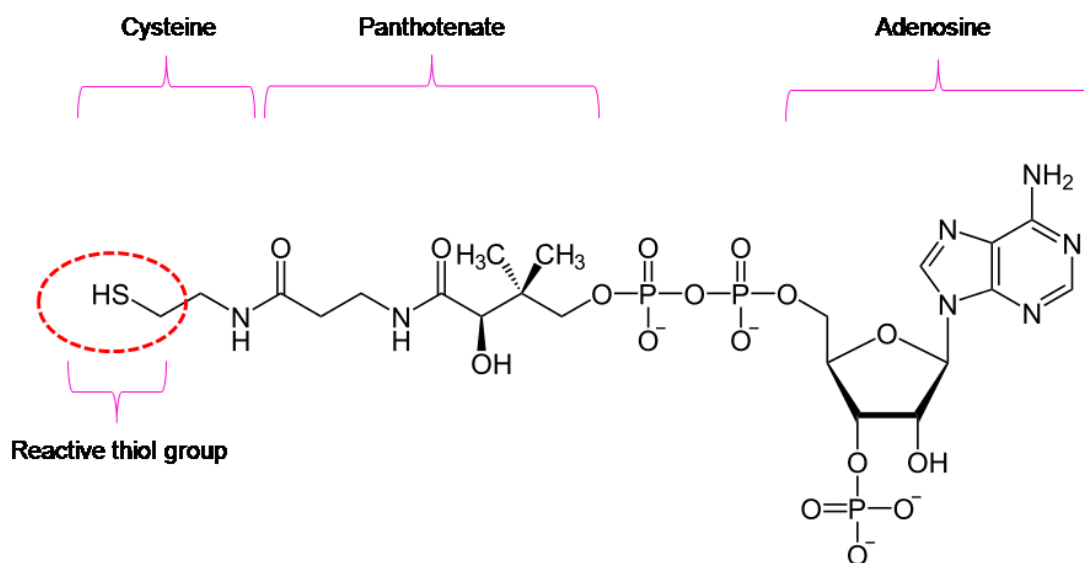


**Figure 6.** The structure of CoA. CoA is synthesized in all living organisms over a series of reactions shown in Figure 7. The complex synthetic pathway was first clarified in bacteria (Brown, 1959), and later in mammals (Abiko, 1967) and other microorganisms (Nishimura et al., 1983; Shimizu et al., 1973).

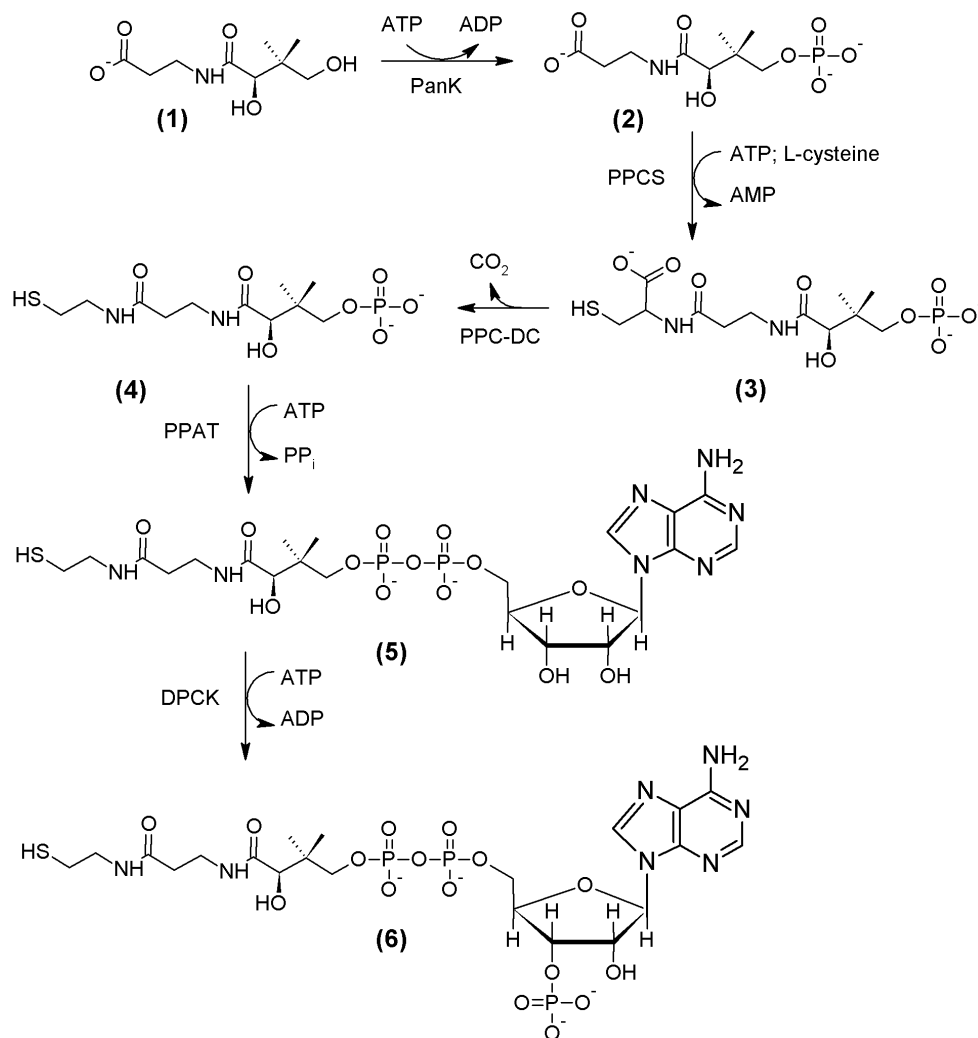


**Figure 7.** The biosynthesis of CoA. The synthetic pathway starts from pantoic acid **(1)** (vitamin B5) which is phosphorylated by the enzyme pantothenate kinase (PanK) yielding 4'-phosphopantotenate **(2)**. In the next step, reaction of condensation of 4'-phosphopantotenate with L-cysteine catalyzed by the enzyme phosphopantotenoylecysteine synthetase (PPCS) gives as a product 4'-phospho-N-pantotenoylecysteine **(3)**, which further undergoes decarboxylation by phosphopantotenoylecysteine decarboxylase (PPC-DC) forming 4'-phosphopantetheine **(4)**. Dephospho-CoA **(5)** is synthesized by coupling  $\alpha$ -phosphate of ATP to 4'-phosphopantetheine by the enzyme 4'-phosphopantetheine adenylyl transferase (PPAT). Finally, 3'-hydroxyl group of dephospho-CoA is phosphorylated by dephospho-CoA kinase (DPCK) and CoA **(6)** is released.

## Acetyl-CoA

Ac-CoA is the most common acyl-CoA thioester present in all living organisms. It occupies a central position in mitochondrial energy metabolism. The end product of glycolysis, pyruvate, enters the TCA cycle in the form of Ac-CoA (Theodoulou et al.,

2014). Additionally,  $\beta$ -oxidation of fatty acids as well as catabolism of amino acids represent remarkable sources of mitochondrial Ac-CoA (Houten and Wanders, 2010; Shi and Tu, 2015). Moreover, Ac-CoA can be directly synthesized through the action of acetyl-CoA synthetase (Schwer et al., 2006) (Figure 8). Beyond its role in energy metabolism Ac-CoA is involved in a variety of anabolic processes including synthesis of fatty acids, cholesterol, ketone bodies or the neurotransmitter acetylcholine (Espenshade and Hughes, 2007; Fukao et al., 2004; Taylor and Brown, 1999; Tehlivets et al., 2007). It has been recognized as an allosteric regulator of enzyme activity (Jitrapakdee et al., 2008). Ac-CoA serves as acetyl-group donor in the reaction utilized by KATs enzymes acetylating a variety of histone and non-histone proteins (Choudhary et al., 2014). Thanks to its chemical reactivity it has been proposed to have a high potential to acetylate proteins through a non-enzymatic mechanism (Wagner and Payne, 2013).

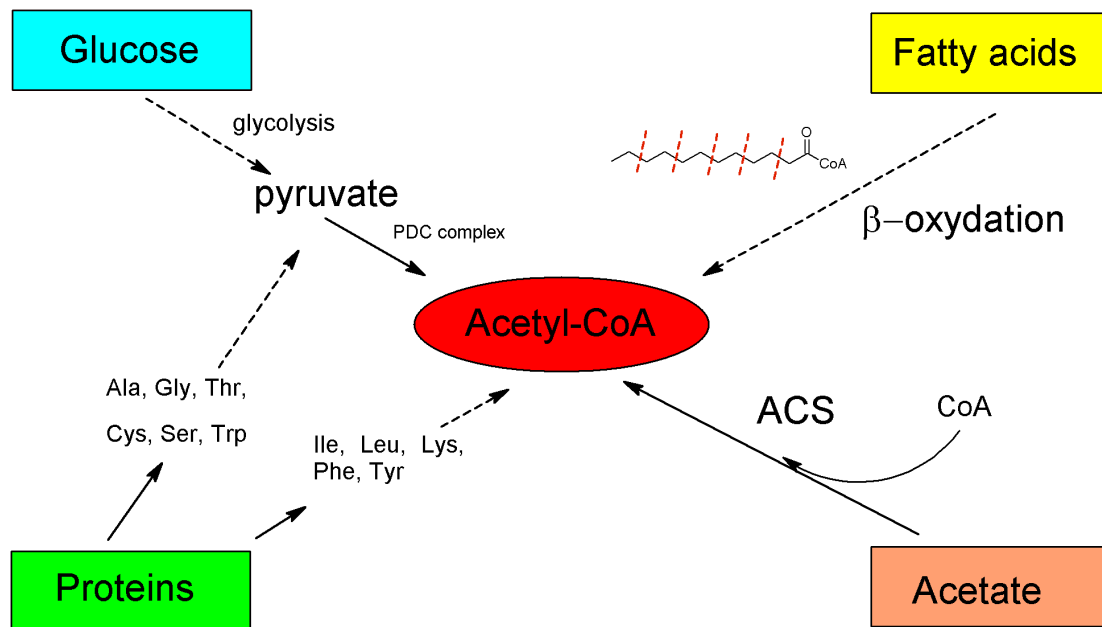


**Figure 8.** Illustration of possible sources of Ac-CoA in the living organisms. Ac-CoA is mainly derived from glucose, but also from fatty acid and amino acid catabolism. Glucose is transformed via the glycolytic pathway into two pyruvate, which are then translocated into the mitochondrion and transformed to Ac-CoA through pyruvate decarboxylase complex (PDC). After lypolysis cytosolic long chain fatty acids are recruited to the mitochondrial matrix for  $\beta$ -oxidation, where the long chains undergo a series of shortenings until Ac-CoA is produced as the end product. Amino acids, especially Ala, Gly, Thr, Cys, Ser and Trp can be degraded to pyruvate, where Ile, Leu, Trp, Lys, Phe and Tyr can be degraded to Ac-CoA. Additionally, less abundant but not less important, is the direct synthesis of Ac-CoA by acetyl-CoA synthetase (ACS) which uses free CoA and acetate to form Ac-CoA.

Acetylation of CoA gives a highly reactive compound (Figure 9). There are some enzymes which can catalyse the formation of Ac-CoA, including Ac-CoA synthetase, phosphotransacetylase, ATP citrate lyase and thiolase (Mishra and Drueckhammer, 2000). Enzymatic reaction of Ac-CoA mainly involves reaction of acetyl-group transfer to a variety of molecules including transfer to N-ε-amino group of lysine residues.

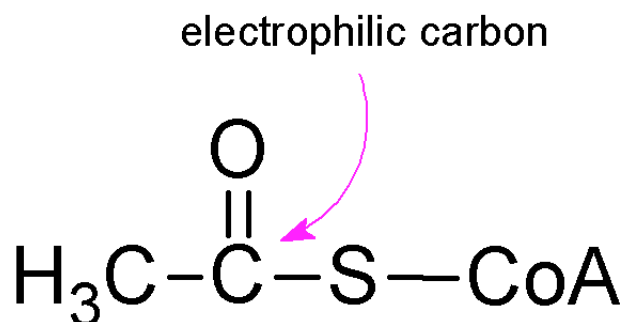


**Figure 9.** Reactivity of Ac-CoA. Partially positively charged carbon in the carbonyl group is electrophilic and thus reactive making the acetyl-group a good leaving group. A thioester bond is characterized by relatively high negative standard free energy of hydrolysis ( $\Delta G^0 = -31.8$  kJ/mol) (Thauer et al., 1977).

Ac-CoA is a widespread metabolite present in different cellular compartments. Although Ac-CoA is ubiquitously distributed within the cell it is a membrane impermeable molecule and thus its mitochondrial pool is strictly regulated. When the mitochondrial concentration of Ac-CoA is increased significantly during the nutrition overloading TCA cycle is running with its full capacity thus the rest of the Ac-CoA can be exported to the cytosol and used as a precursor for fatty acid synthesis. Export of Ac-CoA into the cytosol occurs mainly indirect in form of citrate (Figure 10). Such mechanism keeps mitochondrial concentration of Ac-CoA regulated. It has been observed that mitochondrial concentration of Ac-CoA varies and depends on the metabolic state of the cell (Garland et al., 1965). Mitochondria as the main place for production of Ac-CoA could show concentrations of Ac-CoA in the millimolar range, which is up to tenfold higher in comparison to its cytosolic fraction (Santo-Domingo and Demarex, 2012). As key determinants for protein acetylation the mitochondrial Ac-CoA concentration together with pH value remains a crucial factor of non-enzymatic protein acetylation.

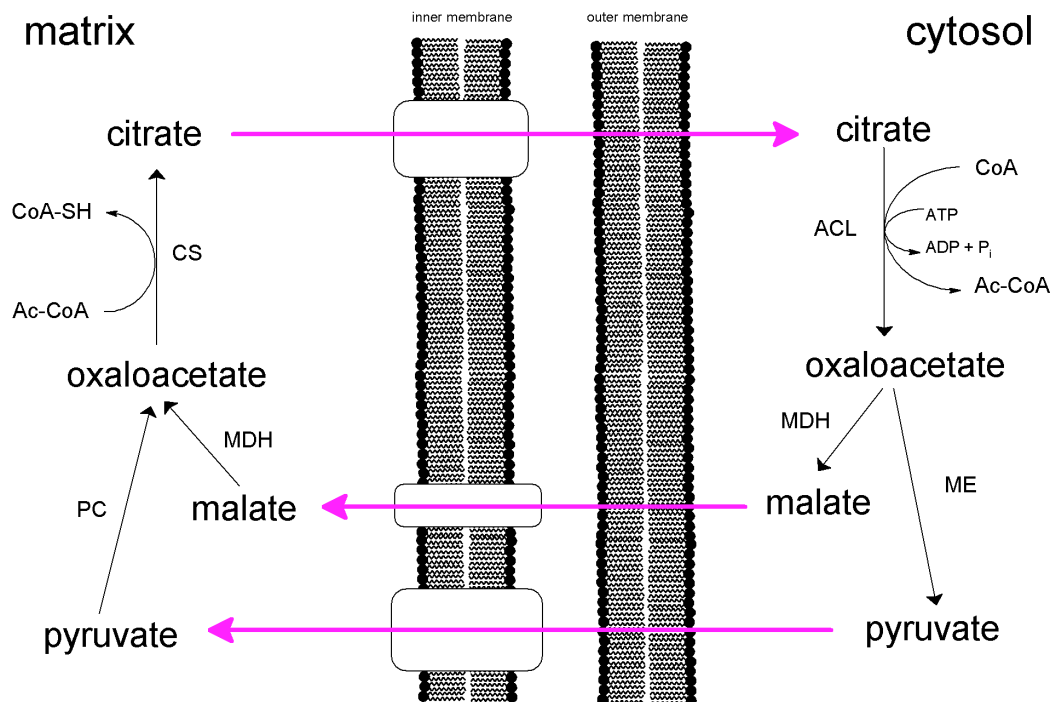


**Figure 10.** Ac-CoA mitochondrial – cytosolic shuttle. Mitochondrial citrate synthase (CS) catalyses reaction of Ac-CoA and oxaloacetate to form citrate as a component of the TCA cycle. Citrate can be translocated to the cytosol through the citrate transporter. In the cytosol, citrate is cleaved by ATP citrate lyase (ACL) releasing Ac-CoA and oxaloacetate. Oxaloacetate is further converted to malate by cytosolic malate dehydrogenase (MDH) and malate further transformed to pyruvate by malic enzyme (ME). Malate and pyruvate are translocated back into the mitochondrial matrix through specific transporters where they could reenter the cycle again. PC – pyruvate carboxylase.

## Acyl-CoA thioesters and PTMs of proteins in mitochondria

Based on sirtuins activity it is obvious that mitochondrial protein posttranslational modifications considerably extend acetylation (Figure 11). Indeed, lysine succinylation and malonylation was discovered as an abundant PTM in mitochondria (Peng et al., 2011; Zhang et al., 2011). Moreover, Tan et al. described lysine glutarylation as a new PTM regulated by mitochondrial SIRT5 (Tan et al., 2014). Short-chain lysine acylation such as lysine propionylation and butyrylation are PTMs initially described on the histones (Chen et al., 2007; Cheng et al., 2009). Later it was demonstrated that lysine butyrylation and propionylation are significantly increased PTMs after knockdown of mitochondrial enzymes like short-chain specific acyl-CoA dehydrogenase (SCAD) and propionyl-CoA carboxylase (PCC), primary as a consequence of resulting increase in concentration of corresponding butyryl- and Prop-CoA thioesters (Pougovkina et al., 2014). Interestingly, it



appears that SIRT6 and other mitochondrial sirtuins are able to remove long-chain acyl moieties from lysine residues (Feldman et al., 2013). These findings open the possibility that such modifications indeed exist as PTMs on the proteins. Except myristoylation, other long-chain acyl PTMs are not discovered so far *in vivo* (Stevenson et al., 1992, 1993).

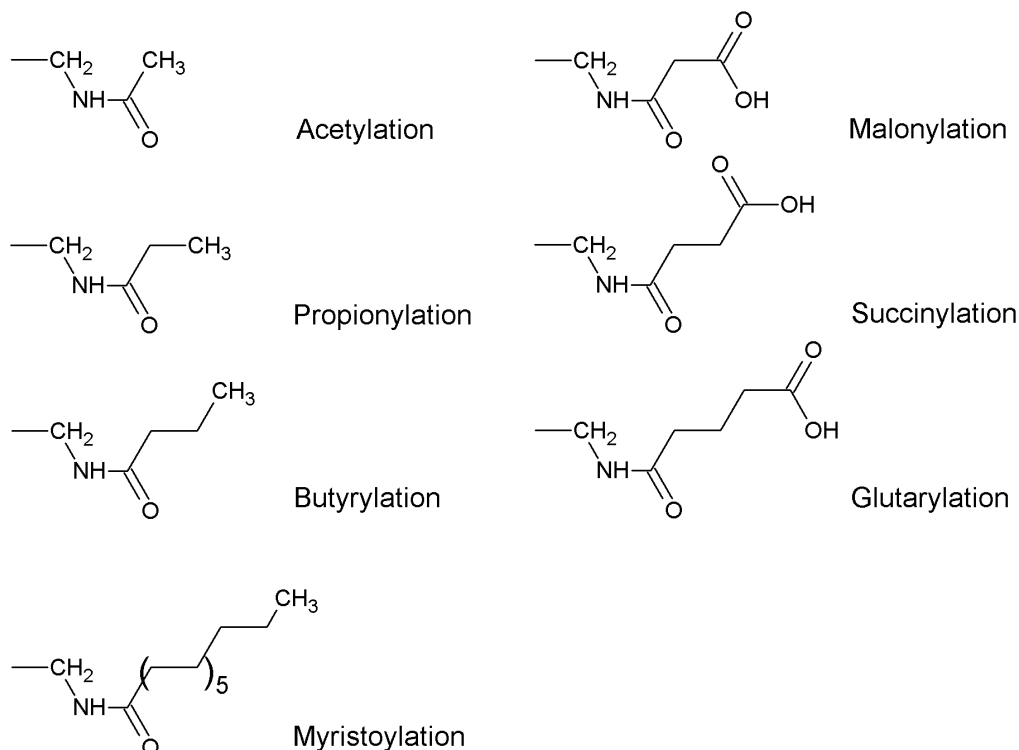


**Figure 11.** Known acyl-lysine posttranslational modifications found in mitochondrial proteome.

It is assumed that all above lysine PTMs are derived from corresponding acyl-CoA thioesters, but enzymes which are responsible for such modifications are still remain elusive. Very limited evidence is provided demonstrating that classical lysine acetyltransferases, such as p300, are able to utilize CoA thioesters different from Ac-CoA, such as But- and Prop-CoA to acylate histone and non-histone proteins (Chen et al., 2007; Cheng et al., 2009). Additionally, Tan et al. demonstrated that p300 efficiently succinylates and glutarylates peptides derived from histone H4 using Succ-CoA and Glut-CoA, respectively (Tan et al., 2014). Recently it was proposed that well known metabolic enzyme  $\alpha$ -ketoglutarate dehydrogenase complex is involved in the succinylation of mitochondrial proteins (Gibson et al., 2015). Nevertheless, it seems more than likely that p300 and other conventional lysine acetyltransferase are not mitochondrial residential

proteins. Therefore, it is increasingly believed that most of mitochondrial acyl-lysine modifications are a result of non-enzymatic action of corresponding acyl-CoA thioesters. Such hypothesis is strongly supported by findings that most of the identified protein acylations overlap with each other in mitochondrial proteome (Weinert et al., 2013). It is already known that mitochondrial content of Ac-CoA reach millimolar level and that Succ-CoA show approximately ten times lower mitochondrial concentration in comparison to its acetyl thioester (Garland et al., 1965; Hansford and Johnson, 1975; Santo-Domingo and Demarex, 2012). Because of their similarities, determination of intracellular acyl-CoAs content as key factors for protein acylation remains challenging for decades. Recently it appeared that Succ-CoA is a relatively abundant intracellular CoA thioester, in particular in the tissues with high mitochondrial content such as heart and muscle (Sadhukhan et al., 2016). Ac-CoA is most abundant in hepatic tissue, which also shows remarkable content of propionyl- and But-CoA.

## Aim of the thesis

Aim of this work was to understand how proteins undergo posttranslational acetylation in the mitochondria. Mitochondrial proteins show highest level of acetylation in comparison to other cellular compartments but enzymes responsible for the transfer of acetyl groups from Ac-CoA to the lysine residues remain unknown. Few enzymes such as GCN5L1 and ACAT1 were proposed as candidates for mitochondrial lysine acetyltransferases, but their role in such phenomenon is questionable. It was already speculated that Ac-CoA, an energy rich and highly reactive thioester, is able to modify proteins spontaneously *in vitro*. Absence of KATs, together with unique physiological environment in the mitochondrial matrix (high Ac-CoA concentration and basic pH value) lead to the hypothesis that acetylation of mitochondrial proteins occurs spontaneously independent of any enzyme activity.

This thesis was designed in two directions with a similar goal: finding reliable explanations for enriched protein acetylation in mitochondria. In the first part of the work the goal was to provide significant evidences supporting the hypothesis that Ac-CoA is able to modify peptides and proteins *in vitro* under conditions found in mitochondrial matrix. Initially, development of an assay allowing to follow non-enzymatic acetylation was required. In order to determine kinetic and thermodynamic parameters of the non-enzymatic reaction, it was necessary to design a short model peptide. Based on the gained data we focused to answer following questions. Is lysine acetylation by Ac-CoA a spontaneous process? What are additional factors involved in modulation of spontaneous acetylation of N- $\epsilon$ -amino group of the lysine residues by Ac-CoA? Taking in consideration that a variety of other reactive CoA thioesters are prevalent in the mitochondrial matrix their reactivity against model peptide was compared. Further investigations have led to protein substrates where we were faced with additional questions. What are the factors determining which lysine on the protein's surface is going to be acylated? Are sirtuins able to revert non-enzymatic lysine acylation? What are the key players in determination of acylation landscape of the mitochondrial proteome?

In parallel, we have developed a strategy in order to identify mitochondrial enzymes with a potential and so far unknown lysine acetyltransferase activity.

# Materials and Methods

All chemicals used in this study are supplied from Sigma-Aldrich unless stated otherwise.

## Chemical synthesis

### Synthesis of CPS1 peptide and CPS1 peptide derivatives

CPS1 peptide (Bz-GVLKEYGV-NH<sub>2</sub>) was synthesized using standard solid-phase peptide synthesis protocol. Fmoc protected amino acid derivatives (Merck, Darmstadt, Germany) were used. Rink amide MBHA resin (Iris Biotech, Marktredwitz, Germany) was first treated with DMF (Merck, Darmstadt, Germany) at RT for 10 min. The Fmoc protecting group was removed with 20 % (v/v) piperidine (Perkin Elmer, USA) in DMF for 15 min. After removal of the Fmoc protecting group resin was washed (5 × 5 min) with DMF. Prolongation of the peptide was done by treating the resin with 4 eq of the corresponding amino acid, 4 equivalent of PyBOP (Merck, Darmstadt, Germany) and 8 eq of DIPEA (Roth, Karlsruhe, Germany) in DMF at RT for 45 min. The N-terminus of the peptide was modified using 4 eq of benzoic acid anhydride and 8 eq of DIPEA in DMF at RT for 45 min. After washing with DCM (Promochem, Wesel, Germany) (5 × 3 min), peptide was cleaved from the resin and side-chains of amino acids were deprotected by TFA (Roth, Karlsruhe, Germany) (97% v/v) at room temperature for 150 min. Crude peptide solution was treated with cold diethylether. Precipitated peptide was filtered and dried. CPS1 peptide was purified by preparative HPLC and final product purity and identity was confirmed by analytical HPLC and MALDI-TOF-MS (Figure A1).

N-methyl-CPS1 peptide derivative has an additional methyl group at the lysine side chain nitrogen. It was synthesized and purified using the same procedure like CPS1 peptide but using Fmoc-Lys-(Me, Boc)-OH (Merck, Hohenbrunn, Germany) as a building block. Crude N-methyl-CPS1 peptide was purified by preparative HPLC and molecular mass of final product was confirmed by MALDI-TOF-MS (Figure A2).

### Synthesis of TNF $\alpha$ peptide derivatives

The peptide Ac-EALPKK(X)Y(NO<sub>2</sub>)GG-NH<sub>2</sub> (X=modification on lysine residue) was synthesized by standard manual solid-phase-peptide synthesis using Fmoc-protected amino acid derivatives. Rink amide MBHA resin was treated with DMF at RT for 10 min.

The Fmoc-protecting group was removed with 20 % piperidine in DMF (2 × 10 min). After washing with DMF (5 × 5 min) the resin was incubated with 4 eq of amino acid derivative, 4 eq HBTU (Biosolve, France) and 8 eq of DIPEA in DMF at RT (60 min). The N-terminus was modified with 4 eq acetic anhydride and 8 eq DIPEA in DCM (60 min). Nosyl-group was cleaved using 5 eq DBU (Merck) and 5 eq thiophenol in DMF (2 × 90 min). Afterwards the resin was washed with DMF.

Free lysine side chain was modified on-resin with HBTU (4 eq), DIPEA (8 eq) in DCM/DMF mixture (1:1) and 6-Fmoc-amino-caproic acid and N-Boc-anthranilic acid (Bachem) (TNF $\alpha$  peptide 3 and 4). For TNF $\alpha$  peptide 1 free lysine residue was acylated with 11-azidoundecanoic acid as described previously (Gubbens et al., 2009). The resin was treated with a solution of triphenylphosphine (5 eq) in THF/H<sub>2</sub>O (95:5) for several days (small portions of resin were taken for the test cleavage and MS-analysis). After washing N-Boc-anthranilic acid was coupled by the standard method. TNF $\alpha$  peptide 2 and 5 were prepared like TNF $\alpha$  peptide 1 with Dma (substrate 2) or 2-amino-5-nitrobenzoic acid (substrate 5) instead of N-Boc-anthranilic acid as described previously (Loving and Imperiali, 2008). Purity and identity of peptides was confirmed by analytical HPLC and MS (Figures A3, A4, A5, A6 and A7). Peptides 1, 2 and 5 were synthesized by Sabine Schuster and peptides 3 and 4 by Dr. Marat Meleshin.

## Synthesis and purification of acyl-CoA derivatives

Benz-CoA, But-CoA, Glut-CoA and Prop-CoA were synthesized with a modified procedure described previously (Mieyal et al., 1974). Reactions of CoA trilithium salt (Boehringer, Mannheim, Germany) with 3 eq of either benzoyl-chloride or butyryl-chloride or propionyl-chloride or glutaric-anhydride were carried out in aqueous solution at pH 7.0 – 8.0 (with periodic addition of 2N NaOH at 4°C). The reaction was monitored by analytical HPLC, and usually finished within 10–30 min. The pH value of the solution was adjusted to pH 3.0 by adding concentrated HCl, and the thioester product was purified by preparative HPLC. Linear gradient from 5 – 70 % of solvent B (ACN) in 60 min was used. Purity and identity of the compounds was confirmed by analytical HPLC and MALDI-TOF-MS (Figure A8, A9, A10 and A11).

## Synthesis and purification of acetyl-adenylate (Ac-AMP)

Ac-AMP was synthesized as described previously (Ramponi et al., 1975) with minor changes. 1 mmol of 5'-AMP was dissolved in 5 ml of 50 % (v/v) pyridine. 1 ml of NaOH

(1M) was added and reaction was kept on ice for 5 min. After that, 1 ml of acetic anhydride was added slowly with stirring. Reaction mixture was extracted three times with cold ether. Aqueous solution was precipitated with cold acetone. Precipitate was dissolved in a small amount of water and precipitated with cold acetone once again. The product was left to dry overnight.

## Preparative HPLC

For purification of peptides a Merck-Hitachi High Speed LC system, consisting of a L-6200 Intelligent pump, L-4200 UV-Vis detector (Darmstadt, Germany) and a Merck Hibar LiChrosorb RP-8 column (250-25 mm, 7  $\mu$ m) were used. For HPLC separation water (solvent A) and ACN (Promochem, Wesel, Germany) (solvent B) were used; both containing 0.1 % (v/v) TFA. A linear gradient from 20 – 50 % of solvent B in 60 min was used if not stated differently. Flow rate was 8 ml/min. Fractions were manually collected with detection at 260 nm. Residual ACN was removed using a rotary vacuum evaporator (Laborota 4000, Heidolph Instruments, Schwabach, Germany) and sample was frozen using liquid nitrogen and lyophilized using a freeze dryer (Christ Alpha 2-4, Germany).

## Analytical HPLC

To analyze the amount of acylated peptide in the samples a RP-HPLC system 1100 (Agilent Technologies, USA) consisting of a gradient pump (G1312A), an autosampler (G1329A), and a UV-detector (G1315A) was used with a Poroshell 120 EC-C18 column (3.0  $\times$  75 mm, Agilent Technologies). A linear gradient was applied with water (solvent A) and ACN (solvent B), both containing TFA (0.1%): 5 % B (0 min), 5 – 70 % B (0–7 min), 100 % B (7.0–7.6 min), 5 % B (7.6–10.0 min); flow rate was 0.6 ml / min. Benzoylated peptide derivatives were detected at 260 nm. Integrated peak areas were used for quantification. Calibration linearity, reproducibility, and stability of the peptide and acyl-CoA compounds were determined (Figures A12).

## Expression and purification of the enzymes

### Expression and purification of human SIRT2

Human SIRT2 was expressed and purified as described previously (Moniot et al., 2013). Briefly, a gene encoding human Sirt2 (34–356) was cloned into pGEX-4T3 (GE Healthcare, Little Chalfont, United Kingdom) using BamH1 and Xho1 restriction enzymes.

Sirt2 was expressed in *E. coli* at 25°C. After 24 h cells were harvested resuspended in 50 mM Tris-HCl buffer pH 8.0, 500 mM NaCl, and disrupted using a microfluidizer (Microfluidic, Newton, USA). Cell debris was removed by centrifugation and the SIRT2 was purified using GST-Buster QF glutathione resin (Amocol, Teltow, Germany). After intensive washing with 50 mM Tris-HCl pH 8.0, 500 mM NaCl, SIRT2 was eluted with 20 mM reduced glutathione. GST-tag was removed by incubation with thrombin (GE Healthcare) for 48 h at 4°C. After gel filtration on Sephadex-200 (GE healthcare) pure SIRT2 was concentrated and stored at -20°C. Enzyme was expressed and purified in the group of Prof. Dr. Clemens Steegborn, University of Bayreuth, Bayreuth, Germany.

### Expression and purification of human SIRT3 and SIRT5

Human SIRT3 (residues 118–399) and SIRT5 (residues 34–302) were expressed as described by Gertz et al. (Gertz et al., 2012). Briefly, the coding sequences were cloned into pVFT3S (Korean patent: 10-0690230) and pET151/d-TOPO (Invitrogen, Carlsbad, USA), respectively, and expressed in *E. coli* Rosetta2 (DE3) cells (Merck, Darmstadt, Germany), thereby resulting in proteins with an N-terminal His-tag (SIRT5) or His-thioredoxin tag (SIRT3). After induction of protein expression with isopropyl- $\beta$ -D-thiogalactopyranoside (IPTG) (0.5 mM), cells were grown overnight at 15°C (SIRT3) or 20°C (SIRT5) and disrupted with a Microfluidizer (Microfluidic, Newton, USA). After removal of cell debris by centrifugation (35000 g, 30 min), the supernatant was supplemented with imidazole (10 mM) and incubated with Talon resin (Clontech, Mountain View, USA) for 1 h at 4°C. The resin was washed with ten volumes of Tris-HCl (50 mM pH 7.8) containing NaCl (500 mM), and ten volumes of Tris-HCl (50 mM, pH 7.8) containing NaCl (200 mM) and imidazole (5 mM). Recombinant protein was eluted in Tris-HCl (50 mM, pH 7.8) containing NaCl (200 mM) and imidazole (250 mM), and then subjected to gel filtration on a Superose 12 column (GE Healthcare) in Tris-HCl (20 mM, pH 7.8) containing NaCl (150 mM). SIRT3 was expressed and purified in the group of Prof. Dr. Clemens Steegborn, University of Bayreuth, Bayreuth, Germany and SIRT5 by Theresa Nowak.

### Expression and purification of human SIRT4

To obtain the expression plasmid of human (His)<sub>6</sub>-SUMO-Sirt4 (29–314), the respective DNA fragment was PCR-amplified using gene-specific primers from the plasmid pET101-Sirt4, which carries the Sirt4 gene, and cloned into the Bsal, XbaI sites of

pE-SUMO yielding the plasmid pE-SUMO-Sirt4 (29–314). The protein was overexpressed in *E. coli* BL21 (DE3) cells at 18 °C. The purification of the protein was performed using affinity chromatography on Ni-NTA resin in 10 mM Tris-HCl, pH 7.5, 0.5 M NaCl. The matrix-bound (His)<sub>6</sub>-SUMO-Sirt4 (29–314) was eluted by imidazole in the buffer and further purified by gel filtration in 10 mM HEPES, pH 7.8, 150 mM KCl, 1.5 mM MgCl<sub>2</sub>, and stored at – 20 °C for use. Enzyme was expressed and purified in the group of Dr. Cordelia Schiene-Fischer.

## Expression and purification of human CypA

Human cyclophilin A (CypA) was expressed as described by Fanghänel et al. (Fanghänel and Fischer, 2002). Briefly, CypA (full length) was cloned into pQE70 (Qiagen) and expressed in *E. coli* M15 cells (Qiagen). The protein was consecutively purified by ion exchange chromatography on Fractogel EMD DEAE-650(M), Fractogel TSK AF-Blue, and Fractogel SO3-650(M) (Merck Millipore). Enzyme was expressed and purified in the group of Dr. Cordelia Schiene-Fischer.

## SDS-polyacrylamide gel electrophoresis (SDS-PAGE)

Protein samples were separated using SDS-PAGE as described previously (Laemmli, 1970) with minor modifications using SE250 electrophoresis system (Hoefer Scientific Instruments, San Francisco, USA). Stacking gel was 5 % acrylamide/bis-acrylamide (37.5:1) (Roth, Karlsruhe, Germany) and resolving gel was 12 % acrylamide/bis-acrylamide. APS (Roth, Karlsruhe, Germany) was used for initiating of gel polymerization. Protein samples were mixed with SDS-PAGE sample loading buffer (5X) and boiled in a thermo-mixer for 5 min at 95°C. Samples were loaded on the gel using a glass micropipette and separated at 60-100 mA (Electrophoresis power supply, EPS200, Pharmacia Biotech) using PAGE running buffer until the bromophenol blue line reached the bottom of the gel. Electrophoresis system was cooled using cold water. Gels were further processed to gel staining, MS or transferred to a nitrocellulose membrane. Gels were stained in Gel staining solution for 30 min and destained in Gel destaining solution until the background blue color disappeared with periodical replacement of destaining solution.



SDS-PAGE Stacking gel (5%)	5 % Acrylamide/bis-acrylamide (37.5:1) 126 mM Tris-HCl pH 6.8 0.1 % (w/v) SDS (AppliChem, Germany) 0.01 % (v/v) TEMED 0.1 % (w/v) APS
SDS-PAGE Resolving gel (12%)	12 % Acrylamide/bis-acrylamide (37.5:1) 375 mM Tris-HCl pH 8.8 0.1 % (w/v) SDS 0.01 % (v/v) TEMED 0.1 % (w/v) APS
SDS-PAGE Running buffer	25 mM Tris, 192 mM glycine (Merck), 0.1% (m/v) SDS, pH 8.3
SDS-PAGE sample loading buffer (5X)	250 mM Tris-HCl pH 6.8 10 % (m/v) SDS, 30 % (v/v) Glycerol (Merck) 5 % (v/v) $\beta$ -Mercaptoethanol (Roth), 0.02 % (w/v) Bromphenol blue (Serva)
Gel staining solution (water)	0.25 % (w/v) Coomassie brilliant blue G-250 (AppliChem, Germany) 30 % (v/v) Methanol 6 % Acetic acid
Gel destaining solution (water)	30 % (v/v) Methanol 10 % Acetic acid

## Native-PAGE

Native-PAGE uses a similar experimental procedure like classical SDS-PAGE. Samples were prepared in a sample loading buffer containing no SDS, no  $\beta$ -mercaptoethanol or heat treatment, under so called non-denaturing conditions. Gels and running buffer also contains no SDS. System temperature was kept below 20°C. Gels were stained using the standard Coomassie brilliant blue staining procedure.

## Dot-blot assay

The reaction mixture (2  $\mu$ l) was spotted onto a nitrocellulose membrane (Sartorius, Göttingen, Germany) and allowed to dry at RT. The membrane was blocked with 5 % (w/v) BSA (AppliChem, Darmstadt, Germany) in TBS-T (Tris base Roth, Karlsruhe, Germany; Tween-20 AppliChem, Darmstadt, Germany) for 2 h at RT, followed by incubation with mouse anti-acetylated-lysine antibody (1:1000 in BSA/TBS-T; Cell Signaling) for 1 h at RT. After washing with TBS-T (3  $\times$  5 min), the membrane was incubated with a horseradish peroxidase (HRP)-conjugated goat anti-mouse antibody (1:10000 in TBS-T; Promega) for 1 h at RT. After final washing (2  $\times$  15 min with TBS-T

and 1 × 5 min with TBS) spots were visualized by colorimetric detection with 4-chloro-1-naphthol (4CN). Quantification was performed with ImageJ (<http://rsb.info.nih.gov/ij/>).

TBS pH 7.5	20 mM Tris-HCl 150 mM NaCl
TBS-T	0.05 % (v/v) Tween-20 in TBS
BSA/TBS-T	0.1 % (m/w) BSA in TBS-T

## 4CN Colorimetric detection for Dot- and Western blot assays

Color was developed as described previously (Hawkes et al., 1982). Briefly, we immersed the membrane in HRP color development solution. Proteins became visible as purple bands or dots within 30 min. Color development was stopped by immersing the membrane in dd H<sub>2</sub>O (2 × 10 min). Membrane was allowed to dry before scanning.

<b>HRP color development solutions</b> Solution A : Solution B (1:1 mixture)	<b>Solution A</b> (freshly prepared prior usage and protected from light): 30 mg of 4CN in 10 ml of methanol.
	<b>Solution B</b> (freshly prepared prior to use): 6 µl of ice cold 30 % (v/v) H <sub>2</sub> O <sub>2</sub> (Merck, Darmstadt, Germany) in 10 ml TBS.

## Western-blot

Proteins separated by SDS-PAGE were transferred on a nitrocellulose membrane (Sartorius, Göttingen, Germany) using the semi-dry transfer apparatus Fast-blot B32 (Biometra, Göttingen, Germany) according to the manufacturer's protocols. The success of the transfer was checked by staining the proteins with Ponceau S solution. After successful transfer, the membrane was incubated in blocking solution for 2 h at RT, followed by immunoblotting with mouse anti-acetyl lysine antibody (1:1000; Cell Signaling) for 1h at RT. After washing (3 × 10 min) with TBS-T secondary HRP-conjugated goat anti-mouse antibody (1:10000, Promega) was applied for 1h at RT. After the final washing (3 × 10 min with TBS-T and 1 × 10 min with TBS) immunoreactive proteins were detected using the 4CN colorimetric procedure. Densitometric analysis was performed using ImageJ software.

Transfer buffer pH 8.3	25 mM Tris-base 150 mM Glycine 10 % (v/v) Methanol
Ponceau S - protein staining solution (water solution)	0.1 % (w/v) Ponceau S 0.5 % (v/v) Acetic acid
Blocking solution	5 % BSA in TBS-T

## Determination of protein concentration

UV-Vis spectra were recorded using Specord M500 spectrophotometer (Zeiss, Germany) and also spectra of corresponding buffers as a reference. Protein concentration was calculated through equation 1 (Beer-Lambert law) using absorbance at 280 nm and the known molar absorption coefficient ( $\epsilon$ ) for certain protein. This method was exclusively used for pure protein samples.

(Equation 1) 
$$A = \epsilon * c * l$$

A: absorption

$\epsilon$ : molar absorption coefficient ( $M^{-1}cm^{-1}$ )

c: concentration (M)

l: cell path length (cm)

## Mass spectrometry (MS)

### Sample preparation and MALDI-TOF/TOF MS

Samples were desalted using ZipTip C 18 pipette tips (Merck Millipore) and subjected to mass measurements. Peptides: 1  $\mu$ l of a solution of 2,5-dihydroxy-benzoic acid in methanol (70 mg/ml) was mixed with 1  $\mu$ l sample and 1  $\mu$ l of the mixture was deposited onto a stainless steel target. Proteins: 1  $\mu$ l of a solution of sinapinic acid in 30:70 (v/v) ACN, containing 0.1 % (v/v) TFA in water was mixed with 1  $\mu$ l sample and 1  $\mu$ l of the mixture was deposited onto a stainless steel target.

The peptide mass fingerprint spectra were recorded on an Ultraflex-II TOF/TOF mass spectrometer (Bruker Daltonic, Bremen, Germany) equipped with a MALDI source, nitrogen laser, LIFT cell for fragment ion post acceleration and gridless ion reflector. The

software Flex Control 3.0, Flex Analysis 3.0 and Biotoools 3.0 were used to operate the instrument and analyze the data. For external calibration a peptide or protein calibration mixture (Bruker Daltonics, Bremen, Germany) was used.

### In-gel trypsin digestion

The protein bands were cut out of the gels, incubated 45 min at 50°C with 10 mM dithiothreitol in 100 mM ammonium bicarbonate. After removing the solution the protein bands were incubated with 55 mM iodoacetamide in 100 mM ammonium bicarbonate for 45 min in the dark to modify cysteine residues. The solution was removed and the gel pieces were washed three times with water, twice with 100 mM ammonium bicarbonate and finally with 100 mM ammonium bicarbonate in 50 % ACN. The gel pieces were dried under a gentle stream of nitrogen, suspended in 20 µl 50 mM ammonium bicarbonate buffer (pH 8.0) and digested with trypsin overnight at 37°C.

### Nano-UPLC

Peptides were extracted from the gel pieces and injected into a nanoACQUITY UPLC system (Waters) equipped with a binary solvent manager, sample manager and heating and trapping module. Samples (2 µl) were injected by the “microliter pickup” mode and desalted on-line through a symmetry C18 pre-column (180 µm × 20 mm). The peptides were separated on a BEH 130 C18 analytical RP column (100 µm × 100 mm, 1.7 µm, Waters) by using a typical UPLC gradient 3.0 - 33.0 % ACN over 15 min. The mobile phases were water (0.1 % formic acid) and ACN (0.1 % formic acid). The column was connected to a SYNAPT G2 HDMS - mass spectrometer (Waters).

### ESI-QTOF-MS/MS-Analysis

The SYNAPT G2 HDMS is a hybrid quadrupole tandem time-of-flight (Q-TOF) mass spectrometer, equipped with Tri-wave ion guides that trap and separate ions by ion mobility (Waters). The data were acquired in LC/MSE or LC/HDMSE mode (an unbiased mobility assisted TOF acquisition method) switching between low and elevated energy on alternate scans. Subsequent correlation of precursor and product ions can then be achieved using both retention and drift time alignment. BiopharmaLynx (1.3.2, Waters) was used to analyze the obtained MS data. Searches were conducted with GlobalSERVER™ using a species specific database to which sequence information of BSA and other contaminating species were appended.

## Capillary electrophoresis (CE)

Samples were subjected to CE in a Bio-Focus 3000 CE system (Bio-Rad, Hercules, CA). The separation was carried out on an uncoated silica capillary column (50 cm × 50 μm; Bio-Rad) at 25°C and with an applied voltage of 12 kV. The capillary was washed with NaOH (0.1N) for 30 s followed by sodium phosphate buffer (100 mM, pH 6.5) for 90 s under high injection pressure (100 psi). Then, samples were injected with 5 psi (34.5 kPa). The retained protein was eluted in sodium phosphate buffer (100 mM, pH 6.5), and detected by UV detector at 200 nm. All buffer solutions were filtered before usage.

## Continuous fluorescence assay for measuring sirtuin activity

The fluorescence measurements were performed on a Hitachi F-4500 fluorescence spectrophotometer (Tokyo, Japan) at  $\lambda_{\text{Ex}} = 473$  nm and  $\lambda_{\text{Em}} = 535$  nm, slit Ex = 10 nm, slit Em = 10 nm, PMT = 950 V for TNF $\alpha$  peptide 2. Each reaction mixture contained 20 mM Tris-HCl pH 7.8, 150 mM NaCl, 5 mM MgCl<sub>2</sub>, 0.5 mM NAD<sup>+</sup> and various peptide concentrations (0.5–30 μM) and was preincubated for 5 minutes at 37 °C. The reaction was started by adding human SIRT4 (1 μM) and followed for 5–10 minutes.

Product formation was monitored by increase of relative fluorescence. This signal was converted into product concentration via a calibration curve. The slope of the linear regression of product formation against time yielded the reaction velocity rates in μM/s.  $K_M$  and  $k_{\text{cat}}$  were obtained by non-linear regression according to Michaelis-Menten. All measurements were done at least in duplicates. For determination of reaction velocity rates in μM/s calibration lines were necessary. Therefore a reaction mixture was prepared containing assay-buffer, 2 μM SIRT2, 500 μM NAD<sup>+</sup> and 100 μM of TNF $\alpha$  peptide 2 was incubated overnight at 37 °C. The reaction mixture was analyzed with HPLC, to control if the entire peptide substrate was turned to product. Additionally the mixture was diluted (0.1–25 μM) and measured with a Hitachi F-4500 fluorescence spectrophotometer at the same conditions as described above (Figure A13B).

The microtiter plate fluorescence measurements were performed on a Tecan Infinite M200 microplate reader (Maennedorf, Switzerland) at  $\lambda_{\text{Ex}} = 320$  nm and  $\lambda_{\text{Em}} = 420$  nm. The reactions (total volume 100 μl) were measured in black low-binding 96- well microtiter plates (Greiner Bio-One International). Assay-buffer, 500 μM NAD<sup>+</sup> and 2–100 μM TNF $\alpha$  peptide 1 were pre-incubated at 37 °C for 5 min. The reaction was started by adding

SIRT4 (1  $\mu$ M) and recorded over 60 min. The signals were converted into product concentration via a calibration curve and the resulting data were evaluated as described above (Figure A13A).

## Fluorescence spectroscopy

Protein fluorescence was measured using a Hitachi Fluorescence spectrophotometer model F-4500. Spectra were recorded at 37°C, in 200 mM Tris-HCl buffer pH 8.0 using 1 ml quartz cuvette in a range from 300-400 nm, with excitation at 280 nm. The slit for excitation and emission light was 10 nm.

## Circular dichroism spectroscopy (CD)

CD spectra were recorded using an Aviv Biomedical Circular Dichroism Spectrometer, Model 420. The spectra were measured with quartz cuvettes at 25°C in a 20 mM sodium phosphate buffer, pH 7.3. Data were collected as averages of 5 repetitive scans. Spectrophotometric determination of protein concentration was estimated using absorption at 280 nm and molar absorption coefficient for CypA  $\epsilon=8400 \text{ M}^{-1}\cdot\text{cm}^{-1}$  as described previously in this section. The mean molecular ellipticity  $\Theta$  was calculated using equation 2 and is expressed in  $\text{deg}\cdot\text{cm}^2\cdot\text{dmol}^{-1}$  units.

$$\text{(Equation 2)} \quad [\Theta]_{\text{MRW}} = \frac{\Theta \cdot 100 \cdot \text{Mr}}{c \cdot d \cdot N_A}$$

$[\Theta]_{\text{MRW}}$  : molecular ellipticity ( $\text{deg}\cdot\text{cm}^2\cdot\text{dmol}^{-1}$ )

$\Theta$ : ellipticity (deg)

Mr: molecular weight (Da)

c: protein concentration (mg/ml)

d: path length (cm)

$N_A$ : number of amino acids

## Peptide microarray

All microarray experiments were done using a hybridization station (HS400, TECAN) in a semi-automated mode. Acetylome peptide microarrays were used (Rauh et al., 2013). All steps were performed at 25°C with an exception for the enzyme incubation step which

was carried out at 30°C or 37°C. All buffers were filtered before usage. First, peptide microarrays were washed (TBS-T 2 × 2 min and TBS 1 × 2 min) followed by blocking step (1 h with Roti-Block solution, (Roth, Karlsruhe, Germany)). Subsequently, acetyltransferase was applied in corresponding buffer for 2 hours. After washings (TBS-T 5 × 2 min and TBS 1 × 2 min), an optimized mixture of primary antibodies (Rauh et al., 2013) was applied for 1 h followed by washing with TBS-T 5 × 2 min and TBS 1 × 2 min. Then, a mixture of secondary fluorescence labeled antibodies (Rauh et al., 2013) was applied for 30 min. Finally microarrays were washed (TBS-T 5 × 2 min, TBS 1 × 2 min and dd H<sub>2</sub>O 2 × 2 min) and dried using a stream of nitrogen gas. Peptide microarrays were scanned using a GenPix 4000B scanner (Molecular devices) at 635 nm (red channel) and 532 nm (green channel). Images were analyzed using GenePix Pro 7.0 software (Molecular devices).

Primary antibodies mixture (1:2000 in TBS-T)	
Mouse anti-Ac-Lys	Abcam
Mouse anti-Ac-Lys	Cell Signaling
Rabbit anti-Ac-Lys	Cell Signaling

Secondary fluorescence labeled antibodies mixture (1:5000 in TBS-T)	
Goat-anti-mouse IgG (H+L) DyLight 649 Conjugated 1 ml/ml	Thermo Scientific
Goat-anti-rabbit IgG (H+L) DyLight 649 Conjugated 1 ml/ml	Pierce

# Results

## Non-enzymatic lysine acetylation of model peptide using Ac-CoA

In order to investigate whether a lysine residue within a peptide undergoes non-enzymatic acetylation in presence of Ac-CoA we used Bz-G<sup>524</sup>VLKEYGV<sup>531</sup>-NH<sub>2</sub> as model peptide, which was discovered in a peptide microarray based approach (Rauh et al., 2013) to be an efficient substrate for several sirtuins in the acetylated form, and was demonstrated to be an extraordinary good SIRT5 substrate in its succinylated and glutarylated form (Roessler et al., 2014). The peptide is derived from CPS1, a mitochondrial enzyme involved in the first step of the urea cycle, catalysing formation of carbamoyl phosphate from NH<sub>4</sub><sup>+</sup>, ATP and bicarbonate (Jackson et al., 1986). Schwer et al. showed that K527 is hyperacetylated during the CR and implicated in CPS1 regulation (Schwer et al., 2009). Other studies revealed succinylation of K527 (Weinert et al., 2013), which could be removed by SIRT5, consistent with role of SIRT5 in urea cycle regulation (Du et al., 2011; Nakagawa et al., 2009; Roessler et al., 2014). To measure non-enzymatic acetylation, we treated the CPS1 peptide with 4 mM of Ac-CoA at 37°C and pH 8.0, which reflects the conditions in the mitochondrial matrix (Garland et al., 1965; Hansford and Johnson, 1975; Santo-Domingo and Demaurex, 2012). For detection and quantification of non-enzymatic acetylation of the lysine residue we developed a HPLC based assay. Separation of the reaction mixture using a RP-column showed the appearance of an additional peak (260 nm) at t<sub>R</sub>=5.22 min, thus indicating the formation of a modified CPS1 peptide derivative over time (Figure 12A). Additional analysis of HPLC fractions by nano-UPLC-coupled MS identified the newly emerged peak as acetylated CPS1 peptide (Figure 12B). Because not just lysine residues are able to be modified chemically (for example phenolic hydroxyl group of the tyrosine residue also represent potential site of modification) further analysis was required. Peptide fragmentation analysis by tandem MS proved that only the N-ε-lysine residue was modified by acetylation (Figure 12C).

In this study all acetylation reactions have been done in a Tris-HCl buffer system. Tris itself contains a primary, but sterically hindered amino group, and can potentially effect



acetylation reaction. In order to test this possibility, we performed acetylation reaction in different buffer systems and found no significant difference between them (Figure A14).

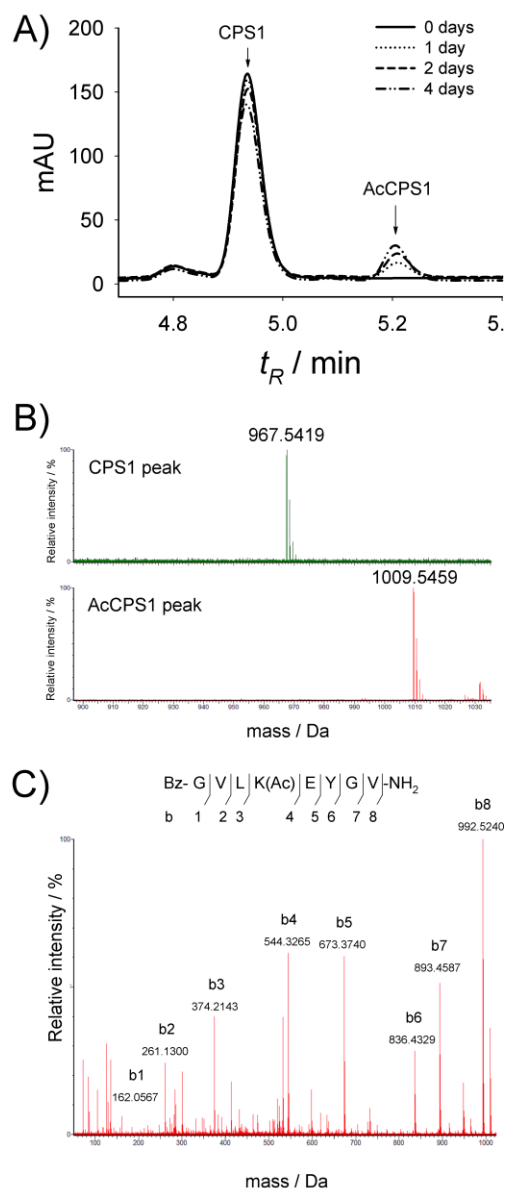


**Figure 12.** Non-enzymatic lysine acetylation of Bz-GVLKEYGV-NH<sub>2</sub> (CPS1 peptide). **A)** Lysine acetylation of the CPS1 peptide was investigated by HPLC (detection, 260 nm). CPS1 peptide (200  $\mu$ M) was incubated with 4 mM Ac-CoA for 0 (—), 1 (·····), 2 (---), or 4 (- · - ·) days at 37°C and pH 8.0. The reaction mixture was separated by RP-HPLC on a Poroshell 120 EC-C18 column. The appearance of an additional peak at 5.22 min indicates the formation of acetylated CPS1 peptide. **B)** Identification of the reaction product by nano-UPLC-coupled MS. The mass spectrum displays a peptide with m/z 1009.5, which corresponds to acetylated CPS1 peptide. **C)** Determination of the acetylation site by nano UPLC-MS/MS analysis. Fragmentation ions observed in the tandem mass spectrum confirmed that the CPS1 peptide is acetylated at the N- $\epsilon$ -position of the lysine residue. Figure is adapted from Simic et al. 2015 with permission (Simic et al., 2015).

## Kinetic and thermodynamic parameters of non-enzymatic lysine acetylation

In order to determine kinetic parameters it was necessary to quantify the amount of acetylated product. A discontinuous HPLC based assay was used. At certain time points reaction was stopped by adding TFA (1 % (v/v) final concentration) and then processed further to HPLC separation. TFA reduces the pH value of the reaction solution, ensuring that N-ε-amino group of the lysine residue is completely protonated, thus no longer being a substrate for the acetylation reaction. After separation of the CPS1 peptide and its acetylated form, chromatogram was integrated and areas under the peaks were used for calculation of the percentage of acetylated product using equation:

$$(Equation\ 3) \quad P_{(\%)} = \frac{A_P * 100 (\%)}{A_P + A_S}$$

With:

$P_{(\%)}$ : Percentage of product

$A_P$ : Area under product peak

$A_S$ : Area under substrate peak

With known starting concentration of the substrate, we can easily calculate the concentration of the product at any time point using equation:

$$(Equation\ 4) \quad [P] = \frac{P_{(\%)} * [S_0]}{100(\%)}$$

With:

[P]: Concentration of the product

$P_{(\%)}$ : Percentage of product

$[S_0]$ : Starting concentration of the peptide substrate

One of the first goals was the determination of the reaction order and reaction rate constant for the non-enzymatic lysine acetylation. Reaction mixture containing 200  $\mu\text{M}$  of CPS1 peptide, 4 mM of Ac-CoA in 200 mM Tris-HCl pH 8.0 was incubated at 37°C. At certain time points the reaction was stopped using TFA and the reaction mixture was analyzed with HPLC to obtain concentration of acetylated product. The concentration of acetylated product was plotted as a function of time. Time-dependence of peptide acetylation displayed a kinetic behavior following a pseudo-first-order reaction with apparent rate constant ( $k_{\text{app}}$ ) of  $6.1 \pm 1.7 * 10^{-7} \text{ s}^{-1}$  (Figure 13A). Starting concentration of Ac-CoA was 20 times higher than for the peptide. For the first few hours nearly linear formation of acetylated product could be detected. Over time, because of spontaneous hydrolysis, concentration of Ac-CoA decreased and course undergoes hyperbolic function. For that purpose, we investigated the stability of different acyl-CoAs in the buffer solution. Ac-CoA and Succ-CoA display a half-life of 18.2 and 3.8 h respectively (Figure A15). All measurements were done within time intervals less than half-life of the corresponding thioester, where its concentration is still high enough to ensure pseudo-first order behavior.

Measurements of peptide acetylation in the presence of different concentrations of Ac-CoA revealed a linear dependence of product formation on Ac-CoA concentration. The slope of the plot of  $k_{\text{app}}$  against Ac-CoA concentration gives a bimolecular rate constant ( $k$ ) of  $1.52 \pm 0.42 * 10^{-10} \mu\text{M}^{-1} * \text{s}^{-1}$  (Figure 13B).

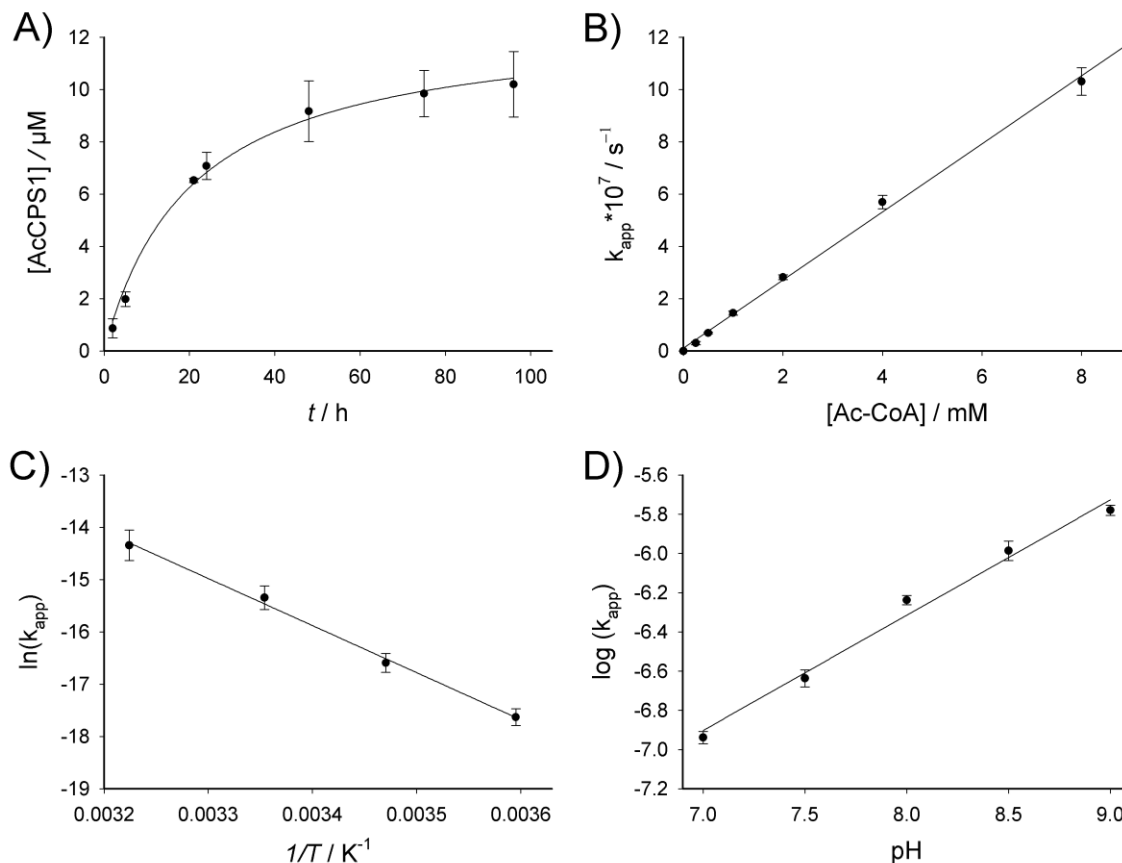


**Figure 13.** Determination of kinetic and thermodynamic parameters of non-enzymatic lysine acetylation by Ac-CoA. **A)** Time-dependent acetylation of the CPS1 peptide, determined by HPLC (detection at 260 nm). The plot shows pseudo-first-order kinetics with a rate constant of  $6.1 \pm 1.7 \times 10^{-7} \text{ s}^{-1}$ . **B)** Ac-CoA concentration dependence. Peptide acetylation rate shows a linear dependence on Ac-CoA concentration. The slope of the plot gives a bimolecular rate constant of  $1.52 \pm 0.42 \times 10^{-10} \mu\text{M}^{-1} \cdot \text{s}^{-1}$ . **C)** Temperature-dependent acetylation. The plot of natural logarithm of the pseudo-first-order rate constants ( $\ln k$ ) versus  $1/T$  is linear, thus indicating that the temperature dependence obeys the Arrhenius law. The calculated activation energy ( $E_a$ ) was  $74.8 \pm 2.8 \text{ kJ} \cdot \text{mol}^{-1}$ . **D)** pH dependence of CPS1 peptide acetylation. The plot  $\log(k_{\text{app}})$  as a function of pH has linear dependence. Error bars represent SD ( $n=2$ ). Figure is adapted from Simic et al. 2015 with permission (Simic et al., 2015).

With intention to investigate temperature dependency of the non-enzymatic acetylation we determined reaction rate constants at different temperatures (5, 15, 25 and 37°C). Our findings revealed that temperature dependence follows the Arrhenius law:

(Equation 5) 
$$k = A * e^{\frac{-E_a}{RT}}$$

With:

k: rate constant of the chemical reaction

A: pre-exponential factor

E<sub>a</sub>: activation energy

R: universal gas constant (R=8.314 J\*K<sup>-1</sup>\*mol<sup>-1</sup>)

T: absolute temperature (in Kelvins)

Taking the natural logarithm of Arrhenius' equation yields:

(Equation 6) 
$$\ln(k) = \ln(A) - \frac{E_a}{R} * \frac{1}{T}$$

With rearrangement:

(Equation 7) 
$$\ln(k) = \frac{-E_a}{R} * \frac{1}{T} + \ln(A)$$

Plotting the logarithm of the rate constant (k) versus the inverse temperature (1/T) shows a linear course (Figure 13C), with a slope of  $-E_a/R$ . Knowing the value for the universal gas constant R it is possible to calculate the activation energy for the non-enzymatic acetylation reaction to be  $E_a=74.8 \pm 2.8 \text{ kJ*mol}^{-1}$ .

Non-enzymatic lysine acetylation strongly depends on the pH value of the solution (Figure 13D). The pK<sub>a</sub> value of the N-ε-amino group of the lysine side chain is around 10.5 (Nolting et al., 2007). At pH values far below the pK<sub>a</sub> of the lysine side chain, N-ε-amino group exist almost exclusively in the protonated, thus not reactive form. Increasing pH accelerates non-enzymatic acetylation by increasing the concentration of reactive (de-protonated) form of the peptide.

## Non-enzymatic acylation of CPS1 peptide by different acyl-CoA thioesters

Recently, large-scale MS studies that identified succinylation, glutarylation and malonylation of the N- $\epsilon$ -amino group of the lysine residue were enriched in the mitochondrial protein fraction (Du et al., 2011; Peng et al., 2011; Sadhukhan et al., 2016; Tan et al., 2014; Zhang et al., 2011). In addition, butyrylation and propionylation, have been recently identified in liver mitochondria (Pougovkina et al., 2014). Nevertheless, enzymes responsible for such modifications in mitochondria remain unknown. All of these modifications are most likely derived non-enzymatically from their corresponding acyl-CoA thioesters. During metabolic flow, many reactive acyl-CoA thioesters are also formed. Some of them are acyl-CoA involved as intermediates in ketone bodies synthesis pathway in mitochondria, like HMG-CoA, and AcAc-CoA. To test our hypothesis, CPS1 peptide was incubated with different acyl-CoA thioesters in Tris-HCl buffer pH 8.0 at 37°C (Figure 14). The highest acylation rate was observed with Succ-CoA (Figure A16), which was about 150 times more efficiently in acylating CPS1 model peptide in comparison to Ac-CoA. Notably, proteomic studies have identified *in vivo* succinylation at K527 of CPS1 in different tissues (Weinert et al., 2013). Glut-CoA (Figure A17) exhibited about sixfold higher acylation than Ac-CoA, whereas Prop-CoA (Figure A18) and But-CoA (Figure A19) displayed three and five times lower acylation rates than Ac-CoA, respectively. Benz-CoA and AcAc-CoA did not react under the conditions used. Interestingly, HMG-CoA (Figure A20) showed the ability to modify lysine residues of model peptide with an acylation rate constant about threefold higher than for Ac-CoA. Based on this discovery, HMG-lysine could be an interesting candidate for a novel lysine posttranslational modification.

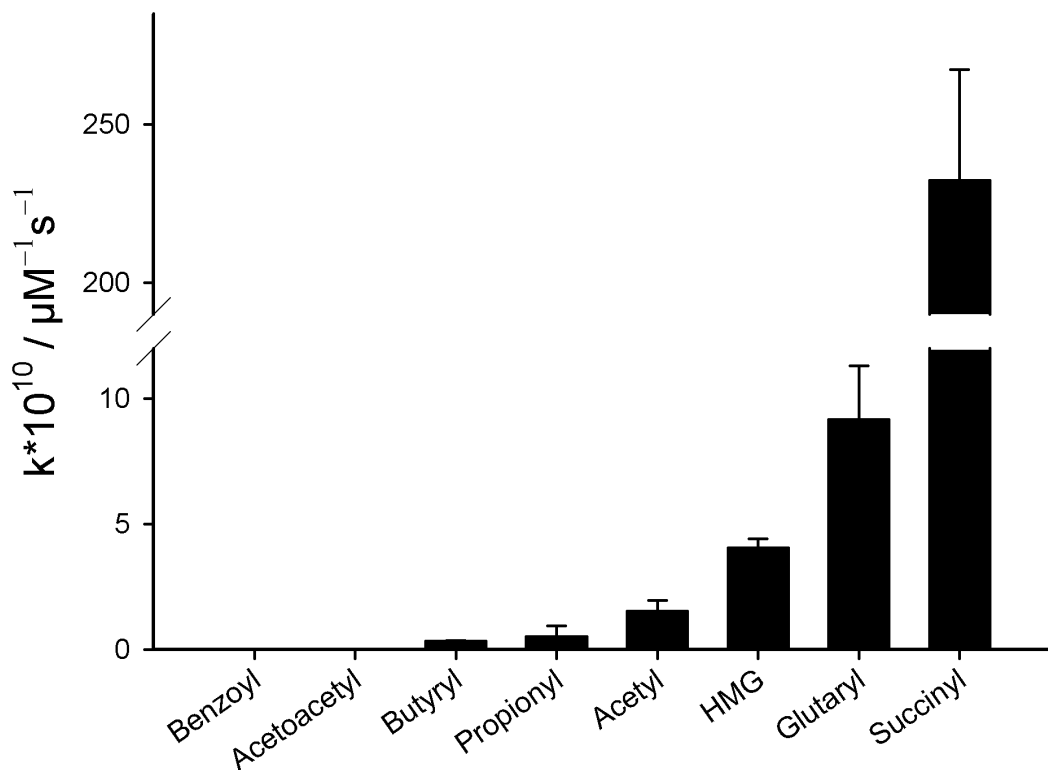


**Figure 14.** Comparison of non-enzymatic CPS1 peptide acylation by different thioesters. CPS1 peptide (200  $\mu\text{M}$ ) was incubated with various concentrations of the different acyl-CoA thioesters in 200 mM Tris-HCl buffer pH 8.0 at 37°C over time. Product formation was determined by HPLC. To obtain bimolecular rate constants for the different thioesters, the slope of the plot of the pseudo-first-order acylation rates versus acyl-CoA concentration was calculated by linear regression. Data represent average  $\pm$  SD (n=3).

## Modulation of non-enzymatic lysine acetylation

### Small molecules

Non-enzymatic lysine acetylation is a slow process compared to histone lysine acetyltransferase p300 catalysed acetylation of a histone-derived peptide ( $k_{\text{cat}}=0.26 \pm 0.01 \text{ s}^{-1}$ ) (Thompson et al., 2004). Here we checked whether 4-(dimethylamino)-pyridine (DMAP), could effect non-enzymatic acetylation. DMAP has been widely used as an efficient acylating catalyst in the chemical synthesis. Indeed, we found that DMAP improved non-enzymatic acetylation in a concentration dependent manner (Figure 15). Next, we examined whether metabolites, cofactors or other small molecules, which are present in mitochondrial matrix in a relatively high concentration, accelerate the non-

enzymatic acetylation. We have tested NAM,  $\text{NAD}^+$ , NADH,  $\text{NADP}^+$ , NADPH, ATP, L-carnitine, mercaptopyruvate, pyridoxal phosphate, thiamin pyrophosphate, ribose-5-phosphate, metabolites of L-tryptophan degradation pathway (like kynurenic acid, picolinic acid and quinolinic acid). None of these compounds shows significant effects on non-enzymatic acylation, even if some of them share similar structure with DMAP.

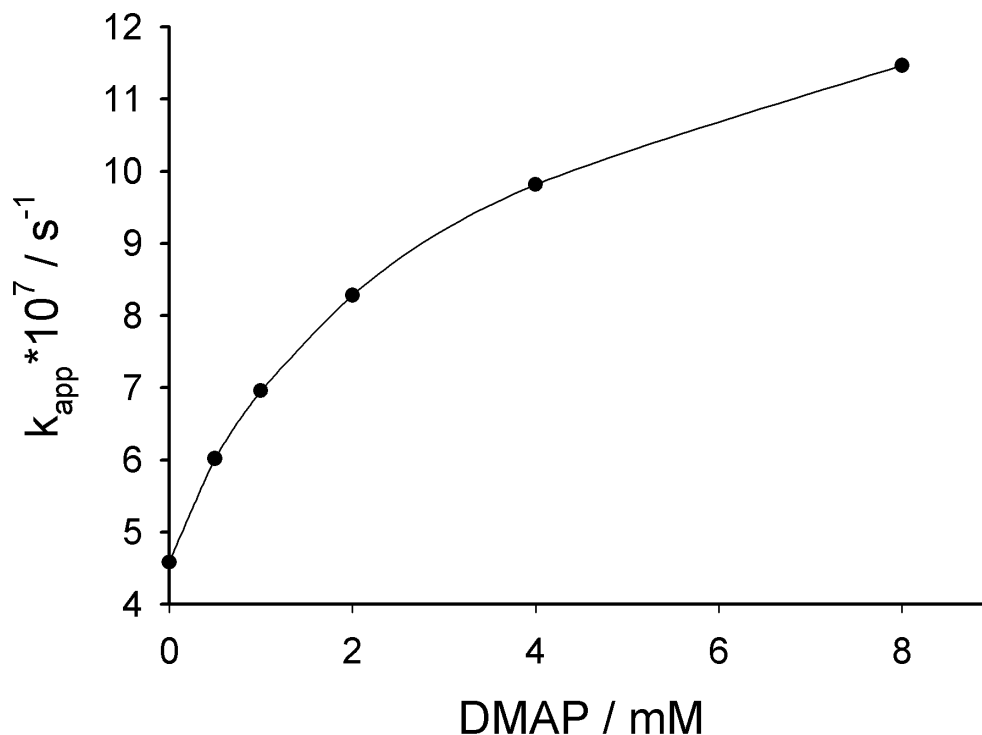


**Figure 15.** DMAP accelerates Ac-CoA-mediated non-enzymatic acetylation of the CPS1 peptide in a concentration dependent manner. Reaction was carried out in 200 mM Tris-HCl buffer pH 8.0 at 37°C for 24 h with 200  $\mu\text{M}$  CPS1 peptide and 4 mM Ac-CoA in the presence of 0 – 8 mM DMAP. Product formation was analyzed by RP-HPLC and calculated rate constants were plotted against the DMAP concentrations. Figure is adapted from Simic et al. 2015 with permission (Simic et al., 2015).

## Water content and ionic strength

It has been shown that mitochondrial matrix space is filled with more viscous material compared to the cytosol. Water content in the cytosol is 3.8  $\mu\text{l}/\text{mg}$  of the protein, and in the mitochondrial matrix it is just 0.8  $\mu\text{l}/\text{mg}$  of the protein (Soboll et al., 1979). Next we wanted to test, whether water content or ion strength effect non-enzymatic acetylation. We reduced water content in the reaction mixture by introducing DMSO (Merck, Darmstadt,



Germany) in the system. Surprisingly, non-enzymatic acetylation was slower in DMSO, than in aqueous solution (Figure 16).

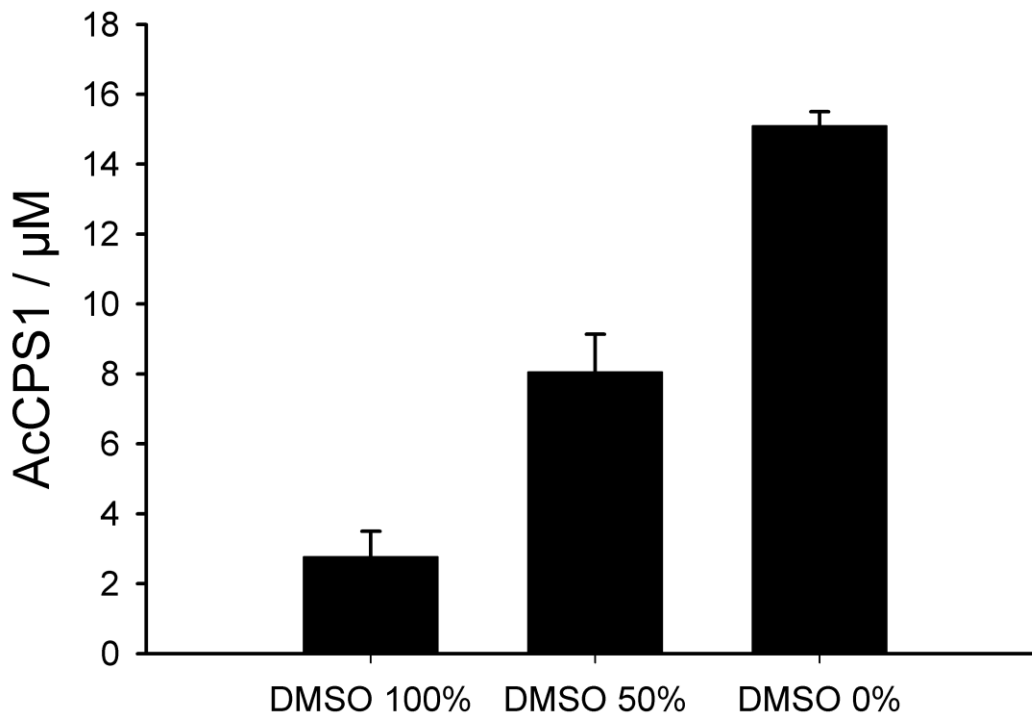


**Figure 16.** Non-enzymatic acetylation of CPS1 peptide by Ac-CoA in the reaction system with reduced water content. Three different reactions were set up. The first one was carried out in 100 % (v/v) DMSO, the second in the mixture 50 % (v/v) DMSO in water and the third one in water. All reactions mixtures contained 200 μM CPS1 peptide, 4 mM Ac-CoA, and 1 % (v/v) DIPEA. After incubation at 37°C for 60 min, reaction mixtures were subjected to HPLC analysis. Data represents average  $\pm$  SD (n = 3).

We performed acetylation reaction at different salt concentrations and found that salt concentration effects acetylation yield in a concentration dependent manner (Figure 17). Sodium chloride shows slightly increased acetylation rate constant, but 1M magnesium sulfate increases the rate constant about two-fold.

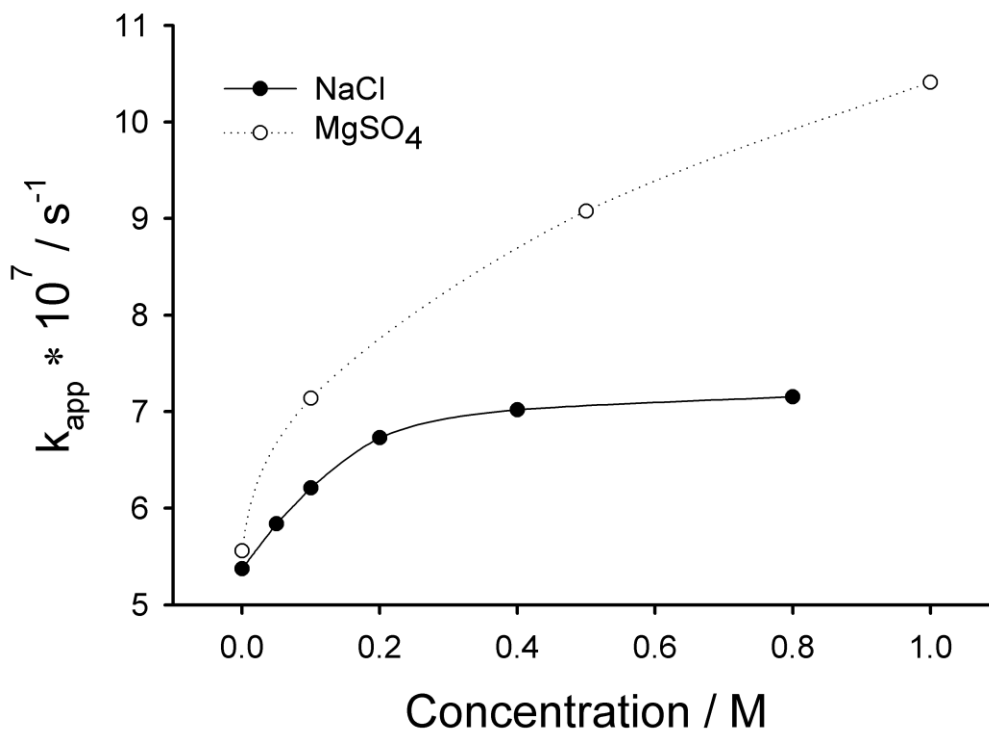


**Figure 17.** Non-enzymatic acetylation of CPS1 peptide by Ac-CoA in the presence of different salt concentrations. Three reactions were carried out in 200 mM Tris-HCl buffer pH 8.0 at 37°C. All reaction mixtures contain 200  $\mu$ M CPS1 peptide, 4 mM Ac-CoA and different concentration of NaCl and MgSO<sub>4</sub>. After different times reactions were stopped and analysed by HPLC.

## The methylation of N- $\epsilon$ -amino group of lysine residue

Protein methylation is a reversible posttranslational modification predominantly found on lysine and arginine residues (Aletta et al., 1998; Ambler and Rees, 1959; Comb et al., 1966). It was originally described on histone proteins to have a role in regulation of chromatin structure and gene transcription (Lee et al., 2005; Murray, 1964). The respective enzymes regulating the methylation state (methyltransferases and demethylases/protein arginine deimidases) have been described to be involved in various diseases (Cloos et al., 2008; Greer and Shi, 2012). Recent studies identified lysine methylation as widespread lysine modification beyond histones (Guo et al., 2014). Lysine N- $\epsilon$ -amino group can be modified with one (monomethylated lysine, Kme1), two (dimethylated lysine, Kme2) or three (three methylated lysine, Kme3) methyl groups. We were interested to see whether lysine methylation could have any influence on lysine non-enzymatic acetylation. Therefore, we used N-methylated CPS1 peptide derivative and

incubated it with Ac-CoA under the same conditions. It was obvious that lysine N- $\epsilon$ -methylation completely prevents non-enzymatic acetylation mediated by Ac-CoA (Figure 18). Additionally, N- $\epsilon$ -methylated CPS1 peptide was incubated with Succ-CoA under the same conditions. Surprisingly, methylated CPS1 peptide easily undergoes non-enzymatic succinylation (Figure 19).

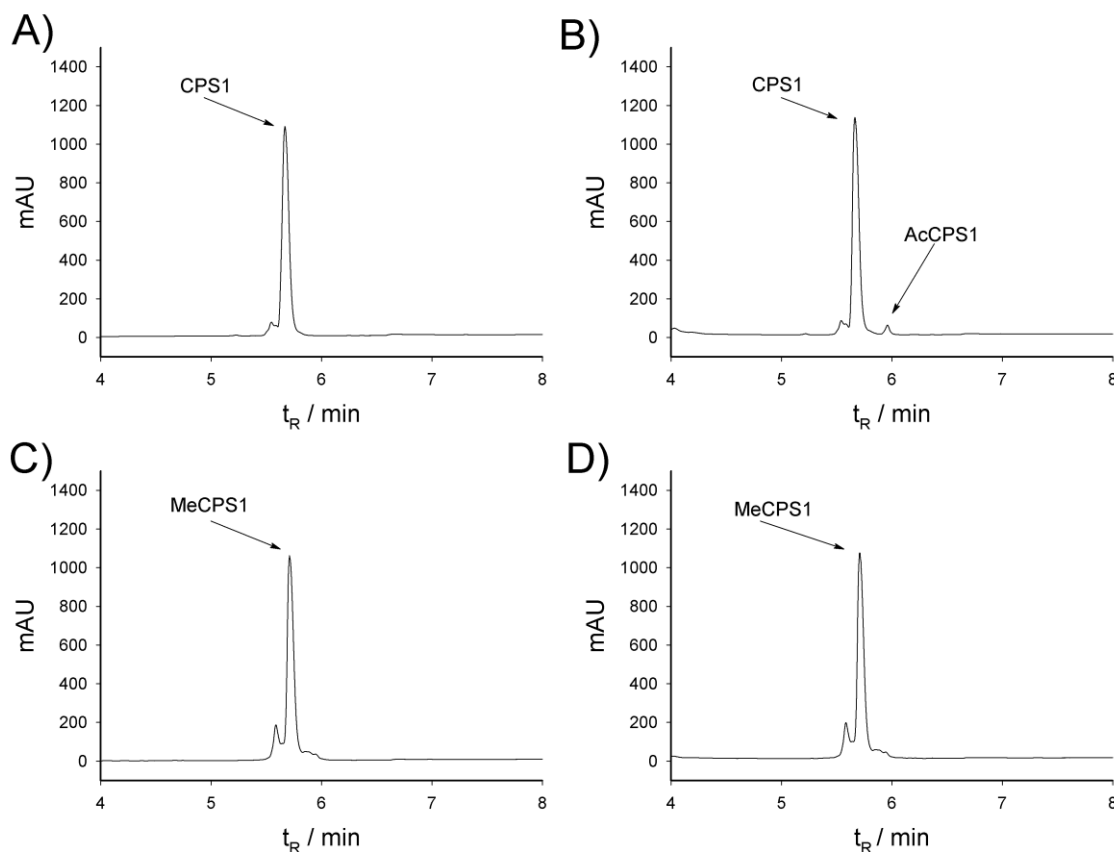


**Figure 18.** Methylation of the  $\epsilon$ -amino group of lysines residues prevents non-enzymatic acetylation by Ac-CoA. **A)** CPS1 peptide and **C)** the methylated form of the CPS1 peptide were incubated in 200 mM Tris-HCl pH 8.0 at 37°C for 24 h and subjected to RP-HPLC analysis. **B)** When CPS1 peptide was incubated in the presence of 4 mM Ac-CoA, formation of acetylated CPS1 peptide can be observed. **D)** However, in the case of the methylated form of CPS1 peptide no acetylated product can be detected in the HPLC chromatogram.

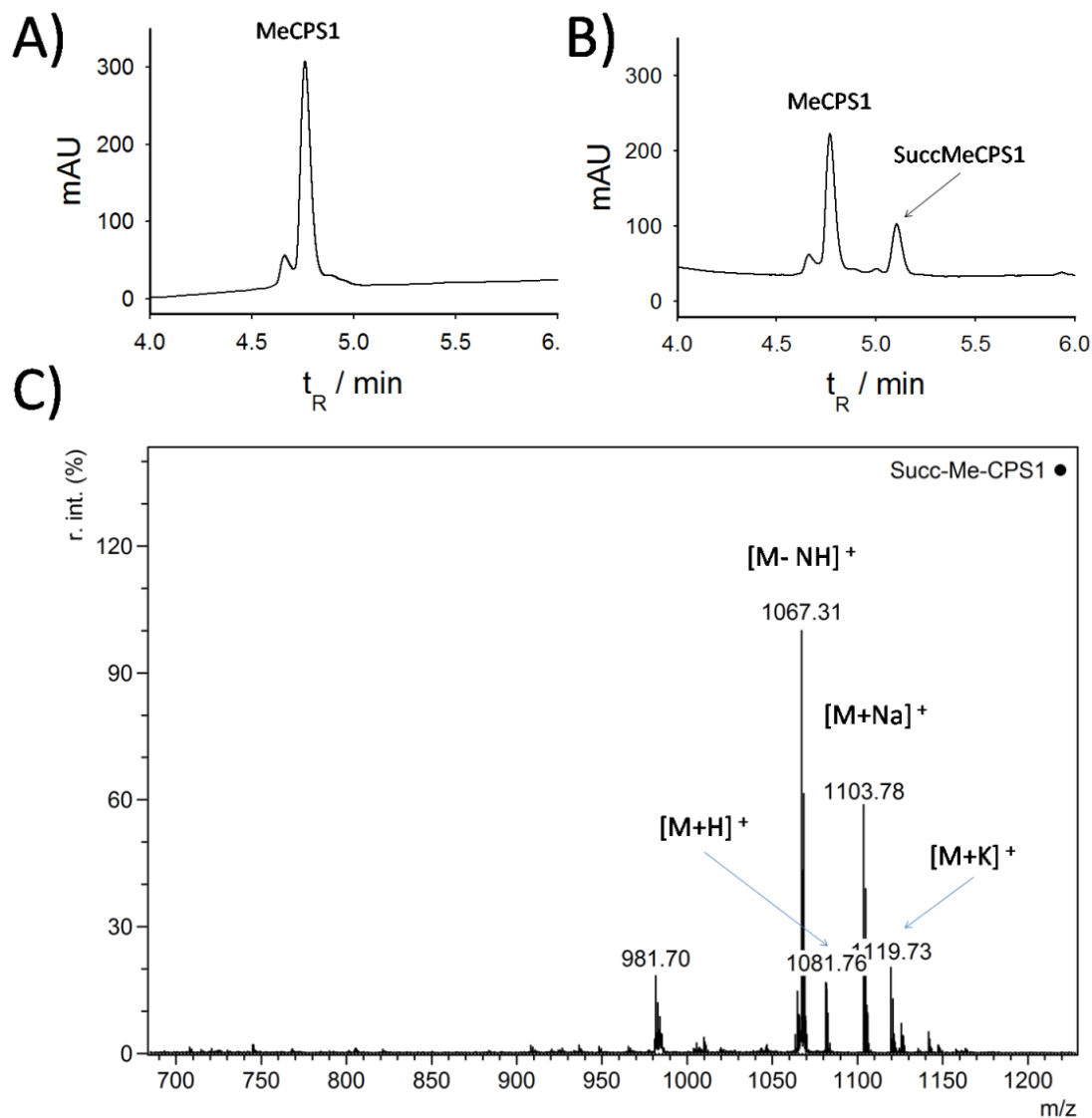


**Figure 19.** Methylation of the  $\epsilon$ -amino group of lysines residues is not able to prevent non-enzymatic succinylation by Succ-CoA. **A)** MeCPS1 peptide. **B)** Methylated form of the CPS1 peptide was incubated in 200 mM Tris-HCl buffer pH 8.0 in the presence of 4 mM Succ-CoA at 37°C for 24 h and then subjected to RP-HPLC analysis. When CPS1 peptide was incubated in the presence of 4 mM Succ-CoA, formation of succinylated MeCPS1 peptide can be observed. **C)** SuccMeCPS1 peak was collected and subjected to MALDI-TOF MS analysis where its identity was confirmed.

## Non-enzymatic acetylation of CypA

Next, we chose CypA, the prototypic member of the cyclophilin family of peptidyl prolyl cis/trans isomerases, as a model protein for non enzymatic acetylation by acyl-thioesters. CypA is a ubiquitously expressed protein with key roles in protein folding, intracellular trafficking, immunity and viral infection (Handschumacher et al., 1984;

Howard et al., 2003; Nigro et al., 2013; Yurchenko et al., 2002). It shares 76.5 % identity in the sequence with its exclusively mitochondrial analogue cyclophilin D (Figure A21). CypA is a highly posttranslational modified protein including phosphorylation and acetylation. Recent studies have revealed that eleven of the fourteen lysine residues of the protein can be acetylated in cells (Table A1). Acetylation of CypA at K82 and K125 inhibits its enzymatic activity, alters its binding capacity to the immunosuppressive drug cyclosporine A, blocks its interaction with the HIV capsid protein, and moreover, prevents its extracellular secretion (Lammers et al., 2010; Soe et al., 2014).

To investigate whether CypA can be acetylated non-enzymatically, the protein was treated with Ac-CoA for various times. Dot-blot analysis showed time-dependent acetylation of CypA (Figure 20A). Analysis of the reaction mixture by MALDI-TOF MS revealed that incubation with Ac-CoA predominantly resulted in monoacetylated and diacetylated forms of CypA (Figure 20B). However, higher acetylated species of CypA (e.g., tri and tetra acetylated) were also observed. In order to identify the lysine residues modified by Ac-CoA, the reaction mixture was subjected to PAGE (Figure A22), CypA bands were cutted out and subjected to tryptic digestion and LC-MS/MS analysis (Figure 21). Tryptic peptides found are listed in the tables (Table A2 and A3). MS data revealed that K155 was the main acetylation site on CypA (Figure 22). More than half of all acetylation signal intensities were from lysine K155. Significant acetylation was also detected for K28, K82 and K125, whereas other residues were only slightly modified. This shows that sequence, microenvironment and accessibility of lysine residues on the protein surface might influence acetylation efficiency. However, it should be noted that label-free MS can lead to misinterpretation of relative peptide abundance under certain circumstances, such as 1) differences in the ionization efficiency and/or detectability of the peptides, 2) variations in biochemical sample preparation of acylated peptides, for example, tryptic digestion and reductive alkylation, and 3) certain peptide structure can become trapped in the LC column, among others. Because of low reproducibility we did not take in consideration the two shortest tryptic peptides NGKTSK and TSKK corresponding to sites K151 and K154, respectively.

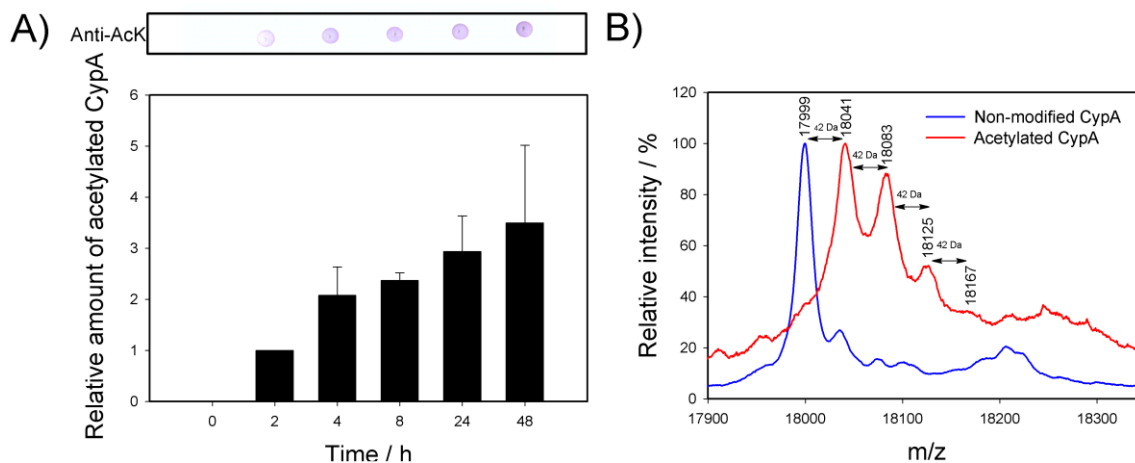


**Figure 20.** Non-enzymatic lysine acetylation of the protein substrate CypA. **A)** Protein (10  $\mu$ M) was treated with 4 mM Ac-CoA in 200 mM Tris-HCl buffer pH 8.0 for 2, 4, 8, 24, or 48 h at 37°C. The reaction mixture was spotted onto a nitrocellulose membrane. Acetylation of retained CypA was determined by immunodetection with anti-acetylated-lysine antibody. Densitometric analysis of the dot blot was performed in ImageJ. Error bars represent SD (n=2). **B)** MALDI-TOF MS analysis of the acetylation reaction mixture after 24 h reveals that CypA is predominantly mono- and diacetylated, although, tri- and tetraacetylated protein are also present. Figure is adapted from Simic et al. 2015 with permission (Simic et al., 2015).

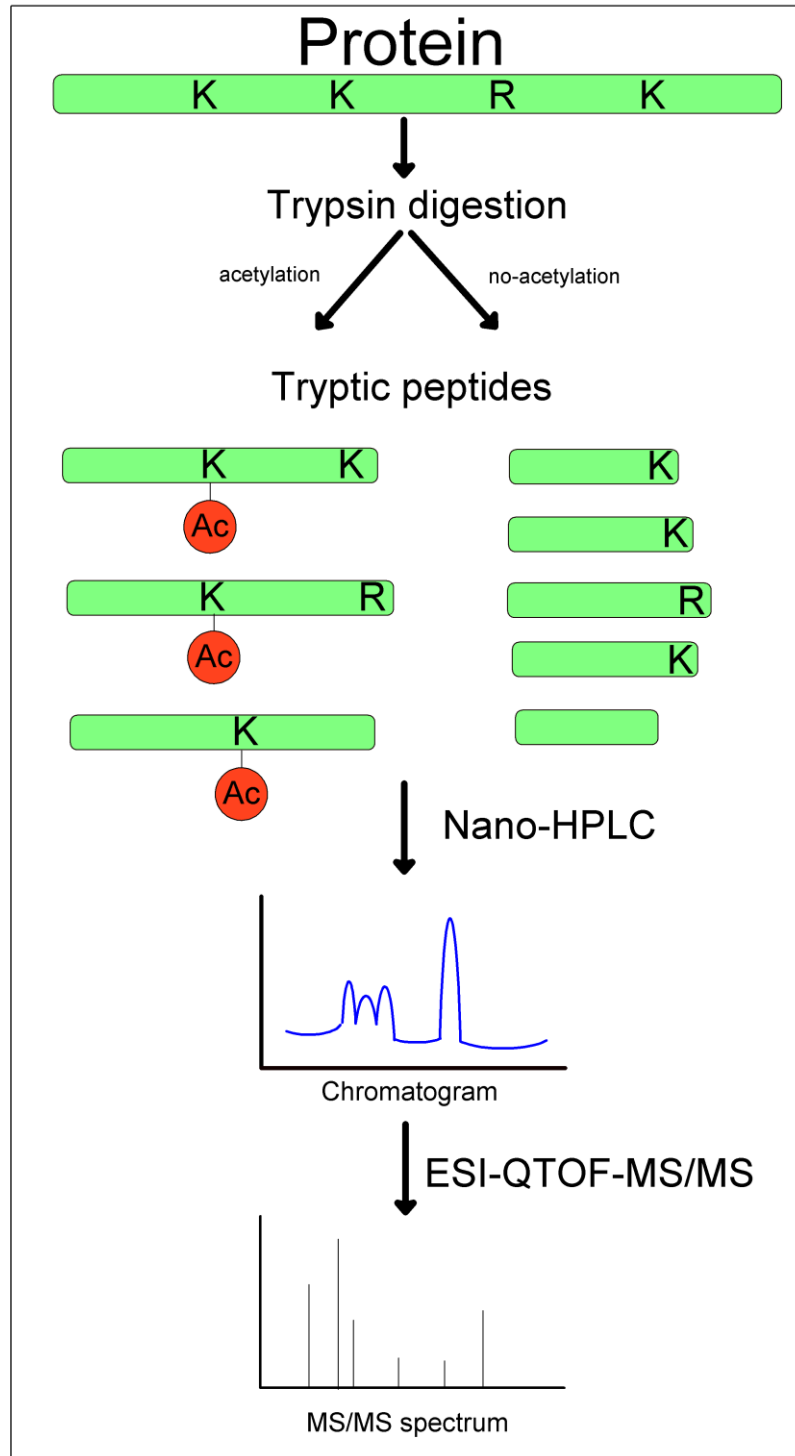


**Figure 21.** Schematic illustration of protein digestion with trypsin and LC-MS/MS analysis of tryptic peptides. Trypsin is able to cut the peptide bound after K and R with an exception when they are followed by proline. Trypsin is not able to cleave peptide bound subsequent to acylated lysine residues. In such case longer tryptic peptides are generated which are indicative for the modification on the respective lysine residue.

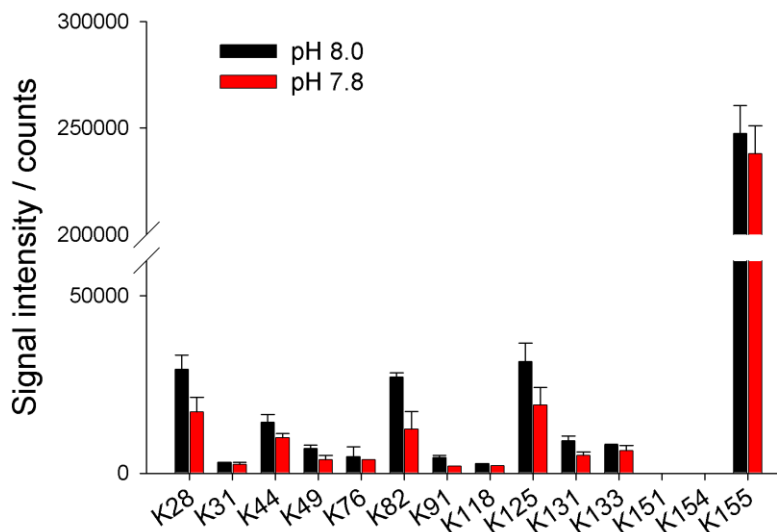


**Figure 22.** Analysis of the lysine acetylation pattern of CypA. CypA is non-enzymatically acetylated at different lysine residues. CypA (10  $\mu$ M) was acetylated with 4 mM Ac-CoA for 24 h at 37°C in 200 mM Tris-HCl buffer pH 8.0 or 7.8. The reaction mixture was subjected to tryptic digestion and LC-MS/MS analysis. The relative intensities of mass peaks reveal that CypA can be non-enzymatically acetylated at twelve of the fourteen CypA lysine residues. K155 is the predominant acetylation site. Data are average  $\pm$  SD (n=3). Figure is adapted from Simic et al. 2015 with permission (Simic et al., 2015).

Acetylation of all lysine residues at pH 7.8 was remarkably lower relative to that at pH 8.0, and acetylation was almost completely restricted to K155. This underlines the importance of the elevated pH in the mitochondrial matrix for acetylation patterns.

In order to test whether the mitochondrial deacetylases SIRT3 and SIRT5 can recognize acetylated CypA as a substrate we performed western blot analysis with an anti acetylated-lysine antibody. The antibody revealed a single band at 18 kDa if CypA was treated with Ac-CoA (Figure 23A). In the presence of the sirtuin cosubstrate NAD<sup>+</sup>, SIRT3 reduced within 4 h the acetylation level of CypA by about 80 %. In the absence of NAD<sup>+</sup>, SIRT3 had no effect on CypA acetylation level. In contrast, SIRT5 removed about 30% of CypA acetylation after 4 h. Native PAGE analysis of the reaction mixtures confirmed the western blot results (Figure 23B) and revealed SIRT3 as an effective deacetylase as well. This experiment also provided evidence that acetylation of CypA significantly alters the surface charge of the protein showing that nonacetylated CypA does not migrate in native PAGE whereas acetylated CypA does. CypA is a small 18 kDa protein and therefore it was easily separated from the acetylated forms using RP-HPLC (Figure A23). These data confirm our findings that CypA is modified mainly at a single lysine residue.



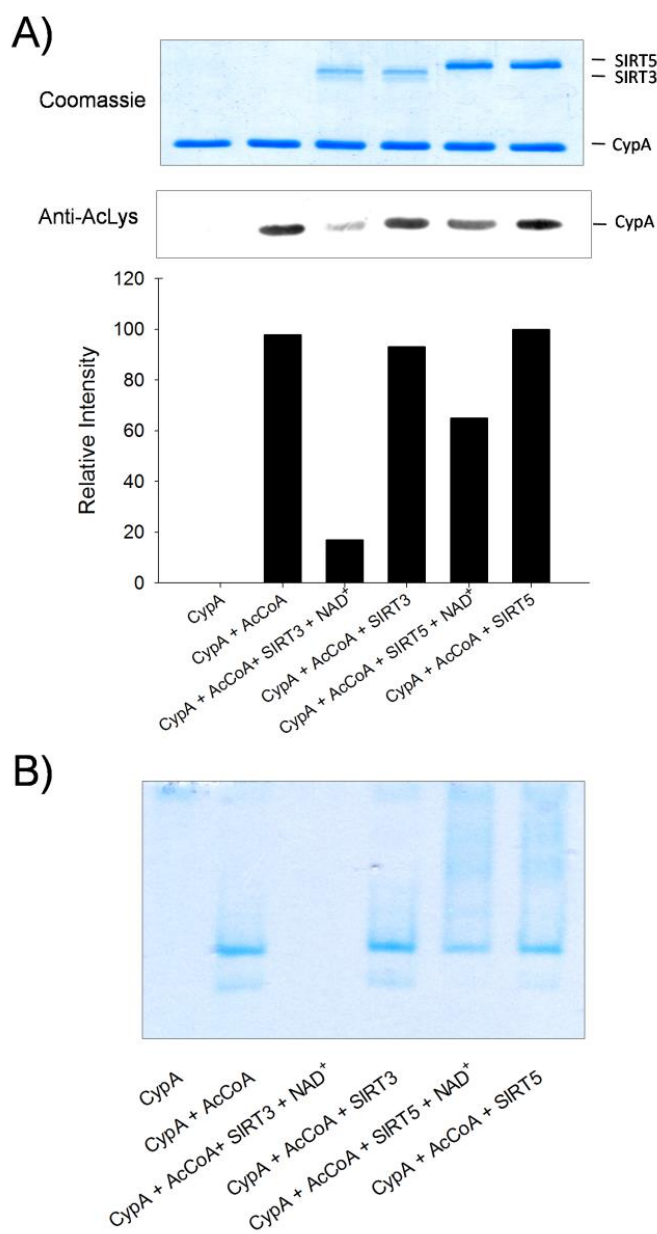


**Figure 23.** Deacetylation of acetylated CypA by mitochondrial sirtuins. **A)** Western blot analysis. CypA (10  $\mu$ M) was incubated with 4 mM Ac-CoA in 200 mM Tris-HCl buffer pH 8.0 for 24 h at 37°C. Incubation was continued for additional 4 h in the presence/absence of 1 mM NAD<sup>+</sup> and either 0.5  $\mu$ M SIRT3 (lanes 3 and 4) or 0.5  $\mu$ M SIRT5 (lanes 5 and 6). Aliquots were separated by SDS-PAGE followed by immunoblotting with antiacetylated-lysine antibody. Densitometric analysis of the Western blot by ImageJ software shows that SIRT3 efficiently deacetylates CypA (lane 3), whereas SIRT5 has only a slight effect (lane 5). In the absence of NAD<sup>+</sup>, neither SIRT3 nor SIRT5 deacetylate CypA (lanes 4 and 6). Controls: non-acetylated CypA (lane 1), and acetylated CypA not treated by sirtuin (lane 2). **B)** Analysis of deacetylation by native gel electrophoresis. Deacetylation reaction mixtures were separated by non-denaturing PAGE followed by Coomassie Blue staining. As only the acetylated form of CypA migrates in the gel, no CypA is detected for non-acetylated CypA (lane 1) or for CypA deacetylated by SIRT3 with NAD<sup>+</sup> (lane 3). Figure is adapted from Simic et al. 2015 with permission (Simic et al., 2015).

## Non-enzymatic succinylation of CypA

Next, we were interested if other acyl-CoA thioesters can also introduce modifications on lysine residues of CypA. Therefore, we incubated CypA with Succ-CoA under the same conditions as applied for Ac-CoA acetylation. CE and MS analysis revealed that succinylation of CypA lysine residues exceeded that of acetylation (Figures 24 and 25). The number of lysine residues modified by succinylation and their relative abundances were higher than for acetylation. This is consistent with the fact that modification of the CPS1 peptide by Succ-CoA was about 150 times faster than by Ac-CoA (Figure 14). In the case of CypA acetylation by Ac-CoA, twelve lysine residues were modified, whereas succinylation was observed for all fourteen lysine residues. Data for the two smallest tryptic peptides NGK(Succ)TSK and TSK(Succ)K (Table A4) representing succinylation at K151 and K154 respectively, were not reproducible so not considered for data analysis.

The patterns differed between acetylation and succinylation: CypA acetylation took place mainly at K155, whereas succinylation was observed at K28 and K82 to a high extent (Figure 24). Succinylation of the principal acetylation site K155 was marginal. The application of lower Succ-CoA concentrations also showed that Succ-CoA prefers other lysine residues in CypA than Ac-CoA. These results show that types of acylation strongly depend on the microenvironment of the target modification sites, and on the nature of the modifying thioester as well as on its concentration. All together, different acylation reactivities may form a specific acylation landscape on the protein surface. Acetylation neutralises the positive charge of the lysine. In the case of succinylation positive charge changes to negative charge which should have more effects on the protein global surface charge resulting in higher differences in migration times in CE (Figure 25).

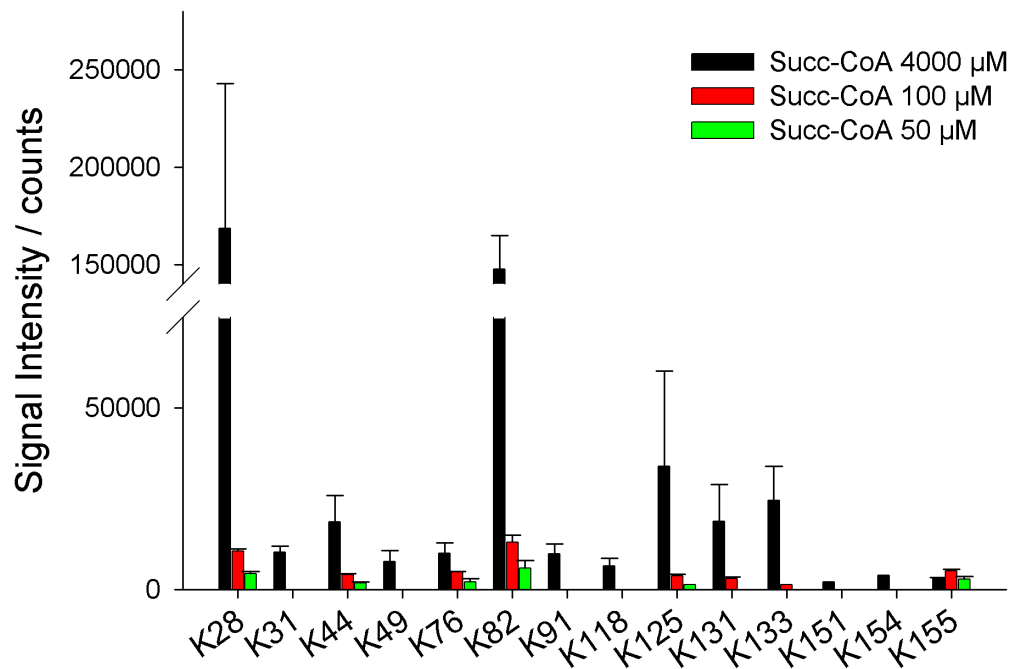


**Figure 24.** Analysis of the lysine succinylation pattern of CypA by LC-MS/MS. CypA (10  $\mu$ M) was incubated with Succ-CoA 4000  $\mu$ M (black), 100  $\mu$ M (red) and 50  $\mu$ M (green) in 200 mM Tris-HCl buffer pH 8.0 at 37°C for 24 h. Then, samples were subjected PAGE. CypA bands were cutted out and further processed by tryptic digestion followed by LC-MS/MS analysis. The relative intensities of the mass peaks reveal that all fourteen lysine residues in CypA can be non-enzymatically modified by Succ-CoA (highest for K28 and K82). Data are average  $\pm$  SD (n=3). Figure is adapted from Simic et al. 2015 with permission (Simic et al., 2015).

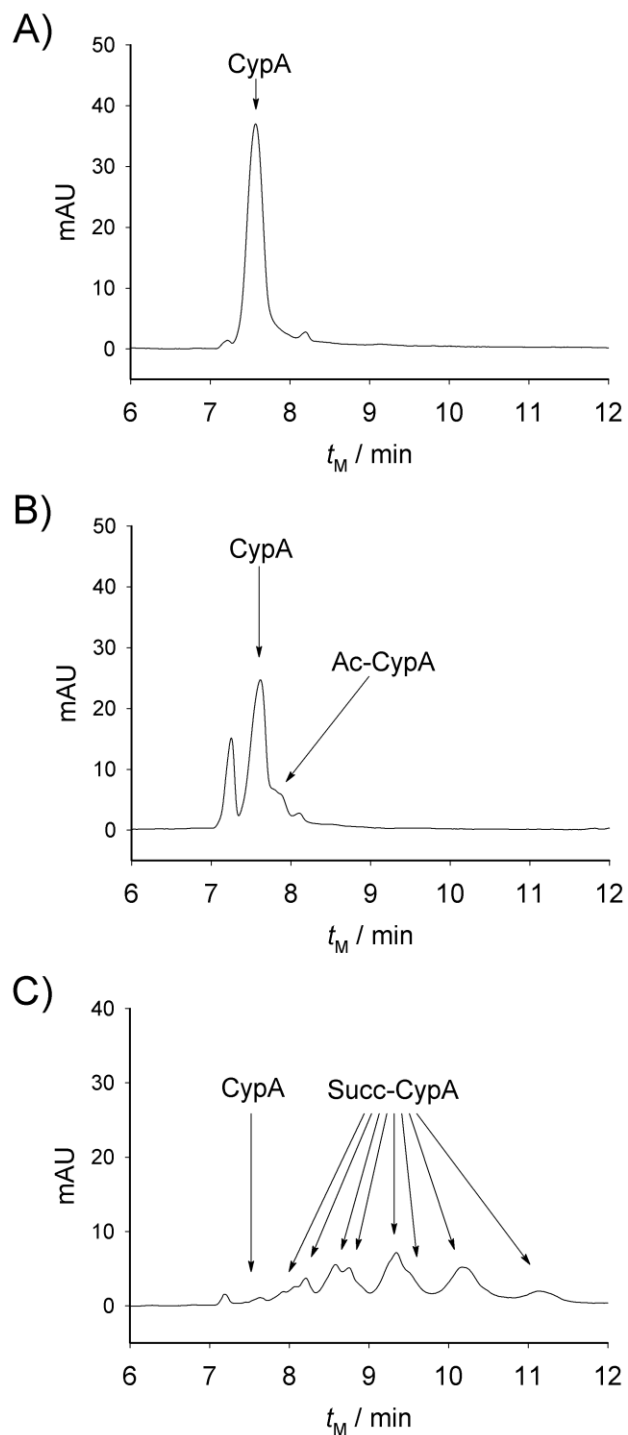


**Figure 25.** Analysis of CypA acylation by CE. **A)** Unmodified CypA (10  $\mu$ M), or **B)** CypA (10  $\mu$ M) acylated with Ac-CoA (4 mM), or **C)** 4 mM Succ-CoA. Acylation were carried out in 200 mM Tris-HCl buffer pH 8.0 containing TCEP (1mM) at 37°C for 24 h and subjected to CE (UV detection at 200 nm). The separation was carried out on a Bio-Rad uncoated silica capillary (50 cm  $\times$  50  $\mu$ m) at 25°C in sodium phosphate buffer applying 12 kV. CypA is almost completely succinylated by Succ-CoA, whereas modification by Ac-CoA was less efficient. Figure is adapted from Simic et al. 2015 with permission (Simic et al., 2015).

## Activity of acylated CypA

In order to check whether acylation of CypA alters the catalytic activity of the protein, peptidylprolyl cis/trans isomerase (PPIase) activity was measured subsequent to 24 h treatment with 4 mM Ac-CoA, Succ-CoA or CoA (control) at 37°C and pH 8.0. Acetylation did not significantly affect PPIase activity, whereas succinylation caused a ~25 % decrease (Figure 26). The moderate decrease in activity of CypA might be caused by succinylation of the K125 residue, which is positioned near the active site of the protein (Figure 27). It was previously shown that acetylation of this lysine led to a significant decrease in PPIase activity (Soe et al., 2014). An effect of K125 acetylation on the PPIase activity was not observed in our experiments probably because the amount of acetylated K125 was too low. The inhibitory effect of K125 succinylation on CypA activity could be explained by the fact that the succinyl moiety occupies more space than the smaller acetyl moiety, thus leading to steric hindrance at the active site. Moreover, succinyl-group introduce negative charge on the protein surface near its active site, which in turn can prevent binding efficiency of the substrate to the active site.

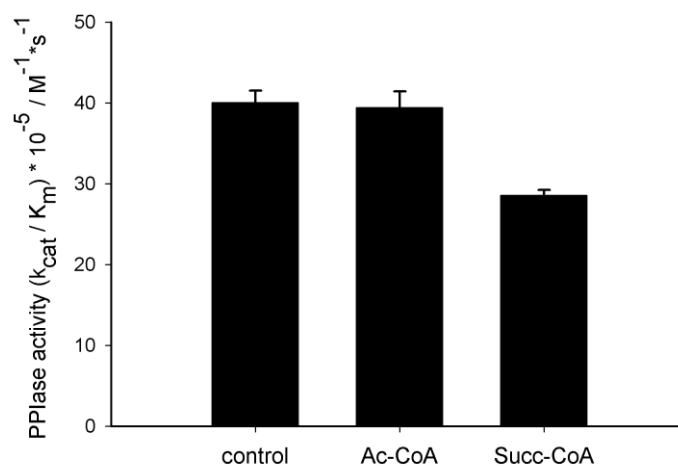


**Figure 26.** Effect of acylation on PPIase activity of CypA. The PPIase activity of CypA was determined using the protease-coupled PPIase assay as described by Fischer et al. (Fischer et al., 1989). The sample contained 5 nM CypA from the acylation mixtures and 40  $\mu$ M Suc-Ala-Ala-Pro-Phe-p nitroanilide as peptide substrate. After preincubation for 6 min at 10 °C in 35 mM HEPES buffer (pH 7.8), reaction was started by addition of the isomer specific protease chymotrypsin (final concentration 1 mg/ml) and the release of 4-nitroaniline was monitored by measuring the absorbance at 390 nm. The PPIase activity of CypA that was incubated with Succ-CoA for 24 h was decreased by 25 %, whereas incubation with Ac-CoA had no effect on PPIase activity. Control represents measurements with CypA treated with CoA. Measurements were performed by Dr. Matthias Weiwad. Figure is adapted from Simic et al. 2015 with permission (Simic et al., 2015).

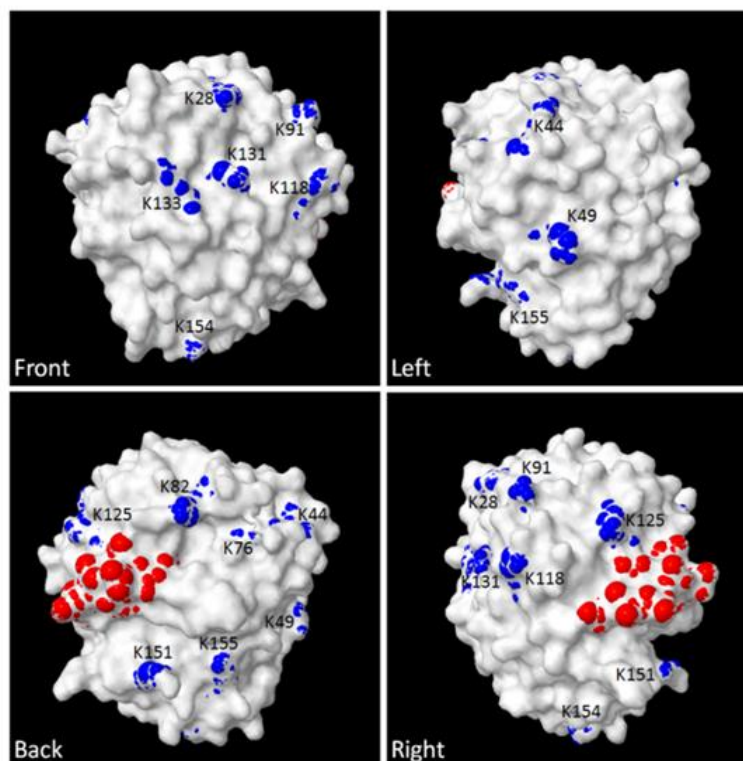


**Figure 27.** Location of lysine residues in the X-ray structure of CypA (PDB ID: 1BCK) in complex with the inhibitor cyclosporine A (**red**). All lysine residues (**blue**) are on the surface of the protein. Residue K125 is near the active site. Figure is adapted from Simic et al. 2015 with permission (Simic et al., 2015).

## Structural alterations of acylated CypA

Additionally, we were interested in whether acylation of CypA affects the folding of the protein. CD spectroscopy revealed that treatment of CypA with Ac-CoA or Succ-CoA did not affect the protein folding. Moreover, the similar shapes of the CD spectra indicate that acylation does not affect the secondary structure of the protein (Figure 28). Most of the lysine residues are located in the random coil, only K31 is located in the  $\alpha$ -helix and K131 and K133 are located in the  $\beta$ -strand (Figure 29). These lysines residues were not significantly modified neither acetylated or succinylated. Fluorescence spectroscopy shows that highly modified lysine residues may cause negligible changes in the protein conformation (Figure A24) but as it was shown by CD spectroscopy secondary structures remain unaltered.

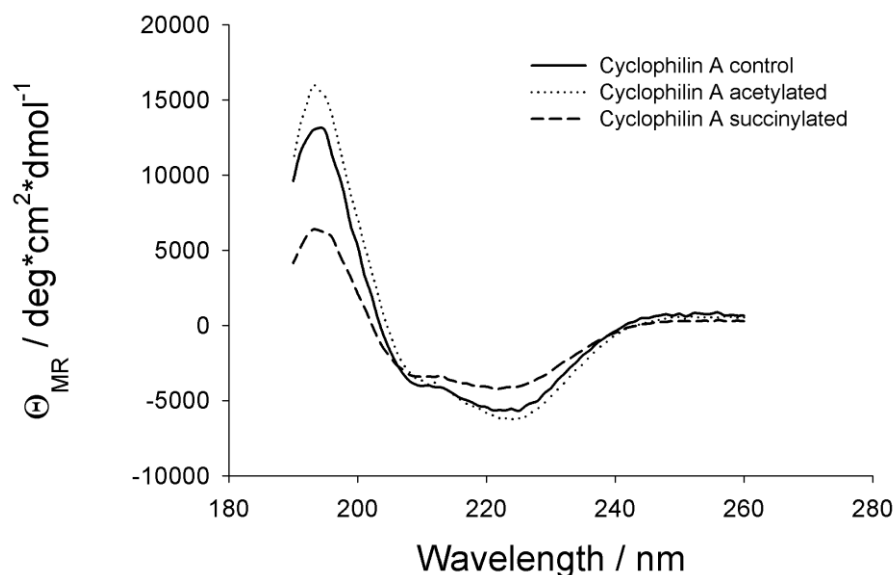


**Figure 28.** Analysis of acylated CypA by CD spectroscopy. CypA was incubated with Ac-CoA or Succ-CoA for 24 h at 37 °C and pH 8.0. Then, samples were dialyzed against 20 mM sodium phosphate buffer pH 7.3. Spectra were recorded with an Aviv Biomedical Circular Dichroism Spectrometer, Model 430 at 25°C. CD spectra show that incubation with Ac- or Succ-CoA does not alter the folding of the protein. Figure is adapted from Simic et al. 2015 with permission (Simic et al., 2015).

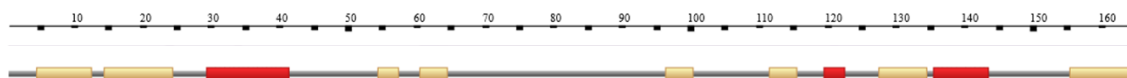


**Figure 29.** Organization of the secondary structure of the CypA. PDB: 1BCK.  $\alpha$ -helix was marked in red,  $\beta$ -strand in dark yellow and random coil in grey. Figure adapted from <http://www.rcsb.org/pdb/protein/P62937>.

## Desuccinylation of succinylated CypA by mitochondrial sirtuins

We wanted to know if mitochondrial lysine deacetylase are able to desuccinylate CypA lysine residues. Succinylated CypA was incubated with either SIRT3 or SIRT5. Our MS data show that SIRT3 was not able to remove any succinyl moiety, but SIRT5 was an effective protein desuccinylase (Figure 30). SIRT5 efficiently removed the succinylation from seven of the twelve investigated lysine residues, but K44 and K155 were only slightly desuccinylated, and there was no activity towards K28, K131, or K133, thus confirming again that SIRT5 exhibits some sequence specificity for succinylated lysine side chains

(Lakshminarasimhan et al., 2013; Rauh et al., 2013) or these lysine were sterically hindered and therefore protected from sirtuin action. These results confirm previous findings that sirtuins differ in their acyl specificity.

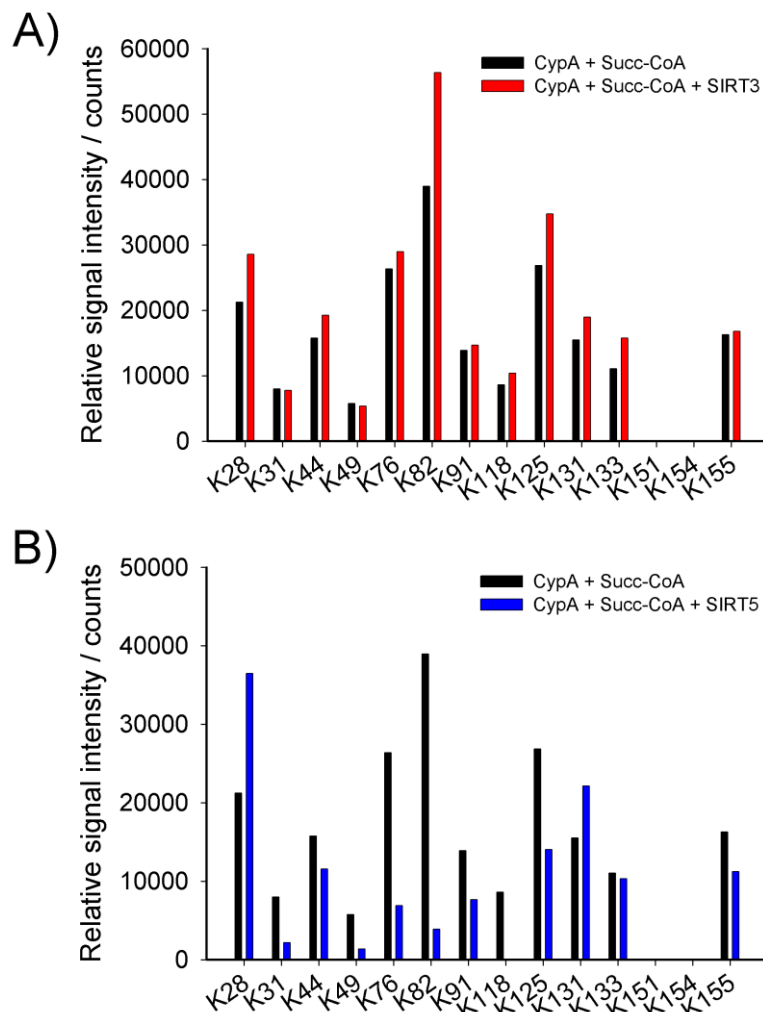


**Figure 30.** Desuccinylation of CypA by SIRT3 and SIRT5. CypA (10  $\mu$ M) was incubated with 4 mM Succ-CoA in Tris-HCl buffer pH 8.0 at 37°C. After 24 h  $\text{NAD}^+$  (1 mM), DTT (1 mM),  $\text{MgCl}_2$  (5mM), SIRT3 (0.5  $\mu$ M) or SIRT5 (0.5  $\mu$ M) were added. Incubation was continued for additional 4 h at 37°C. After that, samples were subjected to PAGE. CypA bands were cutted out and further processed by tryptic in gel digestion followed by LC-MS/MS analysis. Data represent signals normalized to the first non modified tryptic peptide of the CypA sequence (MVNPTVFFDIAVDGEPLGR). **A)** Desuccinylation of modified CypA by SIRT3. The figure shows that SIRT3 was not able to remove any of the succinyl groups from CypA. **B)** Desuccinylation of modified CypA by SIRT5. The resulting plot shows that SIRT5 efficiently removed the succinyl residues from seven of the twelve modified lysine residues of CypA. Two residues, K44 and K155, were only slightly desuccinylated, whereas SIRT5 showed no activity towards the succinylated lysine residues K28, K131, and K133. Figure is adapted from Simic et al. 2015 with permission (Simic et al., 2015).



Next, we investigated whether SIRT5 is able to completely prevent succinylation of CypA. CypA was incubated with succ-CoA in the presence of SIRT5 with or without NAD<sup>+</sup>. CE analysis shows that SIRT5 was able to protect CypA against succinylation but not completely (Figure 31). Some of the residue, most likely K28, K131 or K133 still undergoes succinylation even in the presence of SIRT5 and NAD<sup>+</sup>. In the absence of NAD<sup>+</sup> SIRT5 was not able to remove any of the succinyl-groups from the lysine residues. K131 and K133 were not identified as a site of succinylation *in vivo* so far, but interesting is that K28 is found to be succinylated in mouse liver (Weinert et al., 2013).

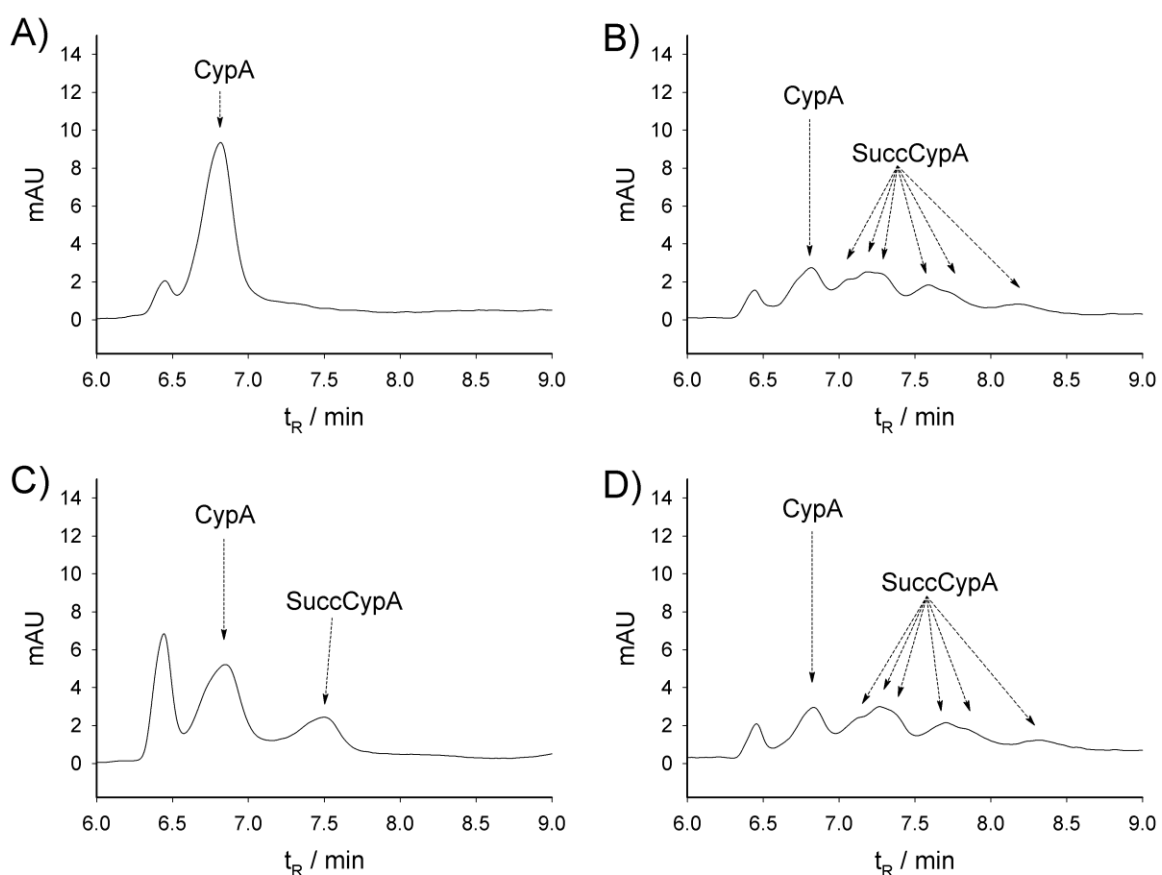


**Figure 31.** Desuccinylation of CypA by SIRT5 followed by CE. CypA (10  $\mu$ M) was incubated with 4 mM Succ-CoA, 0.5  $\mu$ M SIRT5 and with or without 1 mM NAD<sup>+</sup> in 200 mM Tris-HCl buffer pH 8.0 containing MgCl<sub>2</sub> (5 mM) and TCEP (1 mM) at 37°C overnight. **A)** Unmodified CypA. **B)** Reaction mixture contains CypA and Succ-CoA. **C)** Reaction mixture contains CypA, Succ-CoA, SIRT5 and NAD<sup>+</sup>. **D)** Reaction mixture contains CypA, Succ-CoA, SIRT5 but no NAD<sup>+</sup>.

## Acylation of CypA as a function of the lysine $pK_a$ values

There are a variety of ionizable groups on the protein surface including the side chain of Lys, Arg, His, Asp, Glu, Tyr and Cys. These amino acids play a key role in the protein stability, sub-cellular localization, protein-ligand and protein-protein interactions and enzyme activity (Garcia-Moreno, 2009). Most of these residues represent targets for different posttranslational modifications such as lysine acylation, arginine methylation or tyrosine phosphorylation (Cozzzone, 1988; Greer and Shi, 2012; Vidali et al., 1968). Thus,  $pK_a$  values of the ionizable groups represent crucial parameters for characterization and understanding different biological phenomena.  $pK_a$  value of the side chain of a single amino acid differ compared to one incorporated in the protein backbone. Such differences, are caused mostly by micro-environment, and usually strongly depend on protein conformation. In the polar microenvironment  $pK_a$  values are similar to the values found in water, but in a micro-environment which is less polar  $pK_a$  value shifts mostly to neutral state (Isom et al., 2011). The ionization state primarily depends on the pH. This is the reason why intracellular regulation of pH is one of the most important points of all living organisms including even the primitive ones.

Determination of  $pK_a$  can be a useful tool for understanding the basics of many biochemical processes.  $pK_a$  values can be experimentally determined (Dwyer et al., 2000; Harms et al., 2009; Karp et al., 2007) or theoretically predicted (Antosiewicz et al., 1994, 1996; Bashford and Karplus, 1990; Mehler and Guarnieri, 1999; Yang et al., 1993) using biophysical and mathematical based approach for every single lysine in the protein.

The lysine residue has an ionizable  $\epsilon$ -amino group on its side chain with a  $pK_a$  value of 10.5 (Nolting et al., 2007). We used PRO 3.1 software to determine lysine  $pK_a$  values of the CypA protein. PROPKA predicts the  $pK_a$  values of ionizable groups in proteins and protein-ligand complexes based on its 3D structure (free available at <http://propka.org>). All CypA lysine residues with predicted  $pK_a$  values are listed in a Table 3.

**Table 3.** pK<sub>a</sub> values of the CypA lysine residues. PDB: 3K0N

Lys position	pK <sub>a</sub>
K28	10.58
K31	11.33
K44	10.55
K49	10.90
K76	10.34
K82	10.36
K91	10.49
K118	10.73
K125	10.30
K131	10.50
K151	10.42
K154	10.51
K133	10.57
K155	10.60

As mentioned before, ionization state of the lysine side chain strongly depend on solution pH, and therefore on the pK<sub>a</sub> values of the  $\epsilon$ -amino group of the lysine side chain. Next, we wanted to find out if there is any correlation between lysine pK<sub>a</sub> and acylation status of the CypA. We plotted lysine pK<sub>a</sub> values and natural logarithm of the signal intensity (counts) for succinylation and acetylation (Figure 32).

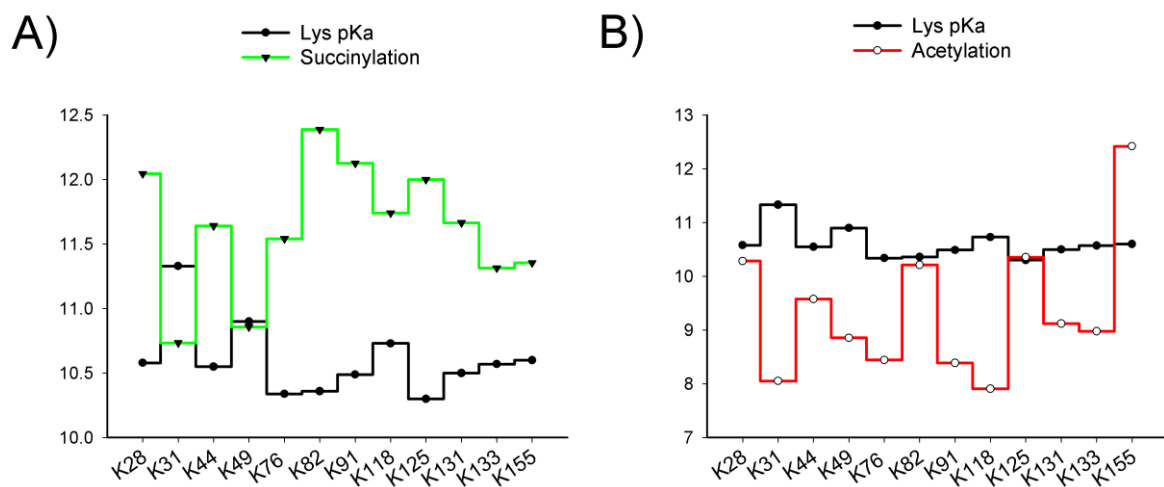


**Figure 32.** Lysine acylation as a function of lysine pK<sub>a</sub>. CypA was acetylated and succinylated as described above. Natural logarithm of signal intensities was plotted against lysine pK<sub>a</sub> values. A plot of CypA **A)** succinylation and **B)** acetylation as a function of lysine pK<sub>a</sub>.

Succinylation of CypA correlate well with the lysine pK<sub>a</sub> values. The lysines with the lowest pK<sub>a</sub> values, K28, K76, K82, K91, and K125 show the highest succinylation intensity. On the other hand, lysines with highest pK<sub>a</sub> values K31 and K49 show less effective succinylation. Lysines with high pK<sub>a</sub> values are occur mostly in protonated form, thus are less reactive. Succinylation pattern (Figure 32A) looks like a mirror image of the pK<sub>a</sub> pattern. Acetylation also correlates well with lysine pK<sub>a</sub>, with few exceptions (Figure 32B). Lysines with highest pK<sub>a</sub> values K31, K49 and K118 show low acetylation intensity. Lysines with low pK<sub>a</sub> values such as K28, K82 and K125 show higher acetylation. Surprisingly, lysine K155 has the average pK<sub>a</sub> and the highest intensity of acetylation. These data support our hypothesis of the existence of super reactive lysine residues within a protein.

## Shift of acylation type by simultaneous action of SIRT3 and Succ-CoA

As it was shown before, acylation largely depends on reactivity and concentration of acyl-CoA thioesters. Additionally it also strongly depends on availability and acyl specificity of the lysine deacetylase. Here, we wanted to test whether simultaneous action of an acyl-specific deacetylase and an acyl-thioester can change the type of lysine acylation (changing the acylation landscape). In this experiment we simulated metabolic conditions in order to test the possibility of replacement of one type of acylation with another. We incubated acetylated CPS1 peptide with the acetyl-specific deacetylase SIRT3 and cosubstrate NAD<sup>+</sup>, in the absence or presence of Succ-CoA. Analysis of the reaction mixture by RP-HPLC revealed that in the absence of Succ-CoA the peptide was deacetylated after 72 h, whereas in the presence of Succ-CoA it was almost completely converted into the succinylated form (Figure 33). Only a small fraction of the peptide was in the non-acylated form. These results suggest that both the concentrations of distinct acyl-CoAs and the acyl-specificity of sirtuin type deacetylases determine the acylation landscape in cells. Additionally, SIRT3 was not just able to keep peptide in its deacetylated form, SIRT3 activity yielded increased succinylation of lysine side chains when Succ-CoA was present.

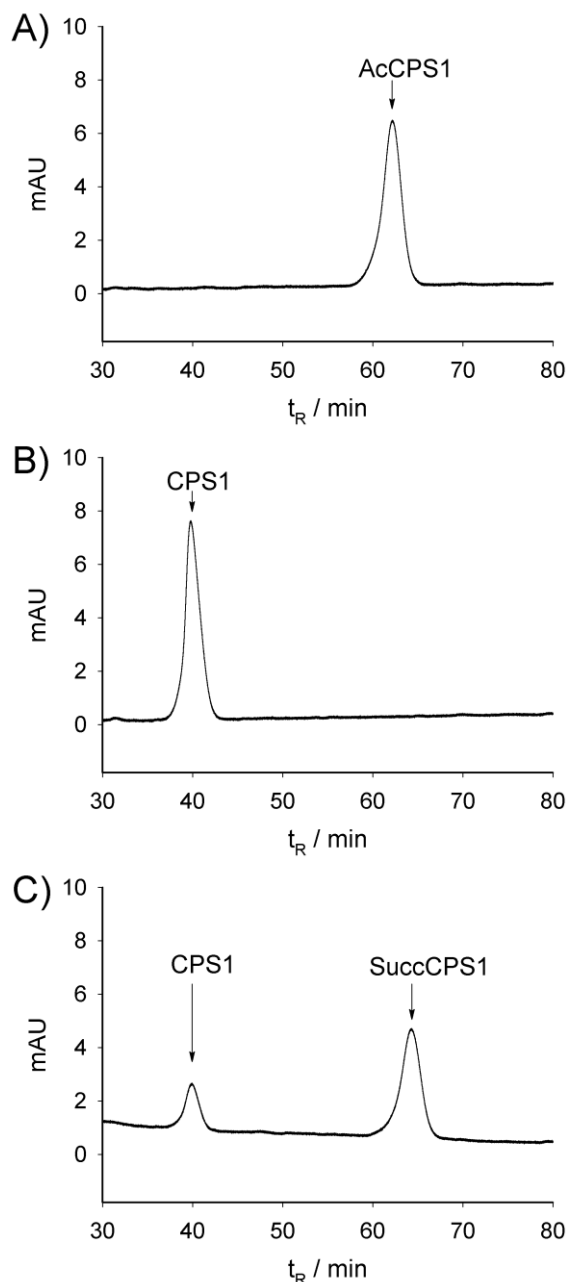


**Figure 33.** Shift in “Acylation landscape” caused by the simultaneous action of specific sirtuin deacetylase and acyl-thioester. The figure shows HPLC analysis of **A)** acetylated CPS1 peptide as well as acetylated CPS1 (100  $\mu$ M) peptide that was incubated for 72 h at 37  $^{\circ}$ C with 1  $\mu$ M SIRT3, and 500  $\mu$ M  $\text{NAD}^+$  either in the **B)** absence or **C)** presence of 4 mM succinyl CoA. In order to ensure equal conditions over the time course of the experiment the concentrations of  $\text{NAD}^+$  and Succ-CoA were kept constant by adding fresh aliquots. Reaction mixtures were separated by RP-HPLC, a linear gradient 20 – 40 % (v/v) ACN over 240 min was used. Detection was performed at 260 nm. The identity of the resulting peaks was determined by MALDI-TOF-MS. The figure demonstrates that the major part of the acetylated CPS1 peptide is converted into the succinylated form in the presence of an active deacetylase and Succ-CoA. Figure is adapted from Simic et al. 2015 with permission (Simic et al., 2015).

## Expanding acyl specificity of SIRT4

As it was mentioned before, SIRT3 represent a main mitochondrial lysine deacetylase and SIRT5 is responsible for removing succinyl, malonyl and glutaryl moieties from the lysine residues. Very little is known about the substrate specificity of the third mitochondrial sirtuin, SIRT4. Different studies describe SIRT4 as a very weak lysine deacetylase (Mathias et al., 2014; Rauh et al., 2013), giving preferences to ADP-ribosylation as a main function of SIRT4 (Ahuja et al., 2007; Haigis et al., 2006).

In order to investigate SIRT4 acyl specificity, we employed the HPLC assay to test different CPS1 peptide derivatives. We found a very weak activity against acetyl, HMG and octanoyl modification and no activity against formyl-CPS1 substrate. Based on the crystal structure of SIRT4 (crystal structure was done by our collaboration partner AG Prof. Clemens Steegborn, University Bayreuth, Bayreuth, Germany, data are not presented) it is obvious that its active site allows accommodation of a more voluminous acyl-group. For further investigations we synthesized different peptides derived from TNF $\alpha$  protein (Figure 34), which have been already used either as model peptide substrate or inhibitors in different sirtuin studies (He et al., 2014; Jiang et al., 2013; Teng et al., 2015).

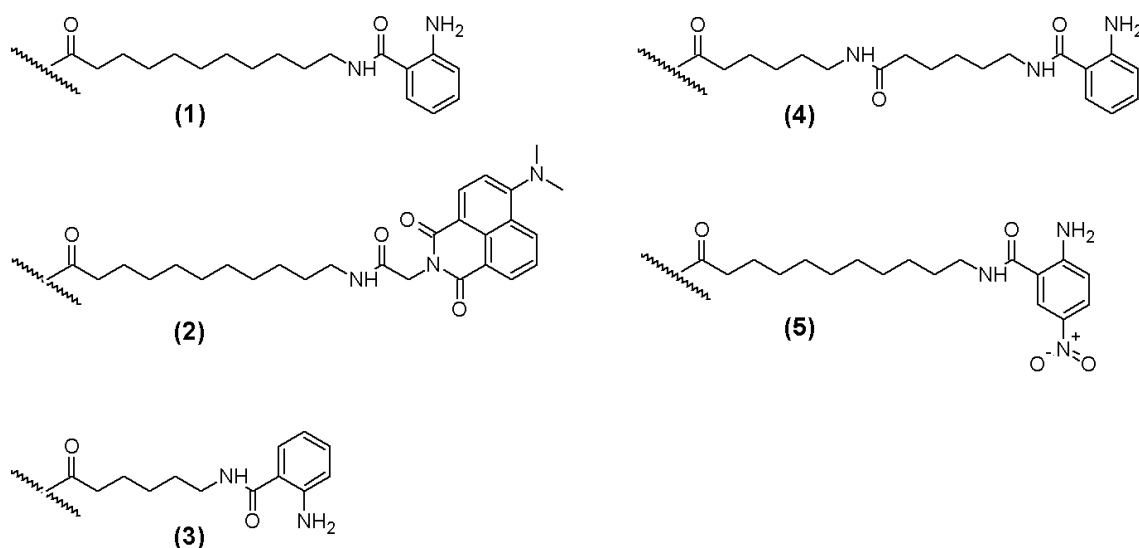


**Figure 34.** Structure of synthesized TNF $\alpha$  peptide substrates. Peptide sequence Ac-EALPKK(X)Y(NO<sub>2</sub>)GG-NH<sub>2</sub> was derived from the TNF $\alpha$  protein. X = different lysine modifications.

Compounds were subjected to HPLC assay to determine whether SIRT4 accept them as a substrate. As it was predicted according to crystal structure three of five peptides were recognized as a substrate by SIRT4 enzyme (Figure 35).

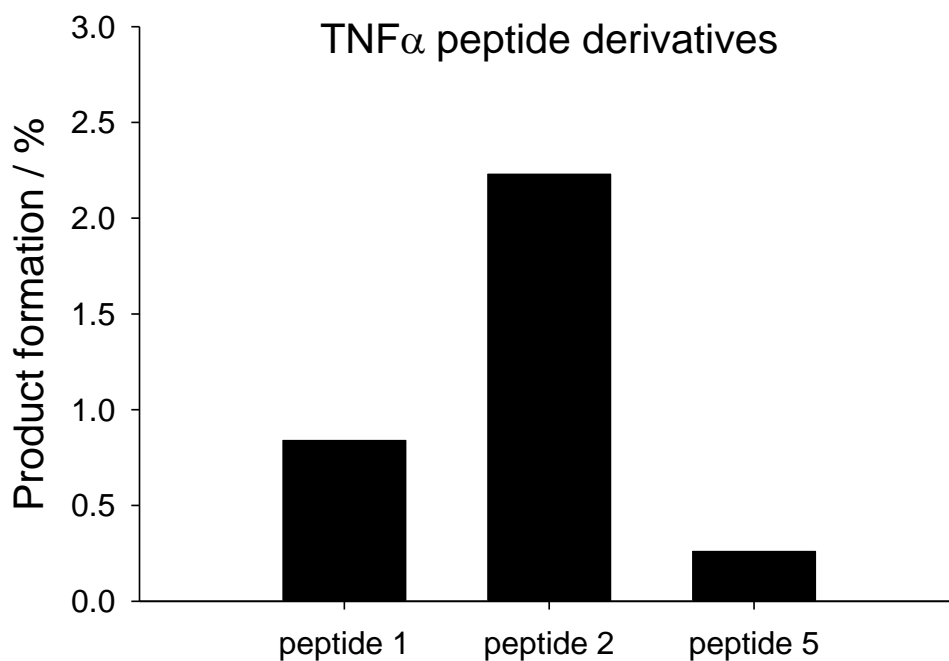


**Figure 35.** HPLC based assay of TNF $\alpha$  peptide substrates for SIRT4. 100  $\mu$ M peptides were incubated in assay buffer (20 mM TRIS-HCl pH 7.8, 150 mM NaCl, 5 mM MgCl<sub>2</sub>), containing 500  $\mu$ M NAD<sup>+</sup> and 1 $\mu$ M SIRT4. Reaction mixtures were incubated at 37°C. After 60 min reaction was stopped by adding TFA (1%, v/v) and subjected to HPLC analysis.

TNF $\alpha$  peptide substrates are specially designed to allow us to follow reaction by following changing in fluorescence intensity (Schuster et al., 2016). All peptides contain fluorophores such as Abz or Dma, which are quenched by nitrotyrosine (Meldal and Breddam, 1991; Schuster et al., 2016). Subsequent to enzymatic action of sirtuin, fluorophore is separated from the quencher moiety resulting in increased fluorescence intensity. Using this fluorescence-based activity assay we were able to determine the kinetic parameters for SIRT4 and TNF $\alpha$  substrates 1 and 2 (Figure 36). Kinetic constants are listed in Table 4.

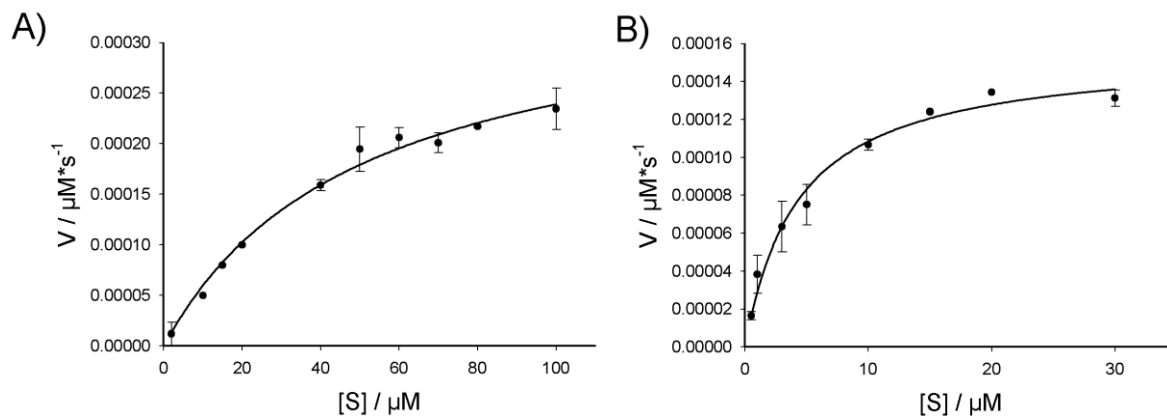


**Figure 36.** Michaelis-Menten plots of TNF $\alpha$  substrate 1 and 2 for SIRT4. Reactions were performed in 20 mM Tris-HCl buffer pH 7.8, 150 mM NaCl, 5 mM MgCl<sub>2</sub> containing 500  $\mu$ M NAD<sup>+</sup> and 1  $\mu$ M SIRT4 and varying concentrations of **A)** TNF $\alpha$  peptide 1 and **B)** TNF $\alpha$  peptide 2. TNF $\alpha$  peptide 1 measurements were performed on fluorescence microtiter plate reader and TNF $\alpha$  peptide 2 on fluorescence spectrophotometer. Data represent means  $\pm$  S.D. (n=2). Figure is adapted from Schuster et al. 2016 (Schuster et al., 2016).

**Table 4.** Kinetic constants for TNF $\alpha$  peptide 1 and 2 and SIRT4. Data represent mean  $\pm$  S.D. (n=2)

SIRT4 substrate	$K_M$ ( $\mu$ M)	$k_{cat}$ ( $s^{-1}$ )	$k_{cat}/K_M$ ( $M^{-1}*s^{-1}$ )
TNF $\alpha$ peptide 1	49.5 $\pm$ 7.5	3.6 *10 <sup>-4</sup> $\pm$ 0.2 *10 <sup>-4</sup>	7.00
TNF $\alpha$ peptide 2	4.32 $\pm$ 0.67	1.6 *10 <sup>-4</sup> $\pm$ 0.1*10 <sup>-4</sup>	35.93



## Enzymatic lysine acetylation

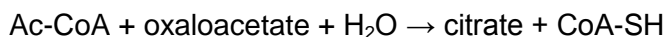
Mitochondria show highest level of acetylation but conventional lysine acetyltransferases are not identified so far. Few attempts were done to assign the existing phenomenon of mitochondrial protein acetylation to a few mitochondrial enzymes, like GCN5L1 (Scott et al., 2012) or ACAT1 (Fan et al., 2014). One part of this study was directed toward the search of an enzyme located in mitochondria with so far undetected lysine acetyltransferase activity. Special focus was on already known metabolic enzymes which use Ac-CoA as a cosubstrate assuming that such enzymes have intrinsic lysine acetyltransferase activity. After intensive literature searching including human metabolome database ([www.hmdb.ca](http://www.hmdb.ca)) we made a short list of the candidates (Table 5). The main criteria were that the enzyme is found in mitochondria, is widely expressed and directly or indirectly uses Ac-CoA as a cofactor/cosubstrate.

**Table 5.** Selected mitochondrial enzymes which use Ac-CoA as a cosubstrate.

CS	Citrate synthase, mitochondrial
ACAT1	Ac-CoA acetyltransferase, mitochondrial
HMGCS2	Hydroxymethylglutaryl-CoA synthase, mitochondrial
CRAT	Carnitine O-acetyltransferase
ACS	Acetyl-CoA synthetase
SAT1	Diamine acetyltransferase 1

### Citrate synthase

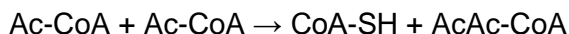
Citrate synthase (CS) is an enzyme involved in the first step of the TCA cycle (Goldenthal et al., 1998). It is present in nearly all living organisms, located in the mitochondrial matrix. CS catalyzes the reaction of condensation of Ac-CoA and oxaloacetate to form citrate thereby releasing free CoA as one product.



We have tested CS (Pig, *Sus domesticus*) as a potential lysine acetyltransferase using a peptide microarray assay. Acetylation reaction was performed in 200 mM Tris-HCl buffer pH 8.0 containing 1 mM Ac-CoA and 0.25 mg/ml CS at 37°C for 2 h. We did not find any lysine acetylation activity for CS under the conditions we used.

## Acetyl-CoA acetyltransferase, mitochondrial

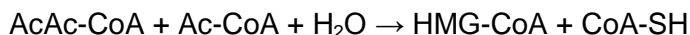
Acetyl-CoA acetyltransferase, mitochondrial (ACAT1) is the enzyme located in the mitochondrial matrix involved in the first step of the ketone bodies synthesis pathway (Fukao et al., 1990; Kano et al., 1991). The enzyme catalyses the following reaction:



It has already been described to have lysine acetylated activity against PDHA1 at lysine K321 and PDP1 at lysine K202 (Fan et al., 2014). We used our acetylome peptide microarray displaying more than 5000 peptides derived from human acetylation sites (Rauh et al., 2013). Acetylation reaction was performed in 40 mM Tris-HCl buffer pH 8.0 containing 75 mM KCl, 1 mM Ac-CoA and 0.2 mg/ml ACAT1 (Human recombinant, ATGEN) at 30°C for 2 h. Our results clearly show that ACAT1 is not able to transfer acetyl the group from Ac-CoA to the amino-group of the lysine residues of the presented peptides.

## Hydroxymethylglutaryl-CoA synthase, mitochondrial

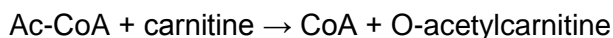
Hydroxymethylglutaryl-CoA synthase, mitochondrial (HMGCS2) is an enzyme located in the mitochondrial matrix and involved in the second step of the ketone bodies synthesis pathway (Boukaftane and Mitchell, 1997; Mascaró et al., 1995). The enzyme catalyses the following reaction:



We have tested HMGCS2 (Human recombinant, Abnova) as a lysine acetyltransferase using a peptide microarray assay. Acetylation reaction was performed in 200 mM Tris-HCl buffer pH 8.0 containing 1 mM Ac-CoA and 0.25 μM HMGCS2 at 30°C for 2 h. We did not find any acetylation activity for HMGCS2.

## Carnitine O-acetyltransferase

Carnitine O-acetyltransferase (CRAT) catalyzes the following reaction:



The enzyme is located in the mitochondria and is involved in the transport of short acyl groups from the cytosol into the mitochondrial matrix (Corti et al., 1994; Wu et al., 2003).

A peptide microarray experiment was performed in 100 mM Tris-HCl buffer pH 8.0 containing 1 mM Ac-CoA or 1 mM O-Ac-carnitine, and 3.2  $\mu$ M CRAT (Pigeon, *Columbidae*). We found that neither Ac-CoA nor O-Ac-carnitine can serve as acetyl group donor for the lysine acetyltransferase reaction mediated by CRAT. Our data revealed that CRAT is not able to act as a lysine acetyltransferase.

## Acetyl-CoA synthetase

Acetyl-CoA synthetase (ACS) is a well conserved enzyme found in a variety of living organisms from bacteria to humans (Campagnari and Webster, 1963; Frenkel and Kitchens, 1977; Karan et al., 2001; Yamashita et al., 2002). ACS catalyses the reaction of conversion of acetate into Ac-CoA which can be further consumed in the TCA cycle, in fatty acids synthesis (Fujino et al., 2001; Howard et al., 1974), ketone bodies synthesis or protein acetylation (Jaworski et al., 2016; Takahashi et al., 2006). ACS catalyzes the following reaction:



There are two iso-forms of the ACS enzymes in mammals, mitochondrial (ACSS2) and nucleo-cytosolic (ACSS1) iso-form (Fujino et al., 2001). Mitochondrial ACS is highly regulated through reversible acetylation of lysine residues in the active site of the enzyme mediated by SIRT3 (Schwer et al., 2006). It has been shown that ACS under low level of oxygen can drive the reaction in a direction of acetate production. This mechanism provides energy production and survival of tumor cells under hypoxia conditions (Yoshii et al., 2009).

Nucleo-cytosolic ACS is essential for histone acetylation and global transcription in the nucleus (Takahashi et al., 2006). It has been shown that ACS represents a rate limiting factor for histone acetylation. This raises the question if it happens just by simply providing Ac-CoA for histone acetyltransferase or if ACS possesses its own capability to modify histone proteins.

We incubated CPS1 peptide with ACS (*S. cerevisiae*) in Tris-HCl buffer pH 8.0 containing  $\text{Mg}(\text{CH}_3\text{COO})_2$ , ATP and CoA at 37°C. At different time points, reaction mixture

was analyzed by RP-HPLC. We observed a new peak at  $t_R = 8.88$  min rising over time (Figure 37A). Product formation shows linear dependence over time (Figure 37B). And indeed, the new peak was confirmed to be an acetylated CPS1 peptide (Figure 37C). It is important to note that reaction in the opposite direction does not give any acetylated peptide product.

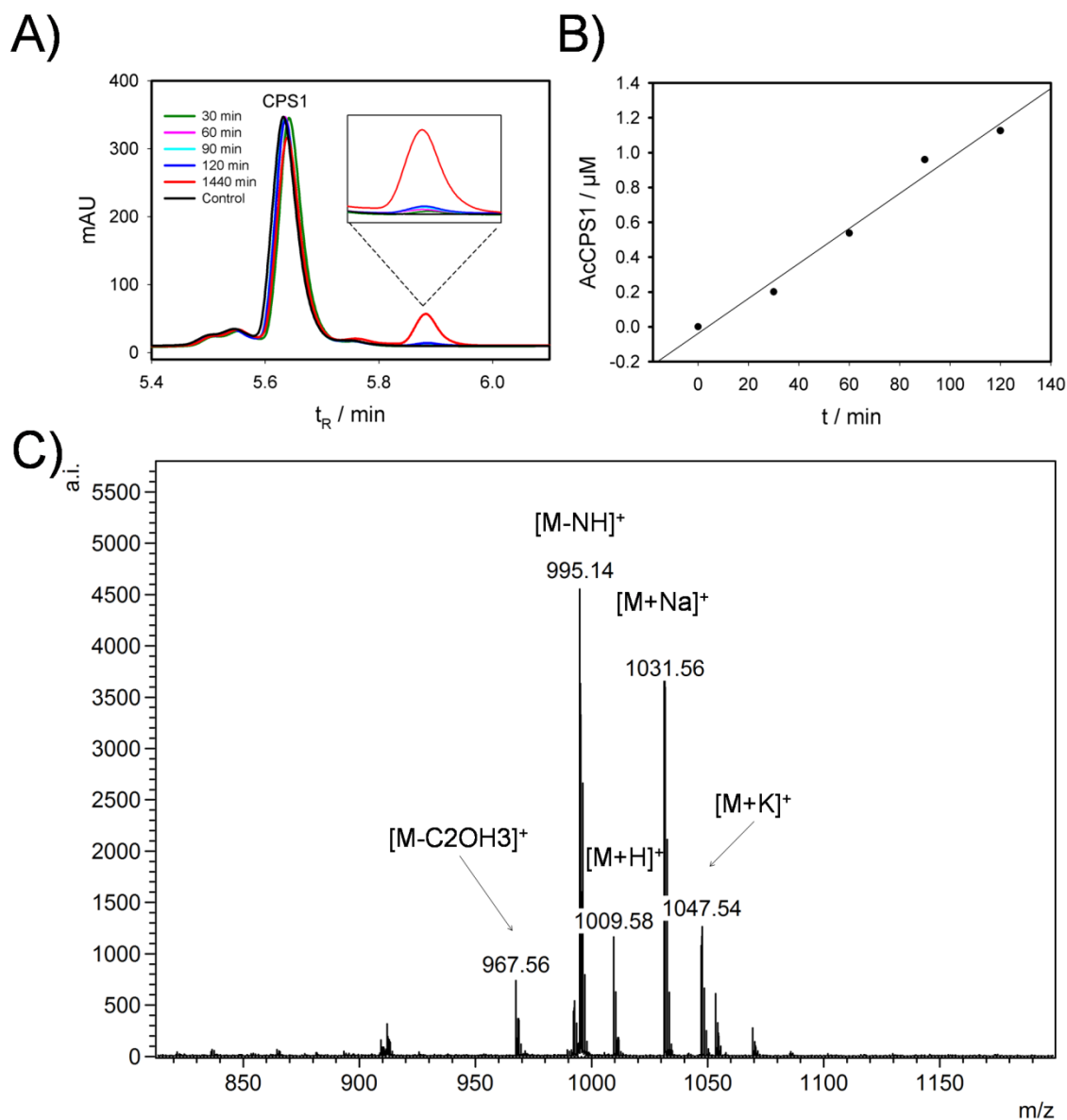


**Figure 37.** Acetylation of CPS1 peptide by ACS. CPS1 peptide (200  $\mu\text{M}$ ) was incubated in 100 mM Tris-HCl buffer pH 8.0 containing  $\text{Mg}(\text{CH}_3\text{COO})_2$  (10 mM), ATP (4 mM), CoA (150  $\mu\text{M}$ ) and ACS (0.1 mg/ml) at 37°C over time. **A)** At different time intervals reaction mixture was analyzed by RP-HPLC with detection at 260 nm. **B)** Amount of product plotted against time. **C)** Product peak at  $t_R = 5.88$  was identified as a acetylated CPS1 peptide using MALDI-TOF MS.

Reaction of condensing acetate and CoA to form Ac-CoA by ACS take place in two steps (Webster, 1967; Webster and Arsena, 1963). In the first step Ac-AMP is formed, which is used in the second step as acetyl group donor for CoA. It has already been shown that Ac-AMP can modify proteins non-enzymatically *in vitro* (Ramponi et al., 1975). Next, we wanted to investigate, whether acetylated CPS1 peptide was formed by the enzymatic activity of ACS or was non-enzymatically generated by the intermediate Ac-AMP. Therefore, Ac-AMP was incubated with CPS1 peptide under the same conditions as in the enzyme catalyzed reaction and indeed we found that acetylated CPS1 product was formed even in the absence of ACS (Figure 38).

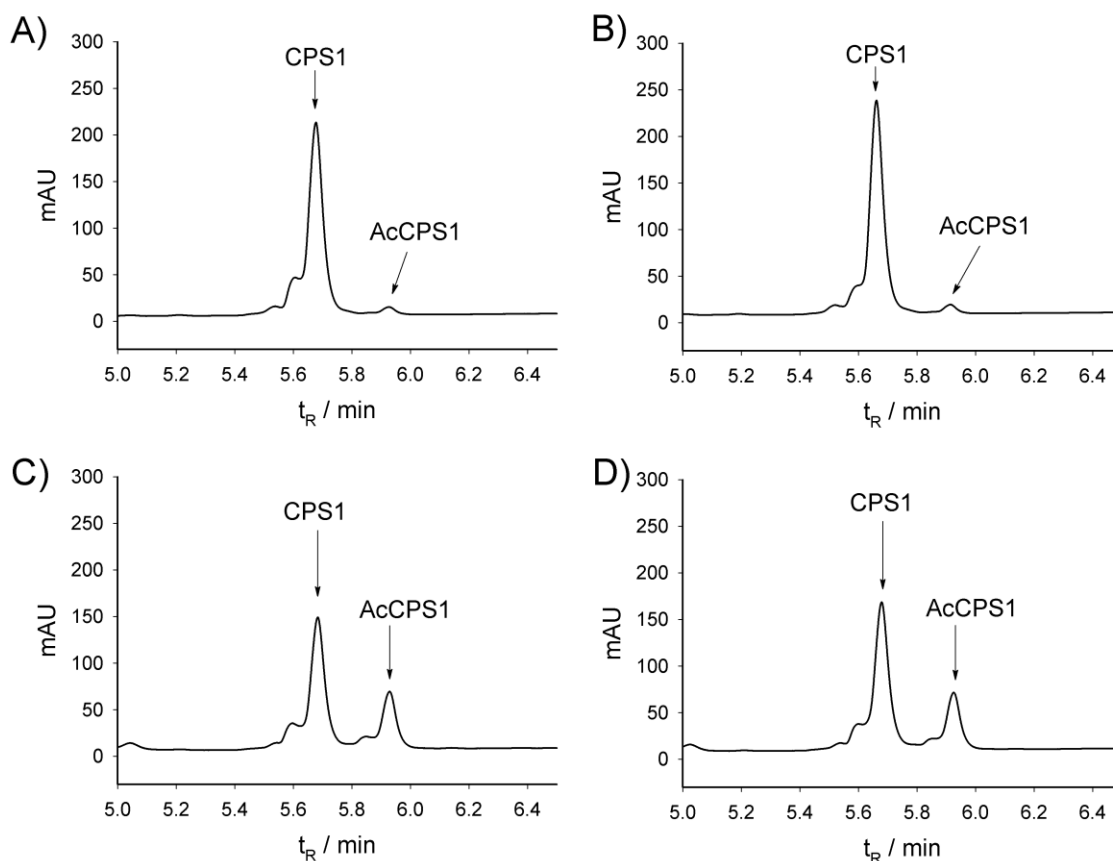


**Figure 38.** Acetylation of CPS1 peptide by Ac-AMP. CPS1 peptide (100  $\mu$ M) was incubated in 200 mM Tris-HCl buffer pH 8.0 containing 5 mM  $MgCl_2$ , 0.4 mM Ac-AMP **A**), **B**) or 4 mM Ac-AMP **C**), **D**) and 1 mg/ml ACS **B**), **D**). After 10 min incubation at 37°C reaction mixtures were analyzed by RP-HPLC with detection at 260 nm. Acetylated CPS1 product was detected at  $t_R = 5.88$  min.

These data revealed that Ac-AMP successfully acetylates CPS1 peptide non-enzymatically. ACS is not able to use Ac-AMP as acetyl donor for peptide acetylation. Acetylation of CPS1 peptide depends only on Ac-AMP concentration and not on ACS presence.

## Diamine acetyltransferase 1

Diamine acetyltransferase 1 (SAT1) is an enzyme involved in acetylation and intracellular regulation of polyamines (Casero et al., 1991; Hegde et al., 2007; Xiao et al., 1991). Small polyamines contain primary amine groups and share a similar structure with lysine side chain (Figure 39).

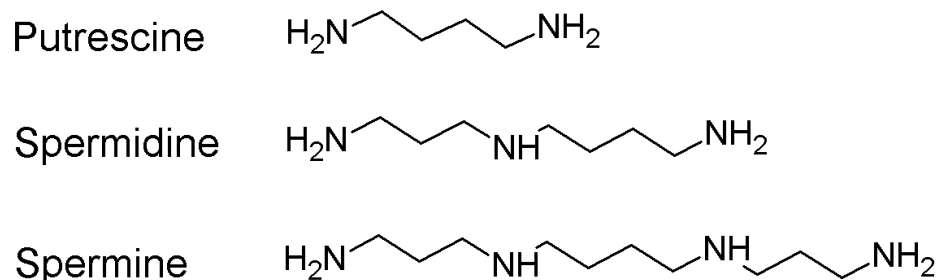


**Figure 39.** Structure of small polyamines molecules. Natural substrates for SAT1.

In order to test, whether SAT1 can act as lysine acetyltransferase, we applied the enzyme on a peptide microarray, presenting thousands of lysine-peptides derived from human proteins. We found a variety of signals corresponding to acetylated peptides (Figure 40). More than ten peptides have a score above five (Figure 41A). Acetylated peptides were mainly derived from cytosolic and nuclear proteins. Mitochondrial fraction represents 15 % of all acetylated peptides (Figure 41B). Based on a comparison between most preferred sequence motifs and ones with lowest acceptance, it seems that SAT1 prefers Arg in +3 and +5 positions, Gln in +1 position, Leu at -2 and Pro in -3 positions (Figure 41C). Top ten substrates for SAT1 are listed in Table 6. We synthesized peptides number 1, 2 and 10 as a nonamers with central lysine residue (Figures A25, A26 and A27; peptides were synthesized by Dr. Marat Meleshin using the same procedure like for the CPS1 peptide). We incubated the peptides with SAT1 in the presence of Ac-CoA up to 24 h. We were not able to confirm SAT1 peptide acetylation in solution using the HPLC based assay.

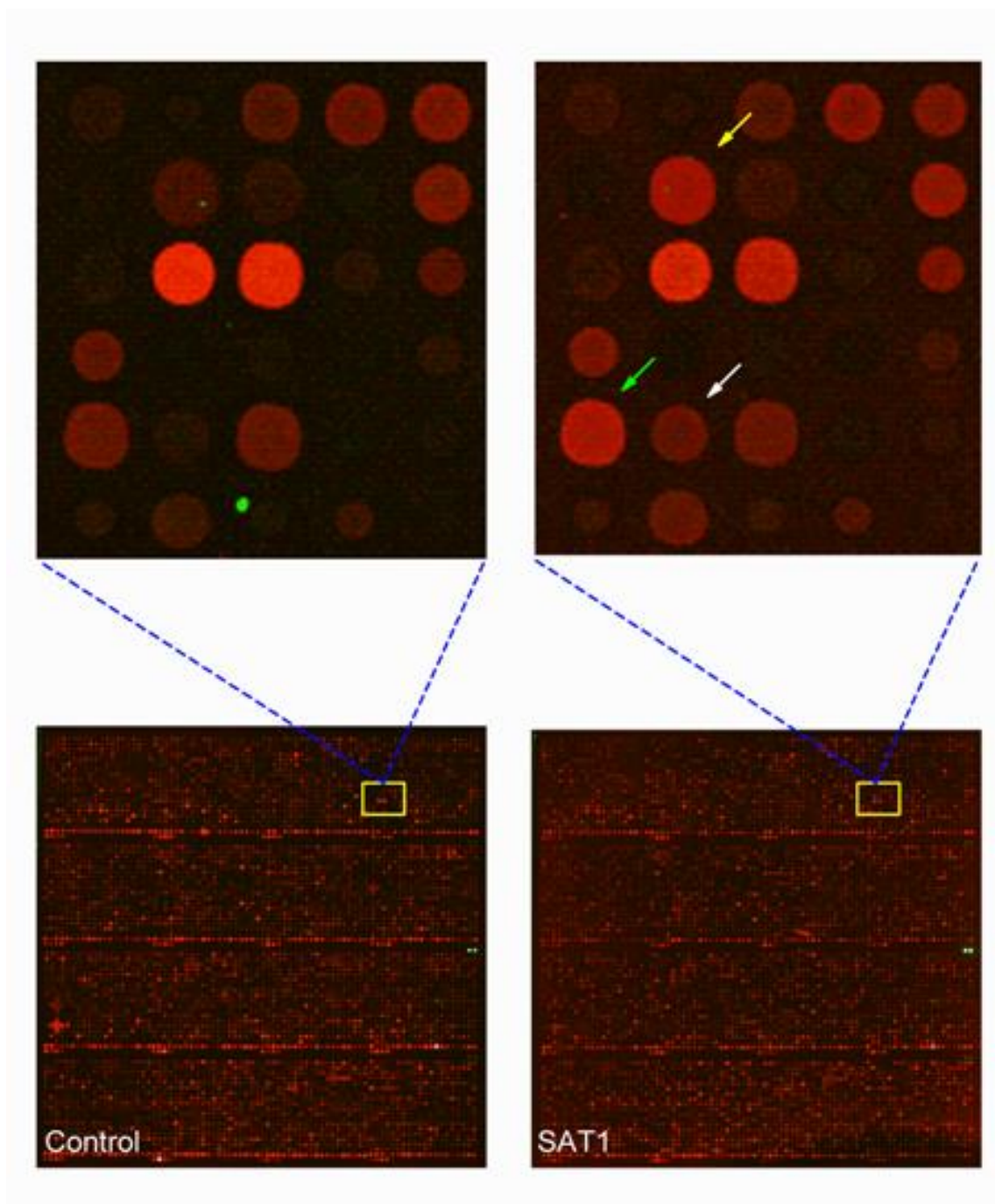


**Figure 40.** SAT1 lysine acetyltransferase activity detected by peptide microarrays. The reaction was performed in 200  $\mu$ l of 50 mM Tris-HCl buffer pH 7.5 containing 100  $\mu$ M Ac-CoA and 5  $\mu$ M SAT1 (Human recombinant, ATGEN) at 30°C for 2 h. The control represents incubation without SAT1. Acetylated peptides were detected using an optimized fluorescence labeled anti acetyl-lysine antibodies mix according to Rauh et al. (Rauh et al., 2013).

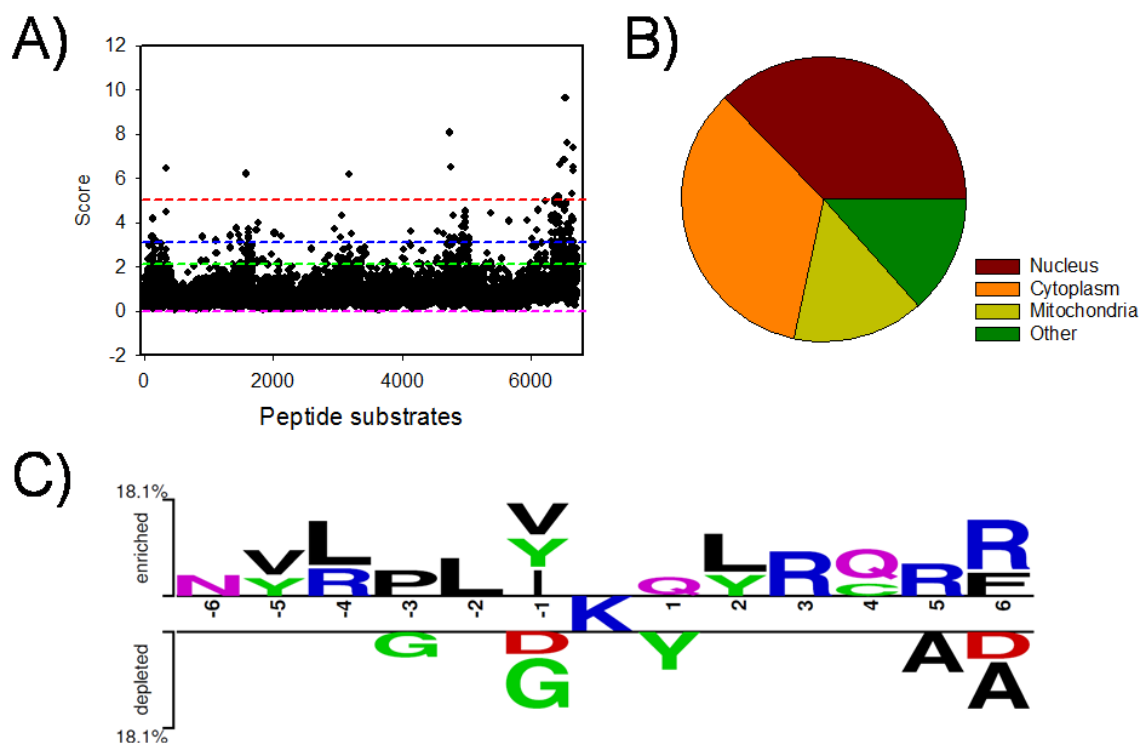


**Figure 41.** Substrate specificity of SAT1. **A)** More than 10 peptide substrates show score above five. The score represent signal intensity normalized to the control. **B)** Subcellular distribution of the proteins from which the detected acetylated peptides are derived. Majority of acetylated peptides are derived from cytosolic (37 %) and nuclear proteins (34 %). Mitochondrial fraction represents 15 % of all acetylated peptides and remaining 14 % represent peptides derived from proteins located in the other cellular compartments such as Golgi, endoplasmatic reticulum or proteins located in the plasma membrane. **C)** Two sample logo for SAT1 and its peptide substrates. Two samples logo is a web-based application free available online ([www.twosamplelogo.org](http://www.twosamplelogo.org)).



Table 6. Top 10 peptide substrates for SAT1.

Peptide No	Peptide sequence	Protein name (UniProt)	Gene name	Cellular compartment	UniProt ID	Score
1	LYPPRA <b>K</b> LVIQRH	TBC1 domain family member 4	TBC1D4	Cytoplasm	O60343	9.64
2	HSDDYI <b>K</b> FLRSIR	HDAC1	HDAC1	Nucleus, Cytoplasm	Q13547	8.07
3	<b>ZZ</b> MIGQ <b>K</b> TLYSFF*	Uracil-DNA glycosylase	UNG	Mitochondrion, Nucleus	P13051	7.62
4	LGAPSR <b>K</b> PDLRVI	Myocyte-specific enhancer factor 2D	MEF2D	Nucleus	Q14814	6.34
5	GHPSLV <b>K</b> ALSYLY	Kynurenine-oxoglutarate transaminase 3	CCBL2	Mitochondrion	Q6YP21	6.52
6	RVGGAL <b>K</b> APSQNR	Mitotic checkpoint serine/threonine-protein kinase BUB1 beta	BUB1B	Cytoplasm	O60566	6.32
7	SLEDRD <b>K</b> PYVCDI	Zinc finger protein neuro-d4	DPF1	Cytoplasm	Q92782	6.21
8	TPLPLI <b>K</b> PYSGPR	Transcription initiation factor TFIID subunit 9	TAF9	Nucleus	Q16594	6.19
9	LRQVRG <b>K</b> ASFLYS	DNA damage-binding protein 2	DDB2	Nucleus	Q92466	5.10
10	PVIELY <b>K</b> SRGVLH	Adenylate kinase 4, mitochondrial	AK4	Mitochondrion	P27144	4.96

\*ZZ represent AA - two alanines were added on N-terminus of the peptide to reach 13 amino acids and to have Lysine in the central position

original motif                   MIGQKTLYSFF  
in the table                       ZZMIGQKTLYSFF  
corresponds to               AAMIGQKTLYSFF   on the peptide microarray

## Protein modifications using modifying agents other than CoA thioesters. Introducing thioacetyl groups into the protein

Introducing thioacetyl-group on the N- $\epsilon$ -amino group of the lysine residues in short peptides has been described (Fatkins et al., 2006).

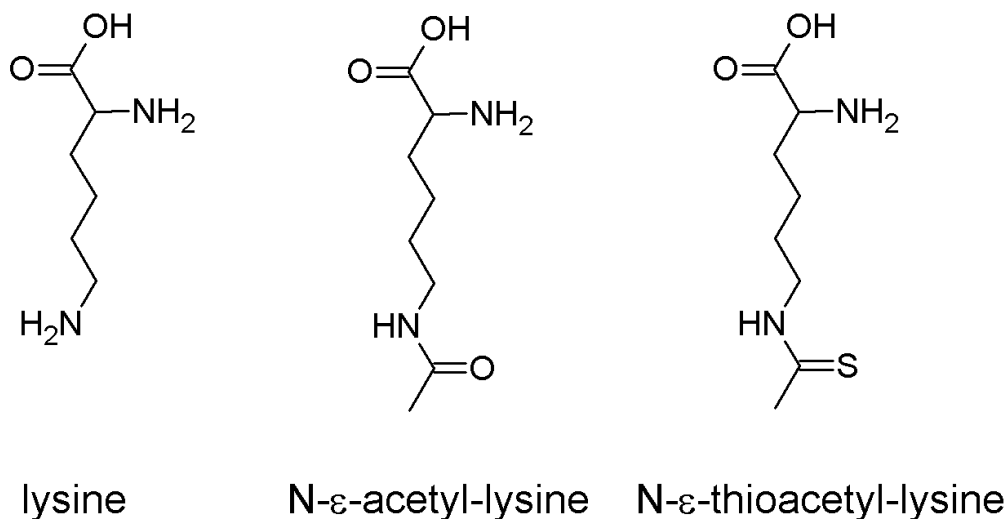


**Figure 42.** Chemical structure of free lysine, N- $\epsilon$ -acetyl-lysine and N- $\epsilon$ -thioacetyl-lysine.

It is known that replacement of the amide oxygen by a sulfur atom transforms peptidic sirtuin substrates into extremely slow substrates/inhibitors generating a stalled intermediate with  $K_i$ -values in the picomolar range (Schuster et al., 2016). Additionally, the conformation of this thioxo amide bond could be selectively switched by UV-irradiation generating stable isomers (Schuster et al., 2016; Zhao et al., 2004).

Here, we want to introduce a thioacetyl-group into protein substrate to generate a unique probe for sirtuin research (Figure 42). We used CypA as a model protein. The reaction solution was ethyl dithioacetate in a Tris-HCl buffer. It is known that ethyl dithioacetate shows low solubility in water. We were able to overcome this problem by heating the solution for 5 min at 65°C. Subsequent to cooling CypA was incubated in the reaction solution for 24 h at RT. Ethyl dithioacetate successfully modified CypA at multiple sites (Figure 43).

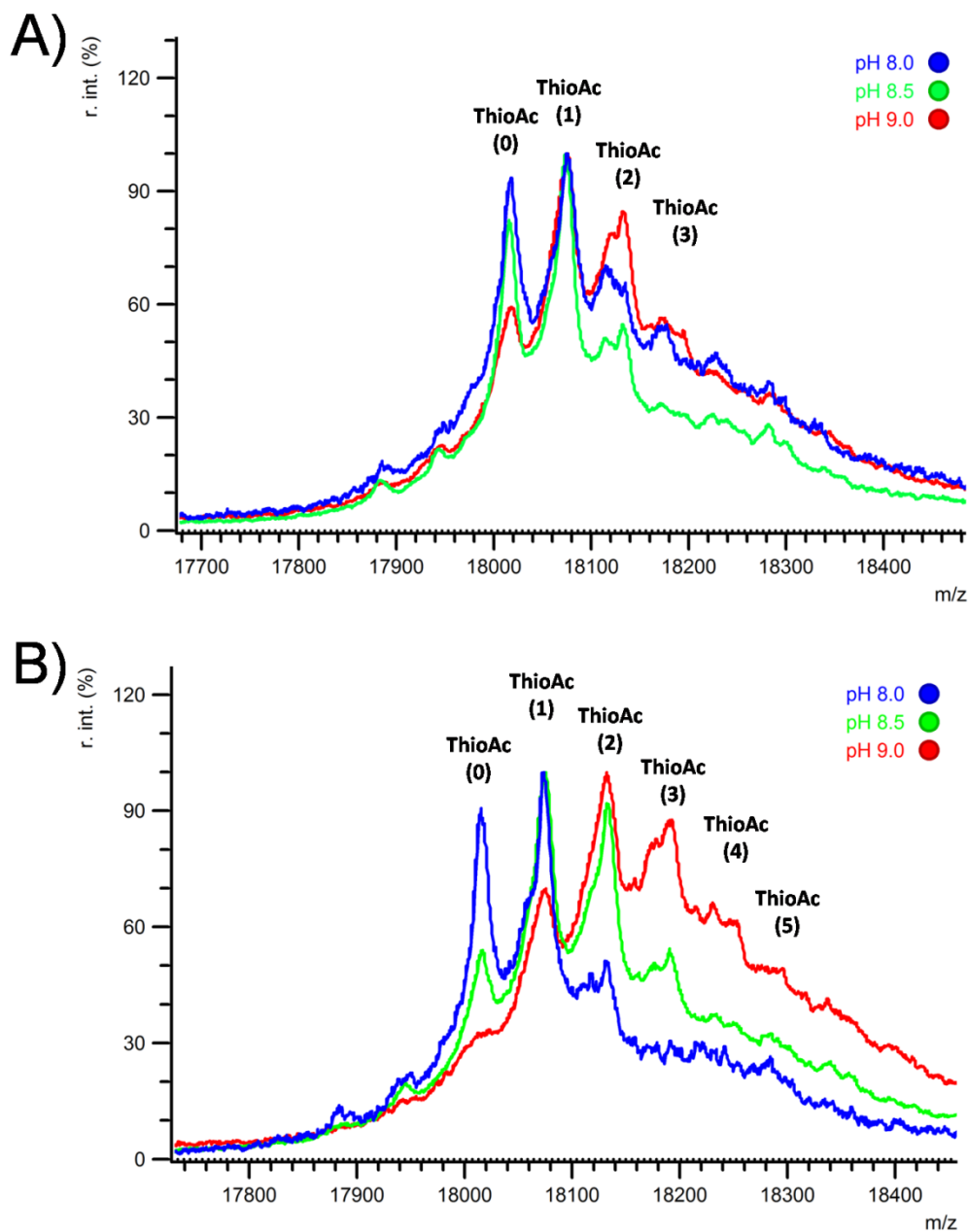


**Figure 43.** Modification of CypA by ethyl dithioacetate. Reaction mixture containing 20  $\mu$ M CypA and **A)** 4 mM or **B)** 8 mM ethyl dithioacetate in 100 mM Tris-HCl buffer pH 8.0, 8.5 or 9.0 was incubated at RT. After 24 hours, CypA was precipitated by adding 5 volumes of cold ( $-20^{\circ}\text{C}$ ) acetone, mixed well and incubated at  $-20^{\circ}\text{C}$  for additional 3 h. After that, samples were centrifuged at  $4^{\circ}\text{C}$  for 10 minutes at  $15000 \times g$ . Supernatant was decanted and pellet was dried. Finally, pellet was re-suspended in 10 mM bicarbonate buffer and analysed by MALDI-TOF MS.

MALDI-TOF/MS analysis shows that at pH 8.0 and 8 mM ethyl dithioacetate concentration, CypA exists almost only in the monoacetylated form. Tryptic digest and

LC/MS analysis revealed that CypA was thioacetylated almost exclusively at K82 (Figure 44). Other sites like K28, K44, K76, K125 and K155 were also observed to be thioacetylated but show lower abundance.

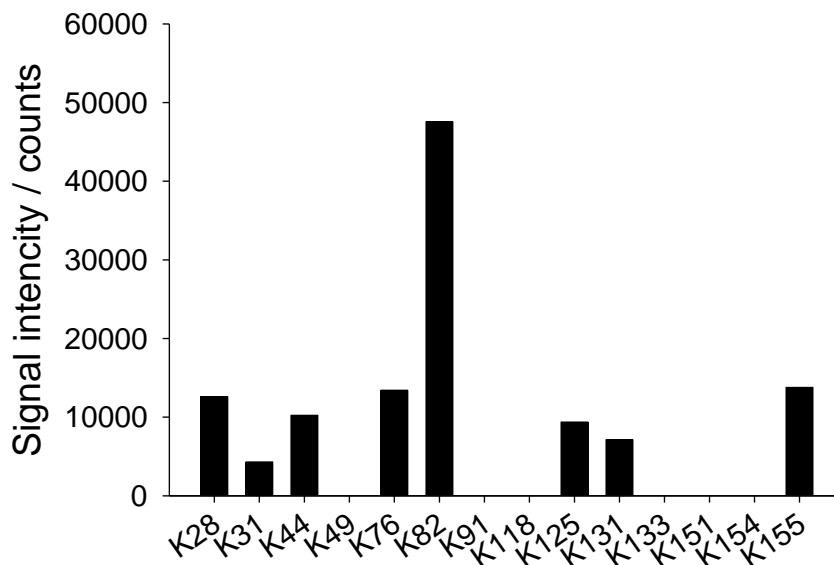


**Figure 44.** CypA is successfully modified by ethyl dithioacetate at multiple lysine sites. Reaction mixture containing CypA 20  $\mu$ M and ethyl dithioacetate 8 mM in 100 mM Tris-HCl buffer pH 8.0 was incubated at RT for 24 h. Precipitated thioacetylated CypA was re-suspended in 10 mM bicarbonate buffer and subjected to trypsin digestion overnight. Reaction mixture was analyzed by LC/MS.

Thioacetylated lysine peptides represent good inhibitors for sirtuins (Smith and Denu, 2007). The key of the inhibition mechanism lies in the 1',2'-bicyclic intermediate which in the case of thioacetyl-lysine is trapped in the deacetylation reaction. The carbon-sulfur bond has a  $\sim 0.4$  Å longer distance in comparison to carbon-oxygen bond, which probably results in a reduced turnover. As there is no such intermediate in the HDACs catalyzed reactions, thioacetyl-based peptide inhibitors selectively inhibit only sirtuin enzymes with  $IC_{50}$  in the low micro molar range (Fatkins et al., 2006). Changing the structure of the peptide from the linear to the cyclic form increases its inhibitory potential and reduce the  $IC_{50}$  value to nano molar range (Huang et al., 2016). Recently it was shown that non-peptide thioacetyl lysine based small molecules efficiently and selectively inhibit SIRT1 (Suzuki et al., 2009). The huge advantage of such inhibitors is that in the most cases they easily cross biological membranes and are protected from the action of intracellular proteases. Therefore, they are more suitable to use in cellular studies in comparison to their peptide analogs.

Thioacetyl lysine based peptides represent a powerful tool to study the reaction mechanism of the sirtuins as well as a good strategy for the further development of new sirtuin inhibitors. Based on the previous studies it is clear that thioacetyl-lysine represent a key structure in the mechanism based inhibition of sirtuin enzymes, but not less important, is the fact that the nature of the entire molecule may affect its potential and selectivity. In one of the recent studies authors described a procedure for the selective incorporation of the thioacetyl-lysine modification in the human histone protein using the flexizyme (Xiong et al., 2016). Here we provide a fast and simple enzyme free procedure for incorporation of thioacetyl-lysine modification in the human CypA. We were able to modify CypA at multiple lysine sites or even at single lysine residues depending on the conditions we used. This method represents a powerful tool for further studies of the mechanisms of protein lysine acetylation and deacetylation as well as its role in protein function. Additionally, caused by the super affinities of the stalled intermediates (covalent fusion of the thioacetylated lysine side chain with the ADP-ribose part of the NAD<sup>+</sup> cosubstrate) with interaction constants in the picomolar range (Schuster et al., 2016) thioacetylated proteins could serve as a starting point for the generation of crystal structures of thioacetyl-protein/sirtuin complexes. Such structures will uncover additional contacts between protein substrates and sirtuin exosites and could explain the complex substrate specificities of sirtuins and give some hints for mechanism of sirtuin activation.

# Discussion

Disorder of mitochondrial function is closely associated with pathogenesis of different diseases including diabetes, cancer and metabolic syndrome. There is strong evidence that hyperacetylation of mitochondrial proteins is implicated in pathophysiology of these diseases (Cheng et al., 2003; Finley et al., 2011a; Hirschey et al., 2011; Toiber et al., 2013). Hyperacetylation of a wide range of mitochondrial enzymes is mostly inhibitory, thereby disrupting mitochondrial metabolic homeostasis (Hallows et al., 2006; Qiu et al., 2010; Schwer et al., 2006; Shimazu et al., 2010; Yu et al., 2012). Nevertheless, there are examples that enzymes, such as malate dehydrogenase and aconitase are activated through their acetylation (Fernandes et al., 2015; Zhao et al., 2010). Acetylation often disrupts binding efficiency or causes mislocalization of the protein (Inuzuka et al., 2012; Yang et al., 2015). Up to 65 % of the mitochondrial proteome is acetylated (Zhao et al., 2010). However, mitochondrial acetyltransferases, which might be responsible for the extensive and frequent mitochondrial acetylation have not been identified so far. Recent studies might provide an explanation for the widespread mitochondrial acetylation. Some of them proposed new enzymes with lysine acetyltransferase activity (Fan et al., 2014; Scott et al., 2012) and others suggest that a non-enzymatic mechanism underlies acetylation (Baeza et al., 2015; Kuo and Andrews, 2013; Wagner and Payne, 2013). Authors demonstrated that alkaline pH and high Ac-CoA concentration present in the mitochondrial matrix are sufficient to cause spontaneous protein acetylation. In this study we provide further evidence that mitochondrial proteins undergo non-enzymatic acetylation.

In contrast to previous investigations, our first approach utilized a model octapeptide derivative representing the well characterized acetylation site K527 of CPS1. Acetylation of K527 *in vivo* has been shown in MS studies (Schwer et al., 2009). Additionally, succinyl-modification has been identified at the same lysine residue in both mice and in humans (Weinert et al., 2013). In one of the previous studies whole mitochondrial lysate was used to demonstrate protein non-enzymatic acetylation (Wagner and Payne, 2013). It is important to mention that use of a model peptide substrate has a number of advantages over a protein substrate and/or using whole cell lysate. Model peptide substrates eliminate the possibility of existing modifications on lysine residues and contaminations with lysine acetyltransferases and deacetylases can be completely excluded. Additionally, cell or

mitochondrial lysate contains not only proteins, but a certain amount of Ac-CoA still remains, and adding a known amount of Ac-CoA in the reaction mixture does not yield the real final concentration within the assay. Our experiments clearly demonstrate that Ac-CoA is able to modify lysine residue non-enzymatically under the conditions present in mitochondria. Even at pH 7.2, Ac-CoA with a concentration below 1 mM was able to acetylate the lysine side chain of the model peptide, thus suggesting that non-enzymatic protein acetylation is not restricted to mitochondria, but can also occur in the cytosol and nucleus, but more slowly. Indeed, histone protein acetylation was observed at pH 6.8 and 200  $\mu$ M concentration of Ac-CoA in the absence of lysine acetyltransferase *in vitro* (Kuo and Andrews, 2013). Our results demonstrate a strong temperature dependence of non-enzymatic lysine acetylation reaction. An increase in temperature of only 2°C results in significant increase in the acetylation rate constant. This finding should be important for the physiological state of prolonged fever, which might induce hyperacetylation. However, our results show that non-enzymatic acetylation is a slow process. It takes hours or days even under the basic conditions of mitochondrial matrix. Nevertheless, our data are consistent with previous findings. It has been shown that fasting induces mitochondrial protein hyperacetylation after 12 – 48 h (Kim et al., 2006). Calorie restriction requires more than 10 weeks for hyperacetylated protein detection (Schwer et al., 2009). In the SIRT3 knockout mice hyperacetylation has also been detected after more than 10 weeks (Hirschey et al., 2011; Lombard et al., 2007). Thus, acetylation can occur at low level under normal basal conditions, but considerably increased during certain physiological or pathological states that cause long-lasting high concentrations of Ac-CoA, such as prolonged fasting, CR, high-fat diet and chronic alcohol consumption. On the other hand, we found that small molecules such as DMAP can increase lysine acetylation. Unfortunately, we did not find any other metabolic small molecule which is involved in basal mitochondrial metabolism accelerating this reaction, but we cannot completely exclude the possibility that such molecules exist. That gives opportunity for further investigation of the mitochondrial metabolome. It is important to be mention, that simulating conditions of the mitochondrial matrix is challenging. Within the mitochondria extremely complex metabolic machinery is condensed to an extremely small space. Mitochondrial water content is 5 times lower in comparison to cytosolic content. This results in a very high protein concentration and gives the mitochondrial matrix more viscous properties. Low water content might results in higher desolvation of lysine residues on the proteins surface, which in turn can lead to reduced  $pK_a$  values.

Nevertheless, our results clearly demonstrated that Ac-CoA still requires water surrounding for its action, most likely because of its highly hydrophilic behavior. On the other hand, increase in ionic strength increases non-enzymatic acetylation, probably by reducing the  $pK_a$  values of the lysine side chain residues. All together it supports our hypothesis that conditions in the mitochondrial matrix are more suited for non-enzymatic acetylation in comparison to other cellular compartments.

During the metabolism many other reactive thioesters are formed and could represent potential acylating agents. We tested whether some of them are able to non-enzymatically acylate the model CPS1 peptide. Notably, the highest acylation rate was observed with Succ-CoA (~150 times faster in comparison with Ac-CoA). Thus, it is not surprising that previous MS studies identified succinylation at K527 in different tissues *in vivo* (Weinert et al., 2013). Our study also revealed that Glut-CoA and HMG-CoA exhibited an approximately six- and threefold higher acylation rate respectively, as compared to Ac-CoA. Consistently, a recent study showed that lysine glutarylation is a broadly conserved posttranslational modification of lysine residues *in vivo*, both in prokaryotic and eukaryotic cells (Tan et al., 2014). The authors demonstrated that glutarylated lysine residues are highly enriched on metabolic enzymes and other mitochondrial proteins. It was found that CPS1 enzyme is glutarylated, including lysine K527 (Tan et al., 2014). However, it is unknown whether acetylation, succinylation or glutarylation of this residue is prevalent in the cells, and which parameters determine the acylation landscape. Moreover, succinylation and glutarylation differ from acetylation, because both succinyl and glutaryl moieties contain an additional carboxyl group which transform the positive charge of the amino group of the unmodified lysine residues into a negative charge. In further investigations it would be interesting to test whether different types of acylation also have distinct effects on protein stability and function. Succ-CoA and Glut-CoA have lower basal cellular level compared with Ac-CoA. Such lower concentrations are compensated with higher reactivity. Thus, it is not surprising that the frequency of these lysine modifications have been proposed to be similar to that of acetylation (Weinert et al., 2013). Therefore, our results provide evidence that different abundance of distinct lysine modifications is based on both reactivity and availability of corresponding CoA-thioesters.

So far, there is no evidence about the existence of HMG lysine modifications *in vivo*. HMG-CoA is a key intermediate in ketone body synthesis. Further investigations should be addressed in particular on the patient with frequent ketoacidosis, caused by different



factors, such as diabetes mellitus type 1, chronic alcohol consumption or low carbohydrate diet (Kitabchi et al., 2009; Krebs et al., 1969; Shah and Isley, 2006; Westerberg, 2013). High concentration of mitochondrial HMG-CoA is detected in patients with HMG-lyase deficiency, an autosomal recessive genetic disorder biochemically characterized by tissue accumulation and urinary excretion of large amounts of 3-hydroxy-3-methylglutarate (Fernandes et al., 2013).

Non-enzymatic propionylation and butyrylation show 3 and 5 times, lower acylation rate respectively, compared to acetylation. Interestingly, we found no reaction in the case of Benz-CoA or AcAc-CoA under the same conditions. Propionylation and butyrylation are well described lysine posttranslational modifications (Chen et al., 2007; Cheng et al., 2009; Liu et al., 2009), while lysine benzoylation or acetoacetylation are not described until now. Recent studies showed that short-chain acyl-CoA deficient mice exhibited increased protein lysine butyrylation as a result of But-CoA accumulation. Similarly, propionyl-CoA carboxylase deficient cells displayed increased propionylation of lysine residues (Pougovkina et al., 2014). Mitochondrial sirtuins SIRT3 and SIRT5 together are able to reverse non-enzymatic lysine acetylation. SIRT3 has a strong preference for acetyl groups (Schlicker et al., 2008), where SIRT5 is able to remove butyryl, acetyl, 3-hydroxy-3-methylglutaryl, succinyl and glutaryl moieties with strong preference for succinyl and glutaryl (Du et al., 2011) (Table 7).

**Table 7.** Kinetic parameters for SIRT5 mediated deacylation of acylated CPS1 peptide derivatives (Roessler et al., 2014).

Lysine modification	$K_M$ [ $\mu$ M]	$k_{cat}$ [ $s^{-1}$ ]	$k_{cat}/K_M$ [ $M^{-1}s^{-1}$ ]
Acetyl	$24.3 \pm 9.1$	$(3.9 \pm 0.6) * 10^{-4}$	16
3-hydroxy-3-methylglutaryl	$7.6 \pm 0.9$	$(3.8 \pm 0.1) * 10^{-3}$	500
Succinyl	$3.8 \pm 0.6$	$(1.9 \pm 0.2) * 10^{-2}$	13995
Glutaryl	$4.1 \pm 1.0$	$(7.7 \pm 0.2) * 10^{-2}$	18669

The investigation of CPS1 peptide modification by different acyl-CoA thioesters revealed that compounds derived from dicarboxylic acids showed much faster acylation rates than those derived from monocarboxylic compounds. The difference in the reactivity of investigated CoA-thioesters cannot be explained by variations in Gibbs free energy ( $\Delta G$ ), because most of the acyl-CoA compounds have nearly the same  $\Delta G$  values

(Thauer et al., 1977). Therefore, higher acylation rate of Succ-CoA compared to Ac-CoA might be explained by succinic-anhydride formation from Succ-CoA, by intramolecular nucleophilic attack of the free carboxylate group on the thioester bond (Bruice and Pandit, 1960). The formed cyclic anhydride could attack the lysine side chain of the peptides and proteins more efficiently than succinyl thioester, because it still represent an "energy rich" compound, yet less sterically hindered than the relatively large Succ-CoA (Figure 45). Intramolecular nucleophilic attack and cyclic anhydride formation might also underlie the non-enzymatic glutarylation and 3-hydroxy-3-methylglutarylation of lysine residues by Glut-CoA and HMG-CoA respectively, but formation of a six membered ring gives a more stable compound and is thus less reactive. Decreasing acylation efficiency from Ac-CoA to Benz-CoA could be explained by steric hindrance of the increasing size of the acyl moieties.

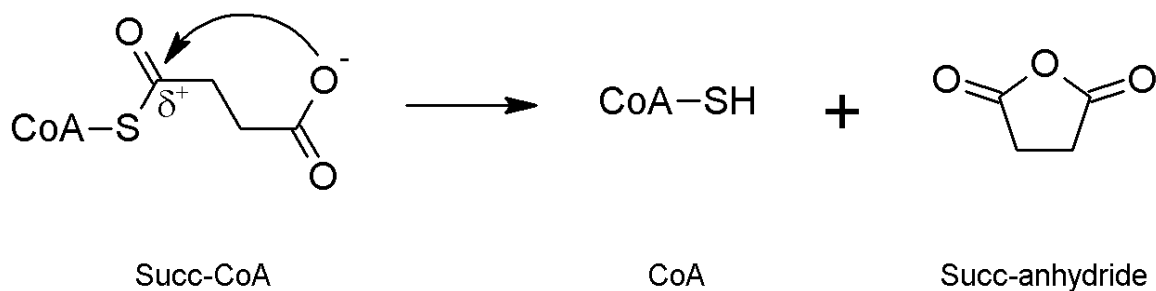


**Figure 45.** Schematic diagram of intramolecular catalysis in Succ-CoA and succinic anhydride formation.

We also characterized non-enzymatic lysine acetylation of the model protein CypA and we showed that Ac-CoA is able to non-enzymatically acetylate CypA. Analysis of CypA acetylation revealed that treatment with Ac-CoA generates predominantly mono and diacetylated forms of CypA. The mapping of acetylation sites revealed that K155 is the main acetylation site on CypA. Other sites have also been identified but with significantly lower abundance. Interestingly, all twelve lysines that were shown to be acetylated *in vivo* could also be acetylated by Ac-CoA. K151 and K154 were found neither to be chemically acetylated nor to be acetylated *in vivo*. These are the two smallest tryptic peptides within the CypA sequences with molecular masses of just 675.35 and 504.3 Da which could be the reason why we did not identify them in the LC-MS analysis and why these lysine residues were not identified as the sites of acetylation in *in vivo* experiments.

Succinylation of CypA exceeds the extent of lysine acetylation. CypA was non-enzymatically succinylated at all fourteen lysine residues. This is in agreement with recent studies demonstrating that succinylation is highly abundant in the cells (Weinert et al., 2013). According to our results it is obvious that Succ-CoA and Ac-CoA generate different lysine acylation patterns in CypA. CypA acetylation took place mainly at K155, whereas succinylation was observed at K28 and K82 at high extent. K155 is located on the surface of CypA in the random coil far away from the active site. Hence, we found that acetylation has no effect on CypA activity or stability. It was shown that K155 is located in the allosteric binding site of CypA (Lv et al., 2012), which indicates that acetylation of CypA at K155 might be important for allosteric regulation of CypA. Succinylation is also not able to induce huge conformational changes in CypA, primary because most of the succinylated lysine residues are located in the random coils. The slight decrease in the activity of succinylated CypA could be caused by succinylation of K125, which is located near the active site of CypA. However, our results clearly show that the sequence and the microenvironment of the target site influence acylation efficiency, and that relative acylation rates of distinct sites vary for different acyl-CoA thioesters.

The diversity of lysine acylations on proteins raises the question, which conditions determine the nature of the introduced acylation moiety and the position of the target lysine residue. There is no evidence about known consensus sequence motifs for different types of non-enzymatic lysine acylation. Previous reports and our present study demonstrate the strong pH dependence of non-enzymatic acylation reaction; thus the  $pK_a$  value of a lysine residue might be an important determinant for its modification. Lysine residues within the protein can exhibit strongly reduced  $pK_a$  values because of local sequence influence such as the presence of positively charged residues in the vicinity, Coulomb interactions and desolvation. Hence, it is not surprising that most of the mitochondrial enzymes show decreasing activity after acetylation. Lysine residues located in the active sites or substrate binding pockets of these proteins occur more frequently in the desolvated state than other lysine residues, and should therefore be more reactive toward acylation in comparison to the surface exposed lysine residues with a high rate of solvent accessibility. Our results clearly show that lysine  $pK_a$  values have one of the key roles in determination of the acylation pattern. In the case of succinylation by Succ-CoA, we observed that modified lysine residues are almost completely consistent with lysine  $pK_a$  values. Lysines with lowest  $pK_a$  value show highest signal intensities and opposite. In

the case of acetylation by Ac-CoA modified lysines were partly consistent with lysine  $pK_a$  values. The obvious exception is K155, which was recognized as the site with the highest rate of acetylation, and does not show the lowest  $pK_a$  value. This phenomenon supports our hypothesis of existence of super-reactive lysine residues, as well as the existence of additional factors, beside lysine  $pK_a$  values. For example accessibility of lysine residues, conformational flexibility of protein backbone, and substrate-binding dynamics, might also be involved in the final determination of protein acylation patterns.

Cross-regulation between lysine acylation and other post-translational modifications might also determine the acylation landscape of proteins. We have demonstrated that methylation of lysine residues completely block non-enzymatic acetylation. Interestingly, it was shown, that monomethylation suppressed acetylation of p53 at K382 (Shi et al., 2007). Contrarily, methylation did not prevent non-enzymatic succinylation by Succ-CoA. This phenomenon raises additional questions. Does this modification affect SIRT5 activity? According to our findings SIRT5 is not able to remove the succinyl group from the MeSuccCPS1 peptide. On the contrary, MeSuccCPS1 peptide represents a good inhibitor for SIRT5 with a  $K_i$  value in the low micromolar range. It would be interesting for further research to investigate what is the mechanism of removing such modification from the lysine residue. One possible mechanism is the release of the "normal" succinylated lysine residue by lysine demethylase which makes it a good substrate for SIRT5. It would also be interesting to find out if such modification triggers other intracellular mechanisms or maybe remains intact and gives signal for follow-up events like protein degradation. Additionally, we investigated deacetylation of CPS1 peptide in the presence of Succ-CoA. The results clearly demonstrated that the acylation landscape of proteins depends not only on the concentration of acyl-CoA metabolites but also on the presence and activity of deacetylases with different acyl specificities. Differential regulation of sirtuins, for example by nutrient deprivation, changes in  $NAD^+/NADH$  ratio or effectors such as nicotine amide or resveratrol could result in completely changed acylation landscape in cellular proteins. It was already shown that SIRT5 catalysed deacetylation and desuccinylation are differently affected by nicotineamide (Fischer et al., 2012).

Deacetylation experiments with SIRT3 and SIRT5 provided further evidence that mammalian sirtuins might target different types of acyl modifications. Previous reports already showed that SIRT5 catalyzes deacylation of acyl groups with negatively charged moieties, such as malonyl, glutaryl, succinyl or adipoyl groups (Du et al., 2011; Roessler

et al., 2014; Tan et al., 2014). Moreover, it was shown that SIRT6 preferably removes myristoyl groups and other long chain fatty acids (Feldman et al., 2013). SIRT1, SIRT2, and SIRT3 mainly remove acetyl groups from lysine residues (Du et al., 2011; Michishita et al., 2005), and also show the ability to remove crotonyl group (Bao et al., 2014). Additionally, it was shown that SIRT2 has demyristoylase and palmitoylase activity (He et al., 2014; Moniot et al., 2013; Teng et al., 2015). Recently, it was shown that SIRT4 is able to transfer lipoyl and biotinyl groups from the lysine side chain to ADP-ribose, both *in vitro* and *in vivo* (Mathias et al., 2014). SIRT4 recognized peptides derived from TNF $\alpha$  protein as a substrate. Kinetic parameters for the TNF $\alpha$  peptide 2 are superior to substrates described in the literature and similar for TNF $\alpha$  peptide 1 (Mathias et al., 2014). Interestingly, TNF $\alpha$  peptide 2 shows a  $K_M$  value tenfold lower in comparison to TNF $\alpha$  peptide 1, indicating that a large hydrophobic group improves binding efficiency to the SIRT4 active site. These data additionally demonstrate that development of substrates with different spectral properties open possibilities for simultaneous detection of enzymatic activities using mixtures of substrates. We were able to analyze reaction kinetics for SIRT2 and SIRT4 using a mixture of substrates (TNF $\alpha$  peptide 1 and TNF $\alpha$  peptide 2) and excitation wavelength of 290 nm for both fluorophores and recording the fluorescence spectra over time (Figure A28 and A29; (Schuster et al., 2016)). Variation of the size and position of fluorophore in the acyl side chain open new possibilities for development of sirtuin isoform specific substrates and/or inhibitors.

It is important to notice that all mammalian sirtuins strictly depend on the availability of the cosubstrate NAD $^+$ . Recently it was demonstrated that NADH at high concentration has inhibitory effect on sirtuin activity (Madsen et al., 2016). Therefore, the acylation state of mitochondrial proteins might also be regulated by the NAD $^+$ /NADH ratio. Thus, metabolic state characterized by simultaneous high concentration of mitochondrial NADH and Ac-CoA, which arise from fatty acid oxidation and amino acid degradation in the case of nutrient depletion, will induce hyperacetylation of mitochondrial proteins by decreased sirtuins activity on one hand and by increased non-enzymatic acetylation on the other hand. Nevertheless, "super substrates" for sirtuins with low  $K_M$  value for NAD $^+$  should be accessible for sirtuin mediated deacetylation under these conditions.

In recent years a big effort has been invested in research to identify the cause of mitochondrial protein acetylation phenomenon. One study suggests GCN5L1 enzyme as a new mitochondrial global lysine acetyltransferase (Scott et al., 2012). Authors showed

that knockdown of GCN5L1 results in an increase of mitochondrial protein acetylation, but they did not provide any evidence of specific substrate recognition and targeting of specific lysine modifications. Moreover, the enzyme is not evolutionary present in all organisms. Thus the idea that GCN5L1 acts as a global lysine acetyltransferase still remains questionable. Another study suggested ACAT1 as mitochondrial lysine acetyltransferase (Fan et al., 2014). Moreover, authors identified that ACAT1 specifically acetylated PDHA1 at K321 and PDP1 at K202, but they did not provide any information about the kinetic parameters using a short peptide substrate.

In this study we have tested few mitochondrial metabolic enzymes which use Ac-CoA as cofactor/cosubstrate for lysine acetyltransferase activity. We found no lysine acetyltransferase activity for CS, CRAT or HMGCS2. Interestingly, even ACAT1 showed no lysine acetyltransferase activity against large number of peptide substrates presented on the peptide microarray under the condition used.

Previously it was shown that ACS is involved in histone acetylation most likely by providing Ac-CoA for non-enzymatic or enzymatic reaction (Takahashi et al., 2006). ACS catalyzes the condensation of acetate with CoA and forms Ac-CoA which can be consumed in the TCA cycle or serve as acetyl group donor for protein acetylation. In the first step acetate and ATP are used to form Ac-AMP with release of diphosphate. In the second step acetyl group from Ac-AMP is transferred to CoA. In the absence of CoA Ac-AMP is released from the ES complex and can non-enzymatically acetylate lysine residues. Here we provide evidence that ACS might indirectly be a part of the mitochondrial acetylation machinery by providing both Ac-CoA and Ac-AMP for non-enzymatic protein acetylation but is not able to use either Ac-CoA or Ac-AMP as a cofactor in direct lysine acetylation reaction (Figure 46). It was shown previously that chronic alcohol consumption results in hyperacetylation of mitochondrial proteins (Harris et al., 2015). In the cytoplasm ethanol is converted to acetaldehyde by ADH; in the mitochondria acetaldehyde is further transformed to acetate by ALDH2 where it can serve for energy production in the TCA cycle after its conversion to Ac-CoA or for ACS mediated protein acetylation.

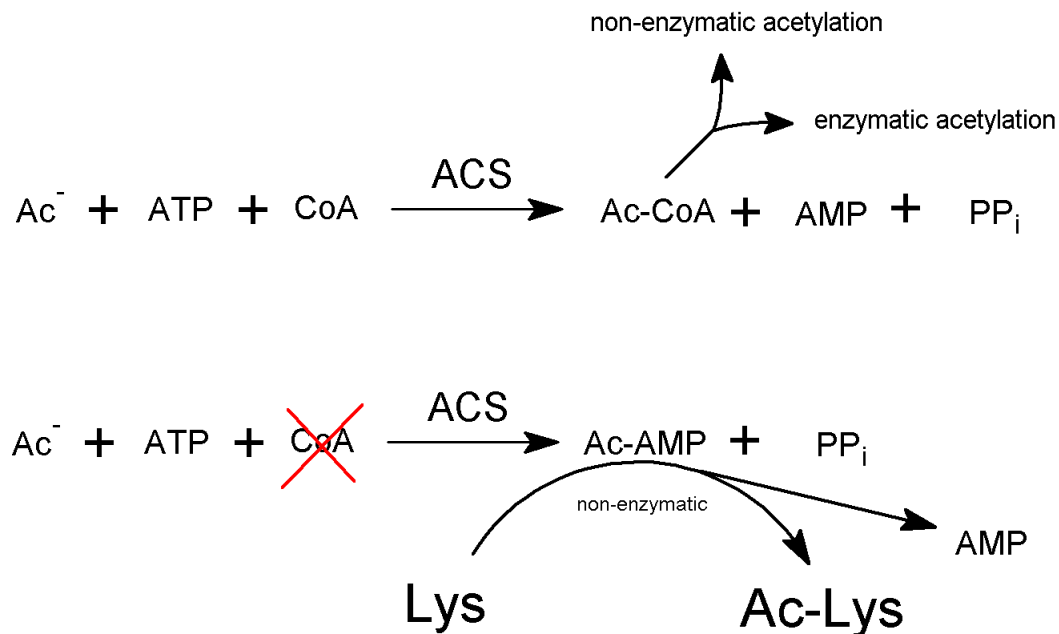


**Figure 46.** Potential role of ACS in the mitochondrial protein acetylation. ACS is indirectly involved in protein lysine acetylation by providing both Ac-CoA and Ac-AMP for non-enzymatic reaction.

SAT1 represent a key enzyme involved in acetylation of polyamines (Casero and Pegg, 2009; Casero et al., 1991; Pegg, 2008). Structural studies revealed that the enzyme shares sequence similarities with the GNAT acetyltransferase family. The enzyme is mainly localized in the mitochondria (Holst et al., 2008). It shows strong binding efficiency for Ac-CoA with  $K_M$  values of 3.8  $\mu\text{M}$  (Hegde et al., 2007). SAT1 natural substrates (spermine and spermidine) contain a primary amine group and share structural similarities with the lysine residue. It was shown that SAT1 undergoes autoacetylation at K26 (Bewley et al., 2006). Also, SAT1 accepts a variety of substrates beside polyamines such as amantadin, glucoseamin-6-phosphate or poly-L-lysine (Bras et al., 2001; Zhang et al., 2012) and shows weak activity to single L-lysine (Lee et al., 2011). Our microarray data reveal that SAT1 has lysine acetyltransferase activity. A range of different peptide substrates were acetylated in the presence of SAT1. Our control completely eliminates peptide acetylation independent of SAT1. Top peptide substrates were derived from proteins located in different cellular compartments like cytoplasm, nucleus and mitochondria. We were not able to confirm SAT1 acetylation reaction in solution using HPLC assay. Most likely, SAT1 activity was too low for detection with our HPLC assay but

still enough for immunochemical detection on microarray. It was previously described that SAT1 shows a low acetylation rate for the poly L-lysine substrate (Zhang et al., 2012), and shows very short half-life *in vivo* (Obayashi et al., 1992). Moreover, peptides for experiments in solution were nonameric, 4 amino acid residues shorter compared with peptides presented on the peptide microarray. According to the fact that SAT1 showed no activity against single L-lysine but action against poly L-lysine substrate was detected, SAT1 might require longer peptides for its action or maybe some of the secondary structure or even entire protein. That reveals that even if SAT1 is involved in mitochondrial acetylation, its action might be restricted to specific lysine modification but the enzyme itself is most likely not responsible for the global mitochondrial protein acetylation. Taking together, we cannot completely exclude the possibility that SAT1 plays a role in the protein acetylation in mitochondria, but further investigation is required.

As it was mentioned earlier Ac-CoA level and pH represent key factors of non-enzymatic protein lysine acetylation in the lumen of the mitochondrial matrix. In the metabolic state of high carbohydrate input, a final product of glycolysis, pyruvate, is imported in the mitochondrial matrix and through pyruvate dehydrogenase complex converted to Ac-CoA. Such formed Ac-CoA can enter the TCA cycle or can be used for ketone body synthesis. When all intermediates of the TCA cycle are available in appropriate concentrations, Ac-CoA enters the TCA cycle and will be oxidized to CO<sub>2</sub> with the main aim of energy production. When the TCA cycle is running with its full capacity protons from the lumen of the mitochondrial matrix are pumped into the intermembrane space to ensure proton motive force necessary for smooth function of ATP synthase and production of ATP. During that process intermembrane space is acidified remaining alkalized pH in the mitochondrial matrix with pH values up to 8.2 (Santo-Domingo and Demareux, 2012). High carbohydrate input makes ideal metabolic conditions for non-enzymatic protein acetylation, by rising concentration of Ac-CoA and increasing the pH value in the mitochondrial matrix. Additionally, during the running of the TCA cycle, NAD<sup>+</sup> molecules are consumed, consequently reducing NAD<sup>+</sup>/NADH ratio, and decrease sirtuin activity which in turn additionally increases acetylation in the mitochondria during nutrient overloading.

Recently, it was discussed that for the normal metabolic flow in the mitochondria free CoA is required (Ghanta et al., 2013). Increasing the Ac-CoA concentration during carbohydrate input reduces the amount of free CoA. Complete depletion of the free CoA



would lead to collapsing of the TCA cycle, because it requires free CoA for normal function. Ac-CoA negatively regulates pyruvate dehydrogenase activity, ensuring always optimal Ac-CoA/CoA ratio for the normal metabolic flow through the TCA cycle (Randle et al., 1978).

Interestingly, low carbohydrate input can also lead to mitochondrial hyperacetylation. In such case low glucose level triggers the alternative mechanisms of lipid and protein catabolism which become the main source of energy production. Oxaloacetate is transformed to malate by MDH2 and exported to the cytoplasm for gluconeogenesis. Under such conditions the TCA cycle is completely blocked, because there is no oxaloacetate available for the reaction with Ac-CoA. Thus, the level of Ac-CoA rapidly increases again and can be used for ketone body synthesis or for non-enzymatic protein lysine acetylation (Figure 47).

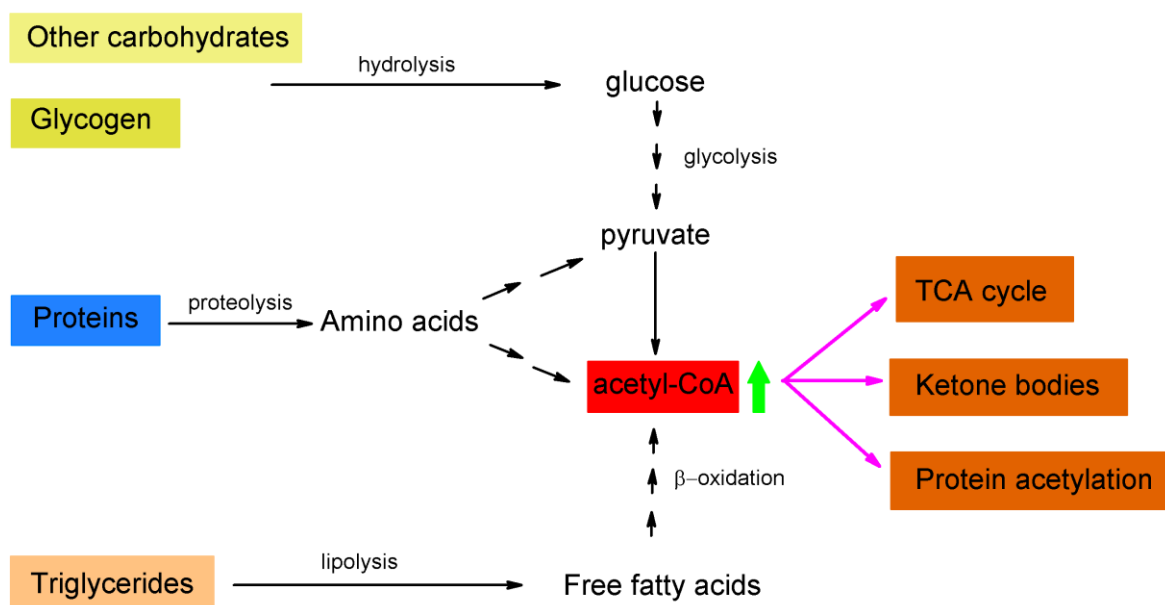


**Figure 47.** Sources and fate of mitochondrial Ac-CoA. Both, high and low nutrient input can induce mitochondrial protein hyperacetylation, through different metabolic mechanisms.

Increasing in  $\text{NAD}^+/\text{NADH}$  ratio, caused by a blocked TCA cycle, leads to activation of sirtuin enzymes. It was shown that the protein acetylation signature induced by calorie restriction differ from the one induced by SIRT3 depletion and even the expression level of SIRT3 is induced during the CR (Hebert et al., 2013). All these findings are in consistence with our results that the acetylation pattern strongly depends on the presence and activity

of certain sirtuin enzymes. Taking together we can clearly distinguish between three types of acetylation sites. Firstly, lysine acetylation sites induced by high calorie input; then lysine sites induced by calorie restriction and finally lysine sites induced by knocking down of SIRT3. In the first case, acetylated sites are the most reactive lysines including SIRT3 targets, while SIRT3 activity is reduced during high calorie input. During CR SIRT3 expression is increased (Hebert et al., 2013) and thus, acetylated sites might include the peptides which are relatively resistant to SIRT3 action. The last group includes lysines which are exclusive substrates of SIRT3 and are easily detected upon SIRT3 deletion (Hebert et al., 2013).

The phenomenon of mitochondrial protein acetylation still remains very questionable. One of the most prominent hypothesis is that protein lysine acetylation in the mitochondrial matrix results of non-enzymatic reaction driven exclusively by Ac-CoA and high pH values in this cellular compartment. The acetylation pattern depends primarily on exposure of the lysine residue on the protein surface, then on its  $pK_a$  values and finally on its resistance to sirtuin enzymes. The entire process occurs spontaneously as a result of specific metabolic conditions.

Evolution determined which lysines should be exposed on the surface, or whether to expose lysine residues in the active site of the enzyme. Highly regulatory lysine residues are in the most cases not sirtuin resistant and are implicated in the regulation of a variety of metabolic pathways. There are lysines completely resistant to sirtuin action. That opens the question if such lysines remain intact until final protein degradation or if such modified sites might cause a signal for final protein degradation.

Only 26 of 700 mitochondrial proteins show functional effects in the acetylated form (Baeza et al., 2016). Most of the acetylated lysine sites have no specific function; they have no influence on the protein activity, stability or structure. Such sites are mainly easily reversed by mitochondrial sirtuins (Weinert et al., 2015). Is such process suitable for the successful energy storage in the form of acetylated proteins? During the nutrient overloading which can lead to an increased level of Ac-CoA and increased pH in the mitochondrial matrix, part of the Ac-CoA could be "stored" on the protein pool. When it is necessary, upon sirtuin action, acetyl groups can easily be restored and get again converted to Ac-CoA through ACS action (Figure 48).

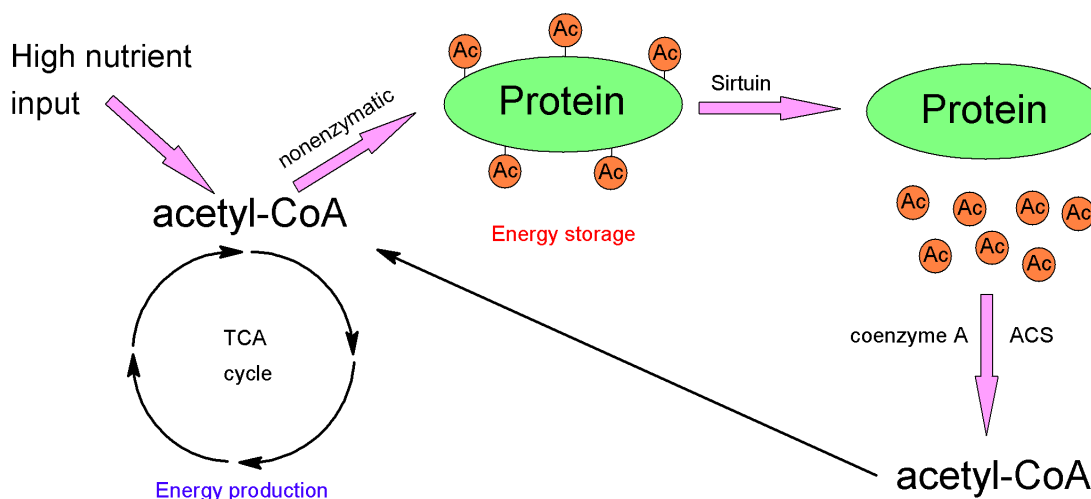


**Figure 48.** Schematic representation of the possible role of non-enzymatic protein acetylation in energy storage. During nutrient overloading part of Ac-CoA could be successfully stored using mitochondrial proteins as an acetyl-group carrier. Later, through sirtuin action and action of ACS, newly synthesized Ac-CoA can re-enter the TCA cycle and can be used for production of ATP.

Diagnose of metabolic syndromes and other disorders remain challenging for years. It was a revolutionary finding that non-enzymatic hemoglobin glycosylation exclusively depends on blood glucose level (Stevens et al., 1977). Determining the amount of the glycosylated hemoglobin represents a powerful tool in diagnostic and monitoring of diabetes mellitus (Koenig et al., 1976). Similarly, protein lysine acetylation depends not just on the concentration of modifying agent but on complex metabolic conditions and might be used as a diagnostic tool. Determination of the specific acylation landscape or acetylation pattern of specific protein markers can reflect metabolic conditions of a certain time period and give a better insight into the metabolic flow during the normal physiological or pathological state. Investment in research and development of this idea can lead to the application of such approach as a powerful diagnostic tool in the future.

And finally the question that arises logically at the end: Is non-enzymatic protein acetylation a biological relevant process? As it was shown in this study non-enzymatic lysine acetylation represents a slow chemical reaction. It appeared recently, that in the case of protein substrate, 2<sup>nd</sup> order rate constants for non-enzymatic acetylation are in a range of  $0.8-978 \times 10^{-5} \text{ M}^{-1}\text{s}^{-1}$  (Baeza et al., 2015). In this study authors used entire protein as a substrate, which could explain the relatively large difference of rate constants in comparison with our data. Moreover, different buffer system and higher pH values were

used. Anyway, our findings agree about differences in reactivity of the individual lysine residues within the same protein. They clearly demonstrated that neighbouring residues surrounding (within 7 Å) the lysine have influence on its reactivity, but they did not connect it with changes of lysine pK<sub>a</sub> values. It was shown that glutamate was the most abundant residue in the lysine surrounding, but in close distance (3.4-4 Å) it shows negative influence on the lysine reactivity. With extending distance (5-6.6 Å) it displays higher reactivity. Taken together, it is likely that protein acetylation in mitochondria does not require enzyme action. The most reactive lysine residues are acetylated sufficiently fast and can be considered to be biologically relevant.

# Summary

Mitochondria represent cellular organelles with a high level of acetylated proteins in comparison to other cellular compartments. Variety of enzymes implicated in pathophysiology of diabetes, cancer, and metabolic syndrome are highly regulated by acetylation but mitochondrial residential lysine acetyltransferases have not been recognized. Here we show that acetylation, as well as other acylations are spontaneous processes that depend on pH value, acyl-CoA concentration and the chemical nature of the acyl residue. In the case of short peptide substrate derived from carbamoyl phosphate synthetase 1, dicarboxylic acyl groups show highest level of reactivity. The rates for succinylation and glutarylation were up to 150 times higher than for acetylation. Reactivities of the CoA-thioesters decrease with extending the acyl chain therefore propionylation and butyrylation show lower acylation rates in comparison to acetylation. Surprisingly, HMG-CoA was found to modify peptide substrate with acylation rates three times higher than for acetylation, which makes HMG a promising candidate for a novel protein posttranslational modification. These results were confirmed by using the protein substrate cyclophilin A (CypA). Deacylation experiments revealed that SIRT3 exhibits deacetylase activity but is not able to remove any of the succinyl group from CypA, whereas SIRT5 is an efficient protein desuccinylase. Considering that we have not found convincing evidence about existence of mitochondrial lysine acetyltransferase so far, it leads us to conclusion that acylation landscape on the lysine residues might largely depend on the enzymatic activities of sirtuins and availability and/or reactivity of certain acyl-CoA thioesters.

# Zusammenfassung

Mitochondrien repräsentieren zelluläre Organellen mit einem hohen Gehalt an acetylierten Proteinen, im Vergleich zu anderen zellulären Kompartimenten. Eine Vielzahl von Enzymen, die in die Pathophysiologie von Diabetes, Krebs und dem metabolischen Syndrom involviert sind, werden stark durch Acetylierung reguliert, im Mitochondrium angesiedelte Lysin-Acetyltransferasen sind jedoch nicht bekannt. Hier zeigen wir, dass Acetylierung, ebenso wie andere Acylierungen, spontane Prozesse darstellen, die vom pH-Wert, der Acyl-CoA-Konzentration und dem chemischen Charakter des Acylrestes abhängen. Im Falle eines kurzen Peptidsubstrates, abgeleitet von der Carbamoylphosphat-Synthetase 1, zeigen dicarboxylierte-Acylgruppen den höchsten Grad an Reaktivität. Die Geschwindigkeiten der Succinylierung und Glutarylierung waren bis zu 150-mal schneller als die der Acetylierung. Die Reaktivität der CoA-Thioester nimmt mit Verlängerung der Acylkette ab, deshalb zeigen Propionyl- und Butyrylierung niedrigere Acylierungsgeschwindigkeiten im Vergleich zur Acetylierung. Erstaunlicherweise, acylierte HMG-CoA Peptidsubstrate mit dreimal höherer Acylierungsgeschwindigkeit im Vergleich zur Acetylierung, damit stellt HMG einen aussichtsreichen Kandidaten für neue posttranslationale Proteinmodifikation dar. Diese Ergebnisse wurden durch Nutzung von Cyclophilin A (CypA) als Proteinsubstrat bestätigt. Deacylierungsexperimente zeigten, dass SIRT3 eine Lysin-Deacetylaseaktivität besitzt, jedoch nicht in der Lage ist, Succinylgruppen von CypA zu entfernen. SIRT5 stellt hingegen eine effiziente Lysin-Desuccinylase dar. Unter Berücksichtigung der Tatsache, dass wir bislang nicht den überzeugenden Beweis für die Existenz einer mitochondrialen Lysin-Acetyltransferase haben, schlussfolgern wir, dass die Acylierungsvielfalt an Lysinresten wahrscheinlich stark von der enzymatischen Aktivität der Sirtuine und/oder der Verfügbarkeit und Reaktivität bestimmter Acyl-CoA-Thioester abhängt.

# Appendix

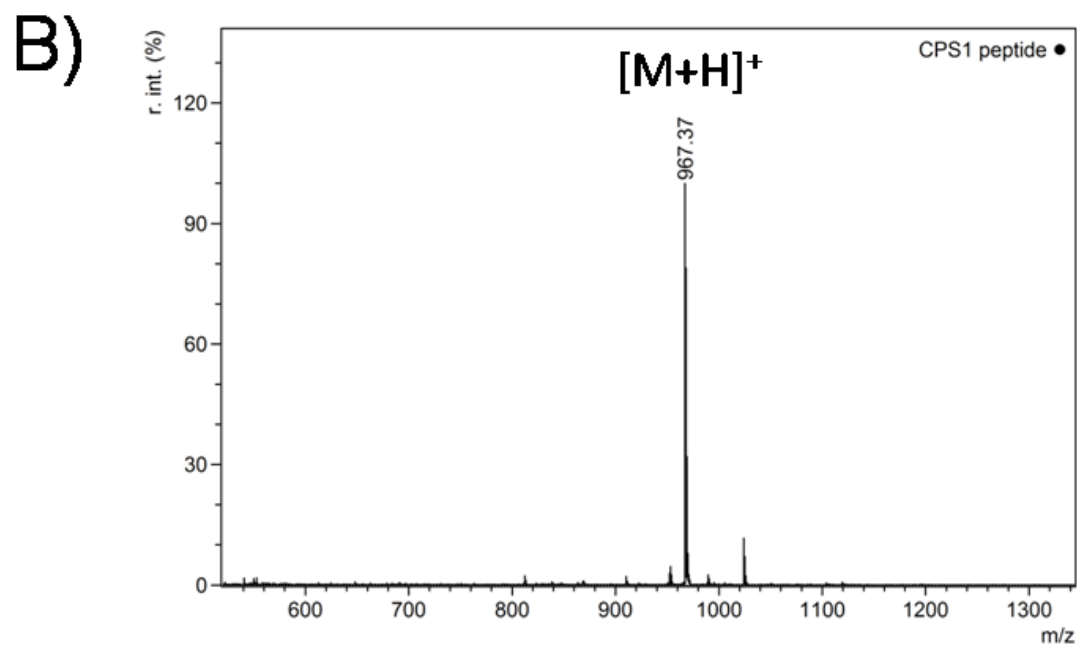
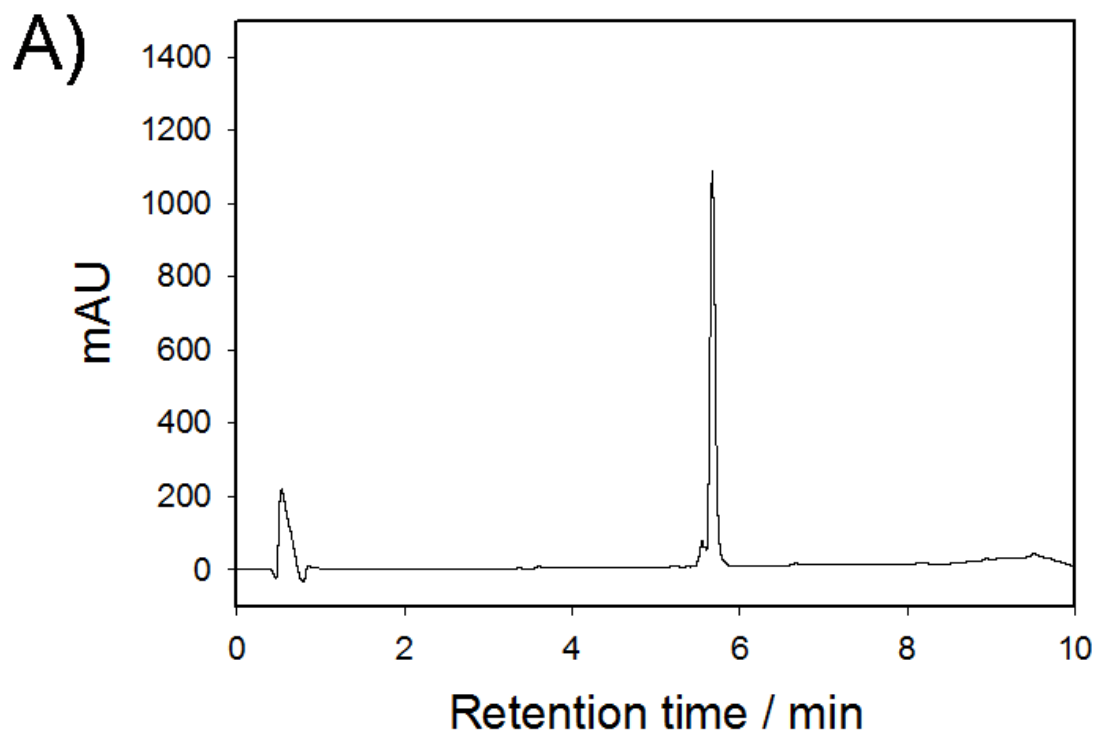


**Figure A1.** Analytical HPLC chromatogram of CPS1 peptide. **A)** Linear gradient 5-70 % ACN over 7 min was applied. Detection was at 260 nm.  $t_R$ : 5.67 min. **B)** MALDI-TOF MS spectrum of CPS1 peptide.  $[M+H]^+ = 967.4$  Da. Theoretical mass: 967.5 Da.



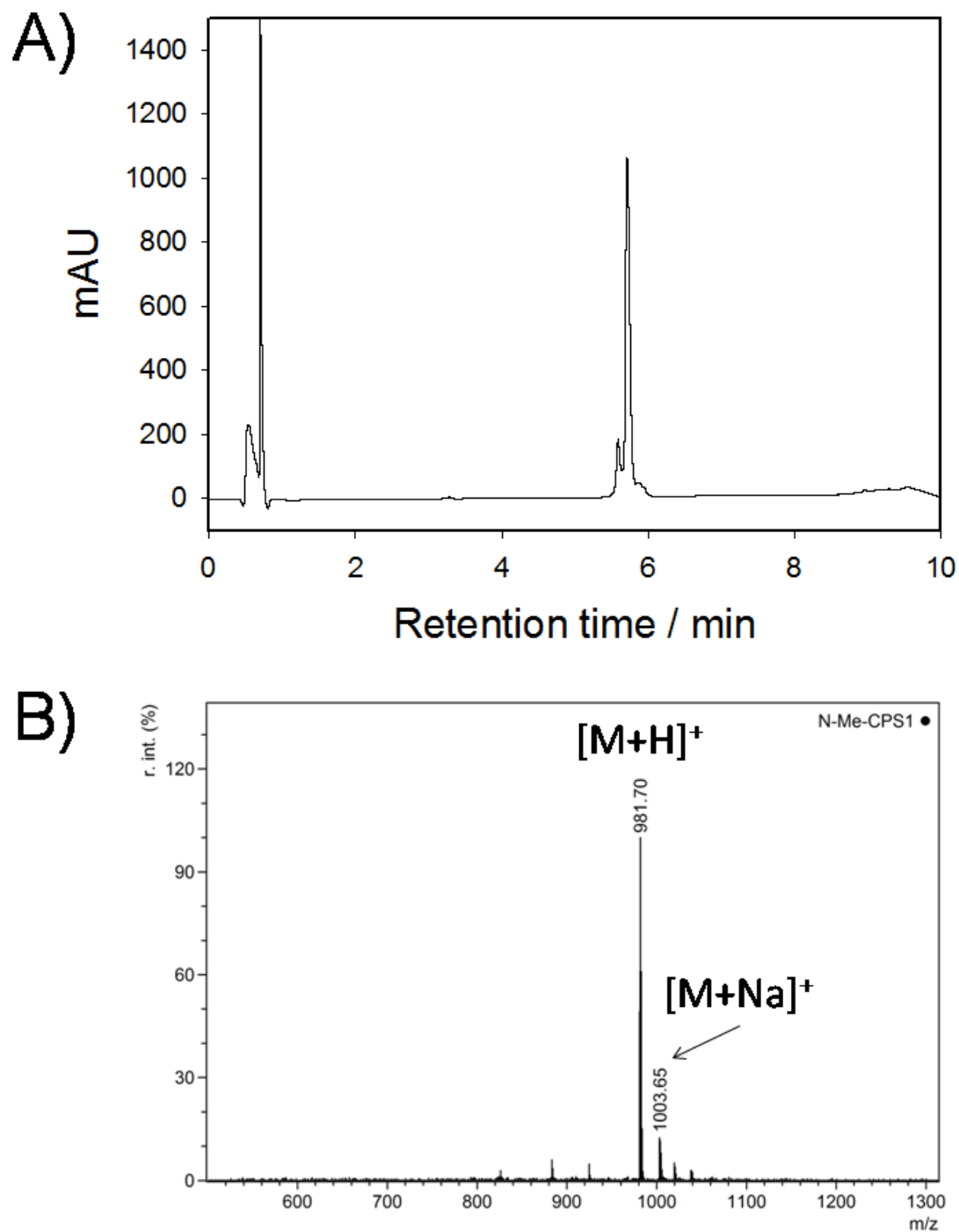


**Figure A2.** Analytical HPLC chromatogram of N-methyl-CPS1 peptide. **A)** Linear gradient 5-70 % ACN over 7 min was applied. Detection was at 260 nm.  $t_R$ : 5.71 min. **B)** MALDI-TOF MS spectrum of N-methyl-CPS1 peptide.  $[M+H] = 981.7$  Da. Theoretical mass: 981.5 Da.

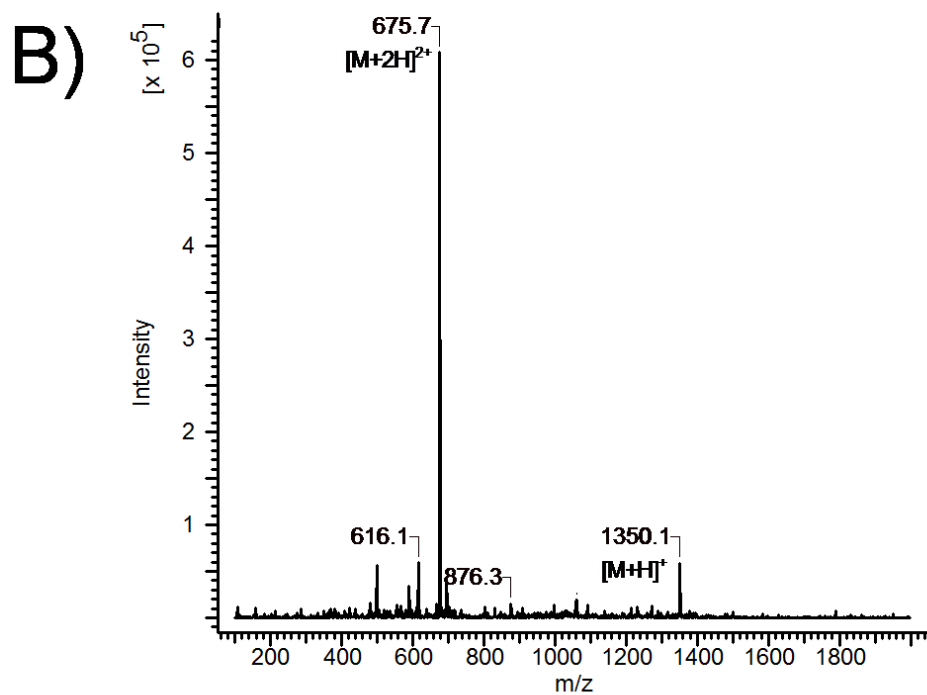
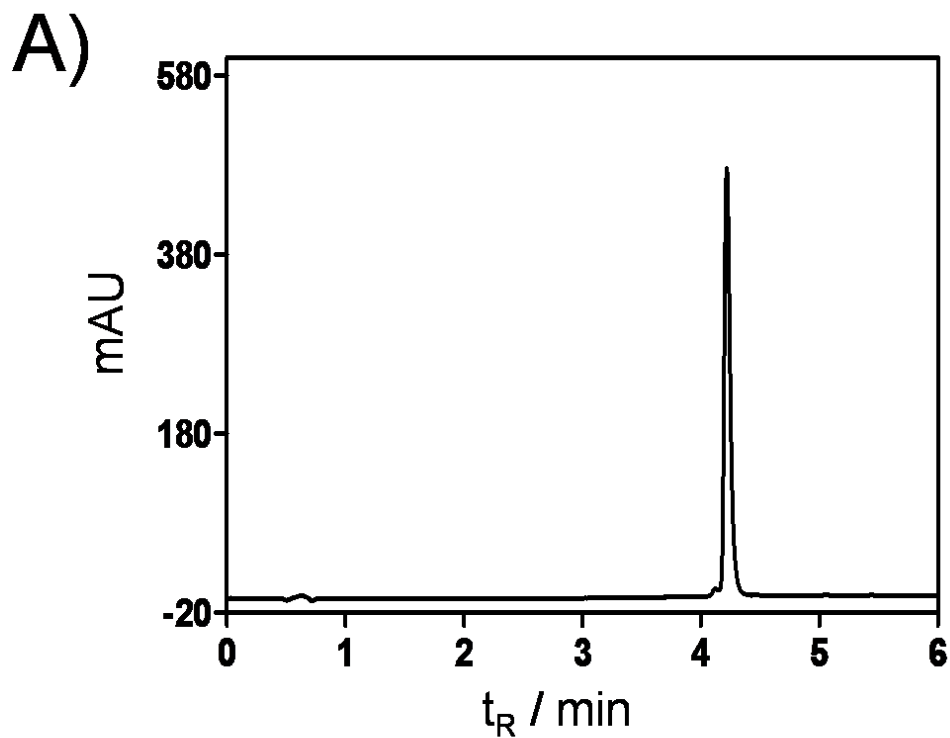


**Figure A3.** Analytical HPLC and MS-spectrum of TNF $\alpha$  peptide 1. Figure is adapted from Schuster et al. 2016 (Schuster et al., 2016).

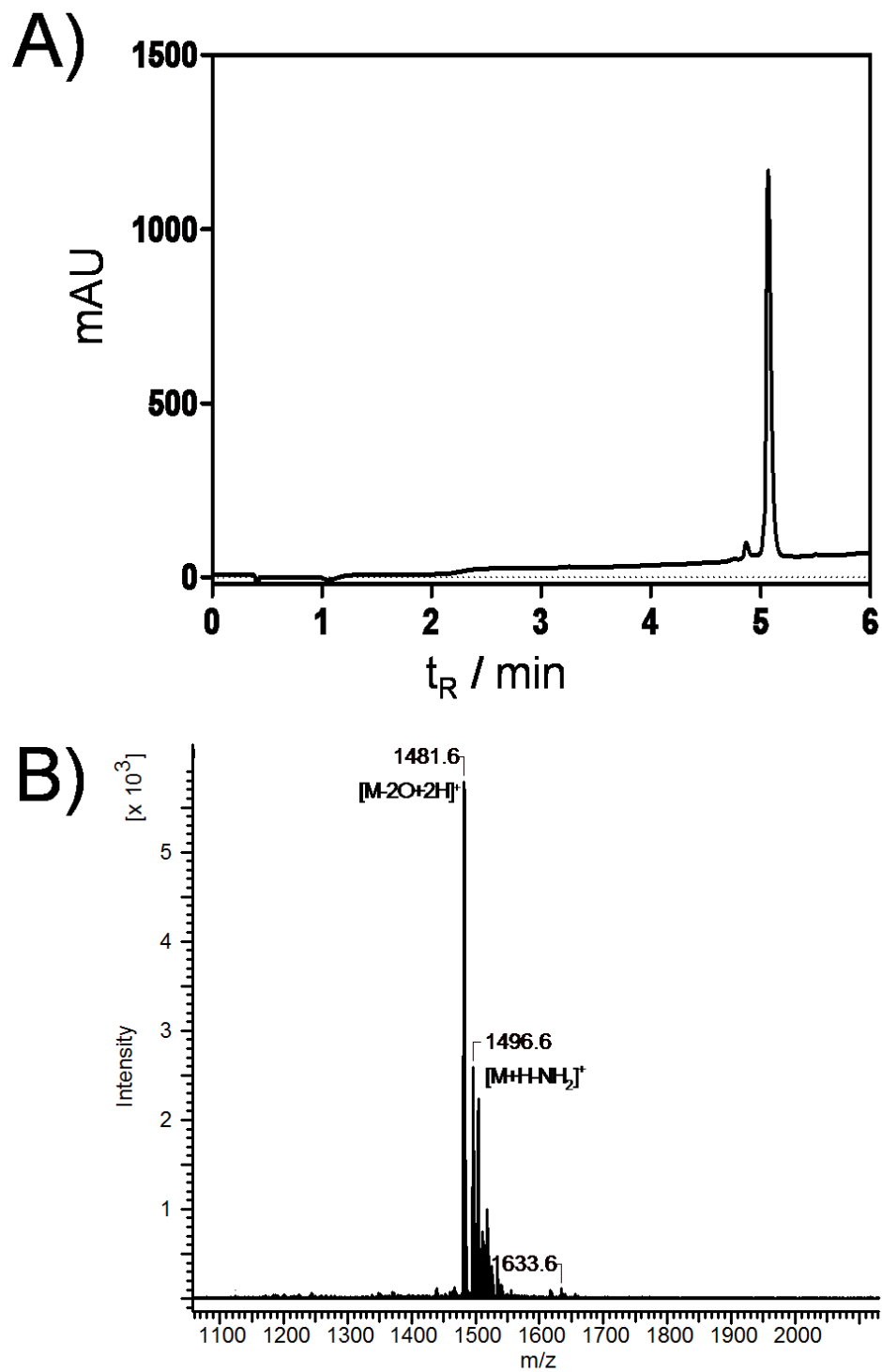


**Figure A4.** Analytical HPLC and MS-spectrum of TNF $\alpha$  peptide 2. Figure is adapted from Schuster et al. 2016 (Schuster et al., 2016).

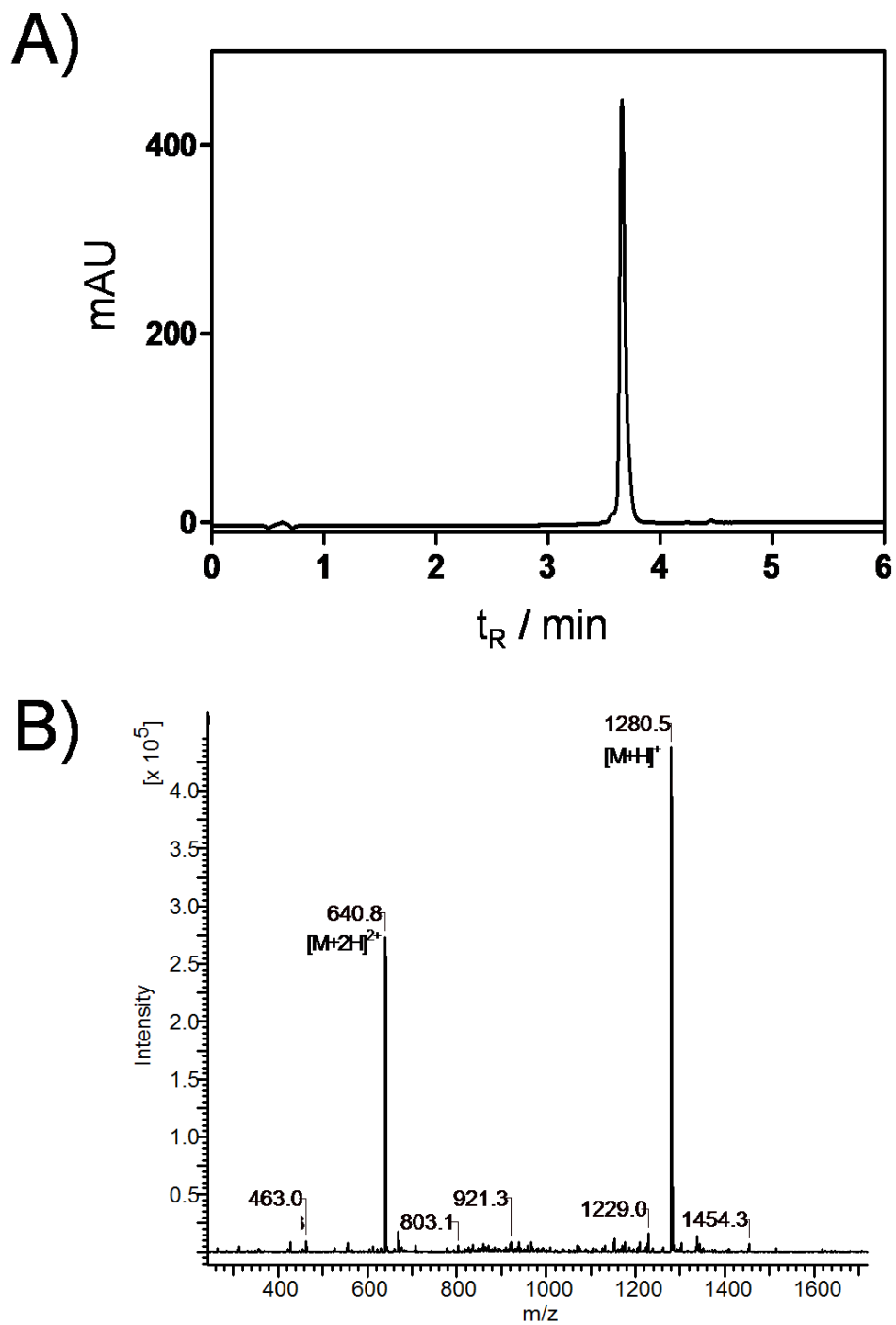


**Figure A5.** Analytical HPLC and MS-spectrum of TNF $\alpha$  peptide 3. Figure is adapted from Schuster et al. 2016 (Schuster et al., 2016).

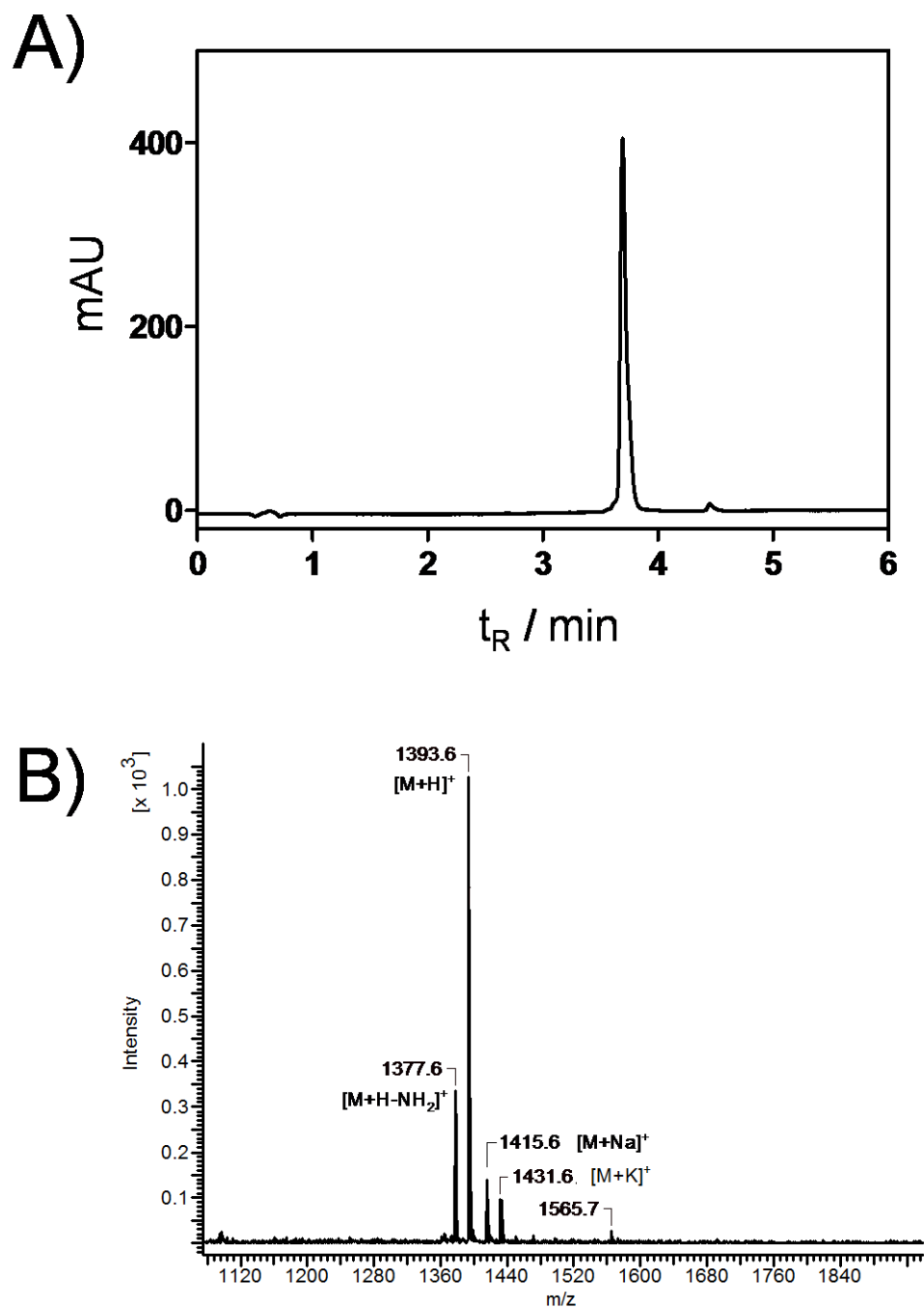


**Figure A6.** Analytical HPLC and MS-spectrum of TNF $\alpha$  peptide 4. Figure is adapted from Schuster et al. 2016 (Schuster et al., 2016).

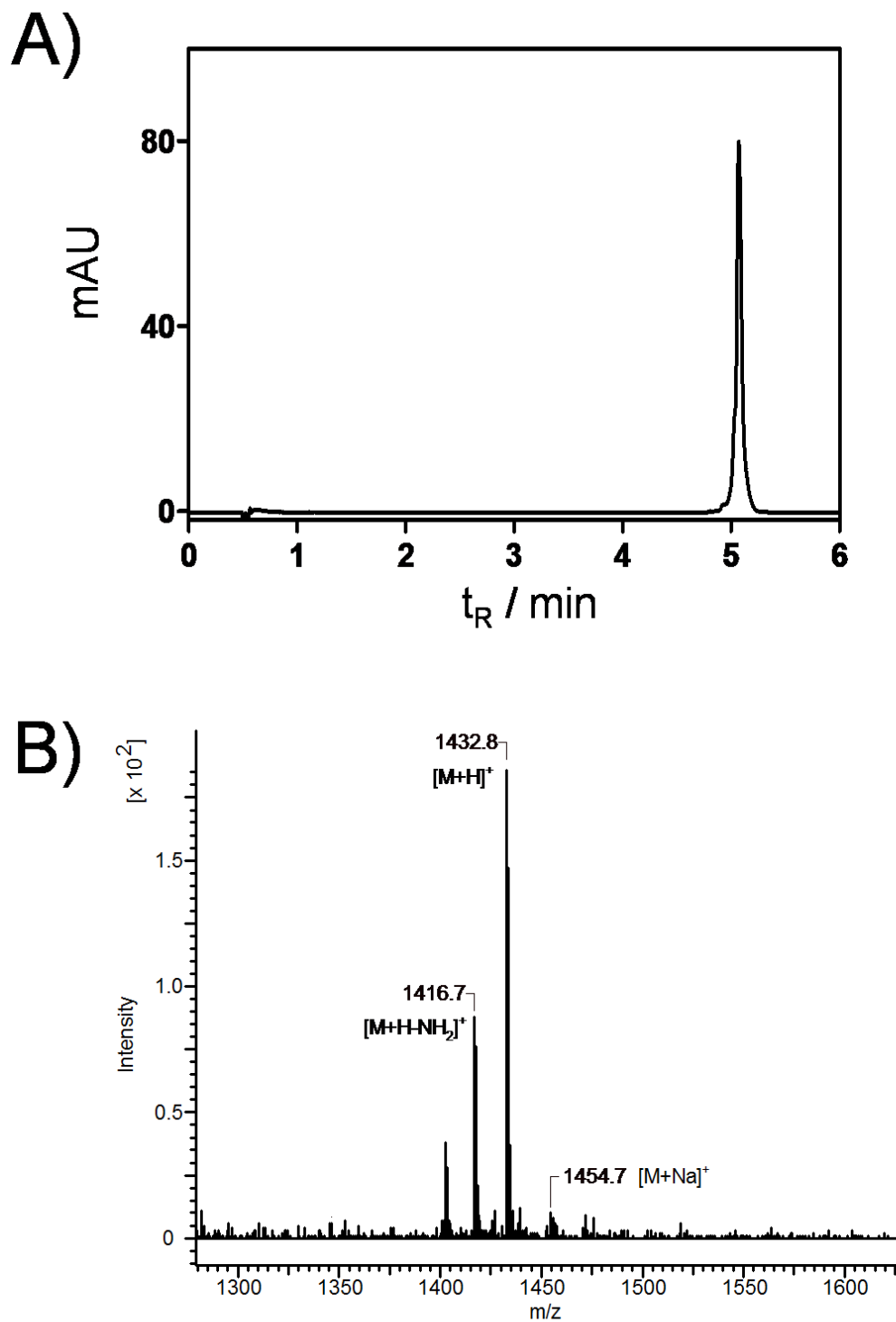


**Figure A7.** Analytical HPLC and MS-spectrum of TNF $\alpha$  peptide 5. Figure is adapted from Schuster et al. 2016 (Schuster et al., 2016).

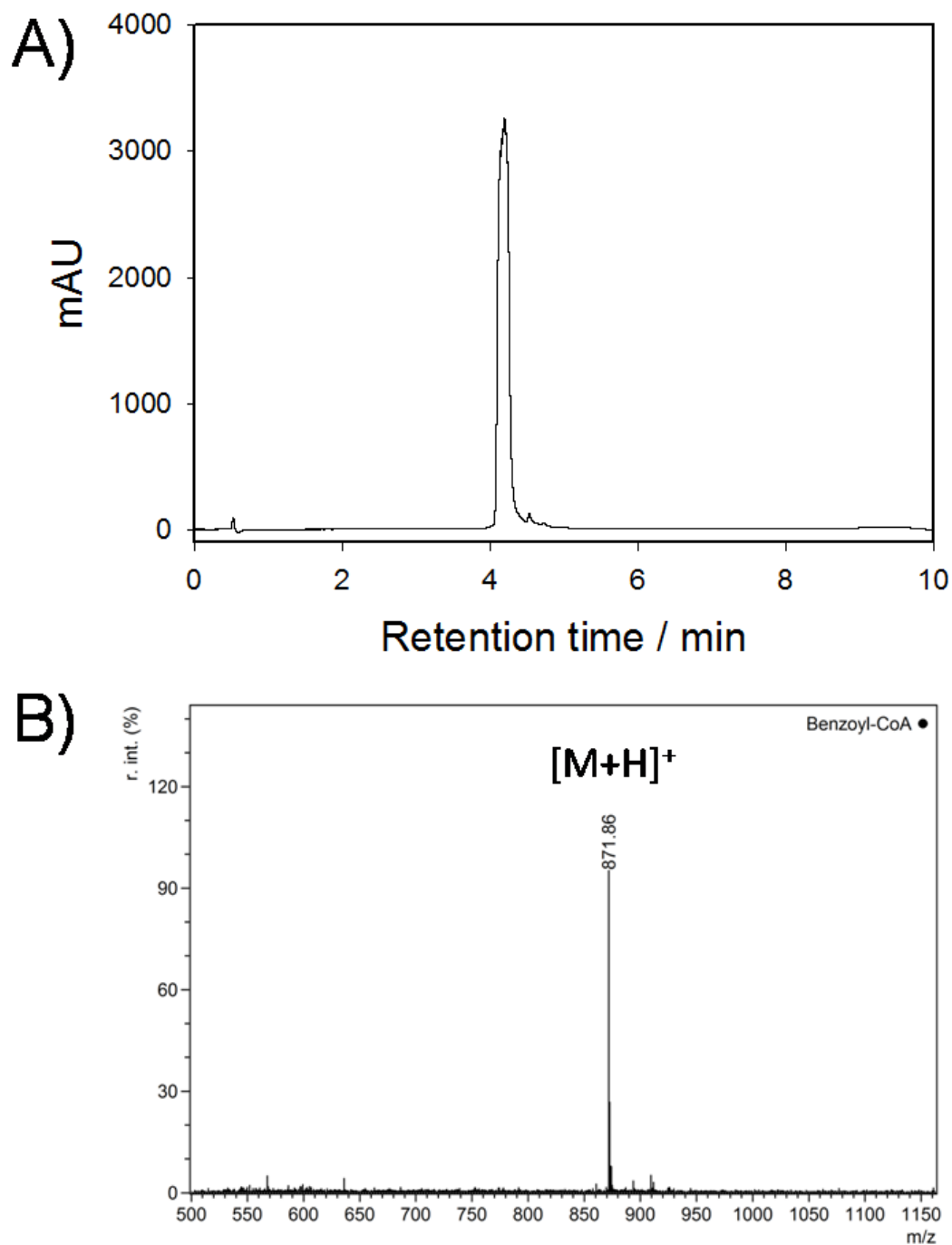


**Figure A8.** Analytical HPLC chromatogram of Benz-CoA. **A)** Linear gradient 5-70 % ACN over 7 min was applied. Detection was at 260 nm.  $t_R$ : 4.2 min. **B)** MALDI-TOF MS spectrum of Benz-CoA.  $[M+H] = 871.86$  Da. Theoretical monoisotopic mass: 871.14 Da.

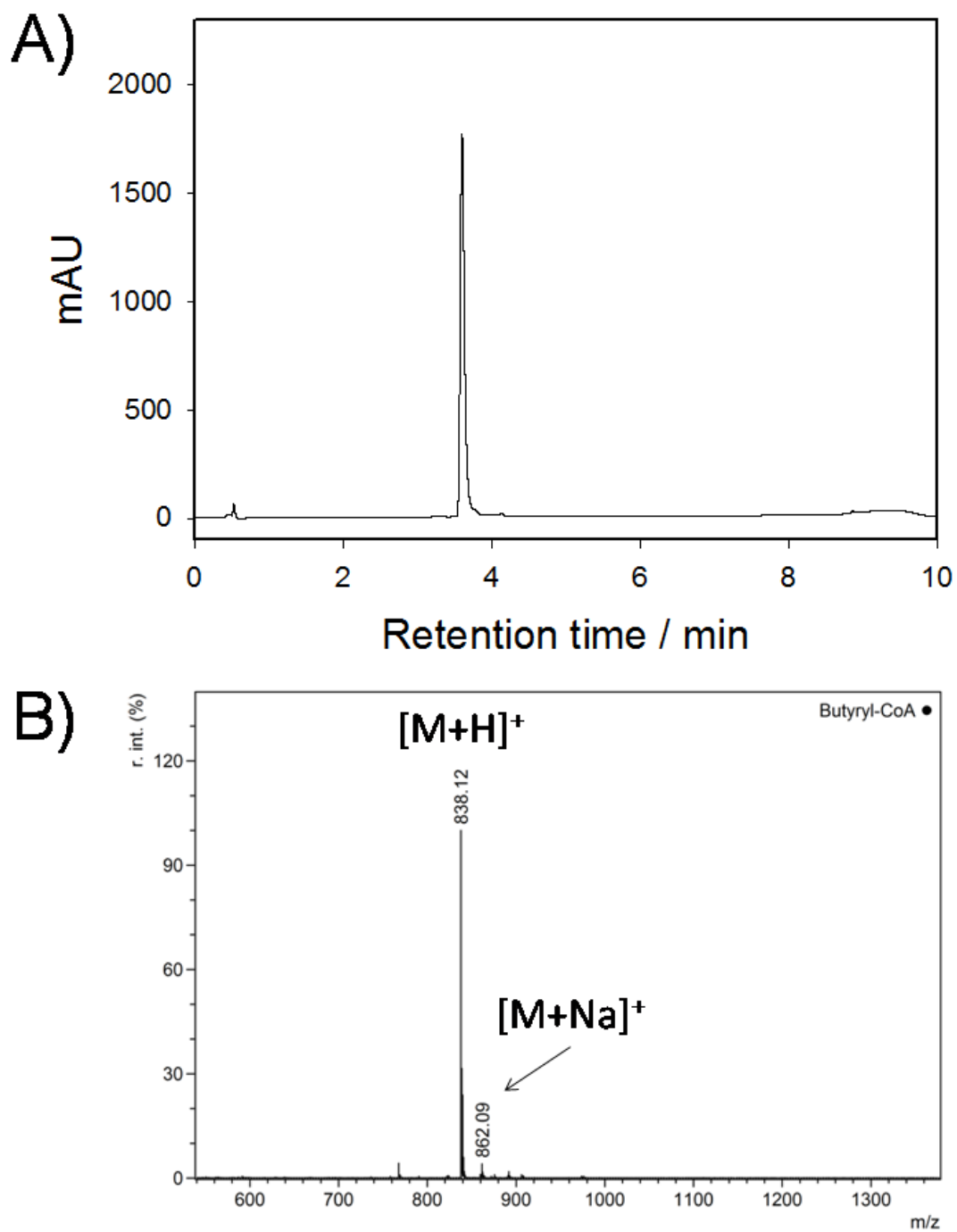


**Figure A9.** Analytical HPLC chromatogram of But-CoA. **A)** Linear gradient 5-70 % ACN over 7 min was applied. Detection was at 260 nm.  $t_R$ : 3.6 min. **B)** MALDI-TOF MS spectrum of But-CoA.  $[M+H]^+ = 838.12$  Da. Theoretical monoisotopic mass: 837.16 Da.



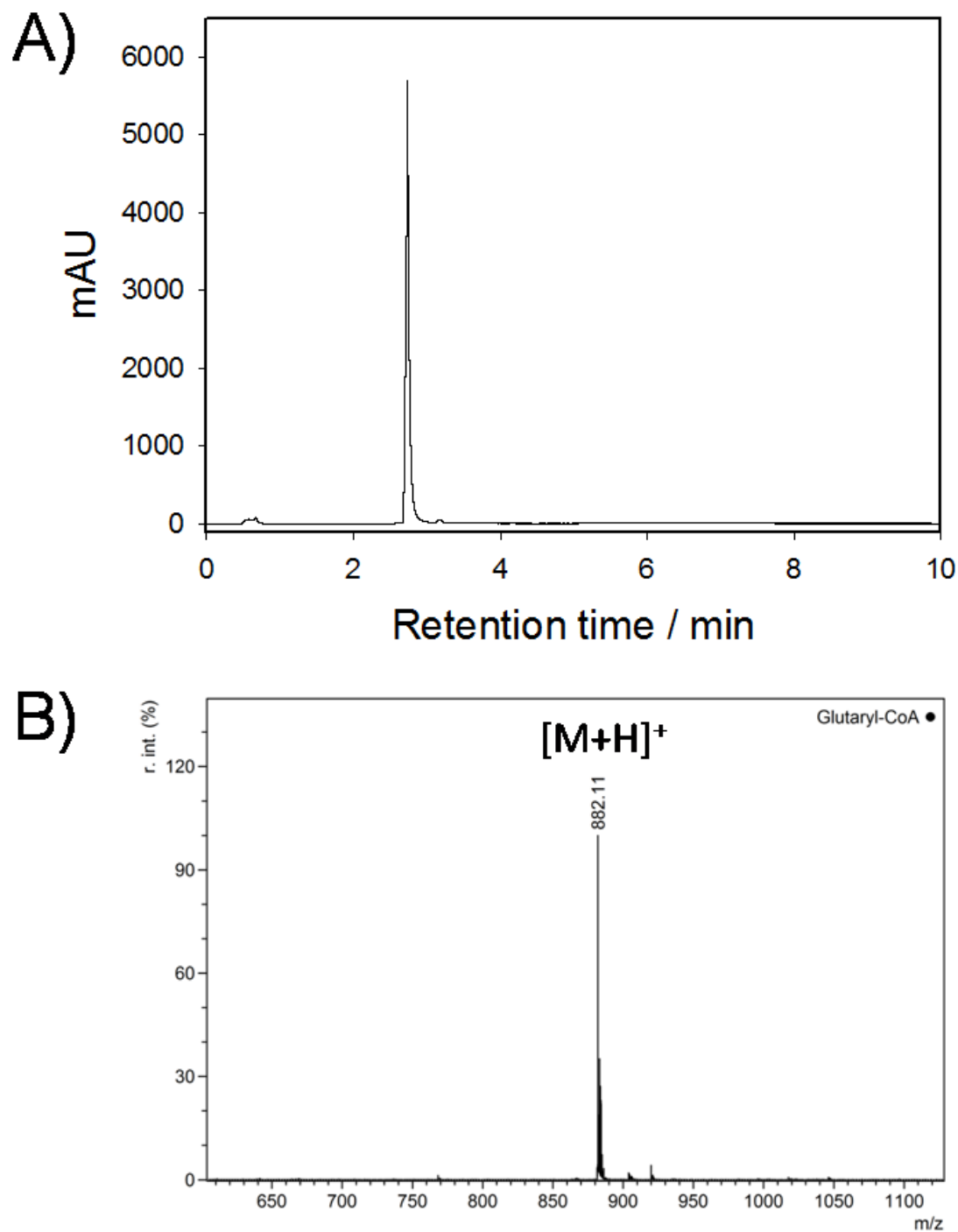


**Figure A10.** Analytical HPLC chromatogram of Glut-CoA. **A)** Linear gradient 5-70 % ACN over 7 min was applied. Detection was at 260 nm.  $t_R$ : 2.7 min. **B)** MALDI-TOF MS spectrum of Glut-CoA.  $[M+H] = 882.11$  Da. Theoretical monoisotopic mass: 881.15 Da.

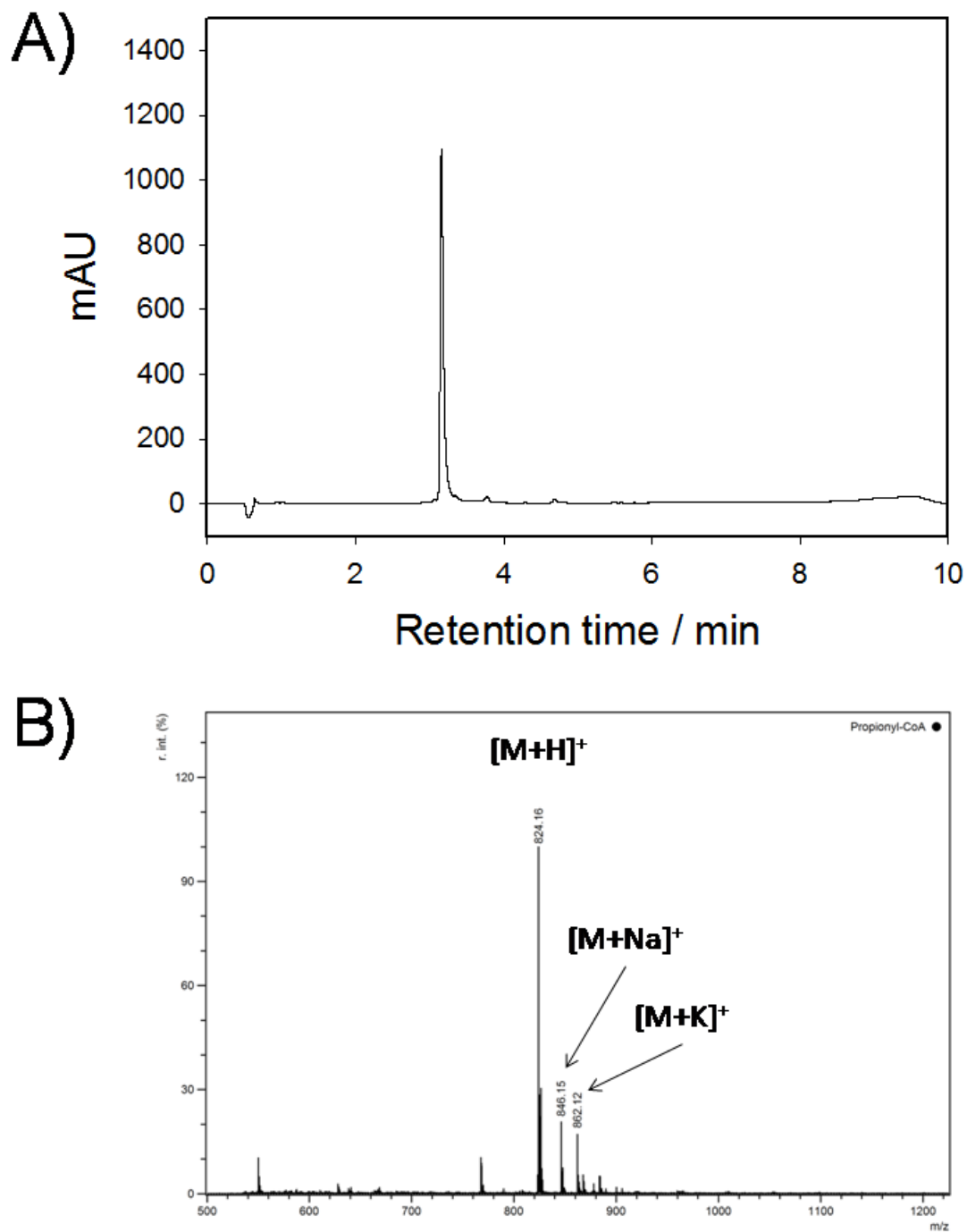


**Figure A11.** Analytical HPLC chromatogram of Prop-CoA. **A)** Linear gradient 5-70 % ACN over 7 min was applied. Detection was at 260 nm.  $t_R$ : 3.16 min. **B)** MALDI-TOF MS spectrum of Prop-CoA.  $[M+H] = 824.16$  Da. Theoretical monoisotopic mass: 823.14 Da.

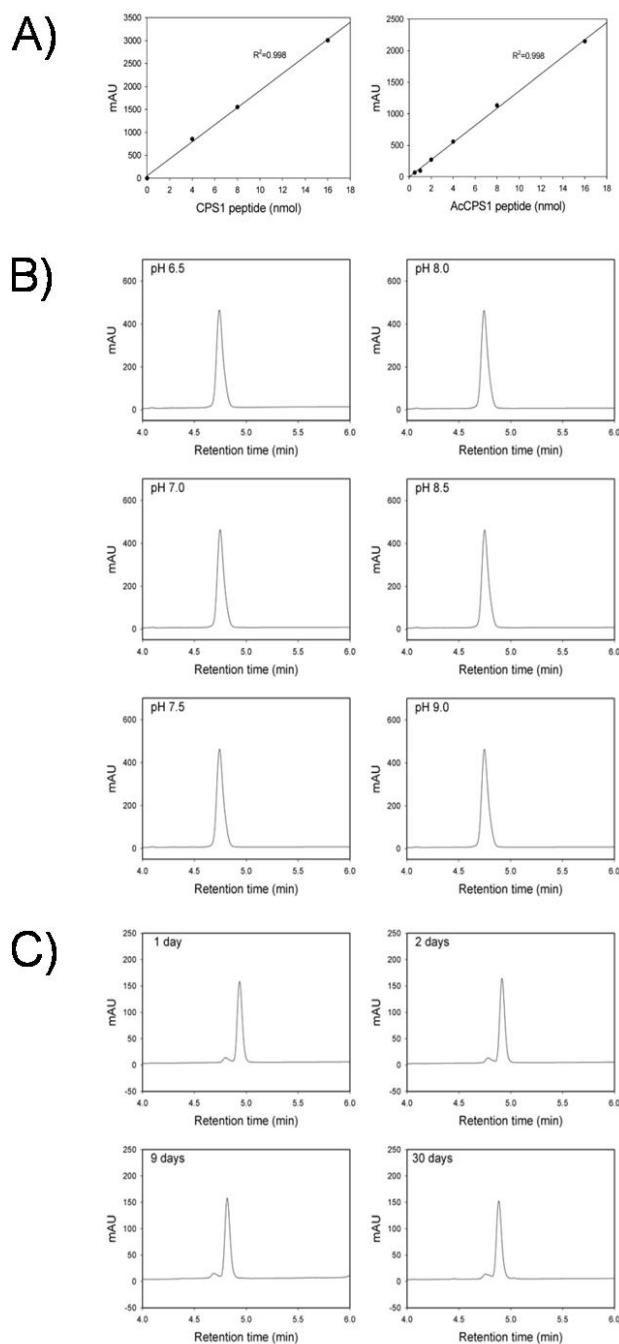


**Figure A12.** Validation of the HPLC method. **A)** Areas under the peaks were plotted against the concentrations of CPS1 peptide and acetylated CPS1 peptide, respectively. The figure reveals that linearity is ensured in the range between 0.5 - 16 nmol peptide. **B)** pH stability of CPS1 peptide. Aliquots of CPS1 peptide solution (400  $\mu$ M) were incubated at 37°C for 60 min at different pH values. Samples were analyzed by RP-HPLC. The figure reveals no decomposition of the peptide in the pH range 6.5 - 9.0. **C)** CPS1 peptide is stable in buffer solution. As shown by RP-HPLC analysis, a solution of 200  $\mu$ M CPS1 peptide is stable for more than 30 days in 200 mM Tris-HCl pH 8.0 at 37°C. Figure is adapted from Simic et al. 2015 with permission (Simic et al., 2015).

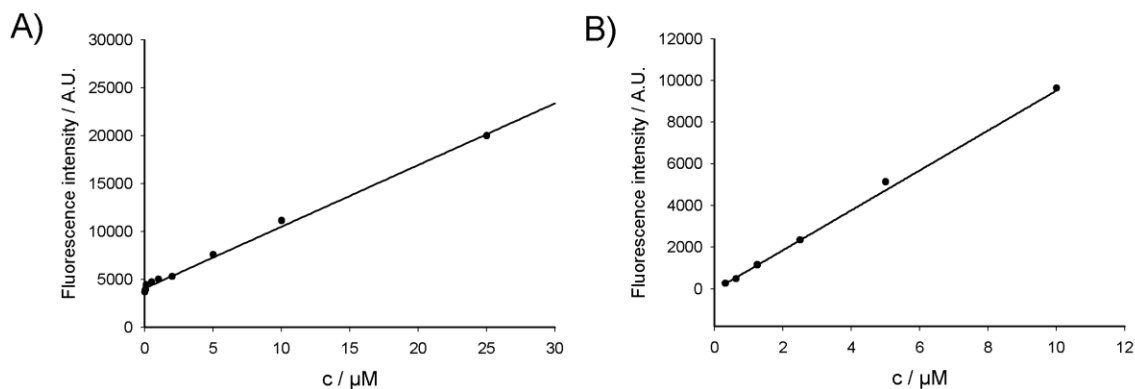


**Figure A13.** Calibration curves for TNF $\alpha$  peptides 1 and 2. The reaction mixtures contained 2  $\mu$ M SIRT2, 500  $\mu$ M NAD<sup>+</sup> and 100  $\mu$ M of TNF $\alpha$  peptides 1 and 2. After complete turnover of peptide substrate, the mixtures were diluted and analyzed by fluorescence measurements; **A)** TNF $\alpha$  peptides 1 and **B)** TNF $\alpha$  peptides 2. Figure is adapted from Schuster et al. 2016 (Schuster et al., 2016).

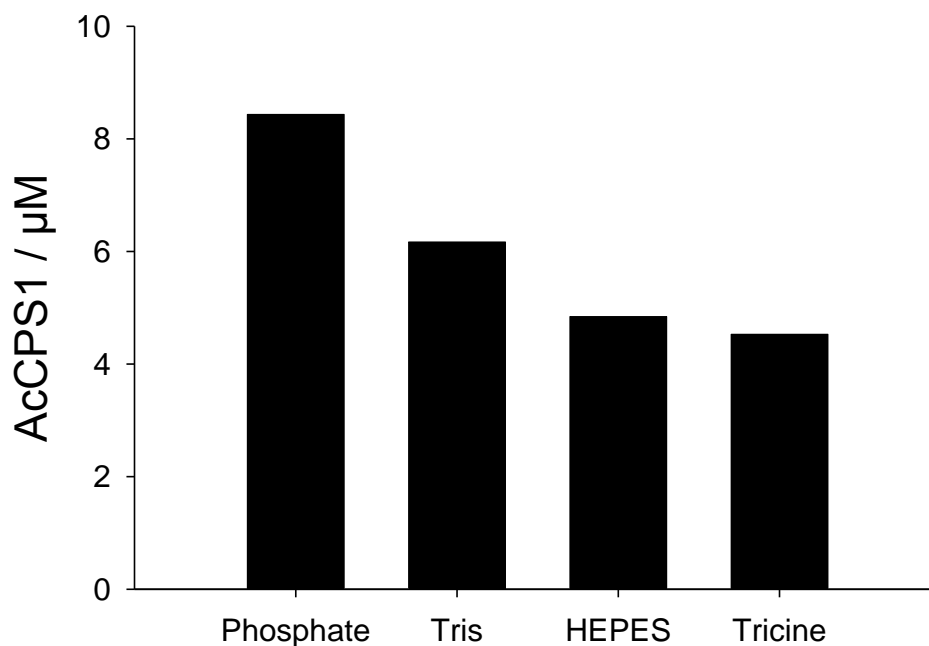


**Figure A14.** Comparison of non-enzymatic lysine acetylation in the presence of a variety of different buffers. 200  $\mu$ M CPS1 peptide was incubated with 4 mM Ac-CoA at 37 °C and pH 8.0 for 14 h in the presence of different 200 mM buffers. Reaction mixtures were analyzed using RP-HPLC. Figure is adapted from Simic et al. 2015 with permission (Simic et al., 2015).

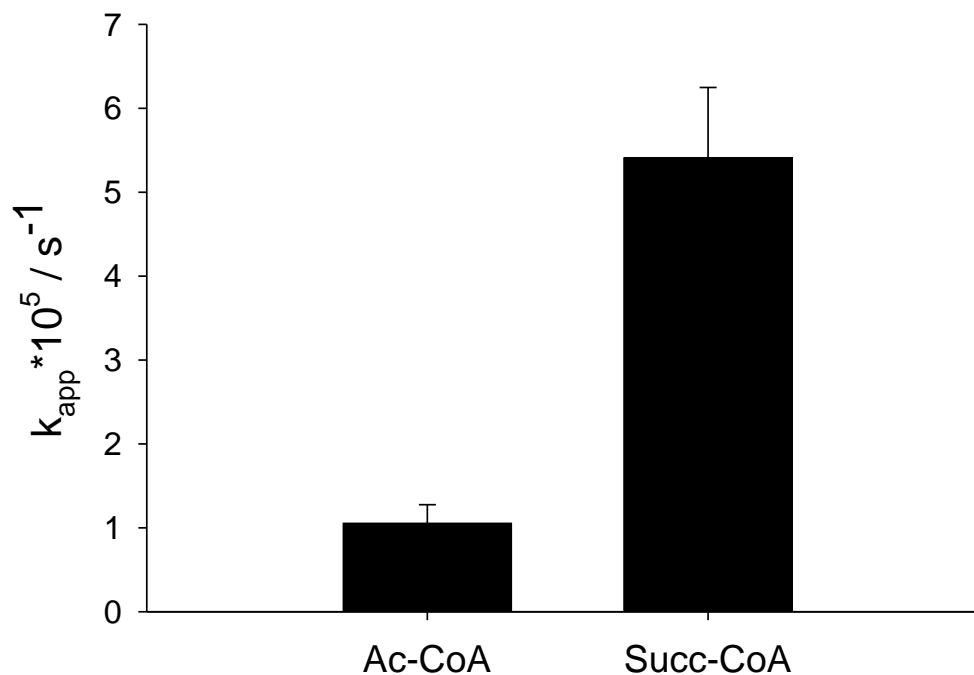


**Figure A15.** Hydrolytic stability of Ac- and Succ-CoA. Different concentrations of Ac- and Succ-CoA were incubated in 200 mM Tris/HCl buffer pH 8.0 at 37° C. At different time points concentrations of free CoA were determined by using RP-HPLC with a 3.0 × 75 mm Agilent Poroshell 120 EC-C18 column and linear gradient 5 - 50 % (v/v) ACN. Hydrolysis rates were calculated according pseudo-first order kinetics. This experiment revealed that Succ-CoA exhibits a five times higher pseudo-first order rate constant for hydrolysis than Ac-CoA. Ac-CoA and Succ-CoA display half-life of 18.2 and 3.8 h, respectively. Error bars represent standard deviations of at least three independent experiments. Figure is adapted from Simic et al. 2015 with permission (Simic et al., 2015).

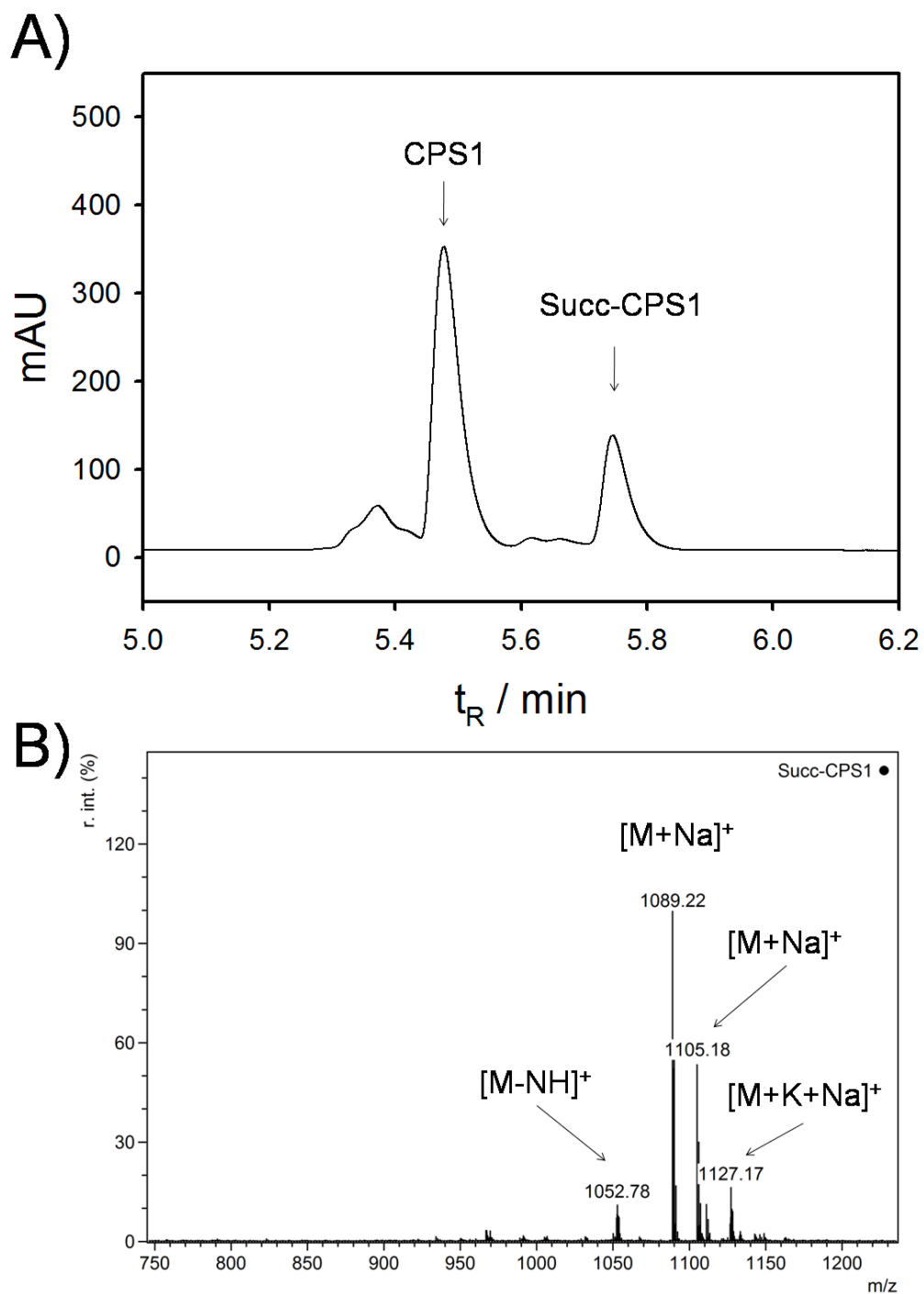


**Figure A16.** Modification of CPS1 peptide by Succ-CoA. **A)** Analytical HPLC chromatogram of reaction mixture of 200  $\mu$ M CPS1 peptide with 1 mM Succ-CoA in 200 mM Tris-HCl buffer pH 8.0 after 5 h at 37°C. Linear gradient 5-70 % ACN over 7 min was applied. Detection was at 260 nm. Peak at  $t_R$ :5.77 min was identified as Succ-CPS1 peptide. **B)** Succ-CPS1 peak was manually collected and confirmed by MALDI-TOF MS.  $[M+Na]^+$ =1089.22 Da. Theoretical monoisotopic mass: 1066.51 Da.

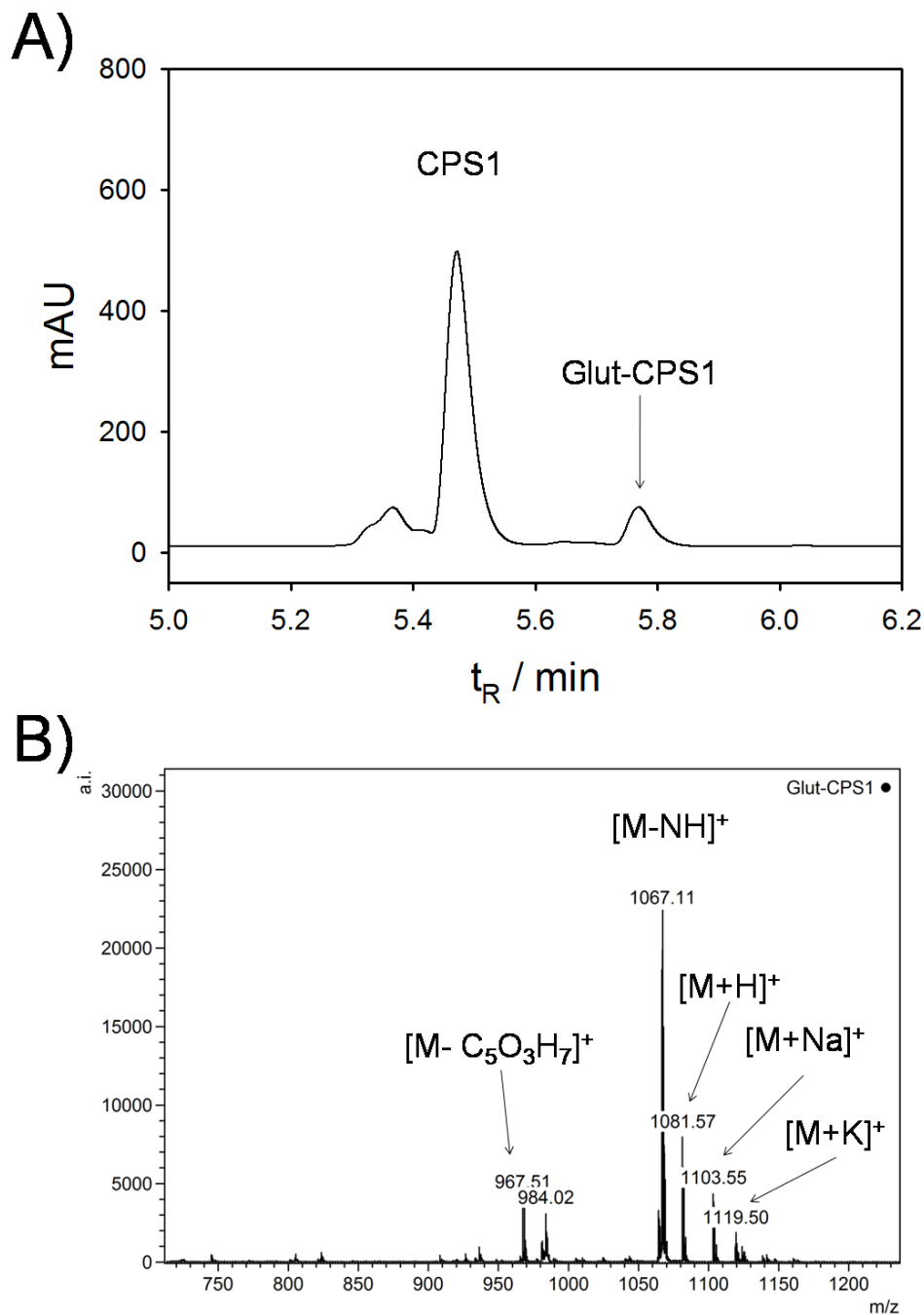


**Figure A17.** Modification of CPS1 peptide by Glut-CoA. **A)** Analytical HPLC chromatogram of reaction mixture of 200  $\mu$ M CPS1 peptide with 4 mM Glut-CoA in 200 mM Tris-HCl buffer pH 8.0 after 24 h at 37°C (**A**). Linear gradient 5-70 % ACN over 7 min was applied. Detection was at 260 nm. Peak at  $t_R$ :5.77 min was identified as Glut-CPS1 peptide. **B)** MALDI-TOF MS spectrum of reaction mixture.  $[M+H]^+$  =1081.57 Da. Theoretical monoisotopic mass: 1080.51 Da.

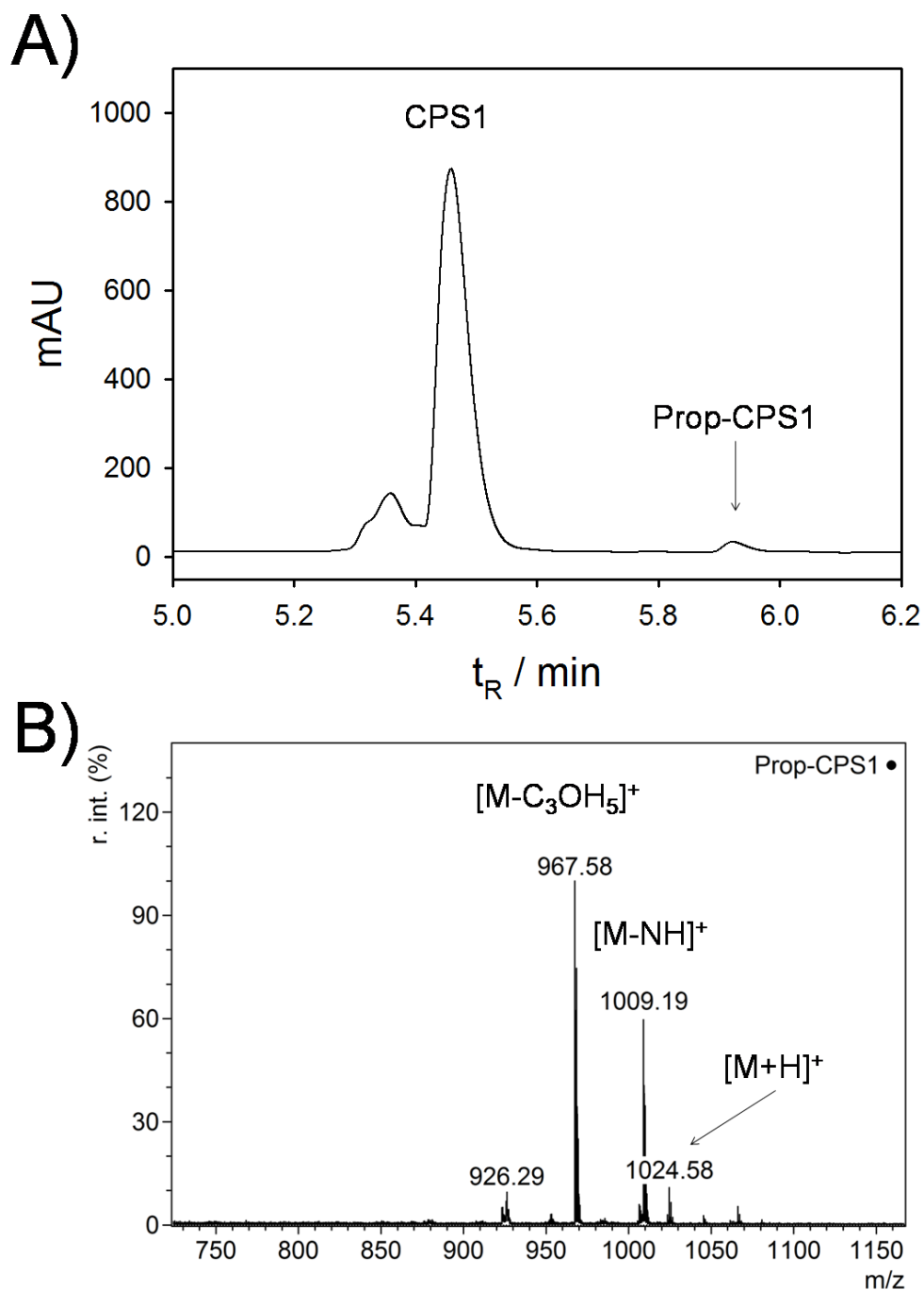


**Figure A18.** Modification of CPS1 peptide by Prop-CoA. **A)** Analytical HPLC chromatogram of reaction mixture of 200  $\mu$ M CPS1 peptide with 4 mM Prop-CoA in 200 mM Tris-HCl buffer pH 8.0 after 24 h at 37°C. Linear gradient 5-70 % ACN over 7 min was applied. Detection was at 260 nm. Peak at  $t_R$ :5.92 min was identified as Prop-CPS1 peptide. **B)** MALDI-TOF MS spectrum of reaction mixture.  $[M+H]^+$ =1024.58 Da. Theoretical monoisotopic mass: 1023.57 Da.



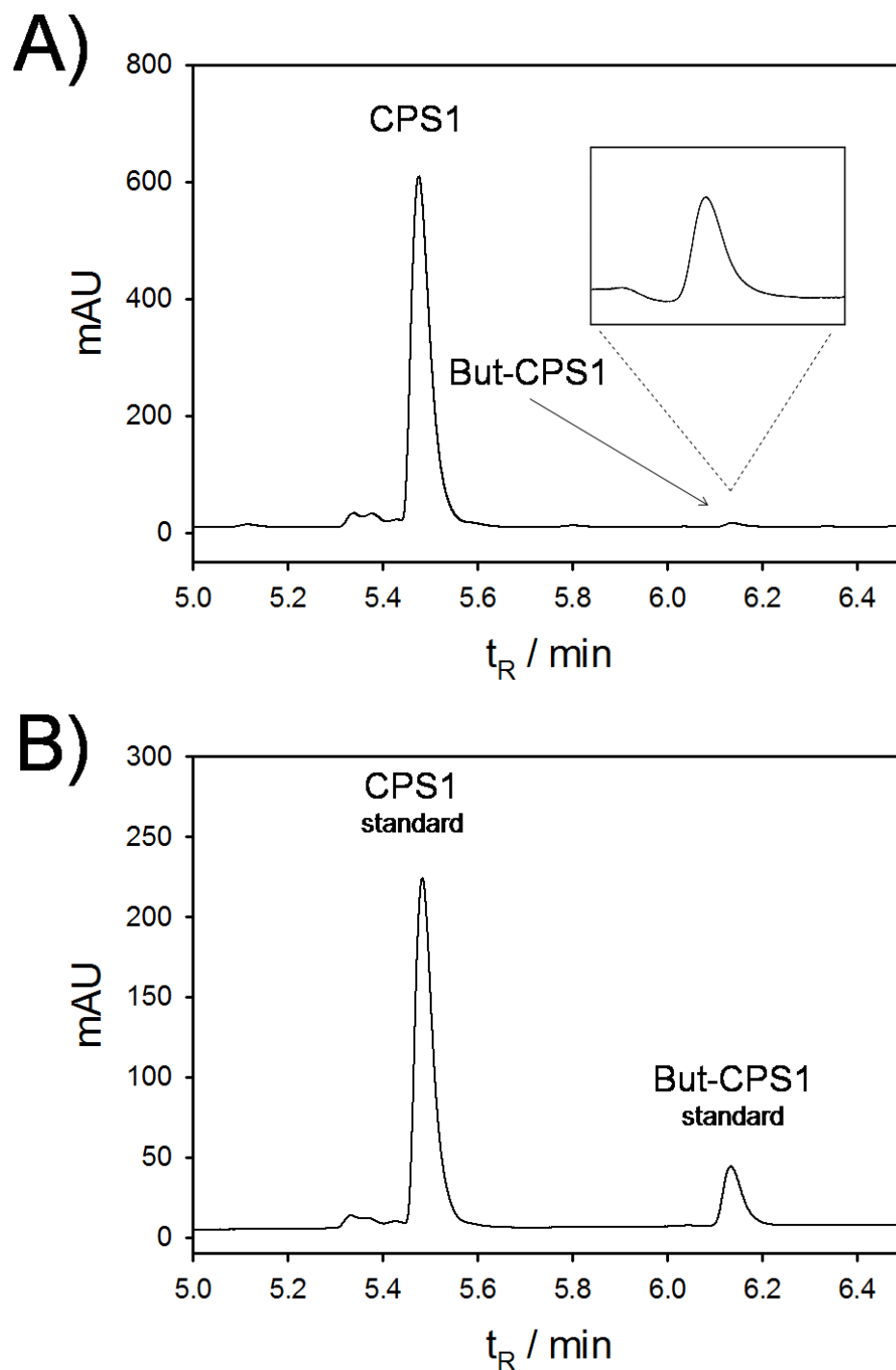


**Figure A19.** Modification of CPS1 peptide by But-CoA. **A)** Analytical HPLC chromatogram of reaction mixture of 200  $\mu$ M CPS1 peptide with 4 mM But-CoA in 200 mM Tris-HCl buffer pH 8.0 after 24 h at 37°C. Linear gradient 5-70 % ACN over 7 min was applied. Detection was at 260 nm. Peak at  $t_R$ :6.14 min was identified as Butyryl-CPS1 peptide. **B)** Analytical HPLC chromatogram of CPS1 and butyryl-CPS1 standards.

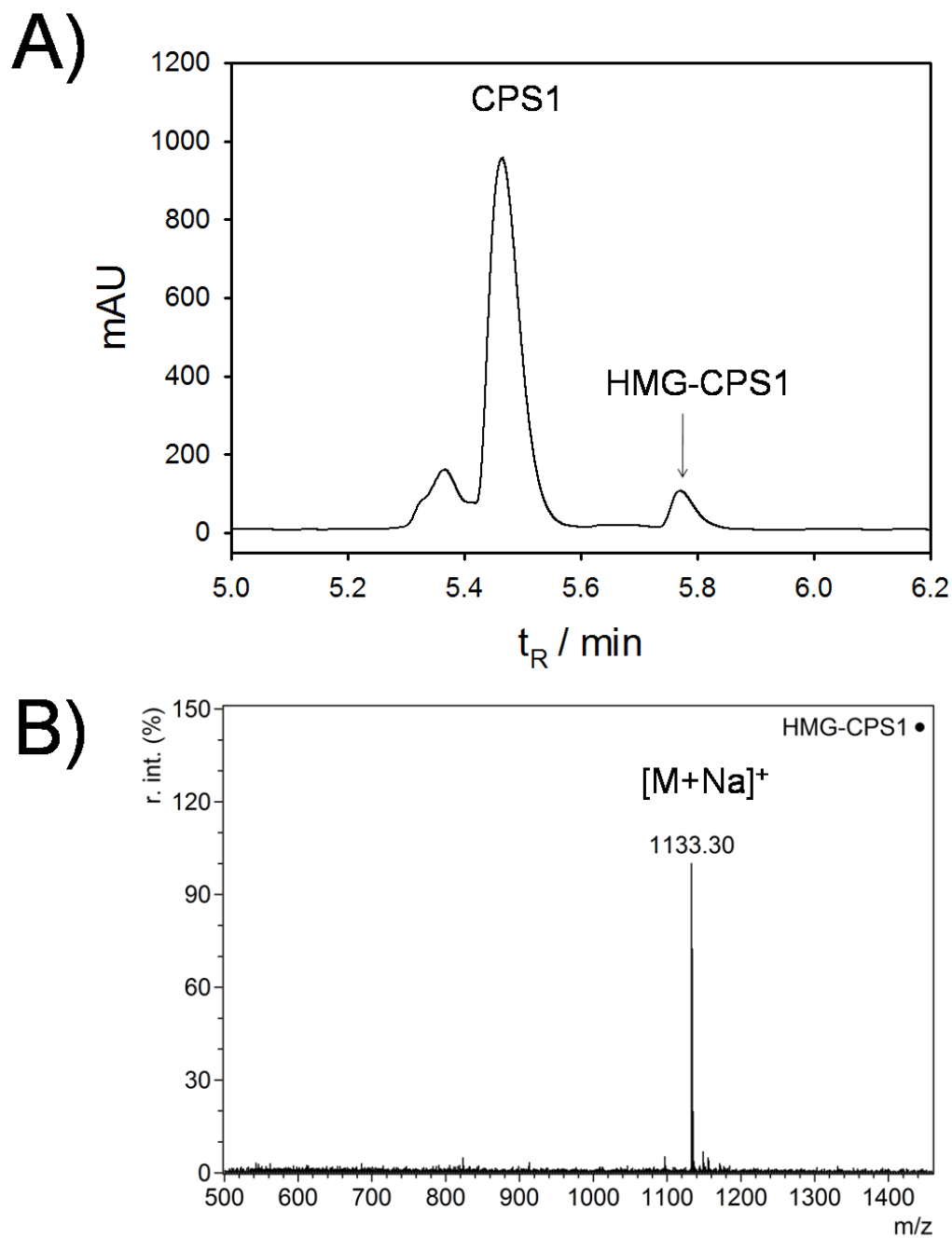


**Figure A20.** Modification of CPS1 peptide by HMG-CoA. **A)** Analytical HPLC chromatogram of reaction mixture of 200  $\mu$ M CPS1 peptide with 4 mM HMG-CoA in 200 mM Tris-HCl buffer pH 8.0 after 24 h at 37°C. Linear gradient 5-70 % ACN over 7 min was applied. Detection was at 260 nm. Peak at  $t_R$ :5.77 min was identified as HMG-CPS1 peptide. **B)** MALDI-TOF MS spectrum of HMG-CPS1 peptide.  $[M+Na]^+$ =1133.3 Da. Theoretical monoisotopic mass: 1110.3 Da.

```

CypA,      3 NPTVFFDIAVDGEPLGRVSFELFADKVPKTAENFRALSTGEKGFYKGSCHFRIIPGFMC
CypD,     45 NPLVYLDVDANGKPLGRVVLELKADVVPKTAENFRALCTGEKGFYKGSTFHRVIPSFMC
          ** * * * * * * * * * * * * * * * * * * * * * * * * * * * * * * * *
          * * * * * * * * * * * * * * * * * * * * * * * * * * * * * * * *

CypA,      63 QGGDFTRHNGTGGKSIYGEKFEDENFILKHTGPGILSMANAGPNTNGSQFFICTAKTEWL
CypD,     105 QAGDFTNHNGTGGKSIYGSRFPDENFTLKHVGPVLSMANAGPNTNGSQFFICTIKTDWL
          * * * * * * * * * * * * * * * * * * * * * * * * * * * * * * * *
          * * * * * * * * * * * * * * * * * * * * * * * * * * * * * * * *

CypA,      123 DGKHVVFVGKVEGMNIVEAMERFGSRNGKTSKKIT IADCGQL
CypD,     165 DGKHVVFVGHVKEGMDVVKIESFGSKSGRTSKKIVITDCGQL
          * * * * * * * * * * * * * * * * * * * * * * * * * * * * * * * *
          * * * * * * * * * * * * * * * * * * * * * * * * * * * * * * * *

```

**Figure A21.** CypA and CypD sequence alignment. CypA shows 76.5 % sequence identity with its mitochondrial protein analogue CypD.

**Table A1.** Posttranslational lysine modifications of CypA.

Position of lysine modification	Peptide sequence	Type of modification	Reference
K28	SFELFADKVPKTAEN	acetylation	(Choudhary et al., 2009)
		succinylation	(Weinert et al., 2013)
K31	LFADKVPKTAENFRA	acetylation	(Weinert et al., 2013)
		succinylation	(Weinert et al., 2013)
K44	RALSTGEKGFYKGS	acetylation	(Choudhary et al., 2009)
		succinylation	(Weinert et al., 2013)
K49	GEKGFYKGSFCFHRI	acetylation	(Choudhary et al., 2009)
		succinylation	(Weinert et al., 2013)
K76	RHNGTGGKSIYGEKF	acetylation	(Choudhary et al., 2009)
		succinylation	(Weinert et al., 2013)
K82	GKSIYGEKFEDENFI	acetylation	(Choudhary et al., 2009)
		succinylation	(Weinert et al., 2013)
K91	EDENFILKHTGPGIL	acetylation	(Weinert et al., 2013)
K118	QFFICTAKTEWLDGK	acetylation	(Choudhary et al., 2009; Sol et al., 2012; Weinert et al., 2013)
K125	KTEWLDGKHVVFVKV	acetylation	(Choudhary et al., 2009; Kim et al., 2006; Mertins et al., 2013; Shaw et al., 2011; Sol et al., 2012; Weinert et al., 2013)
		succinylation	(Weinert et al., 2013)
K131	GKHVVFVKVKEGMNI	acetylation	(Beli et al., 2012; Choudhary et al., 2009; Mertins et al., 2013; Weinert et al., 2013)
K155	RNGKTSKKITIADCG	acetylation	(Mertins et al., 2013)

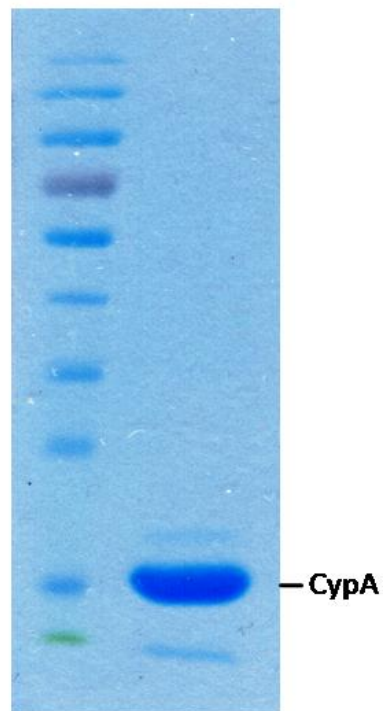


**Figure A22.** SDS-PAGE of CypA. Reaction mixture containing CypA (10  $\mu$ M), 4 mM Ac-CoA in Tris-HCl buffer pH 8.0 after incubation at 37°C over time was subjected to PAGE. CypA band at ~18 kDa was cutted out from the gel and processed further to in gel digestion by trypsin and later to LC-MS/MS analysis.

**Table A2.** List of CypA not-modified tryptic peptides.

Peptide sequence:	Peptide mass (Da)		Calculated Mass Error (ppm)	Peptide RT** (min)
	Calculated	Detected		
<b>MVNPTVFFDIAVDGEPLGR</b>	2076.035	2076.033	-0.8	21
<b>VSFELFADK</b>	1054.533	1054.534	0.3	16.9
<b>VPK</b>	342.216	n.d.		
<b>TAENFR</b>	736.3504	736.3483	-2.9	3.7
<b>ALSTGEK</b>	704.3705	704.3682	-3.3	1.7
<b>GFGYK</b>	570.2802	570.2784	-3.2	9.6
<b>GSCFHR*</b>	762.3232	762.3233	0.1	1.1
<b>IIPGFMCQGGDFTR</b>	1540.717	1540.715	-1	16.7
<b>HNGTGGK</b>	669.309	n.d.		
<b>SIYGEK</b>	695.349	695.3479	-1.6	5.3
<b>FEDENFILK</b>	1153.566	1153.564	-1.6	15.2
<b>HTGPGILSMANAGPNTNGSQFFICTAK</b>	2733.3	2733.313	4.5	17.4
<b>TEWLDGK</b>	847.4076	847.4051	-3	12.1
<b>HVVFGK</b>	685.3911	685.3883	-4.1	9.2
<b>VK</b>	245.163	n.d.		
<b>EGMNIVEAMER</b>	1277.574	1277.572	-1.8	15.4
<b>FGSR</b>	465.223	n.d.		
<b>NGK</b>	317.159	n.d.		
<b>TSK</b>	334.174	n.d.		
<b>K</b>	146.095	n.d.		
<b>ITIADCGQLE</b>	1061.506	1061.505	-1.2	15.5

\*Carbamidomethyl Cysteine      n.d. - not detected

\*\*retention time

**Table A3.** List of tryptic CypA peptides containing acetylated lysine residue.

Tryptic CypA peptides sequences	K position within the protein	Modification of lysine residue	Peptide mass (Da)		Calculated Mass Error (ppm)	Peptide RT (min)
			calculated	detected		
VSFELFADKVPK	K28	K(acetyl)	1420.7603	1420.7596	-0.5	18.3
VPKTAENFR	K31	K(acetyl)	1102.5771	1102.5782	1	11.3
ALSTGEEKGFGYK	K44	K(acetyl)	1298.6506	1298.6519	1	13.2
GFGYKGSFCFHR	K49	K(acetyl)	1356.6034	1356.6067	2.4	12.6
HNGTGGKSIYGEK	K76	K(acetyl)	1388.6685	1388.6682	-0.2	9.8
SIYGEKFEDENFILK	K82	K(acetyl)	1872.9146	1872.9182	1.9	17.9
FEDENFILKHTGPGILSMANAGPNTNGSQFFICTAK*	K91	K(acetyl)	3967.8872	3967.8855	-0.4	19.5
HTGPGILSMANAGPNTNGSQFFICTAKTEWLDGK*	K118	K(acetyl)	3661.7295	3661.7361	1.8	19.7
TEWLDGKHVVFGK	K125	K(acetyl)	1556.7987	1556.8026	2.5	16.1
HVVFGKVK	K131	K(acetyl)	954.5651	954.5667	1.7	11.6
VKEGMNIVEAMER	K133	K(acetyl)	1546.7486	1546.7469	-1	16.7
NGKTSK	K151	K(acetyl)	675.334	n.d		
TSKK	K154	K(acetyl)	504.269	n.d		
KITIADCGQLE*	K155	K(acetyl)	1288.6333	1288.6343	0.8	15.2

\*Carbamidomethyl Cysteine

n.d. - not detected

**Table A4.** List of tryptic CypA peptides containing succinylated lysine residue.

Tryptic CypA peptides sequences	K position within the protein	Modification of the lysine residue	Peptide mass (Da)		Calculated Mass Error (ppm)	Peptide RT** (min)
			calculated	detected		
VSFELFADKVPK	K28	K(succinyl)	1478.7656	1478.7649	-0.5	18.2
VPKTAENFR	K31	K(succinyl)	1160.5825	1160.5801	-2.1	11.2
ALSTGEEKGFGYK	K44	K(succinyl)	1356.6561	1356.6565	0.3	13.3
GFGYKGGSCFHR*	K49	K(succinyl)	1414.6088	1414.6091	0.2	12.7
HNGTGGKSIYGEK	K76	K(succinyl)	1446.6738	1446.6761	1.6	10.1
SIYGEKFEDENFILK	K82	K(succinyl)	1930.9199	1930.9208	0.5	17.9
FEDENFILKHTGPGILSMANAGPNTNGSQFFICTAK*	K91	K(succinyl)	4025.8928	4025.8977	1.2	19.4
HTGPGILSMANAGPNTNGSQFFICTAKTEWLDGK*	K118	K(succinyl)	3719.7349	3719.7334	-0.4	19.5
TEWLDGKHVVFGK	K125	K(succinyl)	1614.8041	1614.809	3	16.1
HVVFGKVK	K131	K(succinyl)	1012.5705	1012.5717	1.2	11.8
VKEGMNIVEAMER	K133	K(succinyl)	1604.7538	1604.7545	0.4	16.7
NGKTSK	K151	K(succinyl)	733.334	733.3606	-5.6	1.1
TSKK	K154	K(succinyl)	562.269	526.2824	-24.5	12
KITIADCGQLE*	K155	K(succinyl)	1346.6388	1346.6404	1.2	15.2

\*Carbamidomethyl Cysteine

\*\*retention time



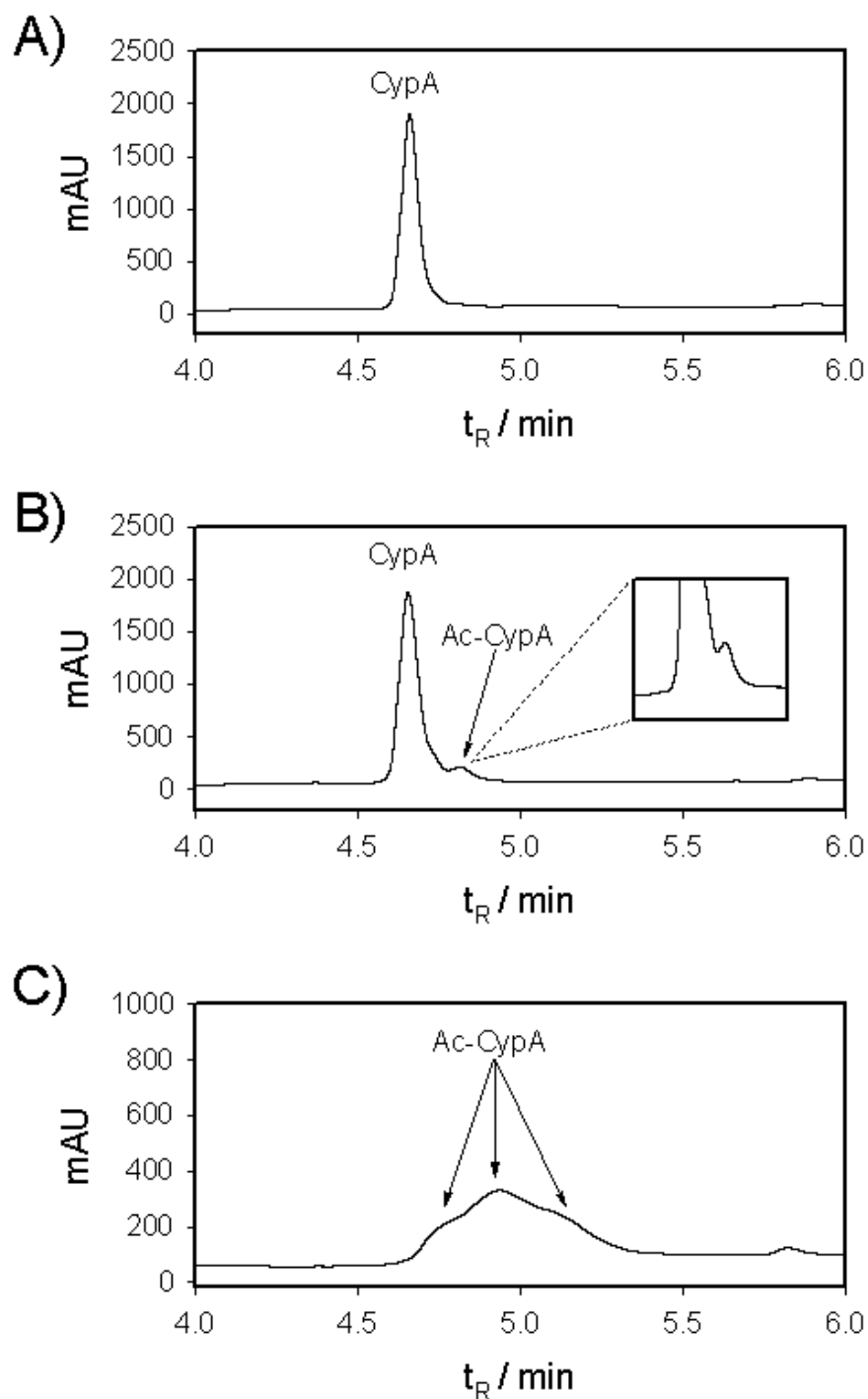


**Figure A23.** RP-HPLC separation of acetylated CypA. **A)** CypA standard, **B)** CypA acetylated with 4 mM Ac-CoA in 200 mM Tris-HCl buffer pH 8.0 at 37°C for 24 h. **C)** CypA acetylated with 0.01 % (v/v) acetic anhydride in same buffer for 30 min at RT.

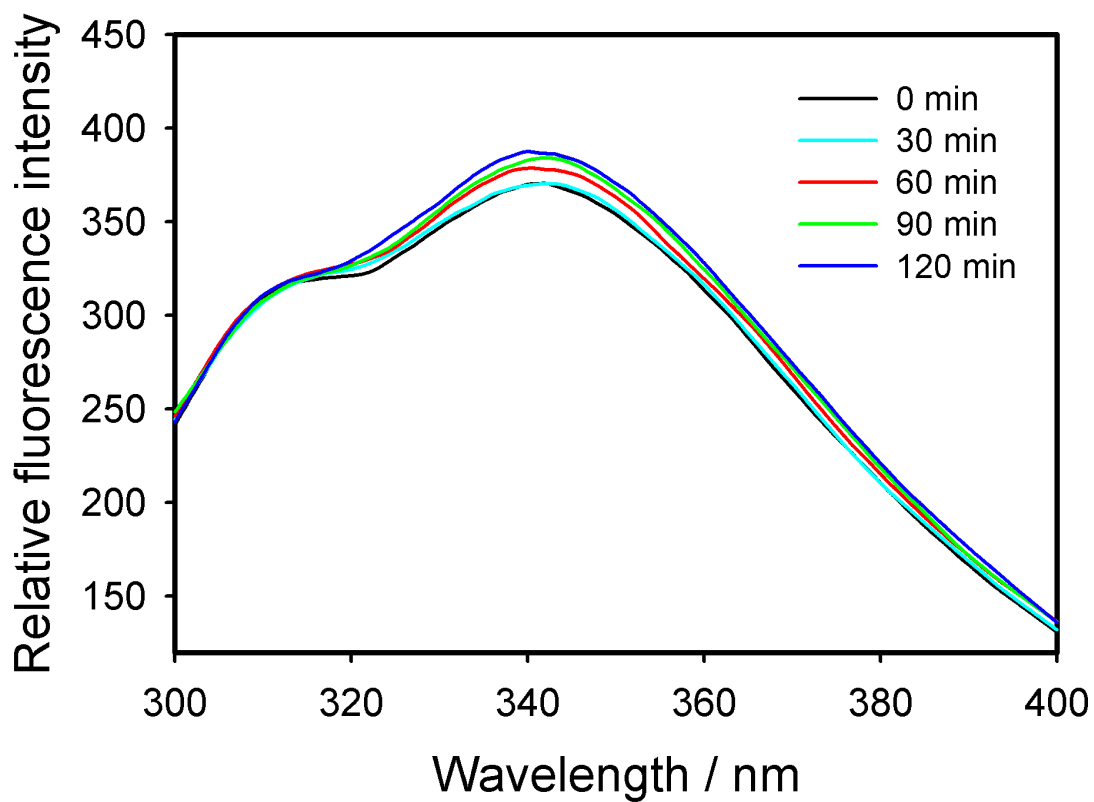


**Figure A24.** Fluorescence spectra of CypA. CypA (10  $\mu$ M) was mixed with Succ-CoA (4mM) in TrisHCl buffer pH 8.0. Fluorescence spectra were recorded in a range 300-400 nm over time at 37°C.

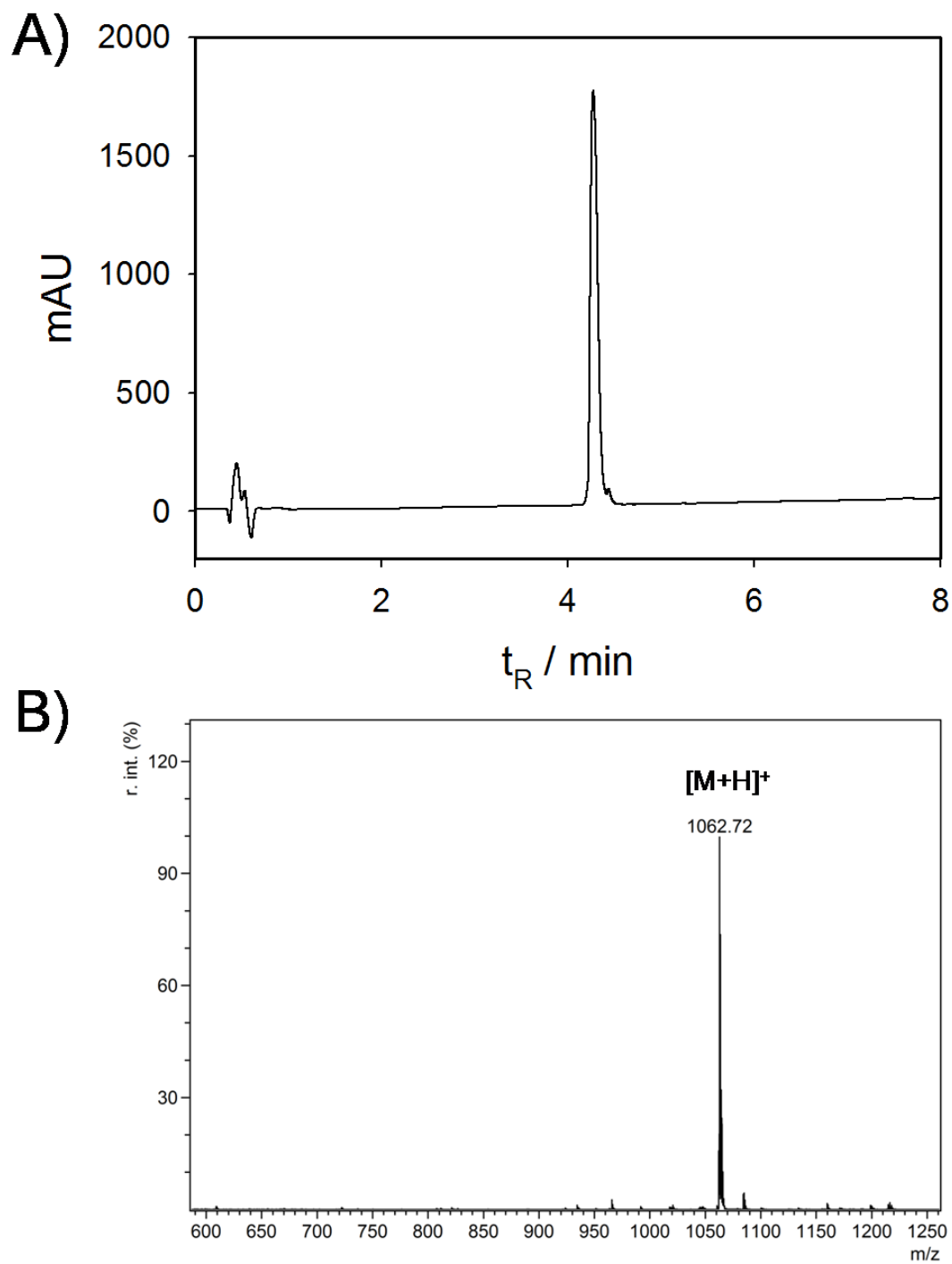


**Figure A25.** Analytical HPLC and MS of SAT1 substrate peptide 1 (Ac-LYPPRAKLVIQRH-NH<sub>2</sub>). **A)** Linear gradient 5-70 % ACN over 7 min was applied. Detection was at 220 nm.  $t_R$ : 4.27 min. **B)** MALDI-TOF MS spectrum of peptide 1.  $[M+H]^+$  = 1062.72 Da. Theoretical monoisotopic mass: 1061.7 Da.

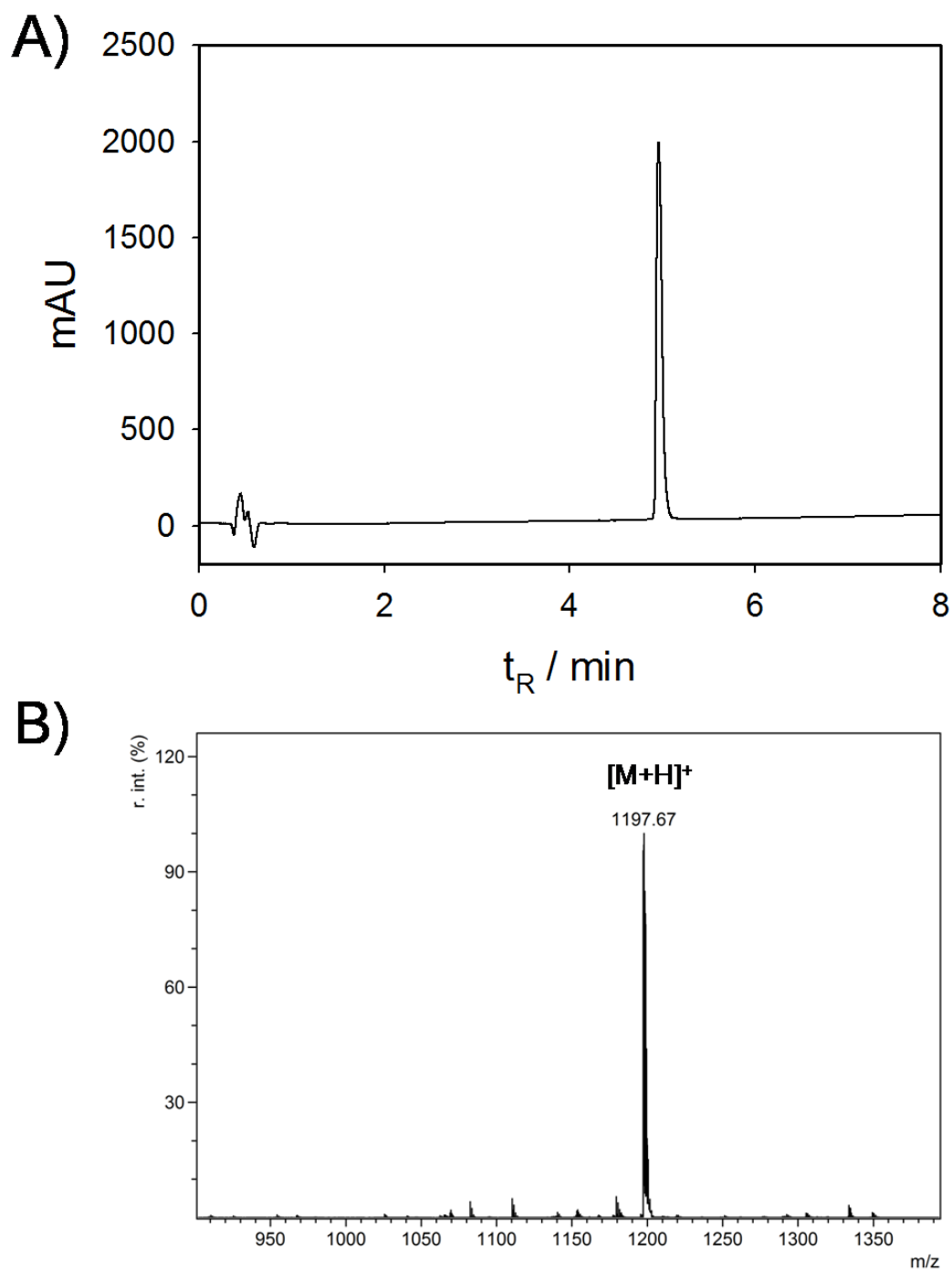


**Figure A26.** Analytical HPLC and MS of SAT1 substrate peptide 2 (Ac- HSDDYIKFLRSIR-NH<sub>2</sub>). **A)** Linear gradient 5-70 % ACN over 7 min was applied. Detection was at 220 nm. t<sub>R</sub>: 4.96 min. **B)** MALDI-TOF MS spectrum of peptide 2. [M+H] = 1197.67 Da. Theoretical monoisotopic mass: 1196.6 Da.

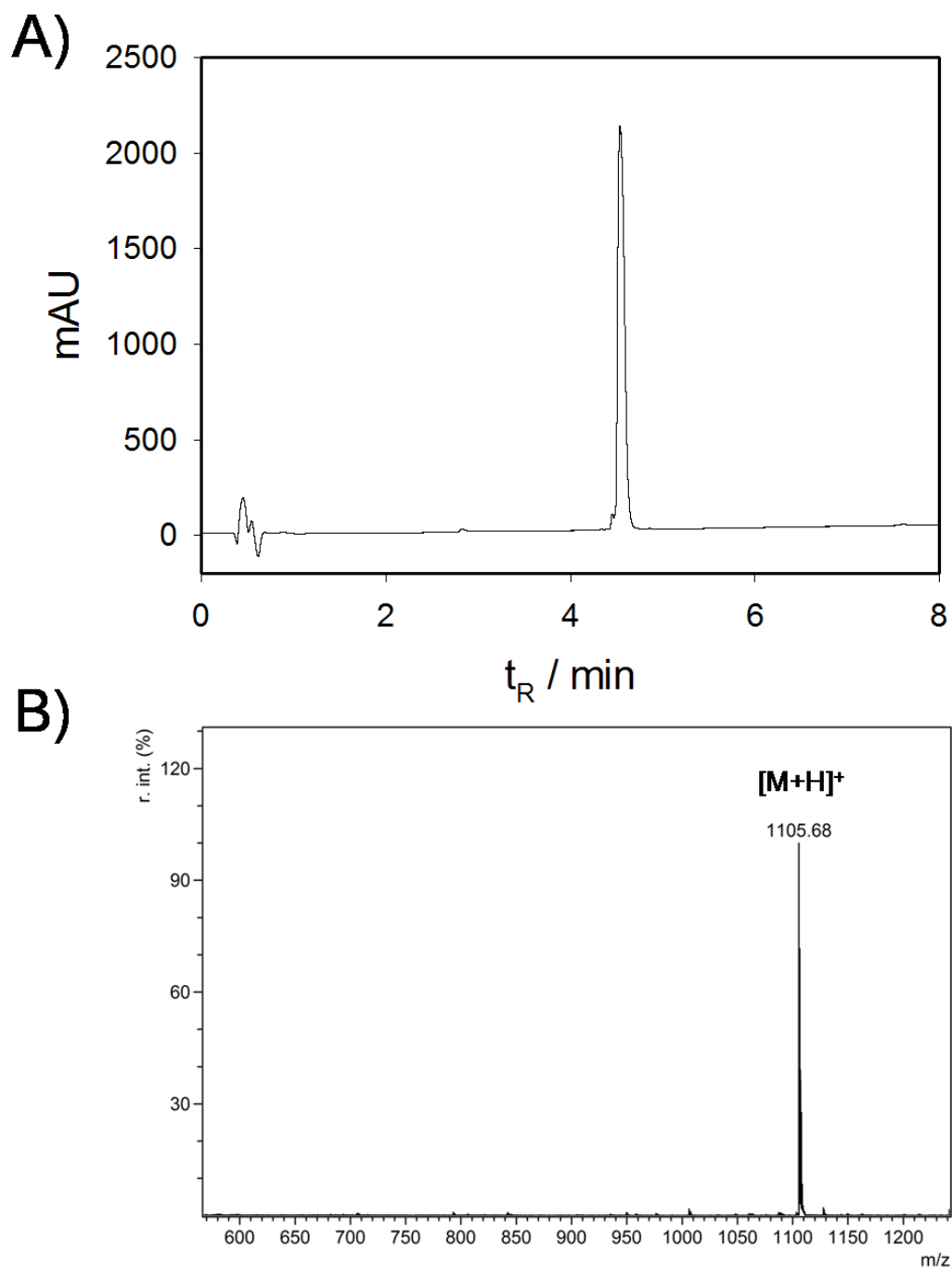


**Figure A27.** Analytical HPLC and MS of SAT1 substrate peptide 10 (Ac-PVIELYKSRGVLH-NH<sub>2</sub>). **A)** Linear gradient 5-70 % ACN over 7 min was applied. Detection was at 220 nm.  $t_R$ : 4.55 min. **B)** MALDI-TOF MS spectrum of peptide 2.  $[M+H]^+$  = 1105.68 Da. Theoretical monoisotopic mass: 1104.6 Da.

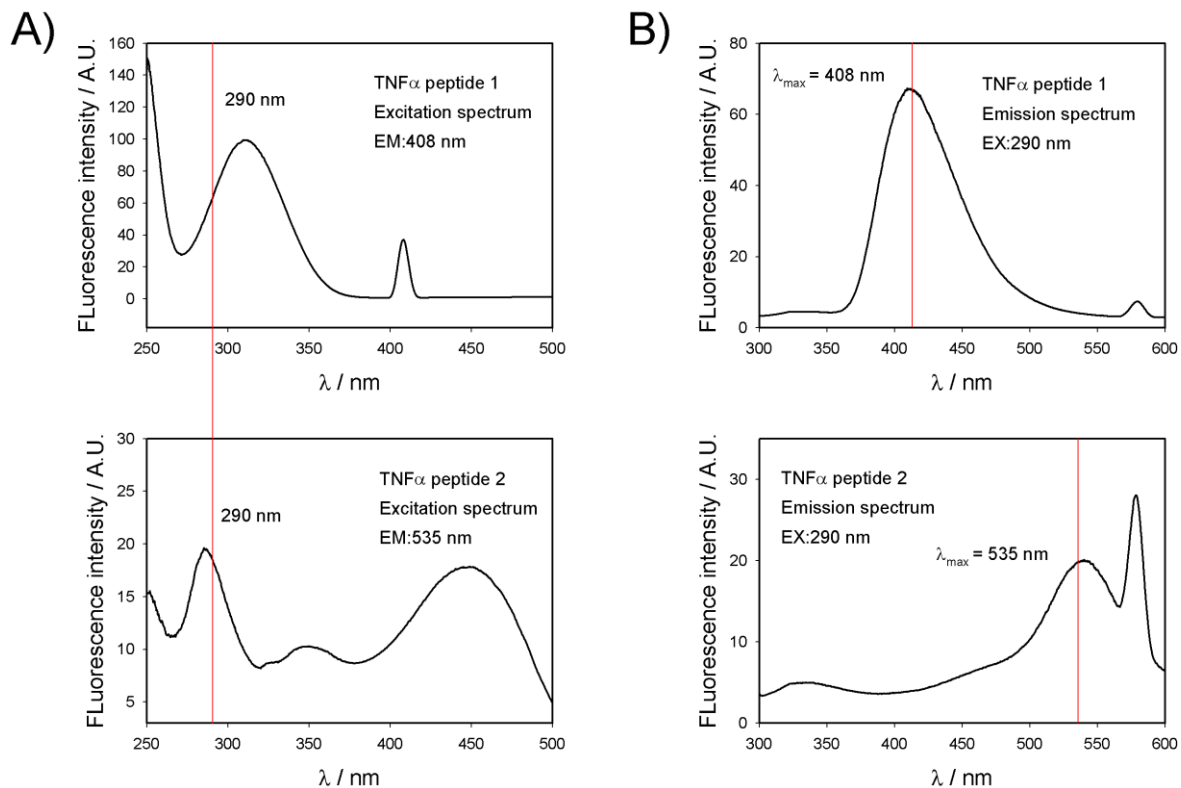


**Figure A28.** Excitation and emission spectra of TNF $\alpha$  peptide 1 and 2. **A)** Reaction mixture containing TNF $\alpha$  peptide 1 and 2 was excited at  $290 \pm 5$  nm. **B)** Emission spectra of the different fluorophores enable simultaneous detection of sirtuin mediated deacylation at 408 nm and 535 nm for TNF $\alpha$  peptide 1 and 2, respectively. Figure is adapted from Schuster et al. 2016 (Schuster et al., 2016).

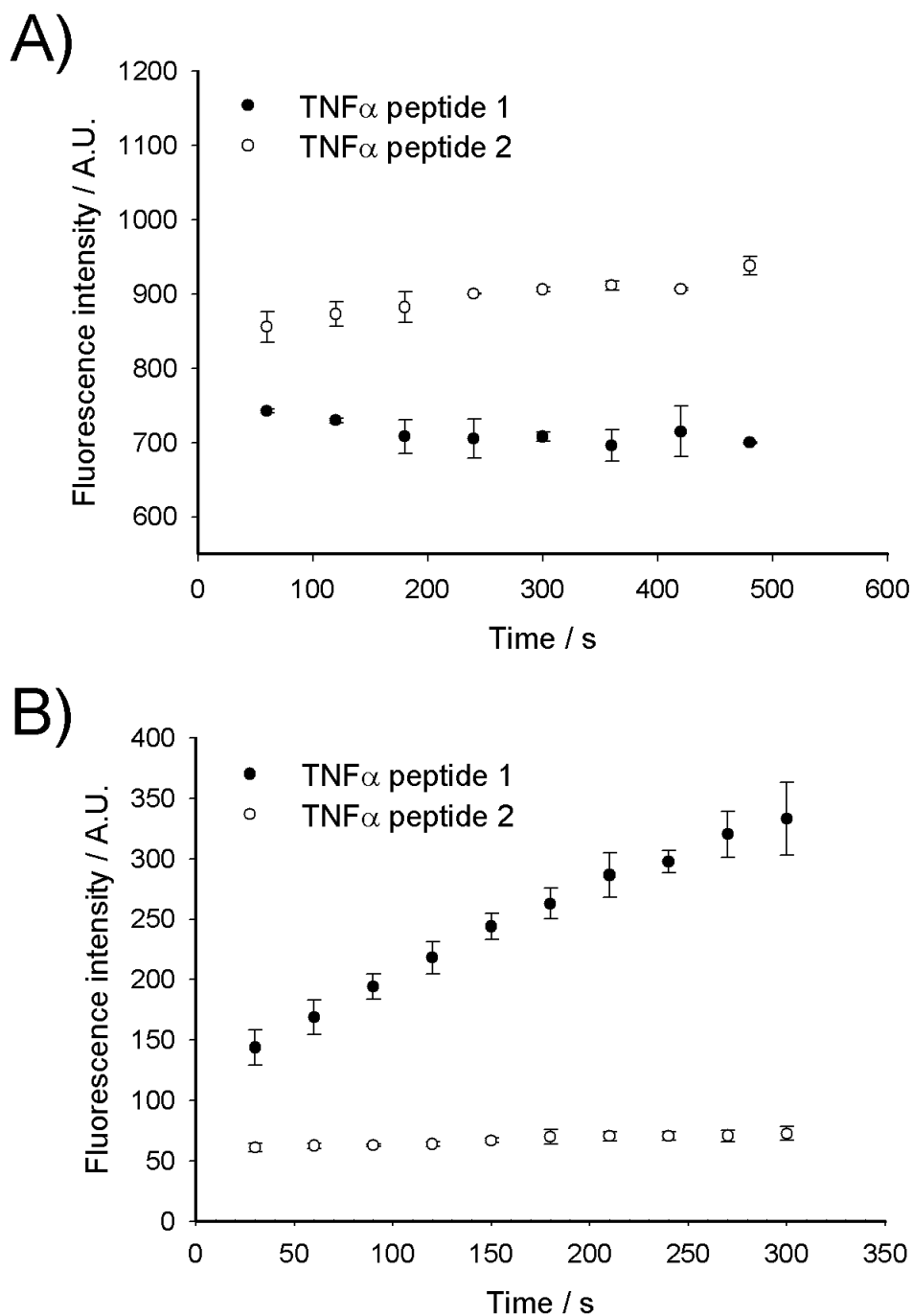


**Figure A29.** Simultaneous measurements of sirtuin activity using two substrates. **A)** Reaction mixtures contained Sirt4 (0.5  $\mu$ M), TNF $\alpha$  peptide 1 (10  $\mu$ M), TNF $\alpha$  peptide 2 (10  $\mu$ M) and NAD $^+$  (500 $\mu$ M) or **B)** Sirt2 (0.01  $\mu$ M), TNF $\alpha$  peptide 1 (1  $\mu$ M), TNF $\alpha$  peptide 2 (1  $\mu$ M) and NAD $^+$  (500 $\mu$ M). Reactions were incubated in assay-buffer at 37°C. Fluorophores were excited at  $290 \pm 5$  nm and emission spectra (350-550 nm) were recorded over time. Fluorescence intensities at 408 nm and 535 nm (maximum of emissions specific for substrates 3 and 6, respectively) were extracted and plotted as a function of time. Data represent average  $\pm$  S.D. (n=2). Figure is adapted from Schuster et al. 2016 (Schuster et al., 2016).

# Bibliography

- Abiko, Y. (1967). Investigations on pantothenic acid and its related compounds. IX. Biochemical studies.4. Separation and substrate specificity of pantothenate kinase and phosphopantothenoylcysteine synthetase. *J. Biochem. (Tokyo)* *61*, 290–299.
- Ahn, B.-H., Kim, H.-S., Song, S., Lee, I.H., Liu, J., Vassilopoulos, A., Deng, C.-X., and Finkel, T. (2008). A role for the mitochondrial deacetylase Sirt3 in regulating energy homeostasis. *Proc. Natl. Acad. Sci.* *105*, 14447–14452.
- Ahuja, N., Schwer, B., Carobbio, S., Waltregny, D., North, B.J., Castronovo, V., Maechler, P., and Verdin, E. (2007). Regulation of insulin secretion by SIRT4, a mitochondrial ADP-ribosyltransferase. *J. Biol. Chem.* *282*, 33583–33592.
- Aletta, J.M., Cimato, T.R., and Ettinger, M.J. (1998). Protein methylation: a signal event in post-translational modification. *Trends Biochem. Sci.* *23*, 89–91.
- Allfrey, V.G. (1966). Structural modifications of histones and their possible role in the regulation of ribonucleic acid synthesis. *Proc. Can. Cancer Conf.* *6*, 313–335.
- Allfrey, V.G., Faulkner, R., and Mirsky, A.E. (1964). ACETYLATION AND METHYLATION OF HISTONES AND THEIR POSSIBLE ROLE IN THE REGULATION OF RNA SYNTHESIS. *Proc. Natl. Acad. Sci. U. S. A.* *51*, 786–794.
- Alrob, O.A., Sankaralingam, S., Ma, C., Wagg, C.S., Fillmore, N., Jaswal, J.S., Sack, M.N., Lehner, R., Gupta, M.P., Michelakis, E.D., et al. (2014). Obesity-induced lysine acetylation increases cardiac fatty acid oxidation and impairs insulin signalling. *Cardiovasc. Res.* *103*, 485–497.
- Ambler, R.P., and Rees, M.W. (1959).  $\epsilon$ -N-Methyl-lysine in Bacterial Flagellar Protein. *Nature* *184*, 56–57.
- Antosiewicz, J., McCammon, J.A., and Gilson, M.K. (1994). Prediction of pH-dependent properties of proteins. *J. Mol. Biol.* *238*, 415–436.
- Antosiewicz, J., McCammon, J.A., and Gilson, M.K. (1996). The determinants of pKas in proteins. *Biochemistry (Mosc.)* *35*, 7819–7833.
- Baddiley, J. (1955). The structure of coenzyme A. *Adv. Enzymol. Relat. Subj. Biochem.* *16*, 1–21.
- Baddiley, J., Kekwick, R.A., and Thain, E.M. (1952). A New Method for Acetylating Proteins. *Nature* *170*, 968–970.
- Baddiley, J., Thain, E.M., Novelli, G.D., and Lipmann, F. (1953). Structure of coenzyme A. *Nature* *171*, 76.
- Baeza, J., Smallegan, M.J., and Denu, J.M. (2015). Site-Specific Reactivity of Nonenzymatic Lysine Acetylation. *ACS Chem. Biol.* *10*, 122–128.



Baeza, J., Smallegan, M.J., and Denu, J.M. (2016). Mechanisms and Dynamics of Protein Acetylation in Mitochondria. *Trends Biochem. Sci.*

Bakin, R.E., and Jung, M.O. (2004). Cytoplasmic sequestration of HDAC7 from mitochondrial and nuclear compartments upon initiation of apoptosis. *J. Biol. Chem.* 279, 51218–51225.

Bao, X., Wang, Y., Li, X., Li, X.-M., Liu, Z., Yang, T., Wong, C.F., Zhang, J., Hao, Q., and Li, X.D. (2014). Identification of “erasers” for lysine crotonylated histone marks using a chemical proteomics approach. *eLife* 3.

Bashford, D., and Karplus, M. (1990). pKa's of ionizable groups in proteins: atomic detail from a continuum electrostatic model. *Biochemistry (Mosc.)* 29, 10219–10225.

Beli, P., Lukashchuk, N., Wagner, S.A., Weinert, B.T., Olsen, J.V., Baskcomb, L., Mann, M., Jackson, S.P., and Choudhary, C. (2012). Proteomic investigations reveal a role for RNA processing factor THRAP3 in the DNA damage response. *Mol. Cell* 46, 212–225.

Bewley, M.C., Graziano, V., Jiang, J., Matz, E., Studier, F.W., Pegg, A.E., Coleman, C.S., and Flanagan, J.M. (2006). Structures of wild-type and mutant human spermidine/spermine N1-acetyltransferase, a potential therapeutic drug target. *Proc. Natl. Acad. Sci. U. S. A.* 103, 2063–2068.

Boukaftane, Y., and Mitchell, G.A. (1997). Cloning and characterization of the human mitochondrial 3-hydroxy-3-methylglutaryl CoA synthase gene. *Gene* 195, 121–126.

Bras, A.P., Jänne, J., Porter, C.W., and Sitar, D.S. (2001). Spermidine/spermine n(1)-acetyltransferase catalyzes amantadine acetylation. *Drug Metab. Dispos. Biol. Fate Chem.* 29, 676–680.

Brown, G.M. (1959). The metabolism of pantothenic acid. *J. Biol. Chem.* 234, 370–378.

Bruice, T.C., and Pandit, U.K. (1960). The Effect of Geminal Substitution Ring Size and Rotamer Distribution on the Intramolecular Nucleophilic Catalysis of the Hydrolysis of Monophenyl Esters of Dibasic Acids and the Solvolysis of the Intermediate Anhydrides. *J. Am. Chem. Soc.* 82, 5858–5865.

Campagnari, F., and Webster, L.T. (1963). Purification and properties of acetyl coenzyme A synthetase from bovine heart mitochondria. *J. Biol. Chem.* 238, 1628–1633.

Casero, R.A., and Pegg, A.E. (2009). Polyamine catabolism and disease. *Biochem. J.* 421, 323–338.

Casero, R.A., Celano, P., Ervin, S.J., Applegren, N.B., Wiest, L., and Pegg, A.E. (1991). Isolation and characterization of a cDNA clone that codes for human spermidine/spermine N1-acetyltransferase. *J. Biol. Chem.* 266, 810–814.

Caton, P.W., Richardson, S.J., Kieswich, J., Bugliani, M., Holland, M.L., Marchetti, P., Morgan, N.G., Yaqoob, M.M., Holness, M.J., and Sugden, M.C. (2013). Sirtuin 3 regulates mouse pancreatic beta cell function and is suppressed in pancreatic islets isolated from human type 2 diabetic patients. *Diabetologia* 56, 1068–1077.

- Chen, L., Fischle, W., Verdin, E., and Greene, W.C. (2001). Duration of Nuclear NF- $\kappa$ B Action Regulated by Reversible Acetylation. *Science* 293, 1653–1657.
- Chen, Y., Sprung, R., Tang, Y., Ball, H., Sangras, B., Kim, S.C., Falck, J.R., Peng, J., Gu, W., and Zhao, Y. (2007). Lysine propionylation and butyrylation are novel post-translational modifications in histones. *Mol. Cell. Proteomics MCP* 6, 812–819.
- Cheng, H.-L., Mostoslavsky, R., Saito, S., Ichi, Manis, J.P., Gu, Y., Patel, P., Bronson, R., Appella, E., Alt, F.W., and Chua, K.F. (2003). Developmental defects and p53 hyperacetylation in Sir2 homolog (SIRT1)-deficient mice. *Proc. Natl. Acad. Sci.* 100, 10794–10799.
- Cheng, Z., Tang, Y., Chen, Y., Kim, S., Liu, H., Li, S.S.C., Gu, W., and Zhao, Y. (2009). Molecular characterization of propionyllysines in non-histone proteins. *Mol. Cell. Proteomics MCP* 8, 45–52.
- Choudhary, C., Kumar, C., Gnad, F., Nielsen, M.L., Rehman, M., Walther, T.C., Olsen, J.V., and Mann, M. (2009). Lysine acetylation targets protein complexes and co-regulates major cellular functions. *Science* 325, 834–840.
- Choudhary, C., Weinert, B.T., Nishida, Y., Verdin, E., and Mann, M. (2014). The growing landscape of lysine acetylation links metabolism and cell signalling. *Nat. Rev. Mol. Cell Biol.* 15, 536–550.
- Cloos, P.A.C., Christensen, J., Agger, K., and Helin, K. (2008). Erasing the methyl mark: histone demethylases at the center of cellular differentiation and disease. *Genes Dev.* 22, 1115–1140.
- Colman, R.J., Anderson, R.M., Johnson, S.C., Kastman, E.K., Kosmatka, K.J., Beasley, T.M., Allison, D.B., Cruzen, C., Simmons, H.A., Kemnitz, J.W., et al. (2009). Caloric Restriction Delays Disease Onset and Mortality in Rhesus Monkeys. *Science* 325, 201–204.
- Comb, D.G., Sarkar, N., and Pinzino, C.J. (1966). The methylation of lysine residues in protein. *J. Biol. Chem.* 241, 1857–1862.
- Corti, O., Finocchiaro, G., Rossi, E., Zuffardi, O., and DiDonato, S. (1994). Molecular cloning of cDNAs encoding human carnitine acetyltransferase and mapping of the corresponding gene to chromosome 9q34.1. *Genomics* 23, 94–99.
- Cozzone, A.J. (1988). Protein phosphorylation in prokaryotes. *Annu. Rev. Microbiol.* 42, 97–125.
- Daugherty, M., Polanuyer, B., Farrell, M., Scholle, M., Lykidis, A., de Crécy-Lagard, V., and Osterman, A. (2002). Complete reconstitution of the human coenzyme A biosynthetic pathway via comparative genomics. *J. Biol. Chem.* 277, 21431–21439.
- Du, J., Zhou, Y., Su, X., Yu, J.J., Khan, S., Jiang, H., Kim, J., Woo, J., Kim, J.H., Choi, B.H., et al. (2011). Sirt5 is a NAD-dependent protein lysine demalonylase and desuccinylase. *Science* 334, 806–809.

- Dwyer, J.J., Gittis, A.G., Karp, D.A., Lattman, E.E., Spencer, D.S., Stites, W.E., and García-Moreno E, B. (2000). High apparent dielectric constants in the interior of a protein reflect water penetration. *Biophys. J.* *79*, 1610–1620.
- Espenshade, P.J., and Hughes, A.L. (2007). Regulation of sterol synthesis in eukaryotes. *Annu. Rev. Genet.* *41*, 401–427.
- Fan, J., Shan, C., Kang, H.-B., Elf, S., Xie, J., Tucker, M., Gu, T.-L., Aguiar, M., Lonning, S., Chen, H., et al. (2014). Tyr phosphorylation of PDP1 toggles recruitment between ACAT1 and SIRT3 to regulate the pyruvate dehydrogenase complex. *Mol. Cell* *53*, 534–548.
- Fanghänel, J., and Fischer, G. (2002). Thermodynamic characterization of the interaction of human cyclophilin 18 with cyclosporin A. *Biophys. Chem.* *100*, 351–366.
- Fatkins, D.G., Monnot, A.D., and Zheng, W. (2006). Nepsilon-thioacetyl-lysine: a multi-facet functional probe for enzymatic protein lysine Nepsilon-deacetylation. *Bioorg. Med. Chem. Lett.* *16*, 3651–3656.
- Feldman, J.L., Baeza, J., and Denu, J.M. (2013). Activation of the protein deacetylase SIRT6 by long-chain fatty acids and widespread deacylation by mammalian sirtuins. *J. Biol. Chem.* *288*, 31350–31356.
- Fernandes, C.G., da Rosa, M.S., Seminotti, B., Pierozan, P., Martell, R.W., Lagranha, V.L., Busanello, E.N.B., Leipnitz, G., and Wajner, M. (2013). In vivo experimental evidence that the major metabolites accumulating in 3-hydroxy-3-methylglutaryl-CoA lyase deficiency induce oxidative stress in striatum of developing rats: A potential pathophysiological mechanism of striatal damage in this disorder. *Mol. Genet. Metab.* *109*, 144–153.
- Fernandes, J., Weddle, A., Kinter, C.S., Humphries, K.M., Mather, T., Szveda, L.I., and Kinter, M. (2015). Lysine Acetylation Activates Mitochondrial Aconitase in the Heart. *Biochemistry (Mosc.)* *54*, 4008–4018.
- Finley, L.W.S., Carracedo, A., Lee, J., Souza, A., Egia, A., Zhang, J., Teruya-Feldstein, J., Moreira, P.I., Cardoso, S.M., Clish, C.B., et al. (2011a). SIRT3 opposes reprogramming of cancer cell metabolism through HIF1 $\alpha$  destabilization. *Cancer Cell* *19*, 416–428.
- Finley, L.W.S., Haas, W., Desquirit-Dumas, V., Wallace, D.C., Procaccio, V., Gygi, S.P., and Haigis, M.C. (2011b). Succinate Dehydrogenase Is a Direct Target of Sirtuin 3 Deacetylase Activity. *PLoS ONE* *6*.
- Fischer, F., Gertz, M., Suenkel, B., Lakshminarasimhan, M., Schutkowski, M., and Steegborn, C. (2012). Sirt5 Deacylation Activities Show Differential Sensitivities to Nicotinamide Inhibition. *PLOS ONE* *7*, e45098.
- Fischer, G., Wittmann-Liebold, B., Lang, K., Kiefhaber, T., and Schmid, F.X. (1989). Cyclophilin and peptidyl-prolyl cis-trans isomerase are probably identical proteins. *Nature* *337*, 476–478.

- Frenkel, E.P., and Kitchens, R.L. (1977). Purification and properties of acetyl coenzyme A synthetase from bakers' yeast. *J. Biol. Chem.* *252*, 504–507.
- Fritz, K.S., Galligan, J.J., Hirschey, M.D., Verdin, E., and Petersen, D.R. (2012). Mitochondrial acetylome analysis in a mouse model of alcohol-induced liver injury utilizing SIRT3 knockout mice. *J. Proteome Res.* *11*, 1633–1643.
- Fujino, T., Kondo, J., Ishikawa, M., Morikawa, K., and Yamamoto, T.T. (2001). Acetyl-CoA synthetase 2, a mitochondrial matrix enzyme involved in the oxidation of acetate. *J. Biol. Chem.* *276*, 11420–11426.
- Fukao, T., Yamaguchi, S., Kano, M., Orii, T., Fujiki, Y., Osumi, T., and Hashimoto, T. (1990). Molecular cloning and sequence of the complementary DNA encoding human mitochondrial acetoacetyl-coenzyme A thiolase and study of the variant enzymes in cultured fibroblasts from patients with 3-ketothiolase deficiency. *J. Clin. Invest.* *86*, 2086–2092.
- Fukao, T., Lopaschuk, G.D., and Mitchell, G.A. (2004). Pathways and control of ketone body metabolism: on the fringe of lipid biochemistry. *Prostaglandins Leukot. Essent. Fatty Acids* *70*, 243–251.
- Garcia-Moreno, B. (2009). Adaptations of proteins to cellular and subcellular pH. *J. Biol.* *8*, 98.
- Garland, P.B., Shepherd, D., and Yates, D.W. (1965). Steady-state concentrations of coenzyme A, acetyl-coenzyme A and long-chain fatty acyl-coenzyme A in rat-liver mitochondria oxidizing palmitate. *Biochem. J.* *97*, 587–594.
- Gertz, M., and Steegborn, C. (2016). Using mitochondrial sirtuins as drug targets: disease implications and available compounds. *Cell. Mol. Life Sci. CMLS.*
- Gertz, M., Nguyen, G.T.T., Fischer, F., Suenkel, B., Schlicker, C., Fränzel, B., Tomaschewski, J., Aladini, F., Becker, C., Wolters, D., et al. (2012). A Molecular Mechanism for Direct Sirtuin Activation by Resveratrol. *PLOS ONE* *7*, e49761.
- Ghanta, S., Grossmann, R.E., and Brenner, C. (2013). Mitochondrial protein acetylation as a cell-intrinsic, evolutionary driver of fat storage: chemical and metabolic logic of acetyl-lysine modifications. *Crit. Rev. Biochem. Mol. Biol.* *48*, 561–574.
- Gibson, G.E., Xu, H., Chen, H.-L., Chen, W., Denton, T.T., and Zhang, S. (2015). Alpha-ketoglutarate dehydrogenase complex-dependent succinylation of proteins in neurons and neuronal cell lines. *J. Neurochem.* *134*, 86–96.
- Glozak, M.A., Sengupta, N., Zhang, X., and Seto, E. (2005). Acetylation and deacetylation of non-histone proteins. *Gene* *363*, 15–23.
- Goldenthal, M.J., Marin-Garcia, J., and Ananthakrishnan, R. (1998). Cloning and molecular analysis of the human citrate synthase gene. *Genome Natl. Res. Counc. Can. Génome Cons. Natl. Rech. Can.* *41*, 733–738.

- Greer, E.L., and Shi, Y. (2012). Histone methylation: a dynamic mark in health, disease and inheritance. *Nat. Rev. Genet.* *13*, 343–357.
- Grillon, J.M., Johnson, K.R., Kotlo, K., and Danziger, R.S. (2012). Non-histone lysine acetylated proteins in heart failure. *Biochim. Biophys. Acta* *1822*, 607–614.
- Gu, W., and Roeder, R.G. (1997). Activation of p53 Sequence-Specific DNA Binding by Acetylation of the p53 C-Terminal Domain. *Cell* *90*, 595–606.
- Gubbens, J., Ruijter, E., de Fays, L.E.V., Damen, J.M.A., de Kruijff, B., Slijper, M., Rijkers, D.T.S., Liskamp, R.M.J., and de Kroon, A.I.P.M. (2009). Photocrosslinking and click chemistry enable the specific detection of proteins interacting with phospholipids at the membrane interface. *Chem. Biol.* *16*, 3–14.
- Guo, A., Gu, H., Zhou, J., Mulhern, D., Wang, Y., Lee, K.A., Yang, V., Aguiar, M., Kornhauser, J., Jia, X., et al. (2014). Immunoaffinity enrichment and mass spectrometry analysis of protein methylation. *Mol. Cell. Proteomics MCP* *13*, 372–387.
- Haapalainen, A.M., Meriläinen, G., Pirilä, P.L., Kondo, N., Fukao, T., and Wierenga, R.K. (2007). Crystallographic and Kinetic Studies of Human Mitochondrial Acetoacetyl-CoA Thiolase: The Importance of Potassium and Chloride Ions for Its Structure and Function. *Biochemistry (Mosc.)* *46*, 4305–4321.
- Hafner, A.V., Dai, J., Gomes, A.P., Xiao, C.-Y., Palmeira, C.M., Rosenzweig, A., and Sinclair, D.A. (2010). Regulation of the mPTP by SIRT3-mediated deacetylation of CypD at lysine 166 suppresses age-related cardiac hypertrophy. *Aging* *2*, 914–923.
- Haigis, M.C., Mostoslavsky, R., Haigis, K.M., Fahie, K., Christodoulou, D.C., Murphy, A.J., Valenzuela, D.M., Yancopoulos, G.D., Karow, M., Blander, G., et al. (2006). SIRT4 Inhibits Glutamate Dehydrogenase and Opposes the Effects of Calorie Restriction in Pancreatic  $\beta$  Cells. *Cell* *126*, 941–954.
- Hallows, W.C., Lee, S., and Denu, J.M. (2006). Sirtuins deacetylate and activate mammalian acetyl-CoA synthetases. *Proc. Natl. Acad. Sci. U. S. A.* *103*, 10230–10235.
- Hallows, W.C., Yu, W., Smith, B.C., DeVires, M.K., Ellinger, J.J., Someya, S., Shortreed, M.R., Prolla, T., Markley, J.L., Smith, L.M., et al. (2011). Sirt3 Promotes the Urea Cycle and Fatty Acid Oxidation during Dietary Restriction. *Mol. Cell* *41*, 139–149.
- Handschumacher, R.E., Harding, M.W., Rice, J., Drugge, R.J., and Speicher, D.W. (1984). Cyclophilin: a specific cytosolic binding protein for cyclosporin A. *Science* *226*, 544–547.
- Hansford, R.G., and Johnson, R.N. (1975). The steady state concentrations of coenzyme A-SH and coenzyme A thioester, citrate, and isocitrate during tricarboxylate cycle oxidations in rabbit heart mitochondria. *J. Biol. Chem.* *250*, 8361–8375.
- Harms, M.J., Castañeda, C.A., Schlessman, J.L., Sue, G.R., Isom, D.G., Cannon, B.R., and García-Moreno E, B. (2009). The pK(a) values of acidic and basic residues buried at the same internal location in a protein are governed by different factors. *J. Mol. Biol.* *389*, 34–47.

- Harris, P.S., Roy, S.R., Coughlan, C., Orlicky, D.J., Liang, Y., Shearn, C.T., Roede, J.R., and Fritz, K.S. (2015). Chronic ethanol consumption induces mitochondrial protein acetylation and oxidative stress in the kidney. *Redox Biol.* 6, 33–40.
- Hawkes, R., Niday, E., and Gordon, J. (1982). A dot-immunobinding assay for monoclonal and other antibodies. *Anal. Biochem.* 119, 142–147.
- He, B., Hu, J., Zhang, X., and Lin, H. (2014). Thiomyristoyl peptides as cell-permeable Sirt6 inhibitors. *Org. Biomol. Chem.* 12, 7498–7502.
- Hebert, A.S., Dittenhafer-Reed, K.E., Yu, W., Bailey, D.J., Selen, E.S., Boersma, M.D., Carson, J.J., Tonelli, M., Balloon, A.J., Higbee, A.J., et al. (2013). Calorie restriction and SIRT3 trigger global reprogramming of the mitochondrial protein acetylome. *Mol. Cell* 49, 186–199.
- Hegde, S.S., Chandler, J., Vetting, M.W., Yu, M., and Blanchard, J.S. (2007). Mechanistic and structural analysis of human spermidine/spermine N1-acetyltransferase. *Biochemistry (Mosc.)* 46, 7187–7195.
- Hirschey, M.D., Shimazu, T., Goetzman, E., Jing, E., Schwer, B., Lombard, D.B., Grueter, C.A., Harris, C., Biddinger, S., Ilkayeva, O.R., et al. (2010). SIRT3 regulates mitochondrial fatty-acid oxidation by reversible enzyme deacetylation. *Nature* 464, 121–125.
- Hirschey, M.D., Shimazu, T., Jing, E., Grueter, C.A., Collins, A.M., Auizerat, B., Stančáková, A., Goetzman, E., Lam, M.M., Schwer, B., et al. (2011). SIRT3 deficiency and mitochondrial protein hyperacetylation accelerate the development of the metabolic syndrome. *Mol. Cell* 44, 177–190.
- Holst, C.M., Nevsten, P., Johansson, F., Carlemalm, E., and Oredsson, S.M. (2008). Subcellular distribution of spermidine/spermine N1-acetyltransferase. *Cell Biol. Int.* 32, 39–47.
- Houten, S.M., and Wanders, R.J.A. (2010). A general introduction to the biochemistry of mitochondrial fatty acid  $\beta$ -oxidation. *J. Inherit. Metab. Dis.* 33, 469–477.
- Howard, B.R., Vajdos, F.F., Li, S., Sundquist, W.I., and Hill, C.P. (2003). Structural insights into the catalytic mechanism of cyclophilin A. *Nat. Struct. Biol.* 10, 475–481.
- Howard, B.V., Howard, W.J., and Bailey, J.M. (1974). Acetyl coenzyme A synthetase and the regulation of lipid synthesis from acetate in cultured cells. *J. Biol. Chem.* 249, 7912–7921.
- Huang, Y., Liu, J., Yan, L., and Zheng, W. (2016). Simple N $\epsilon$ -thioacetyl-lysine-containing cyclic peptides exhibiting highly potent sirtuin inhibition. *Bioorg. Med. Chem. Lett.* 26, 1612–1617.
- Inuzuka, H., Gao, D., Finley, L.W.S., Yang, W., Wan, L., Fukushima, H., Chin, Y.R., Zhai, B., Shaik, S., Lau, A.W., et al. (2012). Acetylation-dependent regulation of Skp2 function. *Cell* 150, 179–193.

- Isom, D.G., Castañeda, C.A., Cannon, B.R., and García-Moreno, B. (2011). Large shifts in pKa values of lysine residues buried inside a protein. *Proc. Natl. Acad. Sci. U. S. A.* *108*, 5260–5265.
- Ito, A., Kawaguchi, Y., Lai, C.-H., Kovacs, J.J., Higashimoto, Y., Appella, E., and Yao, T.-P. (2002). MDM2-HDAC1-mediated deacetylation of p53 is required for its degradation. *EMBO J.* *21*, 6236–6245.
- Jackson, M.J., Beaudet, A.L., and O'Brien, W.E. (1986). Mammalian urea cycle enzymes. *Annu. Rev. Genet.* *20*, 431–464.
- Jaworski, D.M., Namboodiri, A.M.A., and Moffett, J.R. (2016). Acetate as a Metabolic and Epigenetic Modifier of Cancer Therapy. *J. Cell. Biochem.* *117*, 574–588.
- Jiang, H., Khan, S., Wang, Y., Charron, G., He, B., Sebastian, C., Du, J., Kim, R., Ge, E., Mostoslavsky, R., et al. (2013). SIRT6 regulates TNF- $\alpha$  secretion through hydrolysis of long-chain fatty acyl lysine. *Nature* *496*, 110–113.
- Jing, E., Emanuelli, B., Hirschey, M.D., Boucher, J., Lee, K.Y., Lombard, D., Verdin, E.M., and Kahn, C.R. (2011). Sirtuin-3 (Sirt3) regulates skeletal muscle metabolism and insulin signaling via altered mitochondrial oxidation and reactive oxygen species production. *Proc. Natl. Acad. Sci. U. S. A.* *108*, 14608–14613.
- Jitrapakdee, S., St Maurice, M., Rayment, I., Cleland, W.W., Wallace, J.C., and Attwood, P.V. (2008). Structure, mechanism and regulation of pyruvate carboxylase. *Biochem. J.* *413*, 369–387.
- Joiner, M.-L.A., Koval, O.M., Li, J., He, B.J., Allamargot, C., Gao, Z., Luczak, E.D., Hall, D.D., Fink, B.D., Chen, B., et al. (2012). CaMKII determines mitochondrial stress responses in heart. *Nature* *491*, 269–273.
- Kano, M., Fukao, T., Yamaguchi, S., Orii, T., Osumi, T., and Hashimoto, T. (1991). Structure and expression of the human mitochondrial acetoacetyl-CoA thiolase-encoding gene. *Gene* *109*, 285–290.
- Karan, D., David, J.R., and Capy, P. (2001). Molecular evolution of the AMP-forming Acetyl-CoA synthetase. *Gene* *265*, 95–101.
- Karp, D.A., Gittis, A.G., Stahley, M.R., Fitch, C.A., Stites, W.E., and García-Moreno E, B. (2007). High apparent dielectric constant inside a protein reflects structural reorganization coupled to the ionization of an internal Asp. *Biophys. J.* *92*, 2041–2053.
- Kim, G.-W., and Yang, X.-J. (2011). Comprehensive lysine acetylomes emerging from bacteria to humans. *Trends Biochem. Sci.* *36*, 211–220.
- Kim, E.Y., Han, B.S., Kim, W.K., Lee, S.C., and Bae, K.-H. (2013). Acceleration of adipogenic differentiation via acetylation of malate dehydrogenase 2. *Biochem. Biophys. Res. Commun.* *441*, 77–82.

- Kim, S.C., Sprung, R., Chen, Y., Xu, Y., Ball, H., Pei, J., Cheng, T., Kho, Y., Xiao, H., Xiao, L., et al. (2006). Substrate and functional diversity of lysine acetylation revealed by a proteomics survey. *Mol. Cell* 23, 607–618.
- Kitabchi, A.E., Umpierrez, G.E., Miles, J.M., and Fisher, J.N. (2009). Hyperglycemic crises in adult patients with diabetes. *Diabetes Care* 32, 1335–1343.
- Koenig, R.J., Peterson, C.M., Jones, R.L., Saudek, C., Lehrman, M., and Cerami, A. (1976). Correlation of Glucose Regulation and Hemoglobin A1c in Diabetes Mellitus. *N. Engl. J. Med.* 295, 417–420.
- Krebs, H.A., Freedland, R.A., Hems, R., and Stubbs, M. (1969). Inhibition of hepatic gluconeogenesis by ethanol. *Biochem. J.* 112, 117–124.
- Kuo, Y.-M., and Andrews, A.J. (2013). Quantitating the specificity and selectivity of Gcn5-mediated acetylation of histone H3. *PloS One* 8, e54896.
- Laemmli, U.K. (1970). Cleavage of structural proteins during the assembly of the head of bacteriophage T4. *Nature* 227, 680–685.
- Lakshminarasimhan, M., Rauh, D., Schutkowski, M., and Steegborn, C. (2013). Sirt1 activation by resveratrol is substrate sequence-selective. *Aging* 5, 151–154.
- Lammers, M., Neumann, H., Chin, J.W., and James, L.C. (2010). Acetylation regulates cyclophilin A catalysis, immunosuppression and HIV isomerization. *Nat. Chem. Biol.* 6, 331–337.
- Laurent, G., German, N.J., Saha, A.K., de Boer, V.C.J., Davies, M., Koves, T.R., Dephoure, N., Fischer, F., Boanca, G., Vaitheesvaran, B., et al. (2013). SIRT4 coordinates the balance between lipid synthesis and catabolism by repressing malonyl CoA decarboxylase. *Mol. Cell* 50, 686–698.
- Lee, D.Y., Teyssier, C., Strahl, B.D., and Stallcup, M.R. (2005). Role of protein methylation in regulation of transcription. *Endocr. Rev.* 26, 147–170.
- Lee, S.B., Park, J.H., Folk, J.E., Deck, J.A., Pegg, A.E., Sokabe, M., Fraser, C.S., and Park, M.H. (2011). Inactivation of eukaryotic initiation factor 5A (eIF5A) by specific acetylation of its hypusine residue by spermidine/spermine acetyltransferase 1 (SSAT1). *Biochem. J.* 433, 205–213.
- L'Hernault, S.W., and Rosenbaum, J.L. (1983). Chlamydomonas alpha-tubulin is posttranslationally modified in the flagella during flagellar assembly. *J. Cell Biol.* 97, 258–263.
- Lin, S.-J., Defossez, P.-A., and Guarente, L. (2000). Requirement of NAD and SIR2 for Life-Span Extension by Calorie Restriction in *Saccharomyces cerevisiae*. *Science* 289, 2126–2128.
- Lipmann, F. (1945). Acetylation of Sulfanilamide by Liver Homogenates and Extracts. *J. Biol. Chem.* 160, 173–190.



- Liu, B., Lin, Y., Darwanto, A., Song, X., Xu, G., and Zhang, K. (2009). Identification and characterization of propionylation at histone H3 lysine 23 in mammalian cells. *J. Biol. Chem.* *284*, 32288–32295.
- Liu, C., Huang, Z., Jiang, H., and Shi, F. (2014). The Sirtuin 3 Expression Profile Is Associated with Pathological and Clinical Outcomes in Colon Cancer Patients. *BioMed Res. Int.* *2014*.
- Llopis, J., McCaffery, J.M., Miyawaki, A., Farquhar, M.G., and Tsien, R.Y. (1998). Measurement of cytosolic, mitochondrial, and Golgi pH in single living cells with green fluorescent proteins. *Proc. Natl. Acad. Sci. U. S. A.* *95*, 6803–6808.
- Lombard, D.B., Alt, F.W., Cheng, H.-L., Bunkenborg, J., Streeper, R.S., Mostoslavsky, R., Kim, J., Yancopoulos, G., Valenzuela, D., Murphy, A., et al. (2007). Mammalian Sir2 homolog SIRT3 regulates global mitochondrial lysine acetylation. *Mol. Cell. Biol.* *27*, 8807–8814.
- Loving, G., and Imperiali, B. (2008). A versatile amino acid analogue of the solvatochromic fluorophore 4-N,N-dimethylamino-1,8-naphthalimide: a powerful tool for the study of dynamic protein interactions. *J. Am. Chem. Soc.* *130*, 13630–13638.
- Lv, M., Shi, T., Mao, X., Li, X., Chen, Y., Zhu, J., Ni, S., Shen, X., Jiang, H., Li, J., et al. (2012). 1-(2,6-Dibenzyloxybenzoyl)-3-(9H-fluoren-9-yl)-urea: a novel cyclophilin A allosteric activator. *Biochem. Biophys. Res. Commun.* *425*, 938–943.
- Madsen, A.S., Andersen, C., Daoud, M., Anderson, K.A., Laursen, J.S., Chakladar, S., Huynh, F.K., Colaço, A.R., Backos, D.S., Fristrup, P., et al. (2016). Investigating the Sensitivity of NAD<sup>+</sup>-dependent Sirtuin Deacetylation Activities to NADH. *J. Biol. Chem.* *291*, 7128–7141.
- Mascaró, C., Buesa, C., Ortiz, J.A., Haro, D., and Hegardt, F.G. (1995). Molecular cloning and tissue expression of human mitochondrial 3-hydroxy-3-methylglutaryl-CoA synthase. *Arch. Biochem. Biophys.* *317*, 385–390.
- Mathias, R.A., Greco, T.M., Oberstein, A., Budayeva, H.G., Chakrabarti, R., Rowland, E.A., Kang, Y., Shenk, T., and Cristea, I.M. (2014). Sirtuin 4 Is a Lipoamidase Regulating Pyruvate Dehydrogenase Complex Activity. *Cell* *159*, 1615–1625.
- Matsushita, N., Yonashiro, R., Ogata, Y., Sugiura, A., Nagashima, S., Fukuda, T., Inatome, R., and Yanagi, S. (2011). Distinct regulation of mitochondrial localization and stability of two human Sirt5 isoforms. *Genes Cells* *16*, 190–202.
- Mattison, J.A., Roth, G.S., Beasley, T.M., Tilmont, E.M., Handy, A.M., Herbert, R.L., Longo, D.L., Allison, D.B., Young, J.E., Bryant, M., et al. (2012). Impact of caloric restriction on health and survival in rhesus monkeys from the NIA study. *Nature* *489*, 318–321.
- Mehler, E.L., and Guarnieri, F. (1999). A self-consistent, microenvironment modulated screened coulomb potential approximation to calculate pH-dependent electrostatic effects in proteins. *Biophys. J.* *77*, 3–22.

- Meldal, M., and Breddam, K. (1991). Anthranilamide and nitrotyrosine as a donor-acceptor pair in internally quenched fluorescent substrates for endopeptidases: multicolumn peptide synthesis of enzyme substrates for subtilisin Carlsberg and pepsin. *Anal. Biochem.* *195*, 141–147.
- Mertins, P., Qiao, J.W., Patel, J., Udeshi, N.D., Clauser, K.R., Mani, D.R., Burgess, M.W., Gillette, M.A., Jaffe, J.D., and Carr, S.A. (2013). Integrated proteomic analysis of post-translational modifications by serial enrichment. *Nat. Methods* *10*, 634–637.
- Michishita, E., Park, J.Y., Burneskis, J.M., Barrett, J.C., and Horikawa, I. (2005). Evolutionarily conserved and nonconserved cellular localizations and functions of human SIRT proteins. *Mol. Biol. Cell* *16*, 4623–4635.
- Mieyal, J.J., Webster, L.T., and Siddiqui, U.A. (1974). Benzoyl and hydroxybenzoyl esters of coenzyme A. Purification and nuclear magnetic resonance characterization; conformation in solution. *J. Biol. Chem.* *249*, 2633–2640.
- Mishra, P.K., and Drueckhammer, D.G. (2000). Coenzyme A Analogues and Derivatives: Synthesis and Applications as Mechanistic Probes of Coenzyme A Ester-Utilizing Enzymes. *Chem. Rev.* *100*, 3283–3310.
- Moellering, R.E., and Cravatt, B.F. (2013). Functional lysine modification by an intrinsically reactive primary glycolytic metabolite. *Science* *341*, 549–553.
- Moniot, S., Schutkowski, M., and Steegborn, C. (2013). Crystal structure analysis of human Sirt2 and its ADP-ribose complex. *J. Struct. Biol.* *182*, 136–143.
- Murray, K. (1964). The Occurrence of  $\epsilon$ -N-Methyl Lysine in Histones. *Biochemistry (Mosc.)* *3*, 10–15.
- Nakagawa, T., Lomb, D.J., Haigis, M.C., and Guarente, L. (2009). SIRT5 Deacetylates carbamoyl phosphate synthetase 1 and regulates the urea cycle. *Cell* *137*, 560–570.
- Nigro, P., Pompilio, G., and Capogrossi, M.C. (2013). Cyclophilin A: a key player for human disease. *Cell Death Dis.* *4*, e888.
- NISHIMURA, N., KAKIMOTO, T., and CHIBATA, I. (1983). Mechanism of Coenzyme A Biosynthesis by *Sarcina lutea*. *J. Ferment. Technol.* *61*, 95–99.
- Nolting, D., Aziz, E.F., Ottosson, N., Faubel, M., Hertel, I.V., and Winter, B. (2007). pH-Induced Protonation of Lysine in Aqueous Solution Causes Chemical Shifts in X-ray Photoelectron Spectroscopy. *J. Am. Chem. Soc.* *129*, 14068–14073.
- Obayashi, M., Matsui-Yuasa, I., Kitano, A., Kobayashi, K., and Otani, S. (1992). Posttranslational regulation of spermidine/spermine N1-acetyltransferase with stress. *Biochim. Biophys. Acta* *1131*, 41–46.
- Ogura, M., Nakamura, Y., Tanaka, D., Zhuang, X., Fujita, Y., Obara, A., Hamasaki, A., Hosokawa, M., and Inagaki, N. (2010). Overexpression of SIRT5 confirms its involvement in deacetylation and activation of carbamoyl phosphate synthetase 1. *Biochem. Biophys. Res. Commun.* *393*, 73–78.

- Onyango, P., Celic, I., McCaffery, J.M., Boeke, J.D., and Feinberg, A.P. (2002). SIRT3, a human SIR2 homologue, is an NAD-dependent deacetylase localized to mitochondria. *Proc. Natl. Acad. Sci. U. S. A.* *99*, 13653–13658.
- Paik, W.K., Pearson, D., Lee, H.W., and Kim, S. (1970). Nonenzymatic acetylation of histones with acetyl-CoA. *Biochim. Biophys. Acta* *213*, 513–522.
- Park, J., Chen, Y., Tishkoff, D.X., Peng, C., Tan, M., Dai, L., Xie, Z., Zhang, Y., Zwaans, B.M.M., Skinner, M.E., et al. (2013). SIRT5-mediated lysine desuccinylation impacts diverse metabolic pathways. *Mol. Cell* *50*, 919–930.
- Pegg, A.E. (2008). Spermidine/spermine-N(1)-acetyltransferase: a key metabolic regulator. *Am. J. Physiol. Endocrinol. Metab.* *294*, E995-1010.
- Peng, C., Lu, Z., Xie, Z., Cheng, Z., Chen, Y., Tan, M., Luo, H., Zhang, Y., He, W., Yang, K., et al. (2011). The first identification of lysine malonylation substrates and its regulatory enzyme. *Mol. Cell. Proteomics MCP* *10*, M111.012658.
- Phillips, D.M. (1963). The presence of acetyl groups of histones. *Biochem. J.* *87*, 258–263.
- Pirinen, E., Lo Sasso, G., and Auwerx, J. (2012). Mitochondrial sirtuins and metabolic homeostasis. *Best Pract. Res. Clin. Endocrinol. Metab.* *26*, 759–770.
- Pougovkina, O., Brinke, H. te, Wanders, R.J.A., Houten, S.M., and Boer, V.C.J. de (2014). Aberrant protein acylation is a common observation in inborn errors of acyl-CoA metabolism. *J. Inherit. Metab. Dis.* *37*, 709–714.
- Qiu, X., Brown, K., Hirschey, M.D., Verdin, E., and Chen, D. (2010). Calorie Restriction Reduces Oxidative Stress by SIRT3-Mediated SOD2 Activation. *Cell Metab.* *12*, 662–667.
- Ramponi, G., Manao, G., and Camici, G. (1975). Nonenzymatic acetylation of histones with acetyl phosphate and acetyl adenylate. *Biochemistry (Mosc.)* *14*, 2681–2685.
- Randle, P.J., Sugden, P.H., Kerbey, A.L., Radcliffe, P.M., and Hutson, N.J. (1978). Regulation of pyruvate oxidation and the conservation of glucose. *Biochem. Soc. Symp.* *47–67*.
- Rauh, D., Fischer, F., Gertz, M., Lakshminarasimhan, M., Bergbrede, T., Aladini, F., Kambach, C., Becker, C.F.W., Zerweck, J., Schutkowski, M., et al. (2013). An acetylome peptide microarray reveals specificities and deacetylation substrates for all human sirtuin isoforms. *Nat. Commun.* *4*, 2327.
- Roche, T.E., Baker, J.C., Yan, X., Hiromasa, Y., Gong, X., Peng, T., Dong, J., Turkan, A., and Kasten, S.A. (2001). Distinct regulatory properties of pyruvate dehydrogenase kinase and phosphatase isoforms. *Prog. Nucleic Acid Res. Mol. Biol.* *70*, 33–75.
- Roessler, C., Nowak, T., Pannek, M., Gertz, M., Nguyen, G.T.T., Scharfe, M., Born, I., Sippl, W., Steegborn, C., and Schutkowski, M. (2014). Chemical probing of the human sirtuin 5 active site reveals its substrate acyl specificity and peptide-based inhibitors. *Angew. Chem. Int. Ed Engl.* *53*, 10728–10732.

- Roth, S.Y., Denu, J.M., and Allis, C.D. (2001). Histone Acetyltransferases. *Annu. Rev. Biochem.* 70, 81–120.
- Sack, M.N. (2011). Emerging characterization of the role of SIRT3-mediated mitochondrial protein deacetylation in the heart. *Am. J. Physiol. - Heart Circ. Physiol.* 301, H2191–H2197.
- Sadhukhan, S., Liu, X., Ryu, D., Nelson, O.D., Stupinski, J.A., Li, Z., Chen, W., Zhang, S., Weiss, R.S., Locasale, J.W., et al. (2016). Metabolomics-assisted proteomics identifies succinylation and SIRT5 as important regulators of cardiac function. *Proc. Natl. Acad. Sci. U. S. A.*
- Santo-Domingo, J., and Demarex, N. (2012). Perspectives on: SGP symposium on mitochondrial physiology and medicine: the renaissance of mitochondrial pH. *J. Gen. Physiol.* 139, 415–423.
- Sastri, M., Haushalter, K.J., Panneerselvam, M., Chang, P., Fridolfsson, H., Finley, J.C., Ng, D., Schilling, J.M., Miyanohara, A., Day, M.E., et al. (2013). A kinase interacting protein (AKIP1) is a key regulator of cardiac stress. *Proc. Natl. Acad. Sci. U. S. A.* 110, E387-396.
- Schlicker, C., Gertz, M., Papatheodorou, P., Kachholz, B., Becker, C.F.W., and Steegborn, C. (2008). Substrates and regulation mechanisms for the human mitochondrial sirtuins Sirt3 and Sirt5. *J. Mol. Biol.* 382, 790–801.
- Schuster, S., Roessler, C., Meleshin, M., Zimmermann, P., Simic, Z., Kambach, C., Schiene-Fischer, C., Steegborn, C., Hottiger, M.O., and Schutkowski, M. (2016). A continuous sirtuin activity assay without any coupling to enzymatic or chemical reactions. *Sci. Rep.* 6, 22643.
- Schwer, B., Bunkenborg, J., Verdin, R.O., Andersen, J.S., and Verdin, E. (2006). Reversible lysine acetylation controls the activity of the mitochondrial enzyme acetyl-CoA synthetase 2. *Proc. Natl. Acad. Sci. U. S. A.* 103, 10224–10229.
- Schwer, B., Eckersdorff, M., Li, Y., Silva, J.C., Fermin, D., Kurtev, M.V., Giallourakis, C., Comb, M.J., Alt, F.W., and Lombard, D.B. (2009). Calorie restriction alters mitochondrial protein acetylation. *Aging Cell* 8, 604–606.
- Scott, I., Webster, B.R., Li, J.H., and Sack, M.N. (2012). Identification of a molecular component of the mitochondrial acetyltransferase programme: a novel role for GCN5L1. *Biochem. J.* 443, 655–661.
- Shah, P., and Isley, W.L. (2006). Ketoacidosis during a low-carbohydrate diet. *N. Engl. J. Med.* 354, 97–98.
- Shaw, P.G., Chaerkady, R., Zhang, Z., Davidson, N.E., and Pandey, A. (2011). Monoclonal antibody cocktail as an enrichment tool for acetylome analysis. *Anal. Chem.* 83, 3623–3626.
- Shen, J., Zeng, Y., Zhuang, X., Sun, L., Yao, X., Pimpl, P., and Jiang, L. (2013). Organelle pH in the Arabidopsis Endomembrane System. *Mol. Plant* 6, 1419–1437.

- Shi, L., and Tu, B.P. (2015). Acetyl-CoA and the regulation of metabolism: mechanisms and consequences. *Curr. Opin. Cell Biol.* 33, 125–131.
- Shi, X., Kachirskia, I., Yamaguchi, H., West, L.E., Wen, H., Wang, E.W., Dutta, S., Appella, E., and Gozani, O. (2007). Modulation of p53 Function by SET8-Mediated Methylation at Lysine 382. *Mol. Cell* 27, 636–646.
- Shimazu, T., Hirschey, M.D., Hua, L., Dittenhafer-Reed, K.E., Schwer, B., Lombard, D.B., Li, Y., Bunkenborg, J., Alt, F.W., Denu, J.M., et al. (2010). SIRT3 Deacetylates Mitochondrial 3-Hydroxy-3-Methylglutaryl CoA Synthase 2 and Regulates Ketone Body Production. *Cell Metab.* 12, 654–661.
- Shimizu, S., Kubo, K., Tani, Y., and Ogata, K. (1973). Purification and Properties of Pantothenate Kinase from *Brevibacterium ammoniagenes* IFO 12071. *Agric. Biol. Chem.* 37, 2863–2870.
- Shirakawa, K., Chavez, L., Hakre, S., Calvanese, V., and Verdin, E. (2013). Reactivation of latent HIV by histone deacetylase inhibitors. *Trends Microbiol.* 21, 277–285.
- Shore, D., Squire, M., and Nasmyth, K.A. (1984). Characterization of two genes required for the position-effect control of yeast mating-type genes. *EMBO J.* 3, 2817–2823.
- Shulga, N., Wilson-Smith, R., and Pastorino, J.G. (2010). Sirtuin-3 deacetylation of cyclophilin D induces dissociation of hexokinase II from the mitochondria. *J. Cell Sci.* 123, 894–902.
- Simic, Z., Weiwad, M., Schierhorn, A., Steegborn, C., and Schutkowski, M. (2015). The ε-Amino Group of Protein Lysine Residues Is Highly Susceptible to Nonenzymatic Acylation by Several Physiological Acyl-CoA Thioesters. *Chembiochem Eur. J. Chem. Biol.* 16, 2337–2347.
- Smith, B.C., and Denu, J.M. (2007). Mechanism-Based Inhibition of Sir2 Deacetylases by Thioacetyl-Lysine Peptide. *Biochemistry (Mosc.)* 46, 14478–14486.
- Soboll, S., Werdan, K., Bozsik, M., Müller, M., Erdmann, E., and Heldt, H.W. (1979). Distribution of metabolites between mitochondria and cytosol of cultured fibroblastoid rat heart cells. *FEBS Lett.* 100, 125–128.
- Soe, N.N., Sowden, M., Baskaran, P., Kim, Y., Nigro, P., Smolock, E.M., and Berk, B.C. (2014). Acetylation of cyclophilin A is required for its secretion and vascular cell activation. *Cardiovasc. Res.* 101, 444–453.
- Sol, E.M., Wagner, S.A., Weinert, B.T., Kumar, A., Kim, H.-S., Deng, C.-X., and Choudhary, C. (2012). Proteomic investigations of lysine acetylation identify diverse substrates of mitochondrial deacetylase sirt3. *PLoS One* 7, e50545.
- Someya, S., Yu, W., Hallows, W.C., Xu, J., Vann, J.M., Leeuwenburgh, C., Tanokura, M., Denu, J.M., and Prolla, T.A. (2010). Sirt3 mediates reduction of oxidative damage and prevention of age-related hearing loss under caloric restriction. *Cell* 143, 802–812.

- Stevens, V.J., Vlassara, H., Abati, A., and Cerami, A. (1977). Nonenzymatic glycosylation of hemoglobin. *J. Biol. Chem.* *252*, 2998–3002.
- Stevenson, F.T., Bursten, S.L., Locksley, R.M., and Lovett, D.H. (1992). Myristyl acylation of the tumor necrosis factor alpha precursor on specific lysine residues. *J. Exp. Med.* *176*, 1053–1062.
- Stevenson, F.T., Bursten, S.L., Fanton, C., Locksley, R.M., and Lovett, D.H. (1993). The 31-kDa precursor of interleukin 1 alpha is myristoylated on specific lysines within the 16-kDa N-terminal propiece. *Proc. Natl. Acad. Sci. U. S. A.* *90*, 7245–7249.
- Suzuki, T., Asaba, T., Imai, E., Tsumoto, H., Nakagawa, H., and Miyata, N. (2009). Identification of a cell-active non-peptide sirtuin inhibitor containing N-thioacetyl lysine. *Bioorg. Med. Chem. Lett.* *19*, 5670–5672.
- Takahashi, H., McCaffery, J.M., Irizarry, R.A., and Boeke, J.D. (2006). Nucleocytosolic acetyl-coenzyme a synthetase is required for histone acetylation and global transcription. *Mol. Cell* *23*, 207–217.
- Tan, M., Peng, C., Anderson, K.A., Chhoy, P., Xie, Z., Dai, L., Park, J., Chen, Y., Huang, H., Zhang, Y., et al. (2014). Lysine Glutarylation Is a Protein Posttranslational Modification Regulated by SIRT5. *Cell Metab.* *19*, 605–617.
- Tao, R., Coleman, M.C., Pennington, J.D., Ozden, O., Park, S.-H., Jiang, H., Kim, H.-S., Flynn, C.R., Hill, S., Hayes McDonald, W., et al. (2010). Sirt3-mediated deacetylation of evolutionarily conserved lysine 122 regulates MnSOD activity in response to stress. *Mol. Cell* *40*, 893–904.
- Taylor, P., and Brown, J.H. (1999). Synthesis, Storage and Release of Acetylcholine.
- Tehlivets, O., Scheuringer, K., and Kohlwein, S.D. (2007). Fatty acid synthesis and elongation in yeast. *Biochim. Biophys. Acta* *1771*, 255–270.
- Teng, Y.-B., Jing, H., Aramsangtienchai, P., He, B., Khan, S., Hu, J., Lin, H., and Hao, Q. (2015). Efficient demyristoylase activity of SIRT2 revealed by kinetic and structural studies. *Sci. Rep.* *5*, 8529.
- Thauer, R.K., Jungermann, K., and Decker, K. (1977). Energy conservation in chemotrophic anaerobic bacteria. *Bacteriol. Rev.* *41*, 100–180.
- Theodoulou, F.L., Sibon, O.C.M., Jackowski, S., and Gout, I. (2014). Coenzyme A and its derivatives: renaissance of a textbook classic. *Biochem. Soc. Trans.* *42*, 1025–1032.
- Thompson, P.R., Wang, D., Wang, L., Fulco, M., Pediconi, N., Zhang, D., An, W., Ge, Q., Roeder, R.G., Wong, J., et al. (2004). Regulation of the p300 HAT domain via a novel activation loop. *Nat. Struct. Mol. Biol.* *11*, 308–315.
- Toiber, D., Erdel, F., Bouazoune, K., Silberman, D.M., Zhong, L., Mulligan, P., Sebastian, C., Cosentino, C., Martinez-Pastor, B., Giacosa, S., et al. (2013). SIRT6 Recruits SNF2H to DNA Break Sites, Preventing Genomic Instability through Chromatin Remodeling. *Mol. Cell* *51*, 454–468.

- Verbrugge, F.H., Tang, W.H.W., and Hazen, S.L. (2015). Protein carbamylation and cardiovascular disease. *Kidney Int.* 88, 474–478.
- Vidali, G., Gershey, E.L., and Allfrey, V.G. (1968). Chemical studies of histone acetylation. The distribution of epsilon-N-acetyllysine in calf thymus histones. *J. Biol. Chem.* 243, 6361–6366.
- Wagner, G.R., and Payne, R.M. (2013). Widespread and enzyme-independent N $\epsilon$ -acetylation and N $\epsilon$ -succinylation of proteins in the chemical conditions of the mitochondrial matrix. *J. Biol. Chem.* 288, 29036–29045.
- Wagner, G.R., Pride, P.M., Babbey, C.M., and Payne, R.M. (2012). Friedreich's ataxia reveals a mechanism for coordinate regulation of oxidative metabolism via feedback inhibition of the SIRT3 deacetylase. *Hum. Mol. Genet.* 21, 2688–2697.
- Wang, R., Cherukuri, P., and Luo, J. (2005). Activation of Stat3 Sequence-specific DNA Binding and Transcription by p300/CREB-binding Protein-mediated Acetylation. *J. Biol. Chem.* 280, 11528–11534.
- Wautier, J.-L., and Schmidt, A.M. (2004). Protein glycation: a firm link to endothelial cell dysfunction. *Circ. Res.* 95, 233–238.
- Webster, L.T. (1967). Studies of the Acetyl Coenzyme A Synthetase Reaction V. THE REQUIREMENT FOR MONOVALENT AND DIVALENT CATIONS IN PARTIAL REACTIONS INVOLVING ENZYME-BOUND ACETYL ADENYLATE. *J. Biol. Chem.* 242, 1232–1240.
- Webster, L.T., and Arsenau, W. the technical assistance of J.D. (1963). Studies of the Acetyl Coenzyme A Synthetase Reaction I. ISOLATION AND CHARACTERIZATION OF ENZYME-BOUND ACETYL ADENYLATE. *J. Biol. Chem.* 238, 4010–4015.
- Weindruch, R., Walford, R.L., Fligiel, S., and Guthrie, D. (1986). The retardation of aging in mice by dietary restriction: longevity, cancer, immunity and lifetime energy intake. *J. Nutr.* 116, 641–654.
- Weinert, B.T., Wagner, S.A., Horn, H., Henriksen, P., Liu, W.R., Olsen, J.V., Jensen, L.J., and Choudhary, C. (2011). Proteome-wide mapping of the Drosophila acetylome demonstrates a high degree of conservation of lysine acetylation. *Sci. Signal.* 4, ra48.
- Weinert, B.T., Schölz, C., Wagner, S.A., Iesmantavicius, V., Su, D., Daniel, J.A., and Choudhary, C. (2013). Lysine succinylation is a frequently occurring modification in prokaryotes and eukaryotes and extensively overlaps with acetylation. *Cell Rep.* 4, 842–851.
- Weinert, B.T., Moustafa, T., Iesmantavicius, V., Zechner, R., and Choudhary, C. (2015). Analysis of acetylation stoichiometry suggests that SIRT3 repairs nonenzymatic acetylation lesions. *EMBO J.* 34, 2620–2632.
- Westerberg, D.P. (2013). Diabetic ketoacidosis: evaluation and treatment. *Am. Fam. Physician* 87, 337–346.

- Wu, D., Govindasamy, L., Lian, W., Gu, Y., Kukar, T., Agbandje-McKenna, M., and McKenna, R. (2003). Structure of human carnitine acetyltransferase. Molecular basis for fatty acyl transfer. *J. Biol. Chem.* *278*, 13159–13165.
- Xiao, L., Celano, P., Mank, A.R., Pegg, A.E., and Casero, R.A. (1991). Characterization of a full-length cDNA which codes for the human spermidine/spermine N1-acetyltransferase. *Biochem. Biophys. Res. Commun.* *179*, 407–415.
- Xiong, H., Reynolds, N.M., Fan, C., Englert, M., Hoyer, D., Miller, S.J., and Söll, D. (2016). Dual Genetic Encoding of Acetyl-lysine and Non-deacetylatable Thioacetyl-lysine Mediated by Flexizyme. *Angew. Chem. Int. Ed Engl.*
- Xue, L., Xu, F., Meng, L., Wei, S., Wang, J., Hao, P., Bian, Y., Zhang, Y., and Chen, Y. (2012). Acetylation-dependent regulation of mitochondrial ALDH2 activation by SIRT3 mediates acute ethanol-induced eNOS activation. *FEBS Lett.* *586*, 137–142.
- Yamashita, H., Fukuura, A., Nakamura, T., Kaneyuki, T., Kimoto, M., Hiemori, M., and Tsuji, H. (2002). Purification and partial characterization of acetyl-coA synthetase in rat liver mitochondria. *J. Nutr. Sci. Vitaminol. (Tokyo)* *48*, 359–364.
- Yang, A.S., Gunner, M.R., Sampogna, R., Sharp, K., and Honig, B. (1993). On the calculation of pKas in proteins. *Proteins* *15*, 252–265.
- Yang, H., Zhou, L., Shi, Q., Zhao, Y., Lin, H., Zhang, M., Zhao, S., Yang, Y., Ling, Z.-Q., Guan, K.-L., et al. (2015). SIRT3-dependent GOT2 acetylation status affects the malate-aspartate NADH shuttle activity and pancreatic tumor growth. *EMBO J.* *34*, 1110–1125.
- Yoshii, Y., Furukawa, T., Yoshii, H., Mori, T., Kiyono, Y., Waki, A., Kobayashi, M., Tsujikawa, T., Kudo, T., Okazawa, H., et al. (2009). Cytosolic acetyl-CoA synthetase affected tumor cell survival under hypoxia: the possible function in tumor acetyl-CoA/acetate metabolism. *Cancer Sci.* *100*, 821–827.
- Yu, J., Sadhukhan, S., Noriega, L.G., Moullan, N., He, B., Weiss, R.S., Lin, H., Schoonjans, K., and Auwerx, J. (2013). Metabolic characterization of a Sirt5 deficient mouse model. *Sci. Rep.* *3*, 2806.
- Yu, W., Dittenhafer-Reed, K.E., and Denu, J.M. (2012). SIRT3 Protein Deacetylates Isocitrate Dehydrogenase 2 (IDH2) and Regulates Mitochondrial Redox Status. *J. Biol. Chem.* *287*, 14078–14086.
- Yuan, H., and Marmorstein, R. (2013). Histone Acetyltransferases: Rising Ancient Counterparts to Protein Kinases. *Biopolymers* *99*, 98–111.
- Yurchenko, V., Zybarth, G., O'Connor, M., Dai, W.W., Franchin, G., Hao, T., Guo, H., Hung, H.-C., Toole, B., Gallay, P., et al. (2002). Active site residues of cyclophilin A are crucial for its signaling activity via CD147. *J. Biol. Chem.* *277*, 22959–22965.
- Zager, R.A., Schimpf, B.A., and Gmur, D.J. (1993). Physiological pH. Effects on posthypoxic proximal tubular injury. *Circ. Res.* *72*, 837–846.



- Zhang, Y., Zhou, J., Chang, M., Bai, L., Shan, J., Yao, C., Jiang, R., Guo, L., Zhang, R., Wu, J., et al. (2012). Characterization of and functional evidence for Ste27 of *Streptomyces* sp. 139 as a novel spermine/spermidine acetyltransferase. *Biochem. J.* *443*, 727–734.
- Zhang, Z., Tan, M., Xie, Z., Dai, L., Chen, Y., and Zhao, Y. (2011). Identification of lysine succinylation as a new post-translational modification. *Nat. Chem. Biol.* *7*, 58–63.
- Zhao, J., Micheau, J.-C., Vargas, C., and Schiene-Fischer, C. (2004). *cis/trans* photoisomerization of secondary thiopeptide bonds. *Chem. Weinh. Bergstr. Ger.* *10*, 6093–6101.
- Zhao, S., Xu, W., Jiang, W., Yu, W., Lin, Y., Zhang, T., Yao, J., Zhou, L., Zeng, Y., Li, H., et al. (2010). Regulation of cellular metabolism by protein lysine acetylation. *Science* *327*, 1000–1004.
- Zhong, L., and Mostoslavsky, R. (2011). Fine tuning our cellular factories: sirtuins in mitochondrial biology. *Cell Metab.* *13*, 621–626.
- Zhu, Y., Yan, Y., Principe, D.R., Zou, X., Vassilopoulos, A., and Gius, D. (2014). SIRT3 and SIRT4 are mitochondrial tumor suppressor proteins that connect mitochondrial metabolism and carcinogenesis. *Cancer Metab.* *2*, 15.

# Acknowledgments

First, I would like to thank Prof. Dr. Mike Schutkowski for giving me opportunity to work on such interesting project, for his helpful discussions, excellent mentoring and supporting during my work in his group.

I would like to extend my appreciation to former and current members of AG Enzymology, especially to our senior researchers PD Dr. Stefan König, Dr. Ilona Born, and Dr. David Rauch for selflessly sharing their knowledge and experience.

Deep gratitude to my labmates, Claudia Rößler, Antonia Masch and Theresa Nowak for nice working atmosphere, which made our work relaxed and productive. Special thanks to Dr. Marat Meleshin for helping me in chemical synthesis. We were able always to find a right way to the final product. Also, I would like to thank Dr. Miriam Arbach and Dr. Michael Schumann for helpful discussions in the final stages of my PhD work.

I would like to thank Dr. Angelika Schierhorn for our successful cooperation in MS experiments. A great thank to the group of Prof. Dr. Thomas Kiefhaber MLU Halle-Wittenberg for providing me opportunity for CD measurements.

I would also like to thank Dr. Cordelia Schiene-Fischer and Dr. Matthias Weiwad from the former Max Planck Research Unit for Enzymology of Protein Folding, Halle (Saale) and Prof. Dr. Clemens Steegborn from University of Bayreuth for helpful discussions and sharing their expertise.

Last but not least I would like to thank my friends and family. Especially thanks to my parents for providing me financial support during the initially phase of this work. The greatest attitude I own to my beloved wife Maja, for supporting me through my work and encouraging when was necessary.

# Curriculum Vitae

---

## Personal data

**Name:** Zeljko Simic  
**Adresse:** Bruckdorfer Straße 5, 06112 Halle (Saale)  
**Date of birth:** 04.02.1982  
**Place of birth:** Bajina Basta, Serbia  
**Citizenship:** Republic of Serbia  
**Family status:** married

---

## Academic education

**1989-1997** Primary School "Sveti Sava", Bajina Basta, Serbia

**1997-2001** High School (Gymnasium) "Josif Pancic",  
Bajina Basta, Serbia  
Subject – natural science and mathematics

**2001-2008** Faculty of Chemistry, Department of Biochemistry,  
University of Belgrade, Belgrade, Serbia

**2012-2016** Postgraduate study (PhD),  
Department of Enzymology,  
Institute of Biochemistry and Biotechnology,  
Faculty of Natural Science I,  
Martin-Luther University Halle-Wittenberg,  
Halle (Saale), Germany

---

# List of publications

Parts of following publications were included in this thesis with permission of the publisher:

**Zeljko Simic**, Matthias Weiwad, Angelica Schierhorn, Clemens Steegborn & Mike Schutkowski. The epsilon-Amino Group of Protein Lysine Residues Is Highly Susceptible to Non-enzymatic Acylation by Several Physiological Acyl-CoA Thioesters, *Chembiochem*, 2015, **16**, 2337–2347

Sabine Schuster, Claudia Roessler, Marat Meleshin, Philipp Zimmermann, **Zeljko Simic**, Christian Kambach, Cordelia Schiene-Fischer, Clemens Steegborn, Michael O. Hottiger, Mike Schutkowski, A continuous sirtuin activity assay without any coupling to enzymatic or chemical reactions, *Scientific Reports*, 2016, **6**, 22643

## Poster presentations on scientific conferences:

SIRT5 is able to reverse spontaneous lysine acylation in mitochondria. **Zeljko Simic**, Claudia Roessler, Martin Pannek, Clemens Steegborn, Mike Schutkowski. 50 Years of Histone Acetylation. Barcelona Conference on Epigenetics and Cancer, 2014, Barcelona, Spain

Non-enzymatic protein acylation by different acyl-CoA thioesters. **Zeljko Simic**, Claudia Roessler, Clemens Steegborn, Mike Schutkowski. 25<sup>th</sup> Faltertage, International conference, 2014, Regensburg, Germany.

## Eigenständigkeitserklärung

Hiermit bestätige ich, dass ich die vorliegende Arbeit selbständig verfasst und keine anderen als die angegebenen Hilfsmittel benutzt habe. Die Stellen der Arbeit, die dem Wortlaut oder dem Sinn nach anderen Werken entnommen sind, wurden unter Angabe der Quelle kenntlich gemacht. Ich versichere weiterhin, dass die Arbeit in gleicher oder ähnlicher Form noch keiner anderen Prüfungsbehörde vorgelegen wurde.

---

Ort, Datum

---

Unterschrift